

Comparative study of cell walls during wheat and rice grain development

By

Richard Andrew Palmer

Submitted in accordance with the requirements for the degree of
Doctor of Philosophy

The University of Leeds
Faculty of Biological Sciences

September 2015

The candidate confirms that the work submitted is his/her own, except where work which has formed part of jointly-authored publications has been included. The contribution of the candidate and the other authors to this work has been explicitly indicated below. The candidate confirms that appropriate credit has been given within the thesis where reference has been made to the work of others.

In chapter 5, the cloning of monoclonal antibody-secreting cell lines and the antibody characterisation was performed by Sue Marcus. Preparation of the AGP wheat extract for immunisation was performed by Dr Alison Lovegrove.

In chapter 5, Figure 5.3 was produced by Sue Marcus. The experiments and sample preparation leading to this image were performed by her.

In chapter 5 all production of the RNAi lines was performed by Dr Mark Wilkinson.

In chapter 5, high pressure freezing of null and RNAi wheat lines was conducted by Dr Paola Tosi. All paraformaldehyde fixation, all sectioning and immunohistochemistry were performed by the candidate.

This copy has been supplied on the understanding that it is copyright material and that no quotation from the thesis may be published without proper acknowledgement.

The right of Richard Andrew Palmer to be identified as Author of this work has been asserted by him in accordance with the Copyright, Designs and Patents Act 1988.

© 2015 The University of Leeds and Richard Andrew Palmer

ACKNOWLEDGEMENTS

I would like to thank my supervisors, Paola Tosi; Peter Shewry and Paul Knox for their continuous support, incisive comments and understanding during the past four years of this PhD. I greatly appreciate all your time and efforts to get me through this in one piece!

I would also like to thank Fabienne Guillon at INRA Nante for her generosity in providing me with several of their cell wall antibodies, which have helped my to complete this project.

ABSTRACT

The cell wall polysaccharides of wheat and rice endosperm represent an important source of dietary fibre with up to 50% of the dietary fibre intake in western diets deriving from cereal consumption. Plant cell walls are complex structures composed of many interlinking polysaccharide chains as well as lignin, phenolics and some proteins. The significance of many of these molecules has yet to be elucidated, however cell walls have been shown to be rapidly modified during growth and differentiation demonstrating that the cell wall is a dynamic structure modified *in muro* to adapt to changing biological constraints. Wheat and rice present near synchronous developmental cycles and significantly different endosperm cell wall compositions, allowing the localization of these polysaccharides to be related to developmental changes. Monosaccharide analysis has been widely used on mature endosperm and flour sample in cereal grains to provide an overview of cell wall composition, but no previous studies have considered different developmental stages. In both wheat and rice four distinct phases of cell wall deposition were detected, with 4-8 days after anthesis (DAA) and 12-20 DAA showing the greatest levels of depositions in all monosaccharides. After 20 DAA significant deposition of pectic polysaccharides was detected in both species, which may reflect preparations for grain dehydration. Monoclonal antibodies specific to cell wall polysaccharides and immunofluorescence microscopy were used to determine the spatial and temporal locations of these polysaccharides. A conserved sequence of polysaccharide deposition during cellularisation was also seen in both species, matching that reported in barley grains. Arabinogalactan-peptides (AGPs) are a significant component of wheat and rice grains and through the use of novel wheat AGP monoclonal antibodies they were shown to be localised either at the plasma membrane or in the cytoplasm, contrary to previous hypotheses that they may be cell wall proteins.

TABLE OF CONTENTS

Chapter 1: Introduction	22
1.1 General introduction	22
1.2 Seed development	22
1.2.1 Pollination and Fertilization	22
1.2.2 Endosperm development	23
1.2.3 Embryo development.....	25
1.3 Differences in wheat and rice transport pathways	25
1.4 Seed protein	27
1.4.1 Storage proteins.....	27
1.5 Starch	31
1.5.1 Starch composition	31
1.6 Cell wall components	33
1.6.1 Arabinoxylan (AX)	34
1.6.2 Mixed-linkage β Glucan (MLG).....	37
1.6.3 Heteromannans.....	39
1.6.4 Callose.....	40
1.6.5 Pectic polysaccharides	40
1.6.5.1 Homogalacturonan	41
1.6.5.2 Rhamnogalacturonan-I (RG-I).....	42
1.6.5.3 RG-II.....	45
1.6.5.4 Biosynthesis of pectin	46
1.6.6 Cellulose	48
1.6.6.1 Cellulose biosynthesis.....	49
1.6.6.2 Function.....	49
1.6.7 Lignin	50
1.6.8 Arabinogalactan peptides.....	51
1.7 Gradients in grain composition.	52
1.8 Usage and limitations of monoclonal antibodies	53
1.9 Aims of project	53
Chapter 2: Materials and Methods	56
2.1 Plant materials	56
2.2 Immunolocalization of cell wall polysaccharides wheat and rice grains.	57
2.2.1 Light microscopy and immunofluorescence analysis.....	57

2.2.2 Sample preparation for high pressure freezing	57
2.2.3 Indirect immunofluorescence labelling and histochemical staining for light microscopy	58
2.2.3.1 Enzymatic unmasking.....	60
2.3 Histochemical stains	60
2.3.1 General morphology	60
2.3.2 Protein body staining.....	60
2.3.3 Starch granule staining	61
2.4 Cell wall chemistry	61
2.4.1 Isolation of cell wall material.....	61
2.4.1.1 Non-starch polysaccharide (NSP) preparation, based on Englyst et al 1992.	61
2.4.1.2 Alcohol insoluble residue (AIR) protocol 1 (AIR1).....	62
2.4.1.2.1 Additional Starch removal step	62
2.4.1.3 AIR protocol 2 (AIR2).....	62
2.4.1.3.1 Additional Starch removal step	62
2.4.1.4 Lai Protocol	62
2.4.1.5 Shibuya protocol:- (Shibuya et al. 1985).....	63
2.4.2 Monosaccharide analysis via HPLC.....	64
2.4.2.1 Chromatographic method for monosaccharides – neutral sugars.....	64
2.4.2.2 Chromatographic method for monosaccharides – acidic sugars	64
2.4.3 Megazyme MLG Assay kit method	65
2.4.3.1 Glucose Standard curve production	65
2.4.3.2 Assay of samples with unknown MLG content	66
2.4.3.3 Optimised method.	67
2.4.4 Klason-Lignin Assay	67
2.4.5 Cellulose assay	67
2.4.5.1 Cellulose quantification using anthrone reagent as per Gillmor et al. (2002) an amalgamation of Scott Jr and Melvin (1953); Updegraff (1969).....	67
2.4.5.2 Optimisation	68
Chapter 3: Morphology and development of wheat and rice grains	69
3.1 Introduction to grain development and morphology.....	69
3.2 Results.....	70
3.2.1 Fixation and embedding of wheat and rice grains for histochemical staining	70
3.2.1.1 Optimisation of fixation protocol for wheat and rice grains.	70

3.2.2 Morphology of starch/ protein/ cell walls/ nuclei and grain structure with histochemical stains.....	73
3.2.2.1 Staining with Toluidine Blue O reveals general tissue morphology in the developing grains	73
3.2.2.2 Cell wall morphology visualised with Calcoflour White 2mr	76
3.2.2.3 Protein body accumulation detected by labelling with Coomassie brilliant blue (CBB)	79
3.2.2.4 Starch accumulation detected using potassium iodide solution.	84
3.2.3 Monosaccharide analysis of cell wall polysaccharides (HPLC/GC)	87
3.2.3.1 Extraction of cell wall polysaccharides from milled grain material.....	87
3.2.3.2 HPLC monosaccharide data.....	89
3.2.3.2.1 Monosaccharide content per gram of sample material shows minimal changes in the proportions of developing wheat, but rice shows significant changes in the ratio of cell wall composition between 4-12 DAA.	89
3.2.3.2.2 Wheat and rice cell wall deposition appears to follow a 4 phase pattern with the periods between 4-8 DAA and 12-20 DAA showing the significantly higher rates of cell wall depositon in both species.	93
3.2.4 Quantification of MLG content in developing wheat and rice grains with Megazyme MLG colorimetric assay kit.	98
3.2.4.1 Optimisation of the Megazyme MLG kit for detection in developing wheat and rice.....	98
3.2.4.2 Determination of MLG content of developing wheat and rice grain with optimised Megazyme procedure.....	100
3.2.5 Colorimetric quantification of cellulose with anthrone reagent.....	103
3.2.6 Klason-lignin content in developing wheat and rice grains.....	107
3.2.6.1 Klason-Lignin content increases steadily throughout the development of both wheat and rice, but rises at a greater rate in wheat than in rice.	107
3.2.7 Total cell wall composition quantification in developing wheat and rice grains.....	109
3.2.7.1 Examining the contribution of each cell wall component as a percentage reveals that MLG is the major component of grain cell walls from 4-20 DAA in both species.....	111
3.3 Discussion.....	117
3.3.1 Cell wall deposition in wheat and rice grains follows a consistent pattern between the five developmental stages examined.	117
3.3.2 The percentage content of MLG and AX changes significantly in both species throughout development	122

3.3.3 Pectin content increases during grain development, increasing almost two-fold during the period from 4-28 DAA in wheat and three-fold in rice.	123
3.3.4 Cellulose content increases throughout development and appears to be a major component of rice endosperm tissue.	124
3.3.5 The Klason lignin method appears unreliable with the small quantities of grain tissue available for analysis.	125
3.3.6 Deposition of protein and starch granules occur up to 4 days earlier in rice than in wheat grains. Whilst endosperm cell wall morphology is more uniform between the two species.	125
3.4 Conclusion	126
Chapter 4: Immunohistochemical analyses of wheat and rice	128
4.1 Introduction to antibodies and methodology	128
4.2 Results	132
4.2.1 Dynamics of non-cellulosic/non-pectic cell wall matrix glycans.....	133
4.2.1.1 Arabinoxylan (AX as detected with INRA-AX1 increases in labelling strength as development progresses in both wheat and rice in all tissues and wheat endosperm cell walls lacks the LM28 glucuronoxylan epitope that is widespread in rice endosperm cell walls	133
4.2.1.2 Callose persists beyond cellularisation in the developing endosperm of both wheat and rice.	136
4.2.1.3 Mixed-linkage glucan is absent from the early endosperm cell walls of both wheat and rice prior to the detection of AX in both species. MLG is absent from the aleurone and nucellar epidermis of rice until 20 DAA, conversely in wheat these cells always display the strongest labelling for MLG.....	138
4.2.1.4 Xyloglucan is detected in the anticlinal cell wall extensions of wheat and rice during cellularisation, and persists in the early endosperm cell walls, but can only be detected in the aleurone cells of rice at maturity.....	139
4.2.1.5 Glucomannan is detected strongly in the endosperm cell walls of wheat, but cannot be detected at any developmental stage in rice endosperm.....	141
4.2.1.6 Dynamics of pectic polysaccharides.....	143
4.2.1.6.1 The presence of glycan domains of pectic supramolecules was studied using sets of antibody probes specific for HG and RG-I polysaccharides. Homogalacturonan methylation state appears to be cultivar dependant in wheat endosperm tissues, whereas LM19 was the major epitope detected in rice endosperm.	143
4.2.1.6.2 Rhamnogalacturonan-I backbone epitope detection is earlier in the endosperm of rice at (12 DAA) than in wheat (20 DAA).....	145

4.2.1.6.3 Galactan (LM5) and arabinan (LM6) RG-I Side chains can be detected earlier in development than RG-I back bone epitopes in both wheat and rice endosperm.....	146
4.2.1.7 Developmental dynamics of Phenolic polysaccharides.	149
4.2.1.7.1 Ferulic acid epitopes more prevalent in the endosperm cells proximal to the crease cavity in wheat grains after 20 DAA, in rice ferulic acid labelling was evenly distributed throughout the endosperm.	149
4.2.1.7.2 p-Coumaric acid is found in both the aleurone and endosperm cells at maturity in rice, but is detected only in the aleurone cells of wheat grains	151
4.2.2 Unmasking of cell wall polysaccharides	153
4.2.2.1 Unmasking of pectic epitopes with a lichenase xylanase (LX) dual enzymatic treatment.....	153
4.3 Discussion.....	157
4.3.1 Callose, arabinoxylan and Mixed link glucan exhibit a conserved order of deposition within the cellularising endosperm of wheat rice and barley.	157
4.3.2 Xyloglucan is detected in the anticlinal cell walls of cellularising endosperm in wheat and rice.....	159
4.3.3 Pectic polysaccharide structure during grain development.....	160
4.3.4 LX unmasking of pectic polysaccharides during grain development.	161
4.3.5 Conclusion	163
Chapter 5: Arabinogalactan proteins: A cell wall component?	164
5.1 Introduction	164
5.2 Results	167
5.2.1 Production of mAbs to water extractable wheat AGPs.	168
5.2.2 Immunolabeling of paraformaldehyde fixed sections.	170
5.2.3 Comparison of different monoclonal antibody lines from the initial immunisation protocol.....	171
5.2.4 Immunolabelling of gsp-1 RNAi Lines.....	174
5.2.5 Immunolabelling of HPF fixed gsp-1 RNAi lines reveals labelling is restricted to the cell membrane.....	176
5.3 Discussion.....	178
Chapter 6: Discussion	180
6.1 Conclusions.....	187
Chapter 7: Bibliography.....	189

LIST OF TABLES

Table 2.1 KOH elution gradient for HPLC neutral monosaccharide method.

64

Table 2.2 Elution gradients for HPAEC acidic monosaccharides method. 65

Table 2.2. Glucose standard curve for GOPOD. 66

Table 3.1. Comparison of the monosaccharide contents of the rice cell wall material extracted from 150mg of milled polished rice and scaled to ug/g of sample material.. 88

Table 3.2. Average monosaccharide content per gram of milled sample material (from three technical replicates), in wholegrain wheat and rice throughout the course of grain development and a mature polished white flour sample, as detected by HPLC analysis of non-starch polysaccharide.

91

Table 3.3. Average monosaccharide content per grain (from three technical replicates), in wholegrain wheat and rice throughout development, as detected by HPLC analysis of non-starch polysaccharide.

96

Table 3.4. Detection of D-glucose (25-100 µg per cuvette) with Megazyme MLG kit for production of D-glucose standard calibration curve. 99

Table 3.5. MLG content in developing wholegrain wheat and rice as detected with the megazyme MLG assay. 101

Table 3.6. Average d-glucose content colorimetrically detected with anthrone reagent in concentrated sulphuric acid, of samples of known d-glucose concentration to produce a calibration or response curve for the subsequent analysis of cellulose content. 103

Table 3.7. Colorimetric quantification of cellulose derived d-glucose of whole grain wheat and rice using anthrone reagent in a dilute sulphuric acid solution. Average results based on 3 technical repeats. 104

Table 3.8. Lignin content of milled wholegrain wheat and rice tissue throughout development, and in milled mature polished grains (white endosperm enriched flour) using Klason-lignin analysis. 108

Table 3.9. Table of cell wall composition (μg / grain) in developing wheat and rice grain, combining HPLC monosaccharide data, MLG and cellulose data. 110

Table 3.10. Table of cell wall composition by percentage in developing wheat and rice grain, combining HPLC monosaccharide data, MLG and cellulose data. 113

Table 3.11. Summary table of percentage composition of developing wheat and rice grains, showing the relative contribution of the major polysaccharides. 114

Table 3.12. Summary of wheat cell wall component content changes per grain during the 4 major grain phases. 119

Table 3.13. Summary of rice cell wall component content changes per grain during the 4 major grain phase 121

Table 4.1. Cell wall directed monoclonal antibodies used in this study. 130

LIST OF FIGURES

- Figure 1.1. Medial transverse sections of mature wheat (A) and rice (B), stained with toluidine blue, showing the hypothesised route of nutrients flow into the developing grain. 26**
- Figure 1.2. Schematic structures of typical HMW (high molecular weight), S-rich (sulphur-rich) and S-poor (sulphur-poor) prolamins (based on sequences in (Bartels et al. 1986; Anderson et al. 1989; Hsia and Anderson 2001)). 28**
- Figure 1.3. Schematic representation of amylopectin structure according to the “Cluster” model, modified from nakamura et al 2002 32**
- Figure 1.4. A schematic representation of glucuronoxyylan and its potential monosaccharide substitutions. Modified from Burton et al. (2010) 35**
- Figure 1.5. Schematic representation MLG structure with a mixture of DP3 and DP4 glucose chains between each 1-3 linkage. 38**
- Figure 1.6. Schematic representation of the components of the pectic molecular complex. Modified from Leclere et al. (2013) 41**
- Figure 1.7. Schematic structure of rhamnogalacturonan II with the 4 side chains A-D (O'Neill et al. 2004) 46**
- Figure 3.1. Changing grain weight in wheat and rice throughout development, based on the average of 50 grains at each time point. 72**
- Figure 3.2. Toluidine Blue O staining general morphology of medial transverse semi-thin (2 µm) sections of developing rice grains a 4 DAA (A, B), 12 DAA (C, D), and 28 DAA (E, F). 75**
- Figure 3.3. Toluidine Blue O staining general morphology of medial transverse semi-thin (2 µm) sections of developing wheat grains a 4 DAA (A, B), 12 DAA (C, D), and 28 DAA (E, F). 76**
- Figure 3.4. Calcofluor white 2mr staining of cell walls in medial transverse semi thin (2 µm) sections of developing wheat (A, C, E, G) and rice (B, D, F, H) grains a 4 DAA (A, B), 12 DAA (C, D), and 28 DAA (E - H). 79**

Figure 3.5. Coomassie Brilliant Blue (CBB) staining protein in medial transverse semi-thin (2 μ m) sections of developing rice grains a 4 DAA (A, B), 12 DAA (C, D), and 28 DAA (E, F). 81

Figure 3.6. Coomassie Brilliant Blue (CBB) staining protein in medial transverse semi-thin (2 μ m) sections of developing wheat grains a 4 DAA (A, B), 12 DAA (C, D), and 28 DAA (E, F). 82

Figure 3.7. Coomassie Brilliant Blue (CBB) staining protein in medial transverse semi-thin (2 μ m) sections of developing wheat (A, C, E) and rice (B, D, F) grains a 8 DAA (A, B), 12 DAA (C, D), and 28 DAA (E, F) showing the deposition of protein bodies in both species. 83

Figure 3.8. Potassium iodide (IKI) staining of starch in medial transverse semi thin (2 μ m) sections of developing wheat grains a 4 DAA (A, B), 12 DAA (C, D), and 28 DAA (E, F). 85

Figure 3.9. Potassium iodide (IKI) staining of starch in medial transverse semi thin (2 μ m) sections of developing rice grains a 6 DAA (A, B), 12 DAA (C, D), and 28 DAA (E, F). 86

Figure 3.10. Monosaccharide content per gram of milled material in developing wholegrain wheat. 92

Figure 3.11. Monosaccharide content per gram of milled material in developing wholegrain rice. 93

Figure 3.12. HPLC Monosaccharide content per grain in developing wheat grains. Average of 3 technical replicates based on an analysis of 100 mg of milled starting material. 97

Figure 3.13. HPLC Monosaccharide content per grain in developing rice grains. Average of 3 technical replicates based on an analysis of 100 mg of milled starting material. 97

Figure 3.14. D-glucose absorbance response curve at 510 nm with GOPOD reagent. 100

Figure 3.15. Average MLG content per gram of milled wholegrain tissue throughout development in wheat and rice, as detected colorimetrically by the Megazyme MLG assay kit. 102

Figure 3.16. Average MLG content per wheat or rice wholegrain throughout development, as detected colorimetrically by the megazyme MLG assay kit. Each data point is the average of 3 technical replicates using separate tissue samples. 102

Figure 3.17. d-Glucose standard response curve with anthrone reagent, showing the working concentration of anthrone to be between 100 and 600nMol of d-glucose 105

Figure 3.18. Average cellulose content per gram of milled wholegrain tissue in wheat and rice throughout development. Colorimetrically assayed using anthrone reagent. 105

Figure 3.19. Average cellulose content per wheat and rice whole grains throughout development, colorimetrically assayed using anthrone reagent. 106

Figure 3.20. Klason-Lignin content per whole grain in wheat and rice throughout development. 109

Figure 3.21. Combined cell wall composition of developing wheat grains, showing data from HPLC monosaccharide analysis, MLG and cellulose assays. 115

Figure 3.22. Combined cell wall composition of developing rice grains, showing data from HPLC monosaccharide analysis, MLG and cellulose assays. 116

Figure 3.23. Summary of the developmental changes in percentage composition of wholegrain wheat cell walls in the major 4 polysaccharides. 120

Figure 3.24. Summary of the developmental changes in percentage composition of wholegrain rice cell walls in the major 4 polysaccharides. 122

Figure 4.1. Indirect immunofluorescence detection of AX, callose and MLG in medial transverse sections of a wheat grain at 4 (a-c), 12 (d-f), and 28 DAA (g-i). Immunofluorescence detection of INRA-AX1 (a, d, g) and callose (b, e, h) and MLG (c, f, i). 134

Figure 4.2. Indirect immunofluorescence detection of AX and callose in medial transverse sections of a rice grain at 4 (b), 6 (a), 12 (c, d), and 28 DAA (e, f). Immunofluorescence detection of AX (a, c, e) and callose (b, d, f). 135

Figure 4.3. Indirect immunofluorescence detection of glucuronoxylan (GUX, LM28) in medial transverse sections of wheat (A, C) and rice (B, D) grains at 4 DAA (A, B) and 28 DAA (C, D). 137

Figure 4.4. Indirect immunofluorescence detection of MLG in medial transverse sections of wheat (a, c) and rice (b, d) grains at 12 DAA. Arrowheads indicate absence of fluorescence labelling in the aleurone and nucellar epidermis. 139

Figure 4.5. Indirect immunofluorescence detection of xyloglucan in medial transverse sections of wheat (a, c, e) and rice (b, d, f) grains at 4 (a, b), 12 (c, d), and 28 days after anthesis (e, f). Inset in micrograph a is a 4x enlargement of the boxed region, showing immunofluorescence labelling of the anticlinal cell walls. 140

Figure 4.6. Indirect immunofluorescence detection of heteromannan in medial transverse sections of wheat (a, c) and rice (b, d) grains at 12 DAA. Micrographs c and d are 4x enlargements of the outer endosperm regions of micrographs a and b to show that the heteromannan signal is present throughout the endosperm and sub aleurone tissues in wheat, but remains absent in rice. 142

Fig 4.7. Indirect immunofluorescence detection of pectic HG in medial transverse sections of wheat (a-d) and rice (e-h) grains at 4 (a, b, e, f) and 28 DAA (c, d, g, h) using JIM7 and LM19 monoclonal antibodies. Inset in micrograph g is a lower magnification image with the boxed region indicating the region imaged for micrographs g and h. 144

Figure 4.8. Indirect immunofluorescence detection of RG-I backbone in medial transverse sections of wheat (a, c) and rice (b, d) grains at 12 (a, b) and 28 days after anthesis (c, d). 146

Figure 4.9. Indirect immunofluorescence detection of pectic arabinan and galactan as in medial transverse sections of wheat (a-f) and rice (g-l) grains at 4 (a, b, g, h), 12 (c, d, i, j) and 28 days after anthesis (e, f, k, l). 148

Fig 4.10. Indirect immunofluorescence detection of feruloylated polysaccharides in medial transverse sections of wheat (a-d) and rice (e-h) grains at 4 (e), 8 (a), 12 (b, f) and 20 DAA (c, d, g, h) using LM12 monoclonal antibody. Micrograph d and h are higher magnifications of c and g. 150

Fig 4.11. Indirect immunofluorescence detection of coumaric acid in medial transverse sections of wheat (a-d) and rice (e-h) grains at 4 (e), 12 (a, b, f), 20 (c) and 28 DAA (d, g, h) using INRA-COU1 monoclonal antibody. Arrowheads indicate aleurone cells unlabelled by INRA-COU1. 152

Figure 4.12. Indirect immunofluorescence detection of pectic epitopes in medial transverse sections of wheat grains at 20 DAA partially digested by lichenase and xylanase (LX) labelled with INRA-AX1 (a, b), Anti-MLG (c), LM19 (d), JIM7 (e), LM20 (f), LM6 (g), INRA-RU1 (h), LM5 (i) monoclonal antibodies. 154

Figure 4.13. Indirect immunofluorescence detection of pectic epitopes in medial transverse sections of rice grains at 20 DAA partially digested by Lichenase and Xylanase (LX) labelled with INRA-AX1(a, b), Anti-MLG (c), JIM7 (d), LM19 (e), LM20 (f), LM6 (g), INRA-RU1 (h), LM5 (i) monoclonal antibodies. 156

Fig 5.1. Proposed model of the many possible structures of the carbohydrate component of wheat AGPs. Modified from Tryfona et al. (2010). 166

Fig 5.2. Consensus sequence of wheat arabinogalactan peptide across different wheat cultivars, as displayed with the Berkley logo software. Modified from Wilkinson et al. (2013). 167

Fig 5.3. Analysis of LM30 binding to wheat grain AGP. A. Western blot of LM30 binding to wheat grain AGP and sensitivity to an arabinofuranosidase B. ELISA of LM30 binding to wheat grain AGP and sensitivity to arabinofuranosidases. 169

Figure 5.4. Immunofluorescence labelling of AGPs with LM30 (C, D, F) and 2H5/E4 (A, B, E) on paraformaldehyde fixed 1 µm thick medial transverse wheat grain sections at 8 DAA (A-D) and 12 DAA (E, F). 171

Figure 5.5. Immunofluorescence labelling of AGPs with 4H8 (A), 5C9 (B), 7F3 (C), 8E11 (D), MAC207 (E), JIM13 (F), JIM16 (G) and LM2 (H) on high pressure frozen 1 µm thick medial transverse null segregant wheat grain sections at 15 DAA (A-H). 173

Figure 5.6. Immunofluorescence labelling of AGPs with LM30 (A-H) on high pressure frozen 1 µm thick medial transverse wheat grain sections null segregants at 15 DAA (A-H). 175

Figure 5.7. Immunofluorescence labelling of AGPs with LM30 (A-H) on high pressure frozen 1 µm thick medial transverse RNAi gsp-1 wheat grain sections at 15 DAA (A-H). 177

LIST OF ABBREVIATIONS

AcE	Acetyl Ester
AG	Arabinogalactan
AGA	Acacia sp. gum arabic
AGP	Arabinogalactan peptides
AIR	Alcohol insoluble residue
APAP	Arabinoxylan pectin arabinogalactan protein
Ara	Arabinose
Arabfase	Arabinofuranosidase
<i>Araf</i>	Arabino furanosyl
<i>Arap</i>	Arabino pyranosyl
AX	Arabinoxylan
CBB	Coomassie brilliant blue
CSC	Cellulose synthase complex
CSL	Cellulose synthase like
Ces	Cellulose synthase
DAA	Days after anthesis
DHA	3-deoxy-D-lyxo-2-heptulosaric acid
DMSO	Dimethyl sulphoxide
DNA	Deoxyribonucleic Acid
DP	Degree of polymerisation
ELISA	Enzyme-linked immunoabsorbent assay
FeA	Ferulic Acid
FITC	Fluorescein isothiocyanate
Fuc	Fucose
<i>Fucp</i>	Fuco pyranosyl
Gal	Galactose
GalA	Galacturonic acid

Galp	Galactopyranosyl
GalpA	galactopyranosyluronic Acid
GAUT	Galacturonosyl transferease
GDP	Guanosine diphosphate
GOPOD	Glucose oxidase/oxidase solution
Glc	Glucose
GlcA	Glucuronic acid
Glc _p	Glucopyranosyl
Glc _p A	Glucopyranosyluronic acid
GPI	Glycosylphosphatidylinositol
GSP	Grain softness protein
GT	Glycosyl transferase
GUX	Glucuronoxylan
HB-AX	Highly branched arabinoxylan
HCl	Hydrochloric acid
HG	Homogalacturonan
HMW-	High Molecular weight
HMW-GS	High molecular weigh glutenin subunit
HPAEC	High-performance anion exchange chromatography
HPF	High pressure freezing
HPLC	High-performance liquid chromatography
IKI	Iodine/potassium iodide solution
IRX	Irregular xylem
kD	Kilodaltons
KDO	3-Deoxy-d-manno-2-octulosonic acid
KOH	Potassium hydroxide
LAG	Larch arabinogalactan
LB-AX	Low branch arabinoxylan

LMW- GS	Low molecular weight glutenin subunit
LX	Lichenase xylanase mixture
mAb	Monoclonal antibody
Man	Mannose
MLG	Mixed linkage $-(1-3),(1-4)-\beta$ -glucan
NMR	Nuclear magnetic resonance
NSP	Non-starch polysaccharide
OD	Optical density
PB-I	Protein bodies type 1
PB-II	Protein bodies type 2
PBS	Phosphate buffered saline
PCD	Programmed cell death
PTFE	Polytetrafluoroethylene
Qua	Quasimodo
RG-I	Rhamnogalacturonan type 1
RG-II	Rhamnogalacturonan type 2
RGXT	Rhamnogalacturonan xylosyltransferases
Rha	Rhamnose
Rhap	Rhamnopyranosyl
RNAi	Interference ribonucleic acids
RT	Room temperature
SDS-PAGE	Sodium dodecyl sulphate- polyacrylamide gel electrophoresis
TEM	Transmission electron microscopy
UDP	Uridine diphosphate
UV	Ultraviolet
XGA	Xylogalacturonan
XRES	Xylan reducing end sequence
Xyl	Xylose

CHAPTER 1: INTRODUCTION

1.1 General introduction

Wheat and rice are the staple crops for up to two thirds of the world's population, providing more than 50% of the daily calorific intake to nearly 3 billion people (<http://faostat.fao.org/site/368/default.aspx>). Cereals also contribute up to 50% of the total dietary fibre in western diets (Nyman and Bjorck 1989; Bates et al. 2011; Bjorck et al. 2012). The major components of cereal grain fibre are cell wall polysaccharides, which account for ~2% of the dry weight of white wheat flour or polished rice grain but up to 20% of whole grain (Juliano 1985a). An understanding of the structures of cereal grain cell walls is therefore of direct relevance to the understanding of the role of cereals in human health. The benefits of increased dietary fibre intake include improved regulation of blood sugar, reduction in serum cholesterol, immune stimulation and decreased risk of some types of cancer (Bingham et al. 1985; Cade et al. 2007; Buttriss 2009; Anderson et al. 2009; Slavin and Jacobs 2010; Gemen et al. 2011; Bjorck et al. 2012; Threapleton et al. 2013). By contrast, lower contents of dietary fibre are required for other end uses with the high viscosity resulting from soluble fibre being detrimental when cereals are used as feed for monogastric livestock such as pigs and poultry (Hesselman et al. 1981) and for the production of ethanol in brewing, distilling and biofuel.

1.2 Seed development

1.2.1 Pollination and Fertilization

Both in wheat and rice plants at anthesis, the styles covering the ovary separate allowing the stamens to elongate and shed the pollen that is stored in the anthers. The majority of the pollen is shed within the spikelet and some comes into contact with the stigmatic surfaces of the styles, where germination may occur if conditions are conducive, leading to the formation of a pollen tube, which penetrates the tissue of the stigma. The biological material required for the formation and initial extension of the pollen tube is readily available within the pollen grain, which is rich in lipid and proteins. However in later stages of pollen tube extension, some of the nutrients required are sourced from the degradation and digestion of stigma cells via

secretion of enzymes into the cells. The nucleus is located at the very tip of the pollen tube and it remains in that position throughout extension of the pollen tube into the stigma. Two male gametes reside directly behind the tip of the pollen tube and are released into the embryo sac via the degradation of the pollen tube nucleus and the degradation of the cell wall of the pollen tube once it has extended sufficiently in to the micropylar region of the ovule tissues. The first male gamete to reach the two polar nuclei, at the far end of the embryo sac, fuses with them and forms a triploid nucleus typically 5-6 hours after pollination. The endosperm tissue of the new grain originates from this triploid nucleus. After a further 12-14 hours the second male gamete fuses with the oosphere and forms a diploid zygotic nucleus, from which the embryo will develop. Subsequently the triploid endosperm nucleus undergoes several rounds of mitotic division, with a characteristic lack of a cell plate separating the daughter nuclei, which generates a multinucleate cell often referred to as the endospermatic coenocyte. There is some evidence that phragmoplast formation is at least initiated between daughter nuclei in barley coenocytes (Brown et al. 1994), and some rudimentary cell wall structures can be identified in wheat (Tian et al. 1998) implicating a suppression of complete phragmoplast development during this stage, although partial formation of these structures may help to separate the daughter nuclei. It has been shown in maize that these nuclei then continue to undergo successive rounds of mitotic cell division in the basal cytoplasm of the cell, to form a single cell with between 256 and 512 nuclei distributed around the outside of the cell (Walbot 1994). Mitotic division ceases from approximately 48 hours, marking the end of the syncytial or coenocytic stage, and this cessation period is proposed to allow microtubule development to occur to generate the cytoplasmic phragmoplasts between adjacent daughter nuclei which will be the site of anticlinal cell wall formation during the following cellularisation phase (Brown et al. 1994).

1.2.2 Endosperm development

Cellularisation begins at around 2 days after anthesis (DAA) and is defined as the formation of cells walls around each nucleus in a multinucleate cytoplasm, transforming it into a multicellular structure. This process continues until, by 4-6 DAA, the entire cavity has been filled with cells (Mares et al. 1975; Brown et al. 1996a; Sabelli and Larkins 2009). The endosperm, which is the largest tissue in the grain, consists of three cell types: the central starchy endosperm cells which comprise most of the tissue, the sub-aleurone cells which comprises 2-3 layers of cells

immediately below the aleurone and the outer aleurone layer of cells. The starchy endosperm comprises large cells packed with storage compounds, which are mobilized during germination, predominantly starch but also storage proteins (Toole et al. 2009). The aleurone layer in wheat and rice is typically a single layer of cells (but may be multi layered in some rice cultivars) that surrounds the endosperm excluding transfer cell region and contain spherosomes (or lipid bodies) and protein bodies. The growth of the aleurone layer is believed to have an effect on the growth and expansion of the endosperm, although the exact effects are still unclear (Olsen et al. 1998; Olsen 2001; Becraft and Yi 2011).

Programmed cell death (PCD) plays an important role in the development of the endosperm in both wheat and rice and it is thought to facilitate nutrient hydrolysis and uptake by the embryo at germination. PCD starts at about 10 DAA and proceeds until 30 DAA when all the endosperm cells have died except the aleurone layer which remains alive and plays a role in reserve digestion during germination (Young and Gallie 1999; Kobayashi et al. 2013).

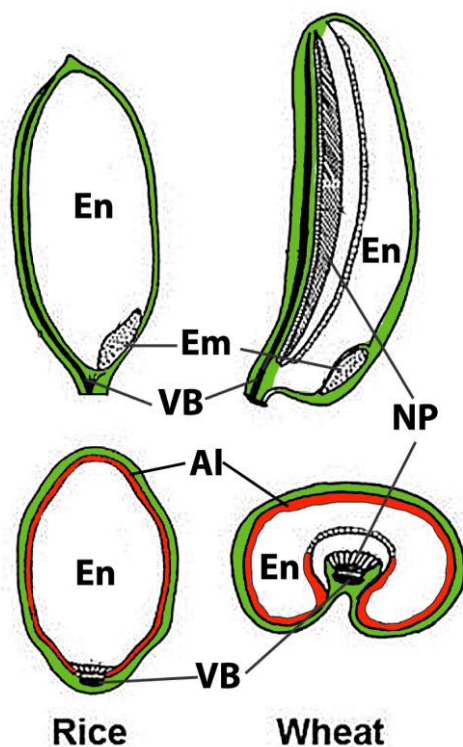


Figure 1.1 Schematic representation of the main tissue types in a Weha and rice grains. The top images represents longitudinal sections through rice (left and wheat (right), the lower images represent transverse sections. Modified from (Fincher and Burton 2014) En = endosperm, Em = embryo, NP = nucellar projection, VB = vascular bundle, Al = aleurone.

1.2.3 Embryo development

After fertilisation the embryonic cell divides in a pre-programmed sequence: - the first division always in the vertical plane to the suspensor, the second is in the vertical plane but at 90 degrees to the first and the third is in the horizontal plane at 90 degrees to both of the first two divisions. This produces 8 equally sized cells, which are known as octants. The next division of the octants produces outer cells, which will form the epidermal tissues of the embryo, and inner cells, which will form the remaining tissues of the developing embryo namely the radicle and hypocotyl regions.

The integument is a protective tissue, which appears to originate at the base of the ovule and extends to surround the entire grain. The integument cells are known to become thickened with lignin and undergo PCD in order to form the seed coat or testa, which protects the developing grain from damage later in grain development.

1.3 Differences in wheat and rice transport pathways

Despite their relatively close genetic relationship, rice (*Oryza sativa*) and wheat (*Triticum aestivum*) exhibit distinct structural differences and have different assimilate uptake pathways. In both cereals the reproductive ear (all the structures above the flag leaf) consists of a central rachis with spikelets arranged alternately at regular intervals; however, in rice the rachilla of each spikelet is extended up to a length of 3 cm, forming a panicle, whereas in wheat the rachilla is reduced down to a few millimetres, so that it is barely distinguishable from the rachis. The architecture of the vascular bundle in the stem also differs significantly between the two plants. In rice there is a distinctive ring of vascular bundles that are equally distributed throughout the parenchymal tissue. These bundles are continuous in their length, stretching from one stem node to the next. By contrast, wheat has vascular bundles that are typically much shorter in length due to the greater number of stem nodes.

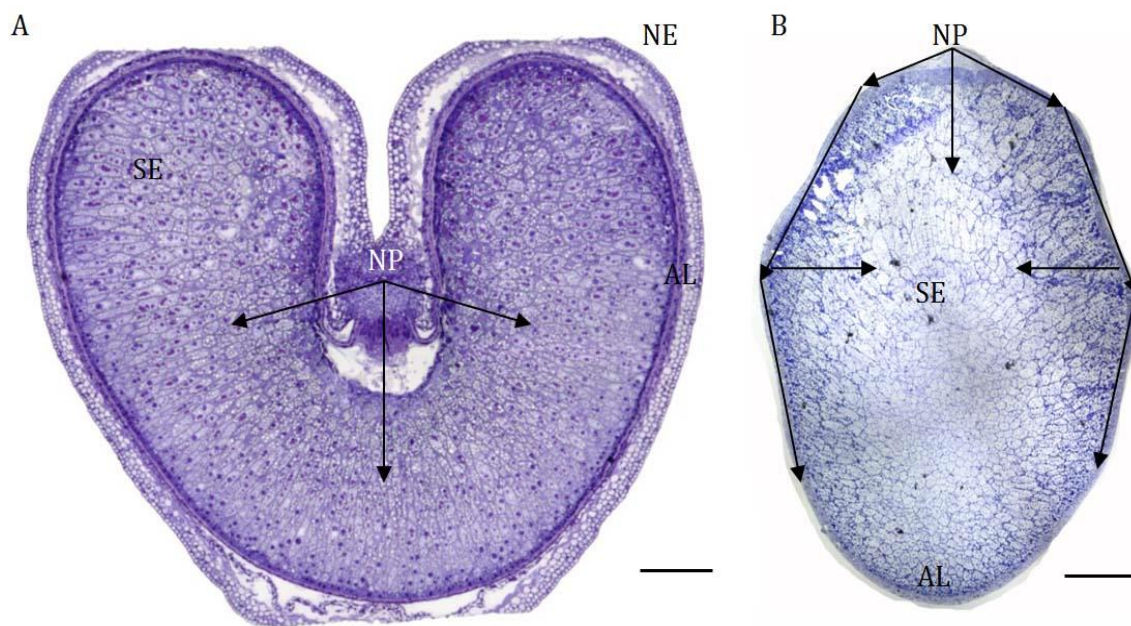


Figure 1.2 Medial transverse sections of mature wheat (A) and rice (B), stained with toluidine blue, showing the hypothesised route of nutrients flow into the developing grain.

Arrows indicate flow of assimilates. NP = nucellar projection, SE = starchy endosperm, NE = nucellar epidermis, AL = Aleurone. Scale bars = 500 μ m

Both rice and wheat have a single vascular trace to supply all assimilates to the grain. However, whereas in wheat and related cereals a crease region develops around the vascular trace, in rice the vascular trace simply lies on the dorsal side of the grain. As shown in Figure 1.1, the pathway of nutrient uptake throughout each grain, from the vascular trace to the endosperm, is different between the two cereals, as a consequence of their different anatomy (Zee and Obrien 1971b, a; Zee and Obrian 1971). In rice, the nutrients leave the vascular bundle and cross the transfer cell region, and the region that will become the pigment strand, to reach the nucellar epidermis. From here the nutrients travel circumferentially (via the apoplastic route) around the endosperm and move radially inwards across the nucellar epidermis/endosperm interface (Zee 1972a, b; Oparka and Gates 1981a, b; Oparka and Gates 1982). Plasmodesmata ensure symplastic transport between cells in the nucellar epidermis and this is also the case in the aleurone cells, but no plasmodesmata have been detected allowing transport between the two cell types (Oparka and Gates 1981b; Oparka and Gates 1982). By contrast, in wheat all assimilates are thought to be transferred into the endosperm cavity via the crease region, and to then diffuse radially through the central endosperm into the outer

endosperm and aleurone layer. This was indicated by uptake studies of fluorescein isothiocyanate (FITC), which is a small membrane-soluble aqueous dye. These studies showed that dye applied to the vascular tissue at the base of an isolated wheat grain penetrated the grain through a radial diffusion pattern from the crease region, whereas in rice the dye was seen to progress along the outside of the nucellar epidermis before some traces of fluorescence were seen in the aleurone and sub-aleurone cells, as well as radially from the vascular bundle (Wang et al. 1994; Wang and Fisher 1994).

1.4 Seed protein

Seed proteins are major storage components of both wheat and rice grains, with between 7-22% of dry weight being protein in wholegrain wheat (Vogel et al. 1978) and between 5-17% in wholegrain rice (Cagam Cagampang et al. 1966). Many types of proteins are present in cereal grains and are often classified on the basis of their solubility in different solvents, with albumins being soluble in water, globulins in dilute salt solution; prolamins in dilute alcohol, and glutenins in dilute acid or alkaline solutions, following the method developed by TB Osborne (1859-1929). However, there are often great differences in the structures and functions of the proteins in any one of these groups, so although this nomenclature survives to this day, a cereal specific classification system has been developed, based on the role of the protein within the grain (i.e. storage, structural or protective) (Shewry et al. 2001).

1.4.1 Storage proteins

Storage proteins are the most abundant type of proteins in cereal grains and are the determinants of cereal grain quality.

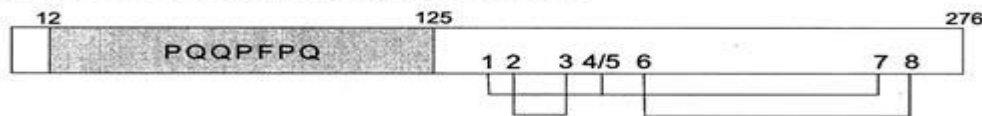
Prolamins are the major storage proteins in wheat, their name reflecting their high contents of the amino acids glutamine and proline. They have been classified based on their structural and evolutionary relationships into three groups (Shewry et al. 2001) (Figure 1.2), including their amino acid sequence and specifically the presence of cysteine residues. Sulphur-rich prolamins have typically 6 or more cysteine residues and comprise both monomeric and polymeric proteins, since they can form intra-chain and/or inter-chain disulphide bridges. Conversely, sulphur-poor prolamins typically contain no cysteine residues and thus are monomeric proteins. High molecular weight (HMW) prolamins are the largest members of the prolamins family at roughly twice the size of sulphur-rich or sulphur poor-prolamins. They

contain fewer cysteine residues than sulphur rich prolamins but are always polymeric. Wheat prolamins contain repetitive domains based on short conserved amino acid sequence motifs, which are detailed in figure 1.2.

HMW PROLAMIN: HMW Subunit (1Dx5)



S-RICH PROLAMIN: γ -type Gliadin



S-POOR PROLAMIN: ω -Gliadin

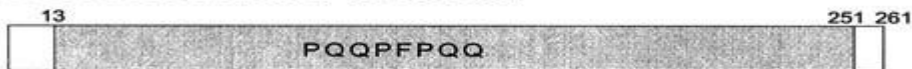


Figure 1.3. Schematic structures of typical HMW (high molecular weight), S-rich (sulphur-rich) and S-poor (sulphur-poor) prolamins (based on sequences in (Bartels et al. 1986; Anderson et al. 1989; Hsia and Anderson 2001)).

Repetitive sequences are shaded and disulphide bonds between conserved cysteine residues (1–8) in the γ -gliadin shown as lines. -SH denotes the positions of cysteine residues in the HMW prolamins taken from Shewry et al., 2001 with permission.

Prolamins differ in their spatial distribution across the endosperm of wheat with the sub-aleurone being enriched in S-rich and S-poor prolamins, whereas the central starchy endosperm is enriched in HMW-prolamins (Shewry et al. 1995; Darlington et al. 2000). Rice prolamins differ from those of wheat with no significant sequence homology, and are much smaller and lack the characteristic repetitive sequences of wheat prolamins. This suggests that rice prolamins have a different origin than the prolamins of other cereals, indicating an earlier evolutionary divergence (Okita et al. 1988; Okita et al. 1989; Xu and Messing 2008).

Globulin proteins are the major storage protein components in oats and rice, but only minor components in wheat. They are concentrated in the starchy endosperm

and have been well characterised chemically. Storage globulins are separated into two major subgroups based on their sedimentation coefficients on the Svedberg scale, and provide no known metabolic or protective function (Shewry et al. 2001). In cereals 7S globulins accumulate primarily in the aleurone and embryo, while 11-12S globulins are present in the starchy endosperm. 11-12S globulins are the major storage protein in rice, accounting for up to 70-80% of the total protein (w/w) in the starchy endosperm (Kim et al. 1993; Shewry et al. 2001). However, rice 11-12S globulins are not soluble in salt solutions and are therefore often referred to as glutelins. Rice α -globulin is a third globulin type which can account for up to 12% w/w of rice grain protein, being present in vacuolar protein bodies (Protein Body type II, PBII), typically in a protein matrix surrounding glutelin crystalloids. α -globulins have significant sequence homology to wheat prolamins (Bechtel and Juliano 1980; Kawagoe et al. 2005).

Gluten is a proteinaceous complex that confers characteristic viscoelastic properties to wheat doughs, and is formed from wheat prolamins: the monomeric gliadins (alcohol-soluble) and polymeric glutenins (dilute alkali and acid-soluble). The synthesis of gluten proteins starts within a few days (6-8 DAA) after anthesis, and deposition increases steadily throughout the grain filling stage. Gluten proteins are synthesised on the ribosomes of the rough endoplasmic reticulum, and there are thought to be two trafficking pathways for gluten proteins in wheat involving either transport to the vacuole via the Golgi apparatus or accumulation within the lumen of the ER to form protein bodies that are subsequently internalised into vacuoles by a process analogous to autophagy. It has also been suggested that the same individual protein could be trafficked by either pathway, possibly depending on the stage of development, and that segregation in the deposition of gluten proteins may occur, both between and within protein bodies (Tosi et al. 2009; Tosi et al. 2011). Monomeric gliadins account for between 30-40% of the total grain protein, and are classified into three groups (α -, γ - and ω -) on the basis of their sequences. The α - and γ -gliadins are sulphur-rich prolamins while ω -gliadins are sulphur-poor prolamins. The polymeric glutenins comprise subunits, which are classified into two groups based on their molecular weights (Dupont and Altenbach 2003). The low molecular weight glutenin subunits (LMW-GS) represents 20-30% of all wheat grain proteins (Gupta et al. 1992). They are S-rich prolamins, are approximately 40 kDa in size and have been shown to resemble γ -gliadins in sequence (Muller et al. 1998). The high molecular weight glutenin subunits (HMW-GS) are ~90 kDa in size and

account for only 5% of total protein. HMW-GS proteins have been suggested to form the main backbone of gluten polymers (Shewry et al. 2001; Shewry et al. 2009).

Storage proteins in cereal grains deposited in protein bodies; in both wheat and rice at least two types of protein bodies have been reported. In wheat PB-I (protein bodies type I) are derived directly from the endoplasmic reticulum and are enriched in high molecular weight glutenin subunits (HMW-GS)(Rubin et al. 1992) whereas PB-II are vacuolar aggregations of protein and are enriched in gliadins. In rice, at least two types of protein body have been reported based upon their characteristic staining pattern with osmium tetroxide when examined with TEM (transmission electron microscopy) (Mitsuda et al. 1967). PB-I are small spherical protein bodies with a maximum size of 3 μm , they are prolamin-rich and have a lamellar structure under TEM visualisation. PB-II are roughly 4 μm in diameter and are not lamellar in structure, they are more abundant in the central endosperm tissue of rice grains and are highly enriched in glutelin and globulin (Tanaka et al. 1980). Most protein is found in the outer 7% by mass of the rice grain (sub-aleurone cells), which contain equal proportions of PB-I and PB-II (Ohdaira et al. 2011). In both rice and wheat protein deposition occurs slightly later than starch granule deposition, with protein bodies first becoming evident at 6-7 DAA in rice and 8-10 DAA in wheat (Harris and Juliano 1977; Ugalde and Jenner 1990). Despite both species containing two types of protein bodies and similar levels of protein per grain, the composition of the storage protein differs between the two species. In wheat prolamins represent the primary storage protein type, with only low amount of glutelin being present, conversely in rice prolamin are minor components (less than 5% of the total) whilst glutelins represent more than 80% of the rice grain storage protein (Palmiano et al. 1968). There are 3 classes of prolamins in rice separated by their molecular weight, 10 kd, 13 kd, 16 kd, the 13 kd sub class is the most prominent and can be further sub-divided into slightly larger 13a and slightly smaller 13b categories (Ogawa et al. 1987). These 3 prolamin classes have only been identified in PB-I (Yamagata et al. 1982). In addition to spatial segregation of storage proteins within protein bodies, spatial differences in the distributions of these protein bodies in the wheat and rice grain can be observed. (Tosi et al. 2009; Tosi et al. 2011) studied storage protein localisation using well-characterised monoclonal antibodies for specific storage protein subunits, and reported that HMW-GS were more abundant in the central regions of the wheat grain endosperm whereas gliadins and LMW-GS were more abundant in the sub-aleurone cells. However, it was noted that even within the gliadin subfamily additional spatial gradients were observed, with γ -gliadins showing

a similar spatial distribution to HMW-GS in the central endosperm region, rather than co-localising with the more closely related α - and ω -gliadins, which were more abundant in the outer endosperm regions. Similar experiments have been conducted in rice grains by Furakawa (2003) who showed that there appeared to be little spatial segregation of 13 kD prolamins, glutelins and gliadins in wild type rice grains with all storage proteins appearing to be evenly distributed throughout the endosperm. However in low glutelin cultivars 13 kD prolamins were found to be more prevalent in the outer regions of the endosperm.

1.5 Starch

1.5.1 Starch composition

Starch is widespread in higher plants where it functions as a carbohydrate storage medium. Typically two sites for starch accumulation are found in monocots: in leaf tissues, where starch represents a transient (short term) carbohydrate storage for product of photosynthesis during daylight hours that can be subsequently digested during the dark night period; and in seeds, which represent a long-term form of starch storage, for use during seed germination. Starch is deposited in the form of granules, which form in plastids referred to as amyloplasts (Tetlow 2011). Starches are the most abundant components of cereal grains, accounting for about 70% of dry weight in wheat grains (Dale and Housley 1986) and up to 88% in rice grains (Juliano 1985b). Starch is suited to being a storage compound as it is chemically inert and water insoluble, allowing for large amounts to be stored without affecting the solute potential within the cell (Tetlow 2011). In most cereals the highest rate of starch deposition is from ~10 DAA until maturity (Bewley and Black 1994), however amyloplasts have been seen to start filling with starch granules almost immediately after cellularisation has completed (Yin et al. 2012). Structurally starch is formed from α -(1-4)-linked glucose polymer chains with branching at α -(1-6)- positions. There are two main types of these glucose polymers in starch: amylose, which is a largely unbranched α -(1-4)-linked chain and typically represent less than 25% of the starch granule, and amylopectin, which is the major component of starch, representing 80-90% of the granule and has α -(1-6)- branches. Typically branching occurs about every 20 residues in amylopectin and is likely to facilitate crosslinking adjacent linear chains to create a larger macromolecular structure through hydrogen bonding between adjacent molecules. At present there are several proposed models for starch granule structure, with the cluster model being the most commonly

favoured. In the cluster model it is proposed that relatively short linear amylopectin chains associate via hydrogen bonding to form parallel left handed double helices, which then in turn pack together into an array to form the lamellae, which are ~9 nm long semi-crystalline regions separated by amorphous regions (Robin 1974; French 1984; Hizukuri 1986; Gallant et al. 1997; Myers et al. 2000) (Fig 1.3). It is proposed that these amorphous layers are composed of amylose chains, producing the growth ring structure evident in starch granules, which is highly conserved in higher plants (Kainuma and Preiss 1988; Zeeman et al. 2002), and is particularly clear in potato starch (Gallant et al. 1997). Bertoft (1986) observed that targeted degradation of cereal starches with enzymatic treatments, released short glucose chains of a length and frequency consistent with the cluster model. The presence of amylose in the amorphous layers is still much debated, but it is suggested that the amylose chains provide easy access points for enzymatic degradation, as starches must be degradable to be a useful storage compound (Fannon et al. 1992; Huber and BeMiller 1997).

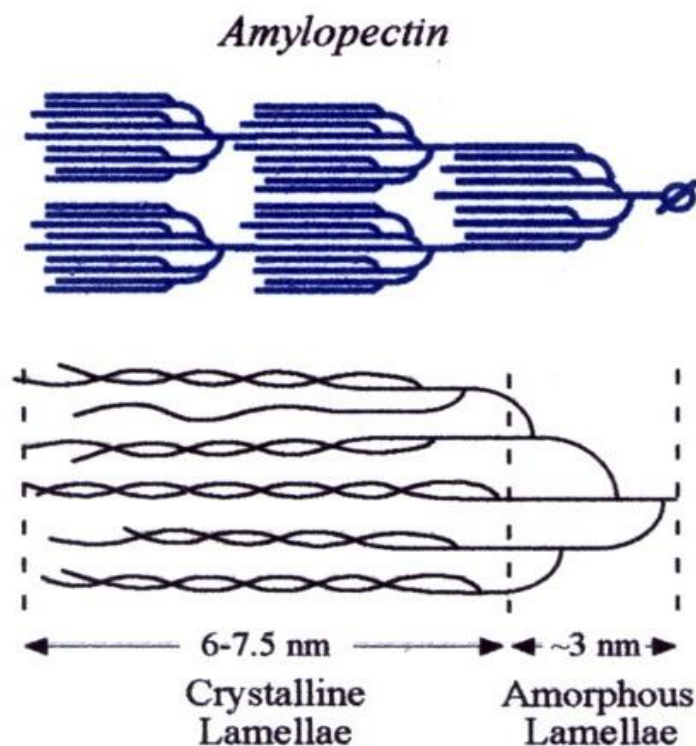


Figure 1.4. Schematic representation of amylopectin structure according to the “Cluster” model, modified from Nakamura et al 2002.

Wheat grain starch granules exist in two types (Kim and Huber 2008), the lenticular A type which are roughly 15-35 μm in size (Meredith 1981) and the smaller spherical

B type which are between 2 and 10 μm (Chiotelli and Le Meste 2002), conversely only one type is present in rice, a polyhedral granule which can be between 2 and 8 μm . The polyhedral structure of the rice starch granule allows the formation of compound starch granules where multiple single granules associate to form large complexes up to 150 μm in diameter. This compound starch is not limited to rice grains but is also found in oat grain starch, but suggests a significantly different granular microstructure to that of wheat and other cereal grains despite very similar levels of amylose and amylopectin (Tester et al. 2004). Asaoka et al (1985b) report that the deposition of both amylose and amylopectin in rice are detectable from immediately after cellularisation (5 DAA) and increases steadily until about 18-20 DAA at which point the starch deposition plateaus. Rice grain starch deposition is reported to be temperature sensitive, with high temperatures during grain development inducing a decrease in amylose content with the starch granules producing a waxy type phenotype with increased crystallinity and brittleness of the starch granules (Asaoka et al. 1985a). In wheat the two types of starch granules appear to have different deposition kinetics implicating differential genetic regulation of starch biosynthesis. A type granules are deposited from 4-15 DAA according to Peng et al. (2000), whereas B type granules only begin to accumulate from 15 DAA onwards (Darlington et al. 2000). Despite this differential accumulation of starch granule types, no differences in the protein sequences extracted from isolated A and B type granules have been observed (Ko et al. 2009). In addition to the temporal differences in starch granule accumulation there are clear compositional differences. A type granules contain about 80-85% amylopectin and 12-18% amylose, whilst B type granules contain a lower amylopectin content at 50-70% and higher amylose content at 25-46% with B type granules displaying larger variation in composition across four cultivars than A type granules (Yin et al. 2012). Jing et al. (2013) have recently reported that both amyloplasts and protein bodies are able to enlarge in wheat endosperm cells that have undergone PCD.

1.6 Cell wall components

Plant cell walls are composites of polymer chains mainly derived from monosaccharides and phenolics, with cellulose and lignin as the fibrous components alongside sets of matrix polysaccharides. These matrix polysaccharides include glucans, heteroxylans, heteromannans (often together referred to as hemicelluloses) and pectic polysaccharides, which are often present in supramolecules containing a range of pectic domains (Burton et al. 2010). The cell walls of the Poaceae species, which include both wheat and rice, exhibit a clear

separation in the composition of their cell walls from all other plant species (with exception of the *Equisetum* genus), in the presence of mixed-linkage β -glucan (MLG) (Sørensen et al. 2008). Monocots also display much lower contents of xyloglucan and pectin and higher levels of MLG and arabinoxylan in the primary cell walls of typical vegetative tissues when compared to the model dicot *Arabidopsis thaliana* (Vogel 2008). The secondary cell walls of monocots also display higher Arabinoxylan (AX) levels than *Arabidopsis* but they also show higher levels of lignin and slightly less cellulose, although the differences are much less pronounced than in the primary cell walls. The endosperm cell walls of the grasses appear to consist only of primary cell walls and typically have low levels of cellulose, lignin, xyloglucan and pectins and high contents of AX and MLG relative to the cell walls of non-graminaceous plants. Although the relative amount of AX and MLG can vary substantially between cereal species and different grain tissues. Thus, AX comprises ~20% total cell wall polysaccharides of the starchy endosperm in barley, 25% in rice and 70% in wheat while MLG accounts for over 70% in barley and ~20% in the other two species. However, rice has significantly higher levels of cellulose (23% compared with 2% in wheat and 3-4% in barley) and about 27% pectin, which is not significant in wheat or barley grain (Mares and Stone 1973b; Bacic and Stone 1980; Shibuya et al. 1983; Shibuya and Nakane 1984; Shibuya et al. 1985; Shibuya 1989). Wheat endosperm cell walls also contain ~7% glucomannan (Mares and Stone 1973b) compared to 3-4% in barley while the presence of low levels of xyloglucan has been shown by immunolabelling in both these cereals (Wilson et al. 2012; Pellny et al. 2012).

1.6.1 Arabinoxylan (AX)

Cereal xylans are predominantly formed of AX and GUX (glucuronoxylan) representing around 20% of primary cell wall composition in vegetative tissues and up to 70% of wheat endosperm cell wall, and are often the most prevalent hemicellulosic components of the primary cell wall.

AX has a backbone of β -1-4 linked xylose residues that can be mono-substituted with arabinofuranose residues at the O-3 or di-substituted at the O-2 and O-3 positions which are common feature of grass AX (Ebringerová et al. 2005). On the contrary, GUX contains arabinofuranose substituted xylan with the additional substitutions of glucuronic acid or 4-O-methyl glucuronic acid substitutions (Hao and Mohnen 2014). The level of glucuronic acid substitutions in GUX is known to vary

significantly with the endosperm tissues of cereals, often displaying very low levels of GlcA substitution relative to the vegetative tissues (Burton and Fincher 2012).

FT-IR spectroscopic analyses have shown that the degree of substitution differs between developmental stages and between cells at different positions within the endosperm (Toole et al. 2010). The variation in substitution level between mono- and di-substituted AX is thought to regulate the hydration status of the cell wall, affecting its flexibility and potentially the nutrient transfer rate (Toole et al. 2011).

The AX of grasses are typically esterified with ferulic acid at the 5 position of arabinose residues and this is thought to provide extra structural strength in the cell wall matrix through the ability to form ether linkages between ferulic acid residues present on adjacent AX chains (Piot et al. 2001).

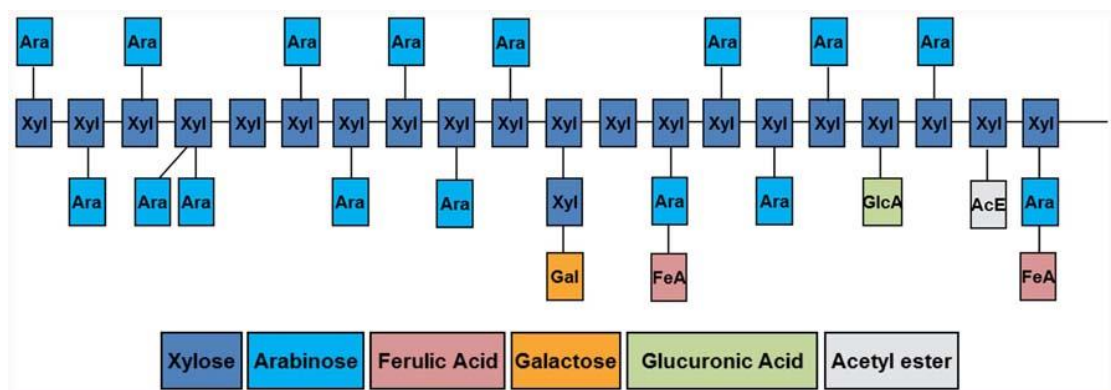


Figure 1.5. A schematic representation of glucuronoxylan and its potential monosaccharide substitutions. Modified from Burton et al. (2010b) Ara = arabinose; Xyl = xylose; Gal = galactose; GlcA = glucuronic acid; FeA = ferulic acid, AcE = acetyl ester.

A recent study by Busse- Wicher et al. (2014) has shown that AX may interact with cellulose microfibrils, and in particular the level of substitution with arabinose or acetylation may regulate the ability of the AX molecule to form these interactions. One current hypothesis is that these interactions can prevent crystalline aggregation of cellulose. AXs are thought to play a key role in regulating cell wall strength especially in the primary cell walls of cereal endosperms where they are one of the most prevalent polysaccharides. Much has been learnt about the biosynthesis of AX, predominantly due to the *irx* (irregular xylem) mutants, as xylem vessels are heavily enriched with xylan polymers. Xylan chain biosynthesis appears to be regulated by 3 genes, IRX9, 10 and 14, which may act together as part of a complex. IRX9 and 14 are members of the GT43 family of glycosyl transferases,

and IRX 10 is a member of GT47 family (Lovegrove et al. 2013). They were first identified as mutations in Arabidopsis with all 3 mutants showing decreases in xylan content and a reduction in average xylan chain length, but without any modification or loss of the xylan reducing end sequence (XRES)(Brown et al. 2007; Peña et al. 2007; Brown et al. 2009; Wu et al. 2009). An IRX10 rice mutant was shown to have a modest decrease in xylan content (~10%) but increased potential for the cell wall to be saccharified or digested into its constituent monosaccharides (Chen et al. 2012b). Whereas IRX9 and 14 overexpression lines in tobacco cell culture lines showed induced xylan xylosyl transferase activity (Lee et al. 2012). Together these data suggest that these 3 genes are non-redundant in Arabidopsis and likely to be involved in the xylan biosynthetic pathway. Anders et al. (2012) have shown that TaXat1 a member of the GT61 family is responsible for most of the monosubstituted arabinose residues on xylan chains in all grasses. However at least 2 other arabinosyl transferases are postulated to be required to generate the O-2, O-3 disubstituted xylan residues, and are yet to be identified. The glucuronic substitutions present in GUX, have been identified as being regulated by GUX1 and GUX2 in Arabidopsis stem, where mutant lines were devoid of the glucuronosyl substitution. GUX1 decorates the xylan backbone at even number xylan locations between 6 and at least 26 residues apart, whereas GUX2 produces more tightly clustered substitutions usually on 5, 6, or 7 units between each substitution (Mortimer et al. 2010; Anders et al. 2012; Bromley et al. 2013).

Due to the identification of many of the xylan biosynthetic components as being located in the Golgi apparatus, it is presumed that all AX synthesis takes place here. However several key questions remain to be answered about the first steps of AX biosynthesis, as it is unclear whether AX synthesis is initiated from a precursor molecule, or whether it is de-novo synthesis with subsequent residues being added at the reducing end. AX synthesis is thought to terminate with a terminal reducing end sequence referred to as XRES (β -D-Xylp-(1-3)- α -L-Rhap-(1-2)- α -D-Galp-(1-4)-D-Xylp.) acting as a signalling molecule for termination of the chain length (Peña et al. 2007).

Phenolic acid residues can also be incorporated into the AX of both monocots and dicots (Ishii 1997b) with ferulic acid and p-coumaric being the most prevalent phenolic components of grass AX. Ferulic acid is thought to be incorporated by feruloyl-CoA transferases encoded by the BAHD gene family, however this remains to be proven (Obel et al. 2003; Pellny et al. 2012). This ferulate ester is attached to

the O-5 position of an L-arabinosyl residue of AX by an ester bond in the Graminae and has been shown to be involved in tissue cohesion, restricting cell expansion and modifying the mechanical properties of cell walls in mature tissues (Tan et al. 1991; Tan et al. 1992; Iiyama et al. 1994; Piber and Koehler 2005). Ferulic acid residues on adjacent AX chains are able to undergo oxidative crosslinking via a peroxidase to form either dimeric or trimeric complexes stabilised by ether bonds, which have been detected *in vivo* (Ralph et al. 1994; Bunzel et al. 2001; Bunzel et al. 2003; Rouau et al. 2003; Funk et al. 2005). Whilst the degree of feruloylation has been identified as being at the basis of AX gel properties *in vitro*, supporting the crosslinking model (Carvajal-Millan et al. 2005).

1.6.2 Mixed-linkage β Glucan (MLG)

Mixed-linkage glucan was thought to be a unique component of the cell walls of the grasses (Buckeridge et al. 2004), however it was recently confirmed that it is also a polysaccharide in fern cell walls (Xue and Fry 2012).

Structurally, mixed linkage β -glucan has been identified as an unbranched and unsubstituted chain of β -glucopyranosyl residues attached by 1-4 linkages, and interspersed with 1-3 linkages at regular intervals along the chain length. Utilising an endo-(1-3)(1-4)- β -glucanase which cleaves proximally to 1-3 linkages it has been shown that mainly trisaccharides or tetrasaccharides are released (Staudte et al. 1983; Woodward et al. 1983a; Woodward et al. 1983b, 1988) (Fig 1.5). However a small fraction of the MLG chain (~10%) is thought to consist of 4 or more contiguous 1-4 linked residues (Böhm and Kulicke 1999), with no contiguous 1-3 linked residues (Lazaridou et al. 2004). The 1-3 linkages have been shown to introduce a kink into the linear chain length, which is thought to induce the increased flexibility and solubility in the molecule through the disruption of hydrogen bonding which generate the aggregation of 1-4 linked glucose in cellulose chains (Kiemle et al. 2014).

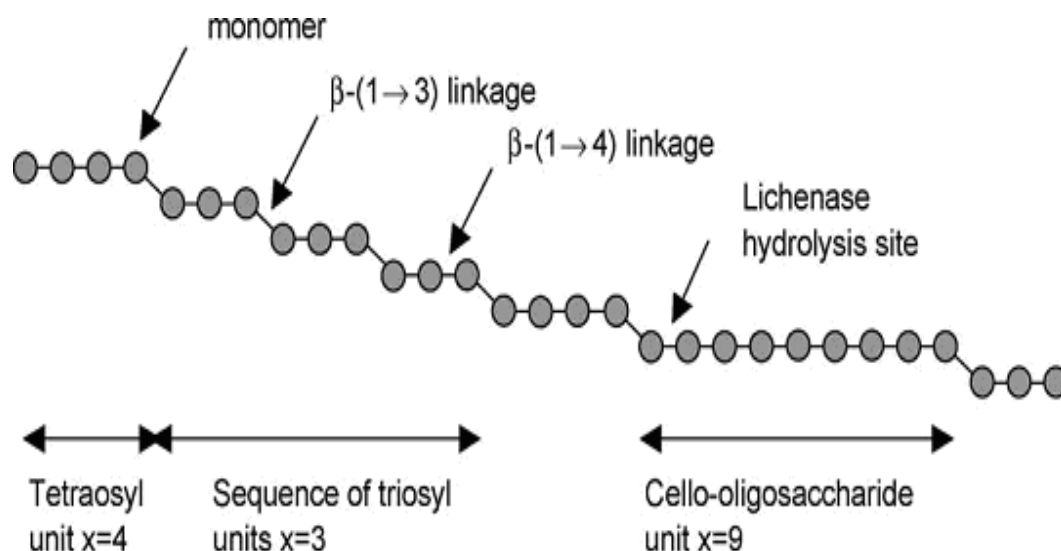


Figure 1.6. Schematic representation of MLG structure with a mixture of DP3 and DP4 glucose chains between each 1-3 linkage. Modified from (Tosh et al. 2004)

MLG is abundant in the endosperm and aleurone tissues of oats, barley, wheat and rice, making up between 20 and 80% of the cell wall material in these tissues.

Although the function of MLG has yet to be established, on the basis of its solubility it has been postulated that it could represent a storage carbohydrate (Buckeridge et al. 2004; Wilson et al. 2006), and may act as an energy source for the germinating embryo (Roulin et al. 2002). However MLG has also been shown to be associated with both cellulose and AX *in muro* (Carpita 1984), and it may act to coat cellulose microfibrils in the same way as xyloglucan (Carpita et al. 2001).

MLG has been shown to be assembled at the Golgi membrane (Urbanowicz et al. 2004), with the current model describing at least a dimeric enzyme complex where even numbered units are synthesised by one enzyme and odd numbered units by another (Buckeridge et al. 2001; Buckeridge et al. 2004). Cellulose synthase-like (CSL) enzymes are thought to be responsible for MLG biosynthesis with the CSLF and CSLH families being specific to the grasses (Hazen et al. 2002). Heterologous expression of CSLF from rice in *Arabidopsis* has shown that CSLF alone is capable of producing MLG (Burton 2006), but that co-expression of CSLF and CSLH resulted in larger amounts of MLG synthesis (Doblin et al. 2009). *In vitro* synthesis experiments with intact Golgi membranes and UDP-glucose have also shown that, depending upon the quantity of substrate provided, the MLG product generated contained either odd or even numbered residues. (Carpita and Gibeau 1993; Buckeridge et al. 1999, 2001; Urbanowicz et al. 2004).

In general, grass MLG contains single 1-3- β -glucan linkages interspersed by sections of three and four glucan molecules connected with 1-4- β -glucan linkages (Burton and Fincher 2009) although continuous stretches of up to fourteen 1-4 linkages being reported in wheat bran although these are a minor components (Cui et al. 2000) (Fig 1.5). The ratio and distribution of these two types of linkages may have profound effects on the structural characteristics, including the ability to form inter-chain interactions (Lazaridou and Biliaderis 2007).

1.6.3 Heteromannans

The unifying feature of all heteromannans is the presence of a β -1-4 linked mannosyl backbone, which is typically acetylated (Scheller and Ulvskov 2010). Glucomannans and galactomannans contain both mannosyl and glucosyl residues in their backbone in a random pattern, and can subsequently be substituted with α -1-6 galactosyl residues on the mannose residues which generates galactomannans or galactoglucomannans (which contain additional glucosyl substitutions on the backbone) (Reid 1997). Heteromannans are synthesised by enzymes encoded by the CSLA gene family; genes from this family encode mannan synthases, which are bifunctional, adding either GDP-mannose or GDP-glucose (Dhugga et al. 2004; Liepman et al. 2005). Yin et al. (2009) reports that CSLD proteins may be galactosyl transferases for mannan, in addition to the GT34 family galactosyl transferase described in fenugreek (Edwards et al. 1999). Analysis of mannan in ivory nut and coconut shows mannan with a very low degree of substitution, which also confers very high insolubility. This, together with the observation of a mannosidase deficient mutant in coconut which possessed a highly substituted galactomannan (Mujer et al. 1984), have led to a model in which mannan are synthesised with galactosyl substitutions, which are known to increase the solubility of the molecule, and subsequently cleaved of their galactosyl residues (Scheller and Ulvskov 2010).

Galactomannans have long been associated with seed development as a carbohydrate storage compound as a cell wall polysaccharide, which is often digested during germination (Mujer et al. 1984; DeMason et al. 1985; Spyropoulos and Reid 1985; Dhugga et al. 2004), but have also been connected with roles in cell signalling, embryogenesis and vascular cell differentiation (Beňová-Kákošová et al. 2006; Liepman et al. 2007; Moreira 2008; Goubet et al. 2009).

1.6.4 Callose

Callose (1,3- β -glucan) has also been demonstrated to be an essential component of the first anticlinal cell wall extensions during cellularisation (Morrison and O'Brien 1976; Fineran et al. 1982; Brown et al. 1997; Wilson et al. 2006) and early cell wall development (cell plate deposition) in wheat, rice, barley and other species (Stone and Clarke 1992; Samuels et al. 1995; Brown et al. 1997; Verma and Hong 2001) where it appears as a transient polysaccharide during cellularisation. Callose is associated with wound healing in many plant species, through rapid production of callose plugs (Verma and Hong 2001). Plasmodesmata also contain a high degree of callose content, and can often be identified in tissue samples through the use of aniline blue staining, which binds to callose and is fluorescent under UV light allowing easy visualisation (Radford et al. 1998).

1.6.5 Pectic polysaccharides

As already mentioned, pectins are very minor components of endosperm cell wall of wheat and barley but substantial components of cell wall polysaccharides in rice endosperm. Pectic polysaccharides are defined as containing galacturonic acid (GalA) residues which are typically 4-linked and can be classified into three main types: homogalacturonan (HG), rhamnogalacturonan-I (RG-I), and rhamnogalacturonan-II (RG-II) (Fig 1.6); although minor fractions of xylogalacturonan and apiogalacturonan also exist, but are not found in cereals. These three types of pectin are important polymers of the cell wall matrix (Caffall and Mohnen 2009) and are proposed to be covalently linked to one another to form a large molecular complex, the structures of which are still poorly understood.

Pectin content varies dramatically depending upon the tissue examined and the species studied. In *Arabidopsis* for example, leaf cell walls pectin accounts for 50% (w/w) of the cell wall (Zabackis et al. 1995) while in wheat endosperm tissue so little pectin is present it has only been detected through the use of monoclonal antibodies (Chateigner-Boutin et al. 2014) and through the presence of GAUT transcripts (Pellny et al. 2012). The ratios of the major pectic components can vary but typically values of 65-70% HG, ~20% RG-I and ~10% RG-II have been reported (Mohnen 2008). These individual molecules are not currently thought of as individual elements, but as covalently linked polymers, which form discrete domains within a larger pectic structure (Fig 1.6) (Caffall and Mohnen 2009; Burton et al. 2010a).

Significant functions have been attributed to pectin molecules, which appear to be essential for cell expansion and contribute to cell-to-cell adhesion in the middle

lamella (Willats et al. 2001a; Øbro et al. 2004; Ogawa et al. 2009).

Homogalacturonan molecules are capable of dimerization through Ca^{2+} binding and egg box motifs, which would assist cell to cell adhesion but would also modify the flexibility of the wall structure. Egg box motifs are so called because the two adjacent HG chains form zig zag structures with every second galacturonic acid molecule in the chain ionically bonding to the adjacent chain via a Ca^{2+} ion; these adjacent zig zag structures look like the insides of egg boxes. Primary cell walls often contain significant proportions of pectic molecules and these are thought to be able to support growth through the modification of cell wall flexibility and hydration level. (Macquet et al. 2007; Moore et al. 2008a). Significant evidence is also building for short pectic oligosaccharides to act as signalling molecules with implications in plant development and growth (Ridley et al. 2001; D'Ovidio et al. 2004; Savatin et al. 2011).

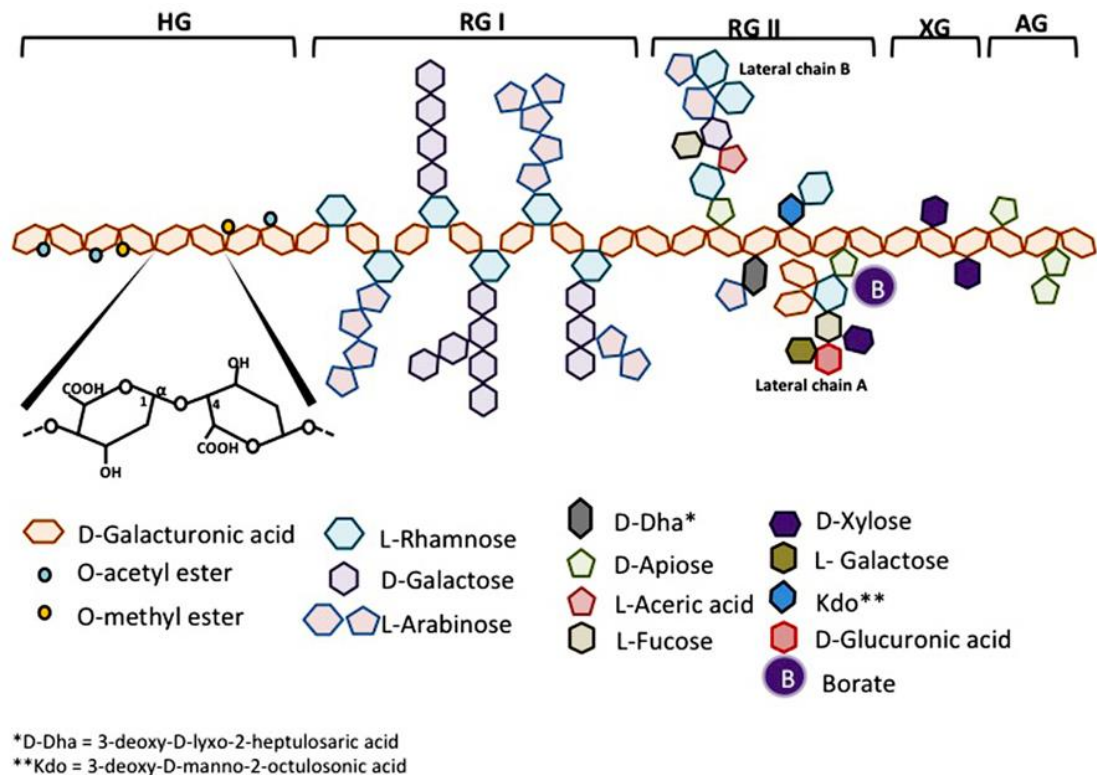


Figure 1.7. Schematic representation of the components of the pectic molecular complex. Modified from Leclere et al. (2013)

1.6.5.1 Homogalacturonan

Homogalacturonan is a homopolymer of D-GalA linked by α -1,4 linkages which may be acetylated on O-2 and O-3 positions and is typically partially methyl esterified on O-6 positions. It is the most prevalent pectic polysaccharide, usually representing

60-80% of the total pectic fraction within a cell wall (Mohnen 2008). HG is synthesised in a methyl-esterified format and then is modified *in muro* through pectin methyl-esterases to modulate the methyl-esterification level of the HG within the wall, however to date no method for methyl-esterifying HG *in muro* has been identified. The degree of methyl esterification is thought to influence the ability of HG to perform intermolecular interactions. It is known that adjacent HG molecules can interact through the egg box motifs and Ca²⁺ ion bridges but the available data suggests that in order for these egg box motifs to form, the stretch of HG must not be methyl-esterified (Caffall and Mohnen 2009; Wolf et al. 2009; Peaucelle et al. 2012). As these sections with ion bridges are thought to provide extra stiffness and stability to the pectic matrix within the cell wall it is hypothesised that methyl esterification is a method for introducing plasticity into the wall and possibly to allow extensibility in cell elongation, as it has been noted that root extension zones label strongly with a monoclonal antibody directed to unmethyl-esterified sections of HG (JIM5) unlike the walls of adjacent cells, which only label with methyl esterified HG specific antibodies (Knox et al. 1990).

1.6.5.2 Rhamnogalacturonan-I (RG-I)

RG-I structure is known to exhibit extensive variation in both the length of the backbone chain, the degree of side chain substitution and the length of the attached sidechains. Thus further understanding of the fine details of its structure and how its variation affects its role *in muro* is a key aim of plant cell wall biology.

RG-I consists of a long backbone molecule made of a homodimer of [-2)- α -L-Rhap-(1-4)- α -D-GalpA-(1] and can contain more than 100 of these subunit in sequence (McNeil et al. 1980) which may be acetylated at the O-2 and O-3 positions of the galacturonic acid residues (Ishii 1997a). This alternating backbone typically contains sidechains of arabinan, galactan or arabinogalactan (AG-I or AG-II) extending from the O-4 position of rhamnose residues (Carpita and Gibeaut 1993), although many other neutral sugar moieties have been recorded as contributing to RG-I structure, with over 30 different oligoglycosyl sidechains being reported to date (Voragen et al. 1995). In rare cases, such as for the pectic mucilage of *A. thaliana* (Penfield et al. 2001) RG-I has been reported to contain few to no side chains. About half of the α -L-rhap residues are substituted with neutral sugar sidechains (dp ~6-7), however this figure varies dramatically depending upon species and tissue examined (Darvill et al. 1985; Lau et al. 1987). These side chains may not be randomly distributed

throughout the RG-I backbone as analysis using endogalactanase and endoarabinanase enzymes to remove particular sidechains, implicates a clustering of sidechains (Sørensen et al. 2000; Skjøt et al. 2002; Vincken et al. 2003). These galactan and arabinan side chains are thought to be orientated in both directions from the backbone in a random pattern rather than being sterically regulated. Arabinan side chains consist of a linear 1-5 linked chain (Nakamura et al. 2001), which may be substituted at O-2 or O-3 positions with 1-3 linked α -L-Araf residues or short oligosaccharide chains (Carpita and Gibeaut 1993). Highly arabinosylated RG-I have been detected in resurrection plants and sugar beet pulp, and have been hypothesised to be related to increasing cell wall plasticity by increasing hydration potential of the cell wall via inhibition of the formation of egg box motifs between adjacent HG regions (Moore et al. 2008b). Galactan side chains are linear chains of 1-4 β -D-Galp residues and have been shown to correlate with fast growing and expanding cell walls in several different species, including Arabidopsis root meristem (McCartney et al. 2003) and carrot root-cap apices (Willats et al. 1999), although these side chains are also reported to be abundant in potato tubers, cucumber mesocarp, sycamore cells, soy bean cotyledons, leek, onion and garlic bulbs (Yapo 2011). Arabinogalactan side chains may be present in two forms, the simpler, more prevalent AG-I and the more heavily branched AG-II. AG-I is highly abundant in sugar beet tubers and leek stems (Yapo 2011) and consists of linear 1-4 β -D-Galp chains, which have single residue 1-2 or 1-3 linked α -L-Araf substitutions. The more varied AG-II contains the same 1-4 linked galactan backbone, but is substituted by short chains of 1-6 β -D-Galp, which may be up to 3 residues in length. Additionally these 1-6 linked galactan residues are also substituted at either O-3, O-4 or O-6 positions or are 1-3/1-5 linked α -L-Araf residues (McCartney et al. 2000). This extremely variable structure is thought to be covalently linked to the RG-I backbone, due to co-extraction and difficulty separating the two. However this is yet unproved, and as this heterogeneous structure is homologous to that of AGPs it may be the result of a multi-component complex (Oosterveld et al. 2002; Immerzeel et al. 2006; Yapo 2011).

The extremely heterogeneous structure of RG-I makes the study and characterisation of this cell wall polysaccharide very difficult, with many questions still remaining to be answered about both the structure and function of this molecule. Several studies have reported correlations between RG-I and certain biological functions ranging from cell wall firmness/elasticity to cell wall elongation and cell division. Study RG-I is of key interest to the fruit industry as depolymerisation of the

RG-I side chains have been linked to key phases in the maturation of apples, strawberries, tomatoes and many other fruits (Gross and Sams 1984; Redgwell et al. 1997; Peña and Carpita 2004; Molina-Hidalgo et al. 2013; Ng et al. 2015). This loss of arabinan and galactan side-chains appears to result in a reduction in fruit firmness, which is hypothesised by Brummell (2006) to occur through increased accessibility to HG for pectate lyase. Pea cotyledons have direct correlations between the appearance of 1-4 link galactan and the modification of the material properties of the cell layers. The galactan enriched cell layers in this legume showed a doubling of the compressive firmness compared to the same cell layers before the detection of galactan (McCartney and Knox 2002). While there are no definitive models for how these RG-I side chains influence mechanical and biological changes in the cell wall, it is hypothesised that arabinan is associated with cell wall plasticity and hydration state modulation, whilst galactan is thought to be involved with cell wall stiffness and elongation. McCartney et al. (2003) have shown that Arabidopsis root meristems only contain galactan in the elongation zone, whereas when the roots were grown on auxin medium, which will inhibit root elongation, the galactan epitope labelling was severely reduced in immunolabelling experiments. This observation of galactan association with cell elongation does not agree well with other reports of galactan side-chains being involved with cell stiffness, leading to the conclusion that other factors such as chain length and ramification may provide additional modulation to the structural properties rather than just the neutral sugar involved.

Arabinan sidechains are involved in regulating the cell walls of stomatal guard cells in order to produce the cell shape change necessary to open and close the stomata. Through experiments using fusicoccin (a chemical inducer of stomatal opening) Jones et al. (2003) were able to show that use of an arabinanase treatment prevented the stomata of epidermal cells from opening upon application of fusicoccin, and that conversely a pre-treatment of the epidermal tissue with LM6 (a 1-5 arabinan specific mAb) allowed for stomatal opening upon fusicoccin application. It was also noted that the double treatment of pectin methylesterase and arabinanase had a higher efficacy in preventing stomatal opening, which implicates interaction of RG-I arabinan with unmethylesterified HG. Jones et al. (2003) hypothesise that the arabinan may provide steric interference between unmethylesterified chain sections preventing the formation of Ca²⁺ cross-linked egg box motifs, which are known to increase cell wall stiffness. This is supported by the work of Renard and Jarvis (1999) who proposed arabinan side-chains as cell wall

plasticizers, and by the work of Moore et al. (2008a) who also suggest arabinan side chains as plasticizers of resurrection plant cell walls in periods of severe dehydration.

The potential for RG-I sidechains to interact with other cell wall polysaccharides is still unclear despite several nuclear magnetic resonance (NMR) studies demonstrating clearly that within the apoplastic space arabinan and galactan side-chains are highly mobile (Fenwick et al. 1999; Ha et al. 2005; Zykwiniska et al. 2006). Evidence for the interaction of RG-I extracted from sugar beet and potato tubers and cellulose exists *in vitro* (Zykwiniska et al. 2005), but may be a result of the co-extraction of hemicelluloses and cellulose along with the RG-I (Cardoso et al. 2007). However a recent study using solidstate-NMR has identified contacts between pectic complexes and cellulose microfibrils in intact arabidopsis cell wall material (Wang et al. 2015). APAP-1 (Arabinoxylan Pectin Arabinogalactan Protein 1) has recently been characterised as a complex of pectin AX and AGP by Tan et al. (2013). APAP-1 appeared to be very minor components of the polysaccharides extracted from suspension-cultured Arabidopsis, but was seen to contain a RG-I backbone moiety linked to an arabinoxylan chain via a 1-4 linkage, with the AGP motif attaching to a GalA residue via a 1-6 linkage. This was the first evidence of interaction between these three polymers, although this complex is yet to be identified *in muro*.

1.6.5.3 RG-II

The structure of RG-II, is very complex, containing 12 different sugar residues arranged in 5 regular side chains surrounding a backbone chain (Fig. 1.7). Whilst RG-II does contain rhamnose and galacturonan, it does not possess a repeating rhamnose-galacturonic acid chain as in RG-I, but a homogalacturonan backbone of at least 8 residues in length. This backbone is substituted by 5 side chains at either O-2 or O-3 positions (Buffetto et al. 2014), which are highly conserved throughout all plants examined to date, ranging from monocots to dicots to bryophytes and beyond, suggesting an ancient heritage and significant functional role (Thomas et al. 1989; Edashige and Ishii 1998; O'Neill et al. 2004). The 5 side chains of RG-II are referred to as A-E, with A + B being oligosaccharides which attach to the O-2 of the backbone, and C-E being short chain saccharides attaching to O-3 positions on the backbone (Melton et al. 1986; Stevenson et al. 1988; Pérez et al. 2003; Ahn et al.

having been identified. HG synthesis was first identified *in vitro* by Lin et al. (1966) however it took 30 further years for the isolation and characterisation of the HG synthetic enzymes to begin. These enzymes are referred to as galactosyltransferases (GAUTs), as they catalyse the transfer of D-GalA from UDP-D-GalA to the non-reducing end of the growing HG chain in the Golgi apparatus (Scheller et al. 1999; Akita et al. 2002; Ishii et al. 2002), although they often require an Mn^{2+} ion as a catalyst. GAUT1 and its homolog GAUT7, were the first GAUTs characterised and were shown to form a complex *in vivo* in *A.thaliana* (Mohnen 2008). Pectin deficient mutants have provided additional detail to the understanding of pectin biosynthesis with Quasimodo1 (Qua) and Qua2, shedding light on the HG biosynthesis. Qua1 is a mutant in GAUT8, and shows a reduction in pectin content (Bouton et al. 2002) *in vivo* leading to a stunted appearance (hence the Quasimodo reference) and shows a specific reduction in the HG-GalA transferase activity, but this is confused by the fact that a reduction in xylan synthase activity was also observed (Orfila et al. 2005). Qua2 was also identified through the reduction in pectin content *in vivo*, however it was discovered to be a putative methyl-transferase rather than GAUT (Mouille et al. 2007). *In vitro* studies have shown that HG can be methyl esterified through s-adenosyl-Met in the Golgi lumen (Goubet and Mohnen 1999). It is yet to be established if qua2 and the other identified putative methyl transferases are indeed directly connected to HG synthesis and how this may affect the reduction in pectin content in the qua2 mutant.

As yet only a few mutants have been identified affecting the biosynthesis of RG-I, leaving the genetics of this complex molecule largely unexplored. Currently only RHM1 (rhamnose modified) and RHM2 mutants have shown direct effects on the RG-I backbone. These mutants were both identified in Arabidopsis and have a 65% reduction in rhamnose and 50% reduction of galacturonic acid content of the seed mucilage. Subsequently these mutants have been characterised as affecting catalytic enzymes in the conversion of UDP-Glc to UDP-Rha (Diet et al. 2006; Oka et al. 2007). Arabinan side chain mutants have also been identified, with ARAD1 (arabinose deficient 1) being the best characterised, an arabinosyltransferase mutant with 46% reduction in leaves and up to 75% reduction in stem tissues of Arabidopsis. Significantly no detectable difference in cellular structure could be detected by Harholt et al. (2006), including no stomatal problems contrary to what may be expected of the stomatal experiments conducted by (Jones et al. 2005). Several other mutants have been generated which show some modification in the structure of the RG-I content, although these mutants also show changes in pectin

networks. For example many of the MUR (murus) ethyl-methane sulphate generated mutants show multiple monosaccharide changes relative to the wild type, but these changes are not associated with specific phenotypes in these mutants (Reiter et al. 1997).

Given the complex structure of RG-II the existence of many glycosyltransferases has been postulated to account for the additions of all 22 separate linkages between the 13 different glycosyl residues, however to date only a few of these enzymes have been reported. The best characterised of these are the RGXTs (rhamnogalacturonan xylosyltransferases), 4 homologs of which have been detected in *Arabidopsis* and characterised through heterologous expression in *Pichia pastoris*, which allowed their role in as adding a UDP-xylose to the L-fucose in side chain A to be established (Egelund et al. 2006; Egelund et al. 2008; Liu et al. 2011). This region of chain A is thought to be relevant to the stabilisation of the RG-II dimer formation, as *mur1* mutants in which the L-fucose residue is replaced with L-galactose have a reduction of ~45% in the formation of RG-II dimers, which is reversible following endogenous L-fucose application.

1.6.6 Cellulose

While cellulose is the most abundant cell wall polysaccharide in the world, accounting for up to one third of the total mass of a plant (Somerville 2006), the endosperm cell walls of cereal grains have very low cellulose contents with wheat, and brachypodium all containing ~2-8% (Guillon et al. 2011). Structurally cellulose is a homopolymer of β -(1-4)-glucose, with chains of this polymer arranged into microfibrils. Within these microfibrils the cellulose chains are oriented parallel to one another, and maintain the form of a flat ribbon through the rotation of every subsequent glucose monomer by 180°, producing repeating units of cellobiose. *In muro*, cellulose can be found either as amorphous or crystalline forms, each form having specific physical and chemical properties, contributing to the structural properties of the cell wall. Crystalline cellulose, which exists in two isoforms 1 α or 1 β (Brown et al. 1996b), is stronger and less malleable than amorphous cellulose and possesses a greater resistance to enzymatic degradation. Both isoforms of crystalline cellulose are typically found in plants although the relative proportions vary from tissue to tissue. The structure adopted is dependent on the opportunity for the glucan chains to form both intra and inter molecular interactions through hydrogen bonding and Van der Waals forces. Cellulose chain aggregation can occur in the presence of these intermolecular interactions resulting in cellulose microfibrils,

which are thought to contain between 24 and 36 glucan chains (Fernandes et al. 2011; Thomas et al. 2013; Newman et al. 2013), Thomas 2013, Newman 2013) although cellulose chain length may be species-specific and extend for up to 14000 glucose residues (Somerville 2006).

1.6.6.1 Cellulose biosynthesis

The regular orientation of cellulose chains in a parallel manner has long been a clue that the biosynthesis of these glucan chains occurs in a highly coordinated fashion (Ha et al. 1998). It is now known that this is the result of cellulose synthase complexes (CSC) which have a characteristic 6 complex rosette, with each complex (CesA) being proposed to synthesise a single glucan chain. Thus each rosette can synthesise 6 glucan chains, so microfibrils in the order of 6, i.e. 24 or 36 are feasible (Harris et al. 2010). CesA proteins are widely reported as elements of the CSC and were discovered in cotton through homology with a bacterial cellulose synthase protein (Pear et al 1996). However it is still unclear whether CesA proteins facilitate the formation of hydrogen bonds. CesA are glycosyltransferases family 2 proteins (Richmond and Somerville 2000) and are integral membrane proteins containing eight transmembrane domains (Somerville 2006), which are predicted to form a pore in the membrane to allow passage of newly formed glucan chains (Morgan et al. 2013; Slabaugh et al. 2014). Dimerisation of CesA proteins is thought to occur through the presence of a c-terminal zinc finger domain in higher plants (Kurek et al. 2002). The location and regulation of CSCs within the plasma membrane has been proposed by Baskin (2001) to be regulated by cortical microtubules adjacent to the plasma membrane after the initial model of Staehelin et al. (1991). These hypotheses are derived from the observation that the cortical microtubules and cellulose microfibrils have very similar orientation (Ledbetter and Porter 1963) and has recently been reinforced by the work of (Bringmann et al. 2012), which elegantly demonstrated that the CesA complexes can interact with cortical microtubules through a intermediary protein POM2/CS11.

1.6.6.2 Function

Cellulose microfibrils are strong and inelastic, and have been shown to interact with a range of other cell wall polysaccharides *in vivo*, such as xylan (Bromley et al. 2013), pectin (Vignon et al. 2004; Zykwincka et al. 2005) and xyloglucan (Hayashi et al. 1987). These interactions are proposed to be through the use of hydrogen bonds, although a recent paper has highlighted the importance of acetylation on

xylan chains to allow interaction with cellulose microfibrils (Busse- Wicher et al. 2014).

Cellulose microfibrils have been shown to be deposited in multiple layers with consistent orientations. This organised structure would provide resistance to the internal osmotic pressure of cells and this turgor pressure in turn would allow plants to stand upright. The relationship of cellulose and cell elongation has been explored in many experiments in *Arabidopsis*, with the root elongation zone in dark grown hypocotyls being the model system. In the elongation zone, cellulose is deposited in a transverse orientation compared to the direction of elongation (Kerstens and Verbelen 2002), which then shifts increasingly towards a longitudinal direction as cell elongation occurs (Anderson et al. 2010). Roland et al. (1975) predicted such a rotation of cellulose microfibril angle in their multi-net growth hypothesis, which describes a passive movement of cell wall layers in response to cell growth.

1.6.7 Lignin

Lignins are structural cell wall components not comprised of polysaccharides, instead it is a phenolic polymer, which is formed from primary hydroxycinnamyl alcohol derivatives. These molecules are joined by oxidative polymerisation, to produce three major lignin components:- H lignin, p-hydroxyphenyl; S Lignin, syringyl; and G lignin, guaiacyl (Vanholme et al. 2008). Catechyl or C-Lignin has recently been added to the list as a minor lignin component only found in vanilla orchid seeds; it derives from a different polymerisation method in which direct polymerisation of caffeyl alcohol and 5- hydroxylconiferyl alcohol form catechyl and 5-hydroxyguaiacyl (5H/5-OH-G) (Chen et al. 2012a; Chen et al. 2013). The major monolignol components are thought to be produced cytosolically (Donaldson 2001; Boerjan et al. 2003) and transported directly to the wall through specific ABC transporters (Miao and Liu 2010; Alejandro et al. 2012) rather than via Golgi vesicles (Kaneda et al. 2008). Additional modulation of lignin synthesis *in muro* has been shown to be in part due to cell wall localised peroxidases and laccases assisting with the polymerisation of the monolignols (Davin et al. 1997; Donaldson 2001; Berthet et al. 2011). The polymerisation of lignin is thought to begin in the middle lamella and functions to stiffen and strength the cell wall by crosslinking to pectins and hemicelluloses *in muro* (Jeffries 1994). Typically lignin is observed in cell walls after cell differentiation and expansion (Lewis and Yamamoto 1990) often around the time of PCD (Albersheim et al. 2010) in what is referred to as the terminal differentiation stage.

1.6.8 Arabinogalactan peptides

Arabinogalactan peptides (AGPs) are heavily glycosylated hydroxyproline rich glycoproteins have been typically considered to be an element of the cell wall matrix. They have been studied in the context of cell walls since their initial discovery due to the very large arabinogalactan motifs that contribute to ~90% of AGPs. Due to this significant content of arabinan and galactan, AGPs were assumed to be associated with the cell wall matrix in some way and at present no known role or cellular location is attributed to the AGP molecules. However AG proteins, which have a much larger protein cores (87-739 amino acids), and slightly different structures in their AG modules, have been postulated to have a wide range of functions from cell signalling to drought tolerance and wound healing (Showalter 2001; Van Hengel et al. 2002; Brownlee 2002; Johnson et al. 2003; Mashiguchi et al. 2004; Lamport et al. 2006; Ellis et al. 2010). However no further explanation of how these AG modules may interact with the cell wall matrix has been provided. Several other cellular locations are possible if compared with hypothesised locations of AG proteins, for example several classes of AG proteins have membrane bound anchors and are thought to be involved in calcium ion signalling (Lamport et al. 2014), or it is possible that they may be cytoplasmic due to the high level of water solubility conferred by the AG modules. Whilst numerous localisation experiments have been conducted on AG proteins, to date none have been probed the cellular location of AGPs in cereals.

In cereal AGPs, the peptide core is highly homologous 15-25 amino acid sequence, containing 3 hydroxyproline residues. The sequence of this peptide is identical to the n-terminal sequence of grain softness protein-1 (GSP-1) and is therefore assumed to originate as a processing product of GSP-1, as the mature protein lacks this 15 amino acid region (Van den Bulck et al. 2005). Additionally specific clades of GSP-1 have been reported to be associated with specific clades of peptide sequence in specific species indicating that it is highly unlikely that the two evolved separately (Wilkinson et al. 2013). The 3 hydroxyproline residues conserved in peptide sequence of cereal AGPs are the sites of attachment for very large arabinogalactan modules. These arabinogalactan modules consist of a β -(1-3)-linked galactopyranosyl backbone chains which in turn have -(1-6)-linked galactopyranosyl side chains which variable in length. Both the side chains and backbone can be decorated with single arabinofuranosyl substitutions at the O-3 position and the side chains can in turn be decorated with single arabinopyranosyl residues at the O-3 position. The β -1-6 galactan side chains may also be decorated

by arabinopyranosyl residues on the arabinofuranosyl residues substitutions present. These side chains also appear to contain glucuronic acid residues at the non-reducing termini (Tryfona et al. 2010). AG modules typically contain somewhere in the region of 100-120 sugar residues.

1.7 Gradients in grain composition.

In addition to the spatial gradients in endosperm storage proteins (Tosi et al. 2009; Furukawa et al. 2003), gradients in the cell wall components are also observed in both wheat and rice. FT-IR and Raman microscopy analysis of cross sections of endosperm revealed differences in the degree of arabinoxylan (AX) substitution in cell walls across the grain (Piot et al. 2001; Barron et al. 2005; Mills et al. 2005; Robert et al. 2005; Barron et al. 2006; Philippe et al. 2006a; Philippe et al. 2007; Toole et al. 2007; Barron and Rouau 2008; Toole et al. 2009; Toole et al. 2010; Guillon et al. 2011; Robert et al. 2011; Toole et al. 2011).

At present, little is known about the factors controlling these compositional gradients. Some of these gradients are assumed to be related to cell age and lineage, since the sub-aleurone layer derives from periclinal cell division of the aleurone layer, occurring later into grain development than divisions of central endosperm cells (Olsen et al. 1998; Olsen 2001). A second hypothesis is that there are positional cues for cell fate; in particular there is some evidence in maize (Becraft and Asuncion-Crabb 2000; Yi et al. 2011) that the endosperm and aleurone do not have fixed cellular fates. Upon application of the appropriate external cue aleurone cells can switch from one cell type to the other and back again. It is yet to be established if this is due to an “outside” signal or if it is the result of a chemical gradient across the grain, much like the hormonal gradients that are commonly found across meristem tissues, i.e. auxin in meristem development patterning (Olsen et al. 1998; Olsen 2001).

A clear pattern in the deposition of cell wall components can be observed in wheat endosperm, a tissue that is still the focus of intense research due to its importance in end use quality. In the cellularizing endosperm of wheat, the walls contain callose (Philippe et al. 2006b; Wilson et al. 2006; Toole et al. 2010). As development continues, callose is replaced by increasing amounts of mixed link β -glucan, and, later on, by highly branched arabinoxylan (HB-AX), which in turn is modified, typically to produce LB-AX (low- branch AX) (Toole et al. 2007).

1.8 Usage and limitations of monoclonal antibodies

Monoclonal antibodies allow for relatively high resolution and highly specific detection of epitopes within a sample material and can detect the presence of absence of an epitope with a very high degree of spatial separation (<1 μm). For example mAbs directed to specific pectic structures can recognise specific sections of cell wall within the cell wall junction whilst no detection is seen along the length of the wall (Willats et al. 2001b). Monoclonal antibodies can be used in many different methods to detect their target epitope, typically immunofluorescence microscopy is one of the most common uses, as it allows the examination of the spatial localisation and separation of the target epitopes. For broader examination of the epitopes present in a sample ELISA assays can be implemented, providing information about both the relative strength of the interaction between the sample and the antibody and which epitopes can be detected in the sample. Further examination of the interactions between different epitopes can be probed with the use of epitope detection chromatography, which utilises chromatographic techniques in conjunction with monoclonal antibodies to examine interactions between different polysaccharides. The wide array of available monoclonal antibodies provides tools to detect almost the whole range of cell wall polysaccharides (Pattathil et al. 2010), which allows for very sensitive analysis of cell wall dynamics and the structural heterogeneity within a single cell wall. This can be used to study both developmental and spatial dynamics of cell wall deposition, maturation and modification in both unfixed and fixed sections. At present the only major polysaccharides not detectable by the available array of mAbs available is RG-II, despite repeated attempts this polysaccharide remains recalcitrant to antibody production, which may be related to its highly complex structure. Monoclonal antibodies are limited in several key dimensions though, firstly generation of monoclonal antibodies specific to a target molecule can be time consuming and it can be problematic to prove that the antibody is specific only to the original immunogen. Antibodies can provide semi-quantitative data about the amount of epitope present in a sample in immunofluorescence microscopy, and detection can be impaired or prevented by steric interference from other molecules, as monoclonal antibodies are relatively large structures.

1.9 Aims of project

As discussed above, qualitative and quantitative gradients in cell wall polysaccharides have been identified across the wheat endosperm, but little is

known about the factors controlling these gradients or their biological roles and not all cell wall matrix polysaccharides have been studied. It is possible that these gradients are related to cell age and lineage, since the sub-aleurone layer is thought to derive from periclinal cell divisions of aleurone cells, occurring later into grain development than the divisions of central endosperm cells that give rise to the central starchy endosperm (Olsen et al. 1998; Olsen 2001). Although the formation of cell walls in the developing rice endosperm is well described and the polysaccharide composition of the mature grain identified, the sequence of deposition of individual cell wall polysaccharides has not been reported. Wheat and rice grain present important anatomical differences, first of all, the presence of a crease in wheat accommodating the vascular bundle and acting as the sole point of entry of assimilates in the endosperm; in rice, on the contrary, nutrients are unloaded from the phloem in the nucellar epidermis, can move circumferentially and enter the endosperm at different points via the aleurone cells. Cell wall composition and formation dynamics in the two species may therefore reflect this different grain physiology. The aim of the present study was therefore to perform a comparative analysis and determine the temporal and spatial patterns of polymer deposition in cell walls of developing rice grain, focusing on the endosperm, and to compare these with the pattern in wheat, which has been more thoroughly described. This was achieved by using immunofluorescence microscopy with sets of monoclonal antibodies (mAbs) to detect the cell wall matrix polysaccharides, focusing on three major time points selected to represent key stages of grain development in both species.

To summarise, three major objectives were pursued during this project:

- To quantify the cell wall polysaccharide content of developing wheat and rice grains, in order to correlate changes in cell wall composition with cell physiological processes in developing grains.
- To use monoclonal antibodies to probe the spatial and temporal regulation of specific cell wall polysaccharides in developing grains of wheat and rice, in order to determine how the cell wall compositions of specific cell and tissue types change in relation to cell/tissue development and the biological roles of tissues.
- To investigate the localisation of arabinogalactan peptides (AGPs), using novel monoclonal antibodies, to confirm the presence of AGPs as cell wall components in developing wheat and rice grains.

CHAPTER 2: MATERIALS AND METHODS

2.1 Plant materials

O. sativa cv. Koshihikari seeds (bred at Fukui Prefectural Agricultural Research Facility) were sterilized in 15 ml falcon tubes in 10% (v/v) bleach and shaken for 20 min. The seeds were then rinsed 5 times in sterile water. Seeds were germinated on damp Whatman's filter paper (Whatmans No.1 90mm diameter filter paper, www.whatman.com) in 90 mm petri dishes in darkened conditions at 22°C for 7 days. Seedlings were transferred to 1 L moldjars (weckjars, weckjars.com) in a pre prepared Murashige and Skoog growth media (Sigma Aldrich, m5519-1L). Once seedlings had reached 15 cm they were transferred to 15cm diameter pots filled with sandy loam soil mixed to a 3:1 ratio with distilled water (Roffey brothers mendip loam, www.nmsb.co.uk). Plants were grown in controlled environment cabinets (Fitotron, SGC-120) at Rothamsted Research with a 12 h photoperiod (4am-4pm) at a day time temperature of 28°C and 22°C night time temperature, relative humidity was maintained at 70%. The pots were placed in deep trays of water; approximately two thirds of the height of the pot, the water level was maintained by regular watering to simulate paddy field conditions. Caryopses were harvested at 4, 6, 8, 12, 20 and 28 DAA from the middle third of the panicle and immediately prepared for microscopy. Anthesis was defined as the point at which the middle third of the panicle had exposed anthers.

Triticum aestivum cv. Cadenza (bred by Cambridge Plant Breeders Ltd) plants were grown in controlled environment rooms at Rothamsted Research at 18°C day/15°C night temperature with a photoperiod of 16 hour provided by banks of 400W hydrargyrum quartz iodide lamps (Osram Ltd., UK) generating a light intensity of ~700 $\mu\text{mol}/\text{m}^2/\text{s}$ photosynthetically active radiation at the pot surface. Caryopses were harvested at 4, 6, 8, 12, 20 and 28 DAA from the middle third of the spikelet and immediately prepared for microscopy.

2.2 Immunolocalization of cell wall polysaccharides wheat and rice grains.

2.2.1 Light microscopy and immunofluorescence analysis

Transverse medial sections of wheat and rice grains (approximately 1 mm in thickness) were cut in paraformaldehyde fixative solution (4% w/v paraformaldehyde, Sigma-Aldrich 158127) and 2.5% w/v glutaraldehyde (Sigma-Aldrich, G7776) in 0.1 M Sorenson's buffer pH7.2 (5.365 g of Na₂HPO₄·7H₂O in 100ml dH₂O + 3.121g of NaH₂PO₄·2H₂O in 100 ml dH₂O mixed in a ratio of 3.6:1.4 and diluted to 0.1M with dH₂O)). Sections were fixed overnight at room temperature (RT) in the same paraformaldehyde fixative solution. After three rinses in Sorenson's phosphate buffer the specimens were dehydrated in an ethanol series: 10% Ethanol (v/v) for 1 h at RT, 30% Ethanol (v/v) for 1 h at RT, 50% Ethanol (v/v) for 1 h at RT, 70% Ethanol (v/v) for 1 h at RT, 100% Ethanol (v/v) for 1 h at RT. Samples were then slowly infiltrated with LR White resin (medium grade, TAAB L012, London Resin Company, London) in increasing concentrations of resin: 25% resin (v/v) in absolute ethanol for 1 h at RT, 50% resin (v/v) in absolute ethanol for 1 h at RT, 75% resin (v/v) in absolute ethanol for 1 h at RT, 100% resin (v/v) for 1 h at RT, the final incubation is repeated twice. Subsequently the samples were incubated in 100% LR White resin for 7 days (in wheat sections) and 28 days (in rice sections), samples were individually encapsulated in flat bottomed polypropylene capsules (Agar Scientific, AGG3759) and polymerised at 55°C in a nitrogen gas saturated environment for 48 h. Semi-thin sections of 1 µm thickness were cut on an UltraCut Microtome (Reichert-Jung, Austria) using glass knives prepared on site, collected in drops of distilled water on multi-well diagnostic slides (Menzel-Gläser, X2XER201B#) coated with 1% v/v poly-L-lysine hydrobromide (Sigma-Aldrich, P1399), and dried on a hot plate at 40°C.

2.2.2 Sample preparation for high pressure freezing.

Transverse thin slices of wheat and rice grains were cut with a razor blade while keeping specimens immersed in MES buffer, pH 5.5 (Sigma Aldrich, 117961-21-4); 2mm punches were taken from the grain slices and loaded into type A planchettes previously dipped in lecithin (100mg lecithin in 1 ml of chloroform) and transferred to Leica EM ICE instrument (Leica Microsystems) for high pressure freezing. Samples were stored in liquid nitrogen until the start of freeze- substitution. Freeze substitution was carried out in a Reichert AFS apparatus (Reichert-Jung, Austria,

using acetone for subsequent low temperature embedding in LR White resin (Agar Scientific, UK) Specimens were brought from -160°C to -85°C in steps of 15 °C h⁻¹, then freeze substitution was started using the following programme T1- 85°C 26 h, S1 +2°C h⁻¹ 12.5 h; T2 -60°C 10.5 h S2 +2°C h⁻¹ 15h; T3 -30°C 6 h.

Samples were take out of planchettes on ice and take from acetone to methanol (1:3, 1:1, 3:1 v/v) while kept at -20°C, then gradually embedded in LR White over a period of 6 days (25%, 50%, 75%, 100%, v/v). UV polymerisation was carried out at -20°C for 24h, followed by another 24h at 0°C Sections were subsequent sectioned as per 2.2.1

2.2.3 Indirect immunofluorescence labelling and histochemical staining for light microscopy.

Slides with LR White-embedded grain sections were incubated (50µl per well) in 5% (w/v) milk powder (Marvel products, UK) in 1 x PBS at pH 7.0 for 1 h, then Washed three times for 5 min each with PBS, then incubated for 2 h in primary antibody. The following monoclonal antibodies were used, diluted in PBS containing 5% (w/v) milk powder: rat probes - LM5 (Jones et al. 1997), LM6 (Willats et al. 1998), LM19 (Verhertbruggen et al. 2009), LM25 (Pedersen et al. 2012), JIM7 (Knox et al. 1990) all diluted 1:5; Mouse monoclonal AX1 (Guillon et al. 2004), anti-callose (Meikle et al. 1991) (BioSupplies Australia, Cat No. 400-2), anti- MLG (Meikle et al. 1994) (BioSupplies Australia, Cat No. 400-3) diluted 1:50; mouse monoclonal INRA-RU1, (Ralet et al. 2010)(INRA Nantes) diluted 1:5. Slides were rinsed three times for 5 min with 1x PBS, then incubated for 2 h, in the dark, with secondary antibody (anti-rat Alexa 568 conjugated or anti-mouse Alexa 568 conjugated, Invitrogen) diluted 1:200 in PBS, 5% (w/v) milk powder (Marvel products, UK). Slides were then washed three times for 5min with PBS, and counterstained with 1% (w/v) Calcofluor White 2mr (Sigma Aldrich, F3543) solution. Sections were then mounted in Citifluor AF-1 glycerol based anti-fade mountant (Agar Scientific, UK) and covered with a glass coverslip. Sections were imaged on a Zeiss Confocal LSM 780 on an Axio Observer microscope, with 32 channel GaAsP detector and 2 PMT, using Zen 2010 software and fitted with 405 nm diode laser; 458 nm, 488 nm, 514 nm from an Argon ion laser; 561 nm and 633 nm HeNe Laser.

Table 2.1. Cell wall directed monoclonal antibodies used in this study.

Antibody	Antigen	Reference
Arabinoxylans		
INRA-AX1	arabinoxylan	(Guillon et al. 2004)
LM28	glucuronoxylan	in preparation
Phenolic components		
LM12	feruloylated polysaccharides	(Pedersen et al. 2012)
INRA-COU1	coumaric acid	(Tranquet et al. 2009)
Mixed Linkage β Glucan		
MLG	mixed linkage β glucan	(Meikle et al. 1994)
Minor non-cellulosic polysaccharides		
Callose	1-3 β -glucan	(Meikle et al. 1991)
LM21	heteromannan	(Marcus et al. 2010)
LM25	xyloglucan	(Pedersen et al. 2012)
Pectic Homogalacturonan		
LM19	un-esterified homogalacturonan	(Verherbruggen et al. 2009)
JIM7	partially methyl-esterified pectic HG	(Clausen et al. 2003)

LM20	methyl-esterified pectic HG	(Verhertbruggen et al. 2009)
Pectic Rhamnogalacturon an-I		
INRA-RU1	rhamnogalacturon an backbone	(Ralet et al. 2010)
LM5	(1-4)- β -D-galactan	(Jones et al. 1997)
LM6	(1-5)- α -L-arabinan	(Willats et al. 1998)

2.2.3.1 Enzymatic unmasking

Enzymatic unmasking was used to investigate the phenomena of polysaccharide masking, via the enzyme pre-treatments on sections. 50 μ l of Xylanase GH10 (X10, Prozomix, pro-E0007) and Lichenase (Prozomix PRO-E0017) solution (20U of Xylanase and 40U of Lichenase in 50 μ l of 50mM PBS buffer pH 7.0) was applied to each section to digest xylan backbone structures of arabinoxylan, and mixed linkage β -glucan and was incubated in a humid chamber (Sigma Aldrich, H6644) for overnight at 37°C.

2.3 Histochemical stains

2.3.1 General morphology

For general morphology and staining of protein bodies, the sections were stained with 0.1% (w/v) toluidine blue O (Sigma Aldrich, 198161) in 1% (w/v) sodium tetraborate, pH 9, for 30 seconds before washing with PBS. Sections were mounted in distilled water under a coverslip and imaged on a Zeiss Axiophot microscope equipped with a Retiga Exi (Qimaging) camera.

2.3.2 Protein body staining

For specific protein body staining, a 1% (w/v) solution Coomassie Brilliant Blue G (CBB, Sigma Aldrich, 27815) in acetic acid, the solution was applied for 30 seconds at 40°C.

2.3.3 Starch granule staining

For specific starch granule staining an iodine/ potassium iodide solution (IKI or Lugol's solution) was used. For 1-2 μm sections the IKI 1 % (w/v) (Sigma Aldrich, 32922) was applied for 1min. IKI was removed with distilled water and air dried at room temperature. Sections were mounted in distilled water under a coverslip and imaged on a Zeiss Axiophot microscope equipped with a Retiga Exi (Qimaging) camera.

2.4 Cell wall chemistry

2.4.1 Isolation of cell wall material

2.4.1.1 Non-starch polysaccharide (NSP) preparation, based on Englyst et al 1992.

Non-starch polysaccharide preparations were completed on wheat and rice flours from 5 developmental time points (4, 8, 12, 20, 28 DAA) as per Englyst et al. (1992) with some amendments.

150 mg of sample flour from each species and developmental time point (in triplicate) was added to 50 ml capped-pyrex tubes (50ml, Cole-Parmer), 2 ml of DMSO was added to each tube and then vortexed repeatedly for 5min. Samples were then boiled in a water bath at 100°C for 30 min. Then 8 ml of α -amylase solution (100U, A3306, Sigma-Aldrich) in 50 mM Acetate buffer at pH5.5 is added to each sample and the samples boiled for a further 10 min. The samples were transferred to a water bath at 50°C and allowed to equilibrate before adding pancreatin V (1494057, Sigma-Aldrich) and pullanase (40U, P2986, Sigma-Aldrich), and incubated for 4 h at 50°C before the enzymes were denatured at 100°C for 10 min. The samples were cooled and 0.15 ml of 5 M HCL was added and topped up to approximately 40 ml absolute ethanol. The cell wall polysaccharides were then allowed to precipitate on ice for 2 h. The precipitates were collected by centrifugation at 1500g for 10 min and the supernatant discarded. The pellet was washed sequentially with 40 ml of acidified 85%(v/v) ethanol (0.15 ml of 5 M HCl per 40 ml of 85% (v/v) ethanol), absolute ethanol and finally acetone. The samples were vortexed and centrifuged between each solvent wash with the supernatant being discarded at each step. Samples dried overnight at RT to ensure no acetone remains prior to further analysis

2.4.1.2 Alcohol insoluble residue (AIR) protocol 1 (AIR1)

150 mg of sample flour, milled to less than 150 µm particle size was weighed into 2 ml microcentrifuge tube, and 1.5 ml of 70% (v/v) ethanol added. The sample was vortexed briefly and centrifuges at 20,000g for 10 min and supernatant removed. The pellet was washed with 1.5 ml of chloroform:methanol (1:1, v/v) and vortexed before centrifugation at 20,000g for 10 min. The supernatant was discarded and the sample dried under a stream of nitrogen.

2.4.1.2.1 Additional Starch removal step

The dried AIR pellet was resuspended in 1.5 ml of 0.1 M sodium acetate buffer at pH 5.2 (pH adjusted with acetic acid). Then 100 µl of α-amylase solution (a3306, Sigma-Aldrich) was added, the sample vortexed and incubated on a shaking heating block at 50°C for 16 h.

2.4.1.3 AIR protocol 2 (AIR2)

150 mg of sample flour, milled to less than 150 µm particle size was weighed into 2 ml microcentrifuge tube, and 1.5 ml of 96% (v/v) ethanol at added, vortexed briefly and then centrifuged at 20,000g for 15 min. The supernatant was discarded and 1.5 ml of absolute ethanol was added to resuspend the pellet. The sample was vortexed briefly and centrifuged at 20,000g for 15 min before discarding the supernatant. 1.5 ml of methanol:chloroform (2:3, v/v) was added and the samples shaken for 1 h at room temperature. The sample was then centrifuged at 20,000g for 15 min and the supernatant discarded. The methanol:cholroform wash and centrifugation was repeated. The sample was then sequentially washed with 1.5 ml of 100% ethanol (v/v), 65% ethanol (v/v), 80% ethanol (v/v) and 100% ethanol (v/v) with the sample centrifuged at 20,000g for 15 min and discarding the supernatant between each wash. The remaining pellet was then dried at room temperature in a sample concentrator (Concentrator 5301, Eppendorf) overnight (~16h).

2.4.1.3.1 Additional Starch removal step

As per chapter 2.4.1.2.1

2.4.1.4 Lai Protocol

As per Lai et al. (2007): 150 mg of wholegrain sample flour, milled to less than 150 µm particle size was weighed into capped pyrex centrifuge tube (50 ml, cole-parmer) de-fatted by refluxing with 10 ml of 80% (v/v) ethanol for 1 h. The sample

was centrifuged at 2,000g for 30 mins and the supernatant discarded. The pellet was incubated in 10 ml of 0.05M MES-TRIS (1.952g of MES (2-(*N*-Morpholino)ethanesulfonic acid (M8250, Sigma Aldrich)) and 1.22 g of TRIS (Tris(hydroxymethyl)aminomethane, T1503 Sigma Aldrich) in 170 ml of dH₂O, adjusted to pH 7.0 with 4 M NaOH and dilute to 200 ml with dH₂O) buffer at pH7.0 with 200U heat stable α -amylase (A3306, Sigma-Aldrich) for 30 min at 90°C. The sample was transferred to a 60°C water bath and allowed to equilibrate before a further incubation of 30 min. Then the pH was adjusted to pH4.0 with HCL prior to the addition of 50U of amyloglucosidase (A7095, Sigma-Aldrich) and mixed continuously for 30 min at 60°C. The enzymes were denatured in a boiling water bath for 15 min. Subsequently 40 ml of 95% (v/v) ethanol was added after the samples had cooled to room temperature, and then the samples were left for 2 h to allow precipitation of cell wall material. Supernatant was removed via by ultracentrifugation (30 mins at 10,000rpm), and the pellet was sequentially washed with 40 ml additions of 80% (v/v) ethanol, 95% (v/v) ethanol and finally acetone, discarding the supernatant after each wash by ultracentrifugation (30 mins at 10,000 rpm). Dry cell wall material was isolated via lyophilisation.

2.4.1.5 Shibuya protocol:- (Shibuya et al. 1985)

150 mg of sample flour, milled to less than 150 μ m particle size was weighed into capped pyrex centrifuge tube (50 ml, cole-parmar) de-fatted by refluxing with 10 ml of 80% (v/v) ethanol for 1 h. The sample was centrifuged at 2,000g for 30 min and the supernatant discarded. The pellet was resuspended in 20 ml of 1% SDS (v/v) and 1% DTT (w/v) in HPLC filtered water, mixed thoroughly and left at RT overnight. The sample was then centrifuged at 2,000g for 30 min and the supernatant discarded. The pellet was resuspended in 30 ml of DMSO (dimethyl sulphoxide) and sonicated using a sonic probe for 5 min then left on a shaker overnight at RT. The sample was decanted into corex tubes in order to remove the DMSO via ultracentrifugation (10,000g for 30 min). The pellet was then washed with 30 ml DMSO twice more, repeating the overnight shaking and ultracentrifugation steps. After the DMSO washes the pellet was washed three more times with 20 ml HPLC filtered water, with removal of supernatant in each wash via ultracentrifugation (10,000g for 30 min). Dry cell wall material was recovered by lyophilisation.

2.4.2 Monosaccharide analysis via HPLC

2.4.2.1 Chromatographic method for monosaccharides – neutral sugars

25 μL of hydrolysed NSP (0.025 $\mu\text{g}/\mu\text{l}$ in dH_2O) was injected into a Thermo Dionex HPAEC-PAD ICS-5000+ equipped with CarboPac PA20 guard and analytical column (3x30 mm – guard; 3x150 mm – analytical) at 0.5 mL/min. Also fitted was an Eluent generator with KOH cartridge, CR-ATC continuously regenerated ion trap, pulse amperometric detector with Gold/PTFE electrode and reference pH electrode, column and detector compartments tempered at 30°C.

The HPLC run was 23 minutes long with a KOH gradient elution (table 2.1).

Calibration curve for each monosaccharide was constructed by injecting known amounts of standards (125, 250, 375 and 625 pmoles). Peak areas for each monosaccharide were then collated and absolute quantities of analyte in each sample were calculated using appropriate calibration curve.

Time [min]	KOH concentration [mM]
0	4.5
13	4.5
14	10
15	13
16	20
17	20
18	4.5
23	4.5

Table 2.2 KOH elution gradient for HPLC neutral monosaccharide method.

2.4.2.2 Chromatographic method for monosaccharides – acidic sugars

20 μL of hydrolysed NSP (0.5 $\mu\text{g}/\mu\text{l}$ in dH_2O) was injected into a Thermo Dionex HPAEC-PAD ICS-3000 equipped with CarboPac PA20 guard and analytical column (3x30 mm – guard; 3x150 mm – analytical) at 0.25 mL/min. Pulse amperometric

detector with Gold/PTFE electrode and reference pH electrode, column and detector compartments were tempered at 25°C.

The HPLC run was 60 minutes long with 0.2M NaOH and 0.1M NaOH in 0.5M sodium acetate gradient elutions (table 2.2). Calibration curve for each acidic monosaccharide was constructed by injecting known amounts of standards (20, 40, 100, 200, 300 and 400 pmoles). Peak areas for each monosaccharide were then collated and absolute quantities of analyte in each sample were calculated using appropriate calibration curve.

Time [min]	0.2M NaOH [%]	0.1M NaOH in 0.5M sodium acetate [%]
0	5	0
5	5	0
30	13.3	0
40	60	40
45	100	0
50	100	0
52	5	0
60	5	0

Table 2.3 Elution gradients for HPAEC acidic monosaccharides method.

2.4.3 Megazyme MLG Assay kit method

2.4.3.1 Glucose Standard curve production

Glucose quantities ranging from 10 µg to 100 µg (10 µg, 25 µg, 50 µg, 75 µg, 100 µg) of D-glucose per test tube were produced by dilution of 1mg/ml d-glucose solution (0.2% w/v benzoic acid, Megazyme International, Ireland) to a final volume of 0.1ml (Table 2.2). To each tube an additional 0.1 ml of HPLC filtered water was added to replace the β-glucosidase solution. In order to detect the glucose present, 3 ml of GOPOD reagent (Megazyme International, Ireland) was added to each tube.

The tubes were then incubated for a final 20 min at 40°C prior to decanting the solution into polypropylene cuvettes and recording the absorbance at 510 nm.

Glucose content in 0.1ml volume	Volume of 1 mg/ml D-Glucose solution	HPLC filtered water
10 µg	10 µl	90 µl
25 µg	25 µl	75 µl
50 µg	50 µl	50 µl
75 µg	75 µl	25 µl
100 µg	100 µl	0 µl

Table 2.4. Glucose standard curve for GOPOD.

2.4.3.2 Assay of samples with unknown MLG content

0.5 g of flour (of a known moisture content) milled to pass through a 0.5 mm screen was weighed out into 50 ml polypropylene falcon tubes in triplicate. An aliquot of 1.0 ml ethanol (50% v/v) was added to each tube, followed by 5 ml of sodium phosphate buffer (20 mM, pH6.5, Megazyme International, Ireland) and vortexed thoroughly. The tubes were incubated at 100°C for 5 min, vortex mixing each tube every 30s to prevent formation of gelatinous lumps. The tubes were cooled to 40°C and 0.2 ml of Lichenase (10U, Megazyme International, Ireland) was added to each tube prior to incubation at 40°C on a thermomixer (Thermomixer Comfort, Eppendorf) for 1 h. The tubes were adjusted to a total volume of 30 ml by the addition of 23.8 ml of HPLC filtered water to each tube. The tubes were then vortexed prior to centrifugation at 1,000g for 10 min in (Eppendorf 5452 Centrifuge). An aliquot of 0.1 ml of supernatant was transferred to a 10 ml pyrex test tube, prior to the addition of 0.1 ml β-Glucosidase solution (0.2U in 50 mM sodium acetate buffer, pH4.0, Megazyme International, Ireland) to each of the tubes. The tubes were incubated in a water bath at 40°C for 15 min. After the incubation 3 ml of GOPOD reagent (Megazyme International, Ireland) was added to each tube. The tubes were then incubated for a final 20 min at 40°C prior to decanting the solution into cuvettes and recording the absorbance at 510nm. The reaction blank consists of a 0.1 ml aliquot of HPLC filtered water to replace the sample supernatant, 0.1 ml of sodium acetate buffer (50 mM, pH4.0) excluding the β-glucosidase and 3 ml of GOPOD. The reaction blank was incubated and vortexed inline with the test samples.

2.4.3.3 Optimised method.

The method was conducted as per chapter 2.4.6.1 with the following exceptions: Firstly, sample flour was reduced to 50 mg from 500 mg. Secondly, sample volumes were not adjusted to 30 ml after incubation with lichenase. Thirdly, 1 ml of supernatant was transferred to new test tubes after centrifugation rather than 0.1 ml. These amendments should produce a 2.5x increase in the glucose concentration detected in the spectrophotometer from each sample in comparison to the original method from Megazyme International, Ireland.

2.4.4 Klason-Lignin Assay

1 g of sample flour (milled to <250 µm particle size) was weighed into pyrex Erlenmeyer flask (125 ml, cole-parmer, 5020-125) and 3 ml of 72% (v/v) sulphuric acid was added and the sample incubated at 30°C for 30 min in a water bath and sealed each vessel with parafilm. The sample was diluted to a 4% (v/v) sulphuric acid solution with the addition of 54 ml of distilled water. The flask was capped with aluminium foil and autoclaved the flask at 120°C for 1 h. Whatman's no.1 filter papers were weighed and added to Buchner funnels the sample solution was then vacuum filtered through the filter papers and washed with a further 1 L of distilled water per sample. Filter papers were dried overnight at 30°C in an oven. Once the filter papers had cooled to room temperature, they were weighed to calculate the lignin content of the sample.

2.4.5 Cellulose assay

2.4.5.1 Cellulose quantification using anthrone reagent as per Gillmor et al. (2002) an amalgamation of Scott Jr and Melvin (1953); Updegraff (1969)

100 mg of sample flour (milled to <250 µm particle size) was weighed into a 2 ml Eppendorf microcentrifuge tube and 1 ml of 70% ethanol (v/v) was added and the Eppendorf locked with a lid lock before incubation at 70°C for 1 hour. The sample was then allowed to cool centrifuged at 20,000g for 10 min and supernatant discarded. The sample was then resuspended in 1ml of acetone and mixed for 10 min, prior to centrifugation at 20,000g for 10 min and removal of supernatant. The pellet was then dried using a sample concentrator (Eppendorf concentrator 5301, Eppendorf) to remove residual acetone and 1 ml of acetic nitric reagent (150 ml of

80% v/v acetic acid + 15 ml of concentrated nitric acid) was added and the sample heated at 98°C on a hot block for 30 min ensuring that the lid is securely fastened. The samples were allowed to cool to room temperature and internal pressure carefully released. The samples were then centrifuged at 14000rpm for 10 min and the supernatant removed. The pellet was resuspended in 1 ml of distilled water and vortexed before being centrifuged at 14000 rpm for 10 min and discarding the supernatant. The sample was then resuspended in 1ml of acetone and centrifuged for 5 min at 14000rpm, with the supernatant discarded. The acetone wash and centrifugation steps were repeated and the pellet was dried overnight in a sample concentrator (Eppendorf concentrator 5301, Eppendorf) at room temperature. The pellet was then covered with 100 µl of 67% sulphuric acid and vortexed thoroughly, and then 400 µl of distilled water was added. 1ml of anthrone reagent (100 mg in 10 ml of concentrated sulphuric acid, must be made fresh daily for the assay, Sigma-Aldrich, 319899) was added and the tubes sealed with a lock lid and boiled on a heating block at 100°C for 5 min. Eppendorf tubes were cooled on ice and before the contents were decanted into glass cuvettes and the absorbances at 620 nm were recorded compared to the reaction blank (100 µl of 67% v/v sulphuric acid, 400 µl of distilled water and 1 ml of anthrone reagent).

2.4.5.2 Optimisation

Both wheat and rice samples were found to be richer in cellulose than anticipated, so additional dilution of the pellet was required to bring the absorbances at 620 nm into the working range of between 0.1 and 1.1 OD. For whole grain samples the method was completed as per chapter 2.1.4.8.1 but the final 500 µl solution prior to the addition of anthrone reagent was diluted by a factor of 50. This was achieved by a serial dilution of 250 µl aliquot of the pellet/sulphuric acid solution added to 750 µl of water, followed by a 250 µl aliquot of this dilution added to 750 µl of water was conducted. Then 500 µl of this solution was added to a clean 2 ml Eppendorf tube and 1ml of anthrone reagent added as per chapter 2.1.4.8.1

CHAPTER 3: MORPHOLOGY AND DEVELOPMENT OF WHEAT AND RICE GRAINS

3.1 Introduction to grain development and morphology

While detailed studies on the physiological and biochemical changes undergone by the developing grain have been carried out on wheat and barley, less is known of the changes occurring in the developing rice grain. Five stages of grain development common to all cereals have been described: cellularisation, differentiation, expansion and deposition of storage compounds, maturation and desiccation. In rice, these phases have been examined in isolation and in differing cultivars but no complete study exists from cellularisation to physiological maturity. The deposition of starch and protein, which are the major storage compounds in developing grains, have been well studied in both species and the progression of their deposition is well understood (Harris and Juliano 1977; Bechtel and Juliano 1980; Oparka and Harris 1982; Yamagata and Tanaka 1986; Nakamura et al. 1989; Jenner et al. 1991; Nakamura et al. 1996; Shewry et al. 2001). A recent study by Chateigner-Boutin et al. (2014) of the developmental dynamics of cell wall polysaccharides using immunofluorescence labelling with monoclonal antibodies has expanded our understanding of the development of the wheat grain by showing that pectin is an element of the wheat endosperm cell wall matrix. In barley and rice studies have focussed on specific developmental phases, in particular cellularisation, and mature grains, leaving a gap in knowledge between these two time points. Monosaccharide analysis is widely used for cereal grain non-starch polysaccharides, with studies focusing on the major hemicellulosic components arabinoxylan and MLG. Monosaccharide analysis of cell wall material provides details of the relative composition of cell walls. However, it does not provide detail of all cell wall components, and it is impossible to separate the relative contributions of cellulose, xyloglucan, callose and MLG using this technique alone. These glucose-derived polymers are all included in a single value for glucose content, which in cereal grains can also be affected by the presence of resistant starch. Specific quantification techniques are available for MLG and cellulose, and rely upon isolating these polymers or fractions of them from the cell wall mixture and then

quantifying the glucose present after conversion to monosaccharides. The cell wall of cereal grain endosperm tissue provides a good model for the study of primary cell wall structure, as there are no reports of secondary cell wall structure in these cells. Significant differences exist in the composition of the cell wall between cereal species, despite a synchronous grain development cycle with similar biological and physical stresses. The study of these differences in wheat and rice and relating them to the biological changes occurring in the two grains has provided new clues for understanding the biological role played by the individual polymers in the cereal cell wall. Thus examining the monosaccharide cell wall composition of both wheat and rice grains at 5 key stages within grain development will provide crucial information about how the cell wall is established within the developing grain and how they correlate with the developmental dynamics taking place at these time points. Comparisons of cell wall polysaccharide composition between the two species may identify homologous patterns of cell wall deposition and differences may indicate how the vastly different final cell wall compositions are established, and if there may be any link between developmental stage and cell wall differentiation in the two species. Histochemical staining of grain morphology and storage product accumulation will allow for accurate tracking of grain development in these cultivars, and provide information on the specific changes occurring within the developing grains of these two species.

3.2 Results

3.2.1 Fixation and embedding of wheat and rice grains for histochemical staining

3.2.1.1 Optimisation of fixation protocol for wheat and rice grains.

Fixation of fresh tissue samples prior to embedding is essential to ensure the preservation of the sample between harvesting and subsequent analysis. Appropriate fixation will allow the sample to remain stable and be examined many months after the initial collection. Paraformaldehyde/ glutaraldehyde fixation is one of the most widely used fixation methods for morphological studies, with the glutaraldehyde crosslinking proteins in situ, and the paraformaldehyde crosslinks adjacent nitrogen atoms in proteins and DNA. In wheat grains, a relatively short fixation period is required in the fixative solution typically 4 hours at room temperature depending on the thickness of the sections prepared from the fresh tissue and its permeability to the fixative (Tosi et al. 2009). In recent years high

pressure freezing (HPF) has also become a relatively popular fixation method for plant materials, having been widely used for the fixation of animal tissues over the last three decades. HPF allows instantaneous fixation and superior preservation of delicate and labile structures within the sample (Dahl and Staehelin 1989; Studer et al. 1992; Eshtiaghi et al. 1994; McDonald 1999; Lonsdale et al. 1999). However, it requires expensive equipment and it has the limitation that only thin sections (<200 μm sections) and small areas (<5 mm x 5 mm) of tissue can be preserved. Thus for morphological studies at the light microscopy level, chemical fixation is still favoured. It was found that rice grains transversely sectioned to 1 mm thick samples required 48 h in paraformaldehyde and glutaraldehyde fixation to achieve a comparable standard of preservation to that of wheat grains (data not shown).

In order to facilitate smooth and precise sectioning of the fixed tissue for microscopy, samples are typically embedded in a solid medium to immobilise the material, typically a specific microscopy resin such as London Resin White (LR White) or Spurr resins are used if thin or semi-thin sections are required (<2 μm) or paraffin wax is used for thicker sections (>5 μm). Sufficient infiltration of the resin throughout the fixed material is essential for structural integrity of the sample when sectioning. Following the method of Tosi et al. (2009), which includes a resin infiltration period of 7 days, good sectioning could be achieved for wheat grains. However, the same method did not give good results for rice grains, with very few sections remaining intact during sectioning, a problem that has previously been reported by Harris and Juliano (1977). In order to alleviate this problem the fixation and embedding steps were repeated with progressively longer infiltration periods in L R White resin (14, 21, 28, 35, 50 days). A progressive increase in structural integrity of the sections was noted as the infiltration period increased, until 35 days when a maximal structural integrity was reached with 1 section in every 4 cut being of sufficient quality.

Several studies have reported the dimensional changes of both wheat and rice grains during development (Briarty et al. 1979; Singh and Jenner 1982; Tashiro and Wardlaw 1990; Ishimaru et al. 2003; Yang et al. 2002). The synchronous development of both wheat and rice grains in terms of DAA allows the direct comparison of the developmental stages of the two species. By recording the dry weight changes of developing wheat and rice grains, it is possible to calculate the average changes of the levels of non-starch polysaccharides from within individual grains. The development of both wheat and rice grains appears to follow 4 phases

of growth, which coincide with developmental changes within the grains (Figure 3.1). After cellularisation, a large increase in size, weight, cross sectional area and endosperm cell number is recorded in both wheat and rice until around 8 DAA when a second phase of grain growth begins. This second phase, spanning 8 to 12 DAA, coincides with the differentiation of aleurone cells from starchy endosperm cells and the production of sub-aleurone cells, as well as with beginning of the synthesis of storage proteins. A clear reduction in the rate of growth of cell number and grain weight can be seen in this phase, by 12 DAA, however the growth rate of both cell number grain size and grain weight, has returned to roughly its initial rate of growth. This third phase of rapid growth occurs at the same time as the fastest phase of deposition of starch and storage protein in both wheat and rice, with increases of large increases in wheat and rice. Around 20 DAA a final phase of growth is recorded, with almost all metrics levelling off. At this point in grain development maturation and preparation for desiccation begins, with synthesis of starch and protein beginning to plateau at around 28 DAA. 28 DAA is often referred to as physiological maturity in wheat grains, as maximal size and weight have been reached by this point, and very little synthesis of starch or protein is recorded from that point onwards (Ishimaru et al. 2003; Shewry et al. 2009).

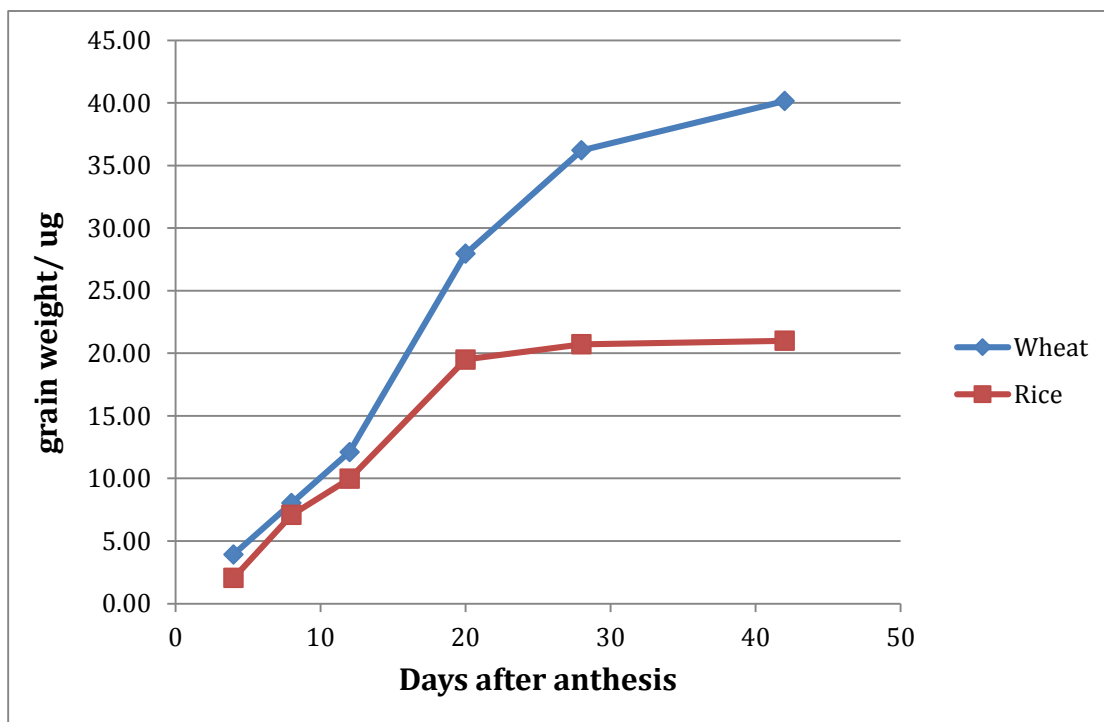


Figure 3.1. Changing grain weight in wheat and rice throughout development, extrapolated from the weight of 100 grains at each time point.

3.2.2 Morphology of starch/ protein/ cell walls/ nuclei and grain structure with histochemical stains.

The morphological changes undergone by the wheat grain during development have been studied in great detail (Briarty et al. 1979; Singh and Jenner 1982; Jenner et al. 1991; Young and Gallie 1999; Olsen 2001; Shewry et al. 2012) often utilising the histochemical stain Toluidine Blue O. Similar detailed studies were lacking in rice, with only few developmental stages having been examined. Thus a direct comparison of the five key developmental stages of grain development was carried out for wheat (cv. Cadenza) and rice (cv. Koshihikari). In order to fully understand the developmental dynamics occurring in the grains during these five phases, four histochemical stains were used: Toluidine Blue O to provide general morphology; Coomassie Brilliant Blue (CBB) to study protein body deposition dynamics, Calcofluor White to determine cell wall morphology and area through staining of cell wall polysaccharides, and potassium iodide solution (IKI) to report polysaccharide deposition (largely starch).

3.2.2.1 Staining with Toluidine Blue O reveals general tissue morphology in the developing grains

Toluidine Blue O is a histochemical stain that is widely used to study morphology of plant tissues in section. It stains proteins, nuclei and carbohydrates in a pH-dependent manner.

In wheat, at 4 DAA, the grain forms a characteristic inverted heart shape consisting largely of maternal tissue surrounding a small central area representing the recently cellularised endosperm (Fig 3.2 a). Unlike in rice the developing grain fills the area within the husk. By 8 DAA the grains of both species have enlarged considerably, although the wheat grain remains larger than the rice grain throughout development. The characteristic crease regions and two lobes become more prominent in the wheat grain at this stage, although the lobes are still relatively small. The aleurone cells become distinguishable at 12 DAA in both species as regular cuboidal cells on the perimeter of the endosperm (Fig 3.2 C, D; Fig 3.3 C, D) adjacent to the nucellar epidermis, and will have developed thick cell walls from 20 DAA onwards. The collapse of the maternal tissue at 12 DAA is much more pronounced in rice grains than in wheat grains, where several cell layers of maternal pericarp are still visible (Fig 3.2 C, D; Fig 3.3 C, D). In wheat, in fact, complete compression of the maternal pericarp does not occur till much later, at 20-28 DAA, and a few cell layers may remain intact especially in the crease region. By 28 DAA both grains have reached

their maximal size and display their characteristic shapes. In wheat this consists of two round cheek regions either side of a large central crease region and linked by a section of endosperm referred to as the prismatic region (Fig 3.3 D). The crease region in wheat contains the vascular bundle; rice lacks this characteristic region since its vascular trace lies on the dorsal surface side of the grain (Fig 3.2 D). At 28 DAA the aleurone cells of both species have strong intracellular labelling with Toluidine Blue O (Fig 3.2 F; Fig 3.3 F), unlike at 12DAA when the aleurone cells are only slightly more labelled than the adjacent sub-aleurone or starchy endosperm cells (Fig 3.2 D; Fig 3.3 D). However the aleurone cells of wheat label more strongly and with a darker hue than those of rice, indicating some differences in the cellular contents between these two species.

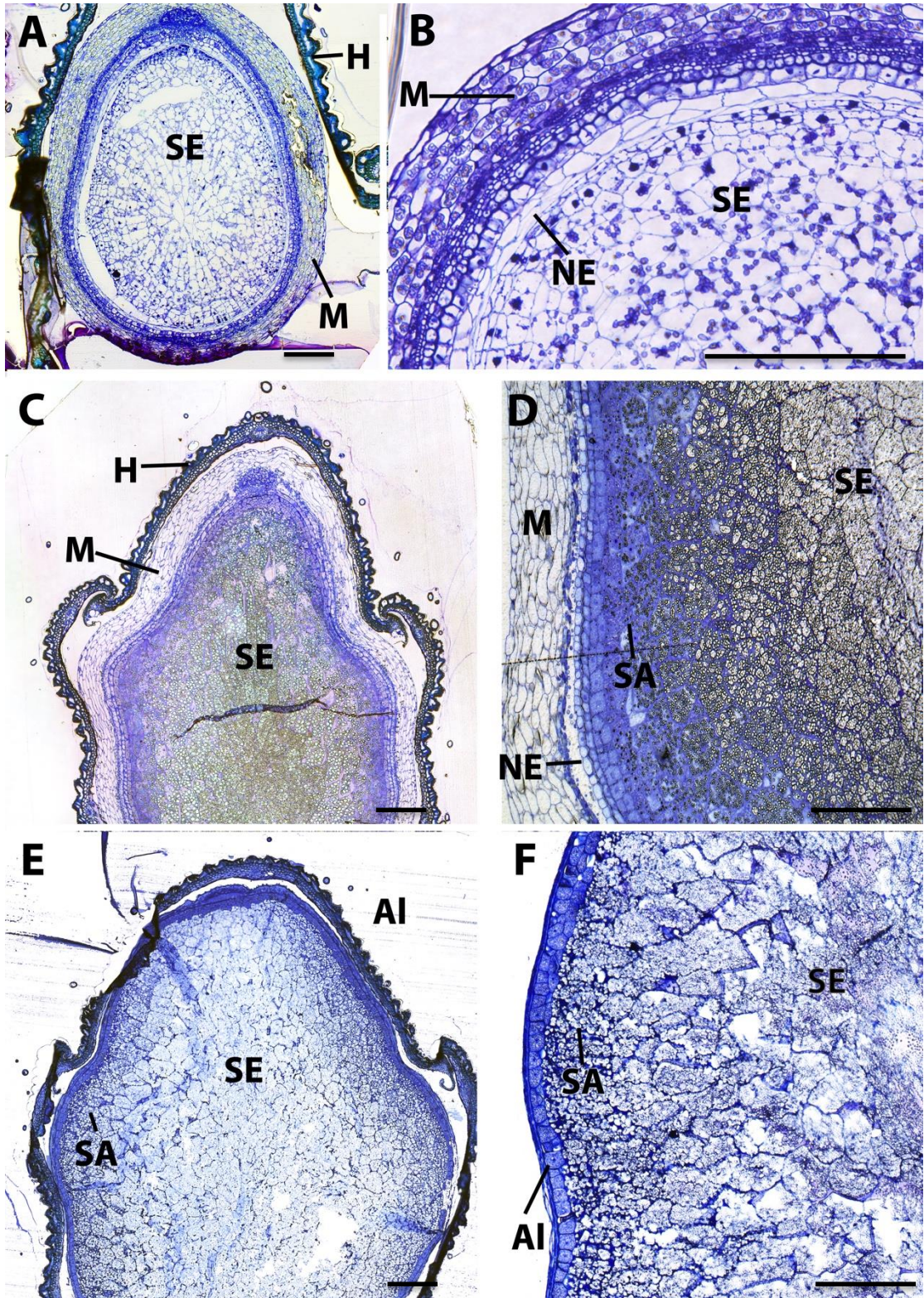


Figure 3.2. Toluidine Blue O labelling general morphology of medial transverse semi-thin (2 μ m) sections of developing rice grains a 4 DAA (A, B), 12 DAA (C, D), and 28 DAA (E, F). Micrographs C, E show half a grain section to demonstrate overall grain morphology. Micrographs B, D, F shows enlargements of the outer endosperm region of micrographs A, C, E. SE =

starchy endosperm, SA = Sub Aleurone, AI = Aleurone, M = Maternal pericarp, H = Husk, VB = Vascular bundle, NE = Nucellar epidermis. Bars = 100 μ m

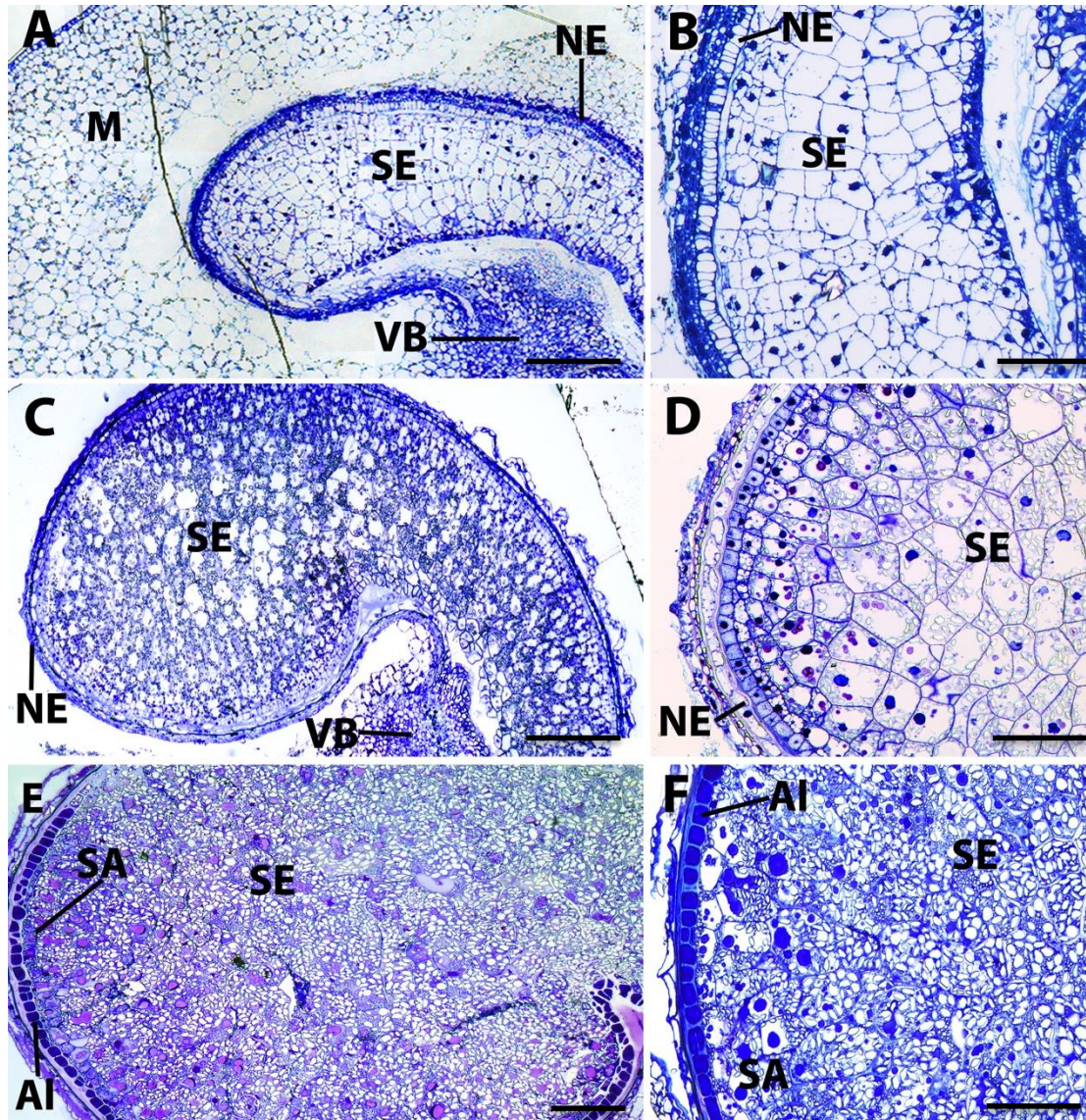


Figure 3.3. Toluidine Blue O labelling general morphology of medial transverse semi-thin (2 μ m) sections of developing wheat grains a 4 DAA (A, B), 12 DAA (C, D), and 28 DAA (E, F). Micrographs A, C, E show half a grain section to demonstrate overall grain morphology. Micrographs B, D, F shows enlargements of the outer endosperm region of micrographs A, C, E. SE = starchy endosperm, SA = Sub Aleurone, AI = Aleurone, M = Maternal pericarp, H = Husk, VB = Vascular bundle, NE = Nucellar epidermis. Bars = 100 μ m

3.2.2.2 Cell wall morphology visualised with Calcofluor White 2mr

Calcofluor White 2mr is a widely used fluorescent dye known to bind to β -glycan structures, which are found in cell walls as component of MLG, callose and cellulose

(Darken et al 1963; Ruchel et al 2001). As such Calcofluor White stain is used as a general cell wall stain allowing the examination of cell wall morphology. At 4 DAA, the cell walls of all maternal tissues are clearly distinguishable and show strong even fluorescence in both species, while the cells of the cellularising endosperm show little to no labelling with this stain (Fig 3.4 A, B). By 8 DAA, all cells of the endosperm have become stained by Calcofluor, however the labelling is stronger in the central cheek regions and the prismatic region closest to the crease cavity in wheat. This labelling pattern persists throughout wheat grain development up to 28 DAA, with the outer endosperm cells exhibiting much lower fluorescence intensity than that of the central cells or the maternal tissues (Fig 3.4 E). The aleurone cells of wheat are easily distinguished from 12 DAA by their typical cuboidal shape and from the significantly brighter fluorescence labelling than other cells of the starchy endosperm (Fig 3.4 C). As the aleurone tissues mature, the characteristic cell wall thickening appears and this new cell wall material is also strongly labelled with Calcofluor White, indicating that these cells possess more β -glycans, probably in the form of cellulose and MLG. The cells of the nucellar epidermis and those of the xylem vessels also exhibit a very strong fluorescence staining with Calcofluor White, which does not change or diminish during development (Fig 3.4 A-D + G, H). The bright fluorescence of the nucellar epidermis in particular is a useful marker to distinguish the maternal tissues of wheat from the endosperm (Fig 3.4 A, C, E, G). Rice also exhibits extensive staining with Calcofluor White, although the early cells of the cellularising endosperm are only weakly stained, unlike in wheat grains. Throughout development a similar gradient is observed, with Calcofluor White labelling more strongly the innermost endosperm cells than the outer cells and sub aleurone tissues; however the difference is less prominent than in wheat grains (Fig 3.4 D, E). Similarly to wheat, the cells of the nucellar epidermis and aleurone of rice exhibit a characteristic strong labelling, providing a reference point to differentiate maternal vegetative tissues and those of the starchy endosperm prior to maternal tissue collapse at 12 DAA. Developmentally the maternal vegetative tissue of rice grains shows a much more rapid compression/degradation than that of wheat grain, with only a couple of intact cell layers remaining by 12 DAA (Fig 3.4 D), whereas 2-4 cell layers can be seen in wheat even in mature grains (Fig 3.4 C, E). By 20 DAA the different layers of the rice maternal tissues are largely indistinguishable and are often referred to as the crushed layer. By staining with Calcofluor white it is apparent that whilst the cells have been crushed, a thick multi-layered cell wall remains externally of the aleurone layer, suggesting that the cell walls themselves are not degraded in this process (Fig 3.4 F).

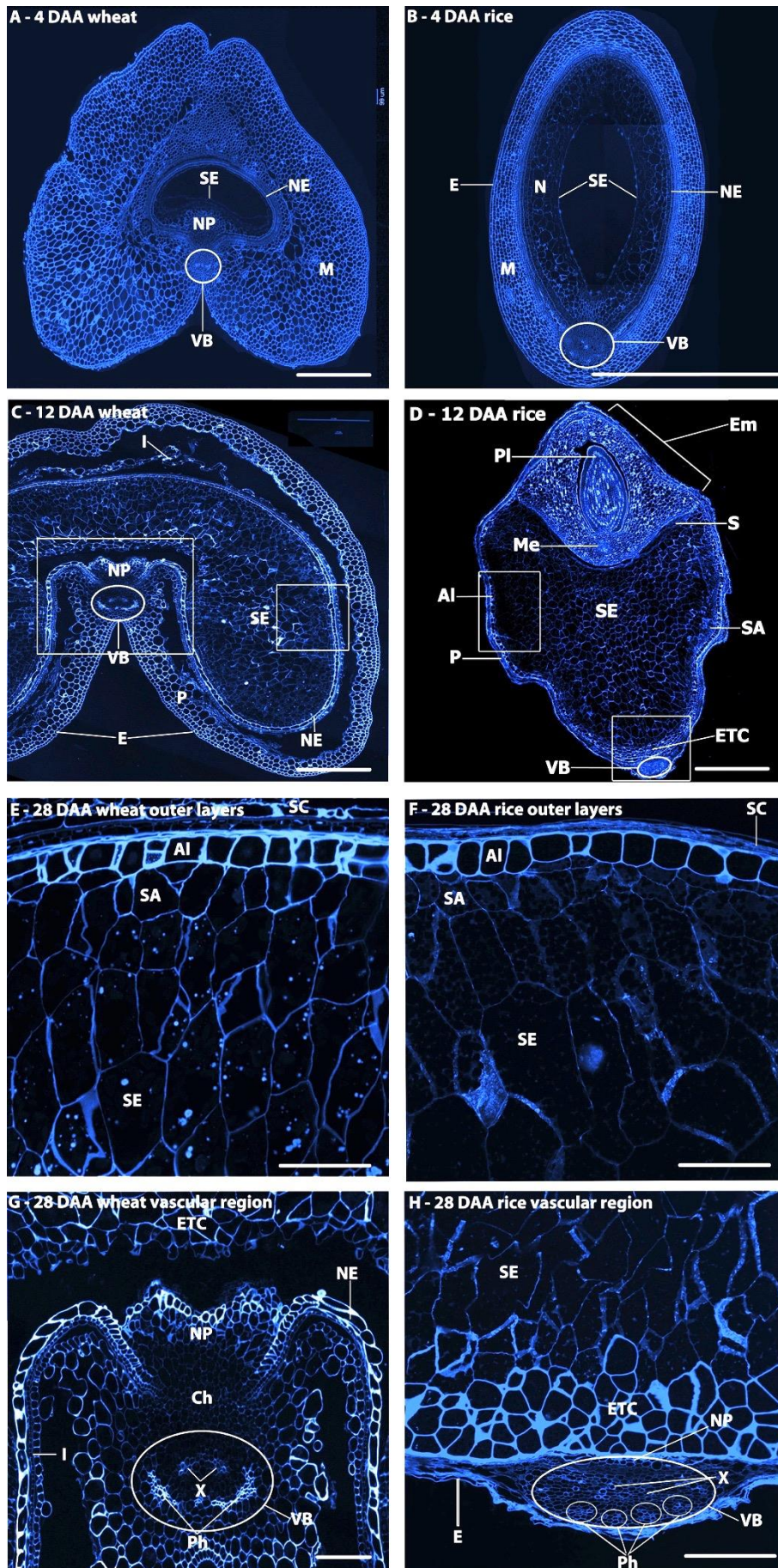


Figure 3.4. Calcofluor white 2mr staining of cell walls in medial transverse semi thin (2 μm) sections of developing wheat (A, C, E, G) and rice (B, D, F, H) grains a 4 DAA (A, B), 12 DAA (C, D), and 28 DAA (E - H). Highlighted areas in micrographs C and D, represent the crease region and outer endosperm regions imaged at 28 DAA in micrographs E-H. SE = starchy endosperm, SA = Sub Aleurone, AI = Aleurone, M = Maternal pericarp, H = Husk, VB = Vascular bundle, NE = Nucellar epidermis, ETC = endosperm transfer cells, Ph = phloem, X = xylem, I = Integuments, Ch = Chalazal region, NP = Nucellar projection, PI = plumule, Me = mesocotyl, S = scutellum, Em = embryo, E = epidermis. Bars = 100 μm

3.2.2.3 Protein body accumulation detected by labelling with Coomassie brilliant blue (CBB)

In wheat the presence of protein bodies in the cells of the endosperm cannot be detected at the light microscope at about 8 DAA, the protein bodies are very small (<1 μm) and very sparsely distributed, until 8-10 DAA when the number and size of protein bodies seen increases (Fig 3.6 A-D; Fig 3.7 A, C). From 10 DAA onwards, most protein bodies will have a diameter of 2 μm or larger, and the number and size of these protein bodies grows throughout development until 28 DAA. During this period many smaller protein bodies appear to merge into larger ones rather than a just few small protein bodies steadily increasing in size up to a maximal size of 30-40 μm (Fig 3.6 E, F). Protein body accumulation is more prevalent in the outer regions of the starchy endosperm in both the cheek regions and in the prismatic cells and includes the sub-aleurone cells from 12 DAA onwards (Fig 3.6 E, F), however the distributions is more even throughout the endosperm than in rice grains, where up to 70% of the grain protein can be found in the outer 10% of the grain.

In rice, protein deposits can first be seen in the developing endosperm from 8 DAA in the form of numerous small circular protein bodies, which reach a maximal size of around 10 μm (Fig 3.7 B, D). A higher prevalence of protein bodies is seen in the outer cells of the endosperm and the sub-aleurone cells, even more so than in wheat (Fig 3.5 C-F). Unlike in wheat, there is no evidence to suggest that the small protein bodies in the sub-aleurone or starchy endosperm cells ever fuse to create larger protein bodies. On the contrary, from 12 DAA onwards an increasing density of small separate protein bodies demonstrates that protein body merging does not occur in rice. By maturity almost all the cytoplasm of the sub-aleurone cells is filled

with protein bodies and some starch granules, and yet they remain as discrete distinguishable bodies with a maximal size of $\sim 10 \mu\text{m}$ (although high magnifications are required to distinguish separate protein bodies due to the density of protein bodies). Using light microscopy it is very difficult to distinguish the separate PB types in rice, identification of these protein body types via microscopy requires either the use of specific fluorescent antibodies for prolamin and glutelin which have been shown to be specific for certain protein body types (Furukawa et al. 2003; Ohdaira et al. 2011) or relying upon the clear differences seen in TEM after osmium tetroxide staining (Tanaka et al. 1980). Protein bodies are more easily detected in rice grains at earlier stages than in wheat with rice protein bodies being numerous and relatively large ($1\text{-}2 \mu\text{m}$) at 8 DAA (Fig 3.7 B) compared to the sparsely distributed and small ($<1 \mu\text{m}$) PBs of wheat at this stage (Fig 3.7 A). At 10 DAA the difference in size between wheat and rice PBs is less noticeable, but the wheat grains still possesses fewer PBs than rice (Fig 3.7 C, D). By maturity a similar distribution of protein bodies is seen in both species, with similar total protein contents per grain being reported ($\sim 7\%$ dry weight of wholegrain)

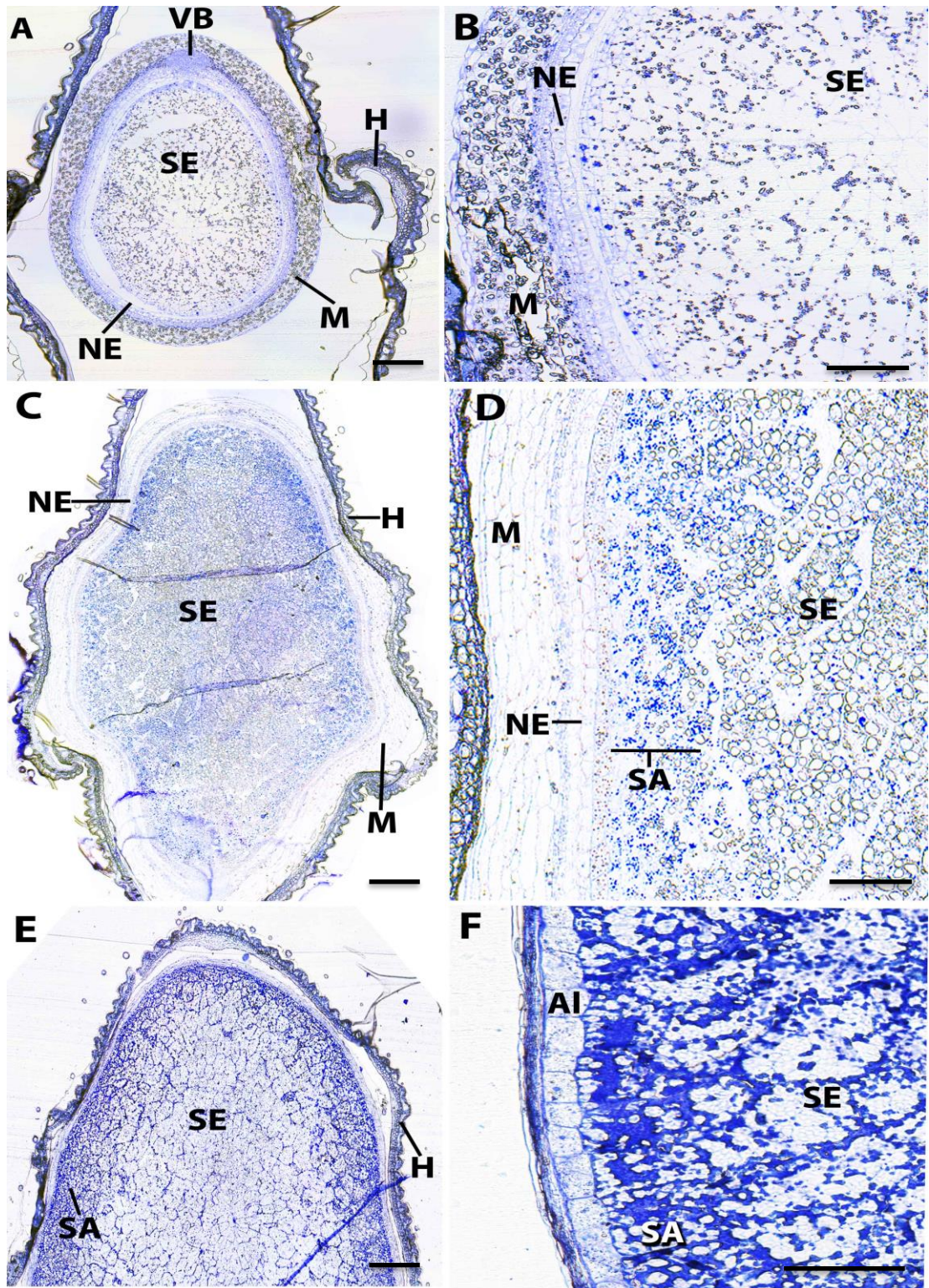


Figure 3.5. Coomassie Brilliant Blue (CBB) staining protein in medial transverse semi-thin (2 μ m) sections of developing rice grains a 4 DAA (A, B), 12 DAA (C, D), and 28 DAA (E, F). Proteins bodies stain a intense blue colour and are approximate 2 μ m in diameter larger circular blue staining represent nuclei, and prevalent in micrograph B. Micrographs B, D, F shows enlargements of the outer endosperm region of micrographs A, C, E. SE =

starchy endosperm, SA = Sub Aleurone, AI = Aleurone, M = Maternal pericarp, H = Husk, VB = Vascular bundle, NE = Nucellar epidermis. Bars = 100 μ m

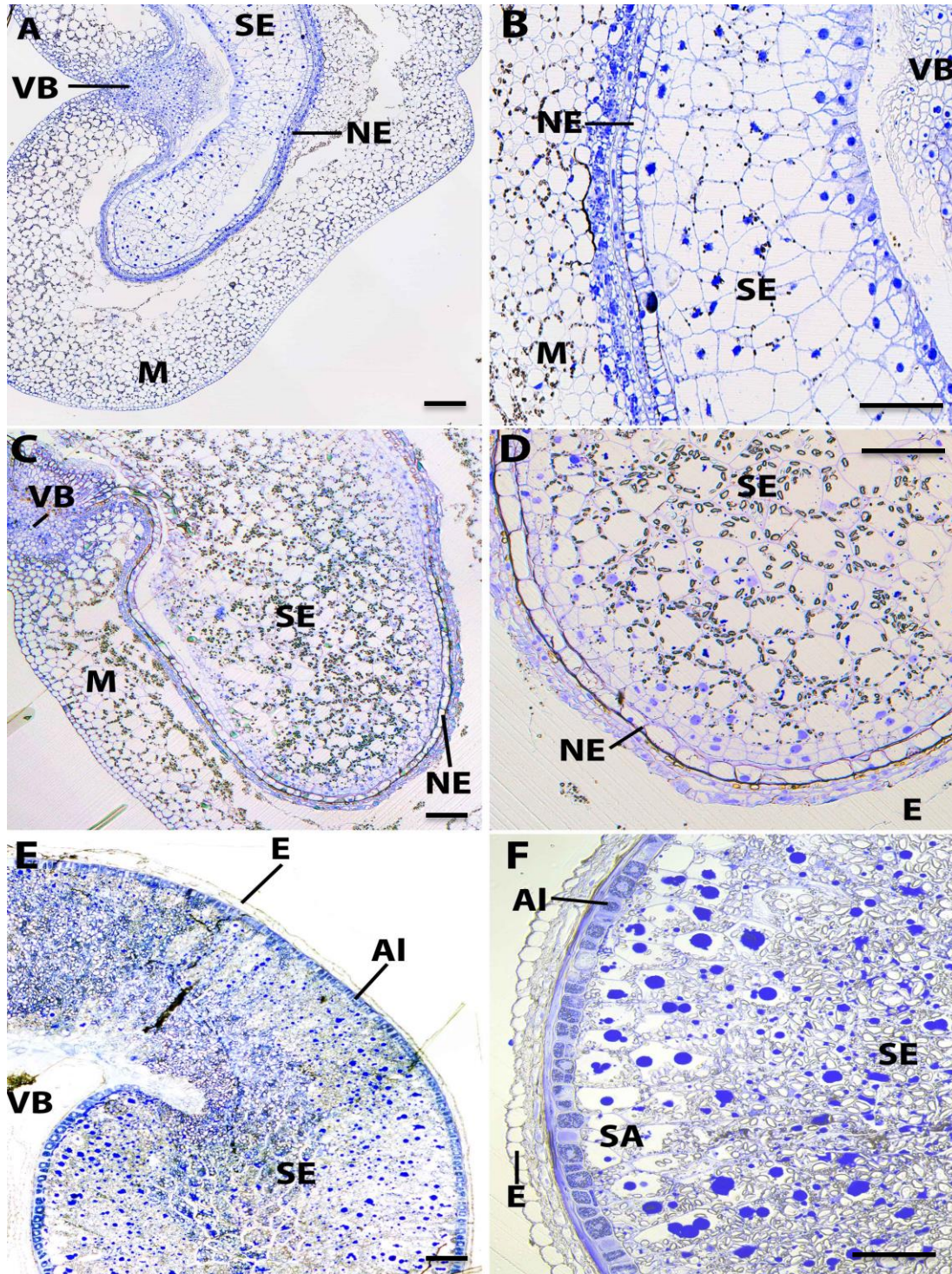


Figure 3.6. Coomassie Brilliant Blue (CBB) staining protein in medial transverse semi-thin (2 μ m) sections of developing wheat grains a 4 DAA (A, B), 12 DAA (C, D), and 28 DAA (E, F). Proteins bodies stain a intense blue colour, paler blue circular staining represents nuclei, which are prevalent in micrographs B and D. Micrographs B, D, F shows enlargements of the outer

endosperm region of micrographs A, C, E. SE = starchy endosperm, SA = Sub Aleurone, AI = Aleurone, M = Maternal pericarp, H = Husk, VB = Vascular bundle, NE = Nucellar epidermis. Bars = 100 μ m

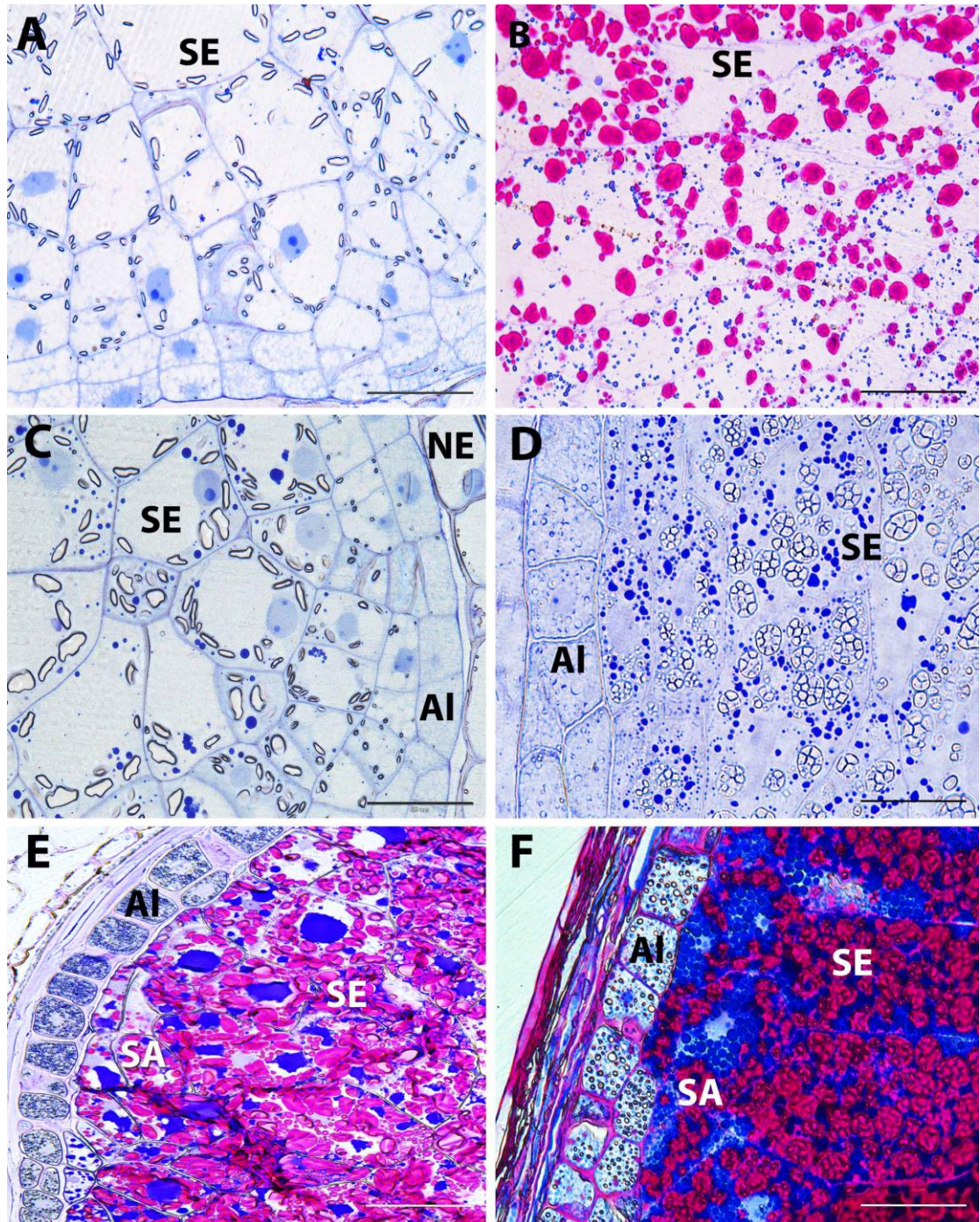


Figure 3.7. Coomassie Brilliant Blue (CBB) staining protein in medial transverse semi-thin (2 μ m) sections of developing wheat (A, C, E) and rice (B, D, F) grains a 8 DAA (A, B), 12 DAA (C, D), and 28 DAA (E, F) showing the deposition of protein bodies in both species. Micrographs B, E, F are counter

stained with PAS which stains carbohydrates red. SE = starchy endosperm, SA = Sub Aleurone, AI = Aleurone, NE = Nucellar epidermis. Bars = 50 μ m

3.2.2.4 Starch accumulation detected using potassium iodide solution.

Starch deposition in rice endosperm appears to begin slightly before cellularisation has been completed, this is in contrast to reports of starch deposition in the *Triticae* where it is commonly accepted that deposition only begins after cellularisation is completed. Starch granules can only be seen from 6 DAA onwards in wheat grains of cv. Cadenza with light microscopy (Fig 3.9 A, B), corroborating these reports. However a recent paper by Yin et al. (2012) has reported amyloplast filling from 4 DAA when examined with TEM. In rice cv. Koshihikari, the deposition of starch granules appears to be more concentrated in the central endosperm region and then extends towards the outer regions along a decreasing gradient with the cells of the sub-aleurone exhibiting very little starch deposition prior to 28 DAA (Fig 3.8 A, C, E). Similarly to rice, starch accumulation in wheat is stronger in the central region of the endosperm, particularly in the lobes, although it never shows the density of starch granules that can be observed in rice central endosperm (Fig 3.9 C, E). Neither wheat nor rice accumulate starch in the cells of the aleurone layer (Fig 3.8 E; Fig 3.9 E).

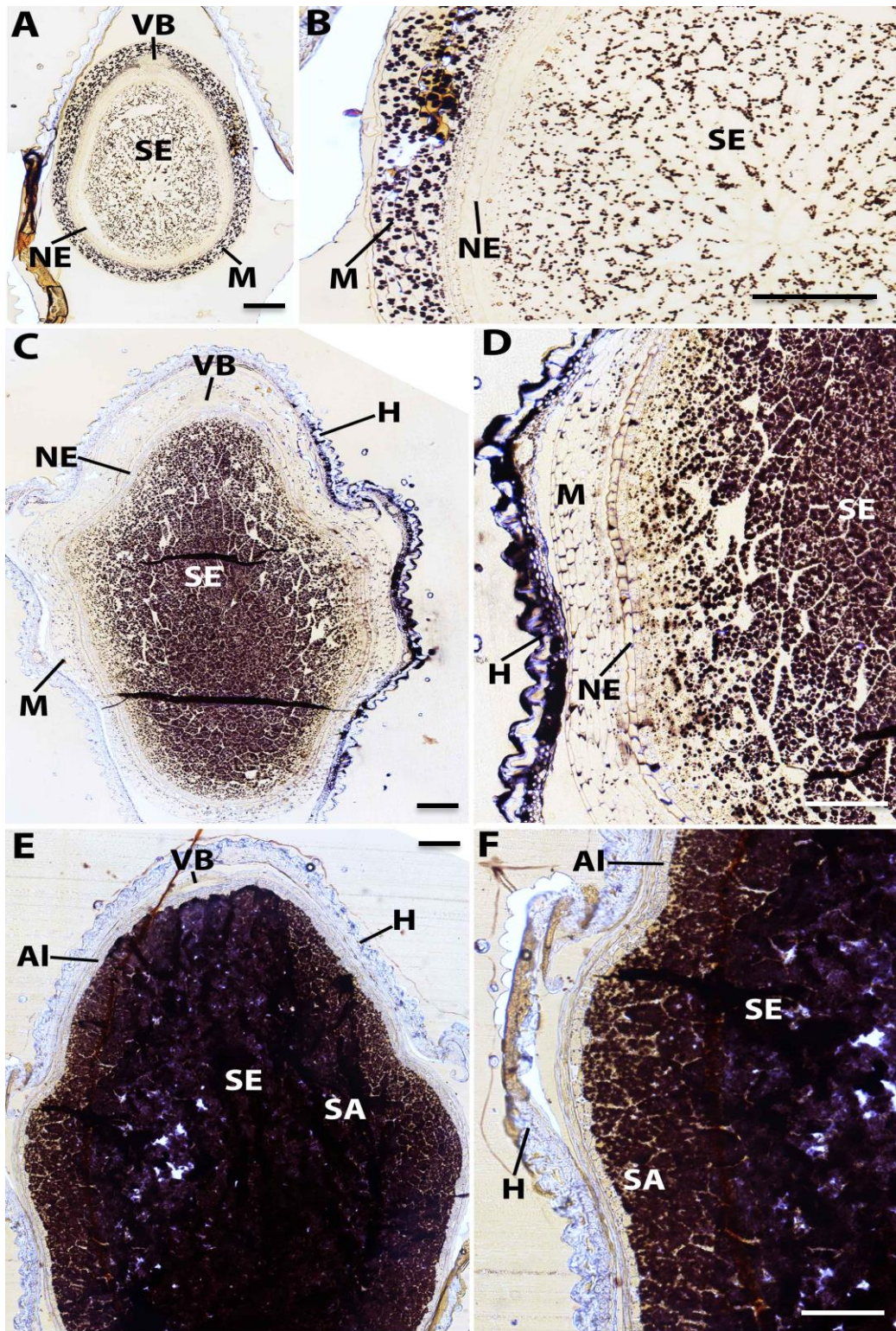


Figure 3.8. Potassium iodide (IKI) staining of starch in medial transverse semi thin (2 μm) sections of developing wheat grains a 4 DAA (A, B), 12 DAA (C, D), and 28 DAA (E, F). Micrographs B, D, F shows enlargements of the outer endosperm region of micrographs A, C, E. SE = starchy endosperm, SA = Sub Aleurone, AI = Aleurone, M = Maternal pericarp, H = Husk, VB = Vascular bundle, NE = Nucellar epidermis. Bars = 100 μm

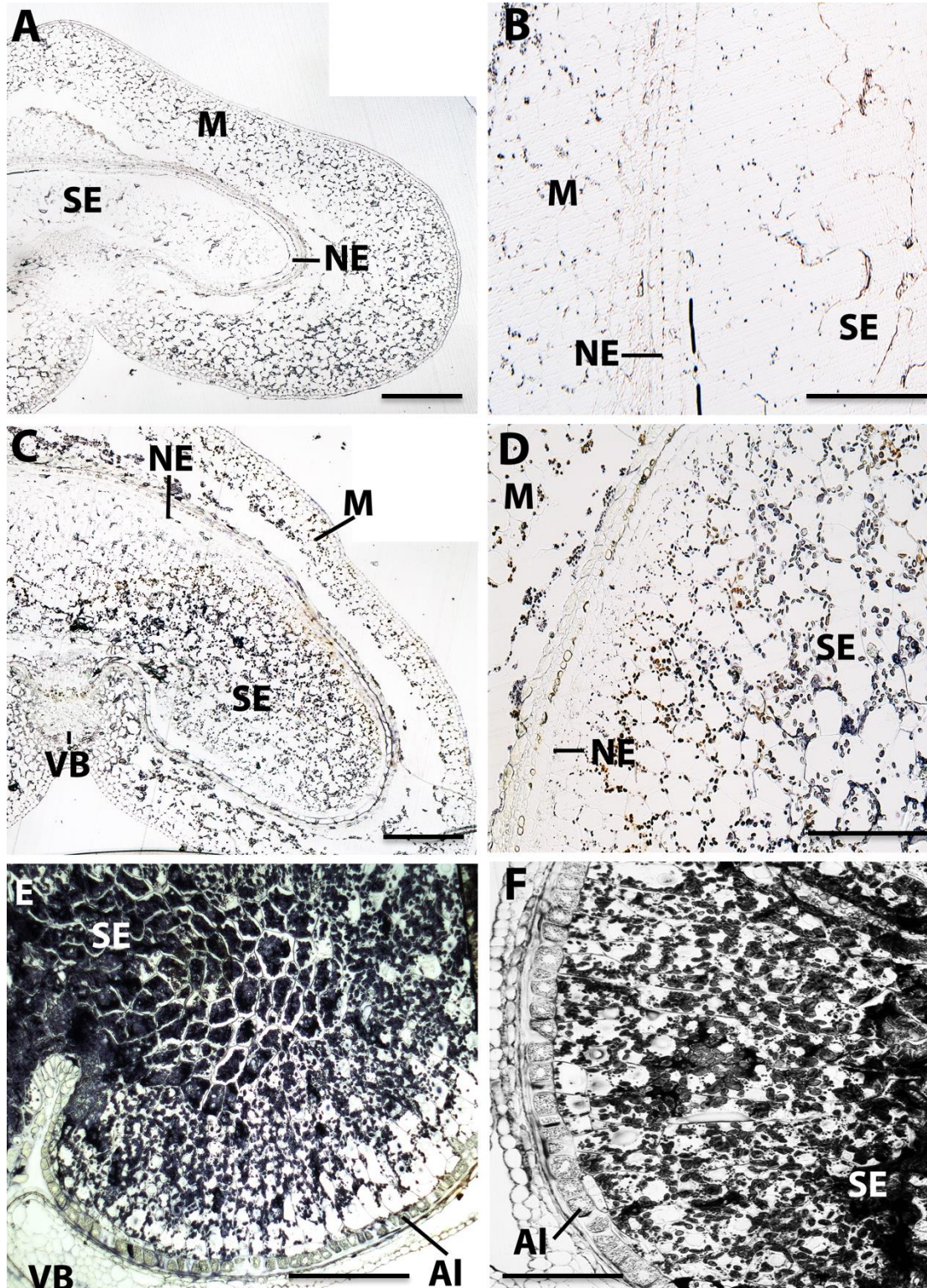


Figure 3.9 Potassium iodide (IKI) staining of starch in medial transverse semi thin ($2\ \mu\text{m}$) sections of developing rice grains a 6 DAA (A, B), 12 DAA (C, D), and 28 DAA (E, F). Micrographs B, D, F shows enlargements of the outer endosperm region of micrographs A, C, E. SE = starchy endosperm, SA = Sub

Aleurone, AI = Aleurone, M = Maternal pericarp, H = Husk, VB = Vascular bundle, NE = Nucellar epidermis. Bars = 100 μ m

3.2.3 Monosaccharide analysis of cell wall polysaccharides (HPLC/GC)

3.2.3.1 Extraction of cell wall polysaccharides from milled grain material

While most studies of the composition of cell wall polysaccharides in wheat flour have used the same non-starch polysaccharide (NSP) extraction method (Englyst et al. 1992; Englyst et al. 1994) giving consistent monosaccharide compositions, the same cannot be said for rice, with many different extraction protocols being reported together with significant differences in rice cell wall composition. In order to explore which method would yield the most complete extraction of cell wall polysaccharides from rice flour, five different cell wall extraction methods were compared, using commercially sourced polished cv.Koshihikari rice (Sushissushi.com) as a proxy for rice flour. Polished rice is >95% starchy endosperm tissue, lacking the outer maternal tissues and most of the aleurone layer due to surface abrasion, and once milled gives a product which is comparable with white rice flour. The five methods selected consisted of two alcohol insoluble residue protocols (AIR 1, AIR 2; Methods 2.5.1.2, 2.5.1.3), which are two variants of the most common cell wall extraction procedure, and two methods taken from Shibuya et al. (1985) and Lai et al (2007). These methods will be referred to herein as the Shibuya method and the Lai method. Finally a direct comparison to the wheat extraction method was made by using a slight modification of the Englyst et al. (1994) method.

The compositions of three technical replicates of the extraction procedures were determined using a Dionex HPLC method (Method 2.5.2). The Englyst method extracted the highest amounts of almost every monosaccharide. (Table 3.1.) The two AIR protocols appeared promising when in the initial phases of analysis, but due to the large amounts of glucose present, which was mainly derived from starch degradation, some data was lost due to overlapping peaks on the chromatograms. In order to reduce the starch and thus glucose content to a level comparable to the other protocols an additional α -amylase digest step was added that was identical to that in the Englyst method. However the inclusion of this additional step appeared to cause the loss of significant proportions of many monosaccharides, rendering the methods unsuitable for further use without further optimisation of the protocol to retain polysaccharides from the α -amylase digest.

The modified Englyst protocol was selected as the optimal procedure for the extraction of cell wall polysaccharides from the samples of developing wheat and rice grains. It has previously proven to be a robust method for wheat grain cell wall extraction, and appears to be the best available option at present for rice grains, while also allowing for direct comparison with wheat cell wall analyses.

Table 3.1. Comparison of the monosaccharide contents of the rice cell wall material extracted from 150 mg of milled polished rice and scaled to $\mu\text{g/g}$ of sample material. Monosaccharide contents are quantified via HPLC, the peaks on the chromatograph can merge together due to their proximity. Average of 3 technical replicates. * indicates xylose peak obscured by the tail of the glucose peak. ** indicates mannose peak obscured by the tail of either glucose peak due to excessive glucose generated by incomplete starch digestion.

Extraction protocol	Monosaccharide content per gram of milled sample tissue. ($\mu\text{g/g}$)							
	Rha	Fuc	Ara	Gal	Glc	Xyl	Man	GalA
AIR 1	70.36	39.27	525.88	91.43	73940.26	0.00*	0.00*	348.83
AIR 1 + α -amylase	66.30	0.00	536.46	130.63	13985.00	708.52	0.00*	658.90
AIR 2	47.64	17.27	642.79	241.40	6	0.00*	0.00*	369.18
AIR 2 + α -amylase	60.74	0.00	575.68	168.55	13508.76	720.82	25.84	806.36
Englyst	81.07	44.73	685.28	156.24	2725.61	869.47	79.11	553.79
Shibuya	14.48	0.00	111.29	45.23	25708.32	0.00*	0.00*	287.61
Lai	16.32	0.00	136.96	52.17	22874.29	0.00*	0.00*	252.48

3.2.3.2 HPLC monosaccharide data.

Monosaccharide analysis using chromatography allows the detection and quantification of very small amounts of carbohydrates. Unfortunately both HPLC and GC methods have their limitations. In GC analysis, for example, the acidic sugars are not labelled by the derivitisation procedure, and thus have to be assayed using a separate methodology. HPLC analysis does not require a complicated derivitisation protocol, and can detect both neutral and acidic sugars, however, several monosaccharides are difficult to separate (notably xylose and mannose), and large quantities of certain monosaccharides (typically glucose in cereal grains) create significant tailing, which may interfere with detection of others.

NSP was prepared using the Englyst isolation procedure (chapter 3.2.4) at all five developmental stages and analysed using HPLC. The peak areas from the chromatograms were correlated with standards of known quantities of monosaccharides, and expressed in two ways: as μg of monosaccharide per gram of starting ball milled wholegrain material, and as μg of monosaccharide per grain at each developmental time point. As the grain weight changes dramatically between developmental stages in both species (fig 3.1) the monosaccharide content must be converted to a per grain basis to allow monosaccharide dynamics to be examined.

3.2.3.2.1 Monosaccharide content per gram of sample material shows minimal changes in the proportions of developing wheat, but rice shows significant changes in the ratio of cell wall composition between 4-12 DAA.

The contents of most monosaccharides change only subtly during wheat development, however arabinose and xylose concentrations decreases from 4748 $\mu\text{g/g}$ and 6139 $\mu\text{g/g}$ to 3500 $\mu\text{g/g}$ and 3852 $\mu\text{g/g}$ respectively between 4 to 12 DAA, before stabilising with xylose showing a slight increase by 28 DAA (Table 3.2). A large rise of 432% was also seen mannose between 4 and 12 DAA. All other monosaccharides show similar content from 4 DAA to 28 DAA (Fig 3.10).

In rice, however several changes were seen in the 4-12 DAA period, with arabinose, xylose and galactose concentrations falling rapidly before levelling off at 12 DAA, whilst fucose, rhamnose and mannose showed a smaller but still large decrease over the same period. All other monosaccharides remained consistent from 4 DAA

to 12 DAA (Fig 3.11). The period from 4-12 DAA coincides with the period of maternal tissue collapse and degradation in the developing rice grain, thus it is likely that the loss of cell wall material provided by the maternal tissues is contributing to the decline in the concentrations of xylose, arabinose and galactose and pectic monosaccharides. In wheat, the maternal cell layers are also seen to degrade and disappear throughout grain development, however, the process occurs steadily and slowly throughout development compared to rice. Thus it is probable that in wheat the increase in cell wall deposition from the expansion and division of the starchy endosperm is at a similar level to the loss of cell wall content from the maternal tissue.

A second phase of monosaccharide changes can be detected in developing rice grains, with galacturonic acid, fucose, rhamnose and galactose content increasing steadily from 12 DAA to a peak at 28 DAA, with galacturonic acid and galactose representing similar levels as arabinose and xylose. This increase in pectin related monosaccharides might be a desiccation tolerance modification, the comparable increases were detected in fucose and rhamnose concentrations suggest that both RG-I content and HG content increase at similar rates during this period.

Table 3.2. Average monosaccharide content per gram of milled sample material ($\mu\text{g/g}$) (from three technical replicates), in wholegrain wheat and rice throughout the course of grain development and a mature polished white flour sample, as detected by HPLC analysis of non-starch polysaccharide. DAA = days after anthesis.

Average wholegrain monosaccharide content per gram of flour (μg) \pm 1 standard deviation																	
Sample	DAA	Fuc	Rha	Ara	Gal	Xyl	Man	GalA	GlcA								
Rice	4	611.9	4.4	1585.2	127.1	6805.6	249.8	5305.4	14.5	5099.2	513.1	1182.6	87.1	1109.3	166.4	203.5	30.5
	8	439.7	21.0	943.7	34.5	2034.1	5.5	3203.9	37.0	2432.0	220.0	489.2	5.2	1219.5	182.9	350.3	52.5
	12	195.5	11.8	543.6	35.3	1531.1	128.9	1403.8	101.3	1311.2	201.4	185.4	16.4	1076.2	161.4	288.8	43.3
	20	296.1	21.3	662.6	72.5	1458.4	51.2	1537.3	160.0	1402.4	64.5	205.1	15.3	1343.9	201.6	288.7	43.3
	28	386.4	67.0	1071.7	124.7	1721.9	85.9	2373.3	287.3	1515.4	27.2	371.8	46.7	1586.4	238.0	288.3	43.2
Wheat	4	79.9	7.4	130.8	9.0	4748.3	1191.3	2133.9	354.5	6139.1	1877.5	347.1	60.5	1280.3	192.0	246.8	37.0
	8	65.0	7.7	53.8	8.3	3981.2	914.1	1326.9	196.8	4854.2	1141.9	986.20	131.1	1420.1	213.0	258.3	38.7
	12	118.7	13.1	69.8	6.7	3500.0	702.0	1220.1	189.8	3852.6	992.6	1309.29	241.5	1106.3	165.9	317.1	47.6
	20	123.5	8.6	33.4	1.9	3120.5	300.3	874.1	70.0	4283.8	748.8	960.14	51.5	1345.2	201.8	343.2	51.5
	28	279.0	5.5	50.0	3.5	3244.2	319.3	1812.1	697.2	4717.8	1003.5	846.26	8.4	1189.2	177.5	227.7	34.2

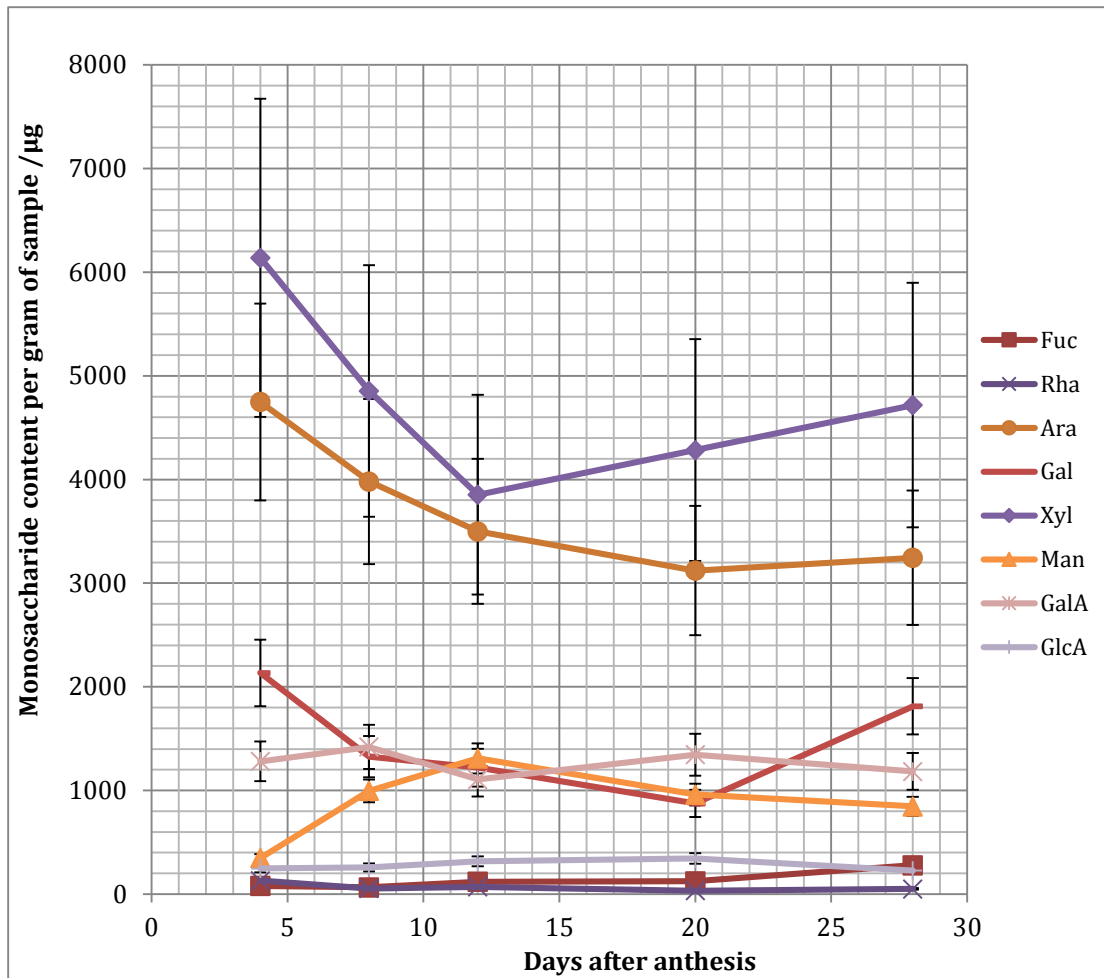


Figure 3.10. Monosaccharide content per gram of milled material in developing wholegrain wheat. Error bars denote the variance of 3 technical repeats.

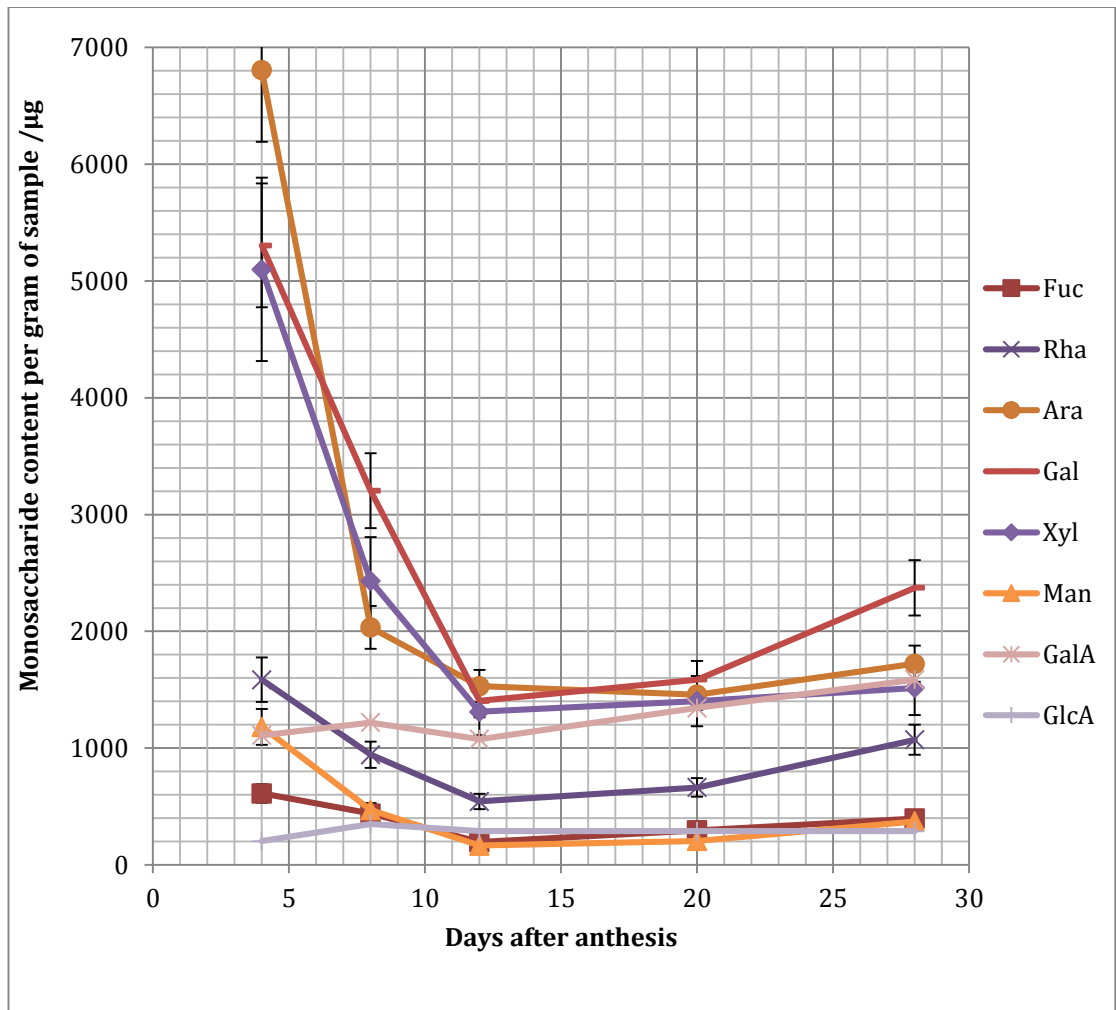


Figure 3.11. Monosaccharide content per gram of milled material in developing wholegrain rice. Error bars denote the variance of 3 technical repeats.

3.2.3.2.2 Wheat and rice cell wall deposition appears to follow a 4 phase pattern with the periods between 4-8 DAA and 12-20 DAA showing the significantly higher rates of cell wall deposition in both species.

In both wheat and rice, four phases of cell wall deposition can be detected. The rates of deposition of different monosaccharides differs slightly, but the four phases are still seen across all monosaccharides, however the pattern is more pronounced in rice grains than in wheat (Table 3.3; Fig 3.12 - 3.13). The first phase from 4-8 DAA is characterised by a rapid deposition of cell wall monosaccharides, which may be expected in line with the rapid cell division and expansion occurring during this phase of grain development. In wheat, most monosaccharides exhibited a large increase in content from 4 DAA to 8 DAA with increases upto 58% in arabinose and 67% xylose and 109 and 122% increases in glucuronic acid and galacturonic acid

respectively (Fig 3.12). A greater variation was seen in the rate of increase of monosaccharide content in rice grains from 4 DAA to 8 DAA, however, rates were higher for rhamnose and galactose, ranging in increases from 106%-109%. Glucuronic acid, galacturonic acid and fucose increased at rates of 248%-490% increase in rice, however the increase in xylose was noticeably lower and more in line with deposition rate in wheat at 64% increase (Fig 3.13). Unexpectedly arabinose content only increased 3% in rice but taken with the 490% increase in glucuronic acid, this may indicate the deposition of a highly substituted xylan without arabinose decoration. The second phase of cell wall deposition from 8-12 DAA exhibits both decreases and increases depending of the particular monosaccharide. In wheat, only no decreases were detected but galacturonic acid, xylose and arabinose and galactose all showed small increases at 19-38%, with all other monosaccharides showing larger increases in content on a per grain basis. In rice, arabinose, galacturonic acid and glucuronic acid showed modest increases at 6-24%, while all other monosaccharides showed modest decreases 19-49% although the ~15% experimental error may account for some of these decreases. The period from 8-12 DAA in wheat and rice is a period of re-differentiation with little grain expansion or cell division occurring, which may account for the small changes in cell wall content in both species at this developmental stage. The third period from 12-20 DAA is a second phase of rapid cell wall deposition, however it is not as rapid as the 4-8 DAA period. In wheat, increases of 67% to 184% were detected from 12-20 DAA, which are roughly half the rate seen in wheat from 4-8 DAA given the time period is 8 days rather than 4. Xylose arabinose, galacturonic acid and glucuronic acid were the monosaccharides with the biggest increase during this period in wheat with 108%-184% increases, implicating increases in AX and HG deposition in this period. Rice similarly showed pronounced increases in arabinose (86%), xylose (109%) and galacturonic acid (184%), with all other monosaccharides showing similar large increases (95%-196%). The 4th phase from 20-28 DAA coincides with maturation of the grain and it has been hypothesised that desiccation tolerance is generated in the grain during this time. This phase of cell wall deposition both in wheat and rice grains, shows a mix of increases in some monosaccharides and levelling off of other monosaccharides. In wheat, the RG-I components fucose, rhamnose, and galactose all show the most prominent increases at this stage (190%, 93% and 166% respectively) with the arabinose and xylose content also increasing (34% and 42% respectively). Galacturonic acid content also increases slightly in this phase (10%) but this is similar to the ~15% experimental error. In rice, arabinose xylose and galacturonic acid shows a small increase (14-25%) in content

while the RG monosaccharides fucose, rhamnose, galactose all show larger increases of 42-72%, but significantly smaller increases than the same monosaccharides in wheat at this time point. The continued deposition of pectin in both species, and in particular RG monosaccharides, may indicate a conserved adaptation mechanism to provide enhanced desiccation tolerance to the maturing cereal grain. (Moore et al. 2008a; Moore et al. 2008b; Moore et al. 2013).

Table 3.3. Average monosaccharide content per grain (μg) (from three technical replicates), in wholegrain wheat and rice throughout development, as detected by HPLC analysis of non-starch polysaccharide. DAA = days after anthesis.

		Wholegrain monosaccharide content/ μg per grain															
Sample	DAA	Fuc	Rha	Ara	Gal	Xyl	Man	GalA	GlcA								
Rice	4	1.26	0.01	3.25	0.26	13.96	0.51	10.89	0.03	10.46	1.05	2.43	0.18	2.27	0.34	0.42	0.06
	8	3.12	0.15	6.69	0.24	14.42	0.04	22.71	0.26	17.24	1.56	3.33	0.04	8.64	1.30	2.48	0.37
	12	1.95	0.12	5.43	0.35	15.28	1.29	14.01	1.01	13.09	2.01	1.65	0.16	10.74	1.61	2.88	0.43
	20	5.77	0.41	12.92	1.41	28.44	1.00	30.95	3.12	27.35	1.26	4.00	0.30	26.21	3.93	5.63	0.84
	28	8.21	1.39	22.21	2.58	35.68	1.78	49.18	5.95	31.40	0.56	7.70	0.97	32.87	4.93	5.97	0.90
Wheat	4	0.32	0.03	0.52	0.04	18.99	4.77	8.54	1.42	24.56	7.51	1.39	0.24	5.12	0.77	0.99	0.15
	8	0.52	0.06	0.43	0.07	31.85	7.31	10.61	1.57	38.83	9.13	7.97	1.05	11.36	1.70	2.07	0.31
	12	1.42	0.16	0.84	0.08	42.00	8.42	14.64	2.28	46.23	11.91	15.71	2.90	13.28	1.99	3.81	0.57
	20	3.46	0.24	0.93	0.05	87.38	8.41	24.47	1.96	119.95	20.97	26.88	1.44	37.66	5.65	9.61	1.44
	28	10.04	0.20	1.80	0.13	116.79	11.50	65.24	25.10	169.84	36.13	30.47	0.30	41.41	6.21	7.97	1.20

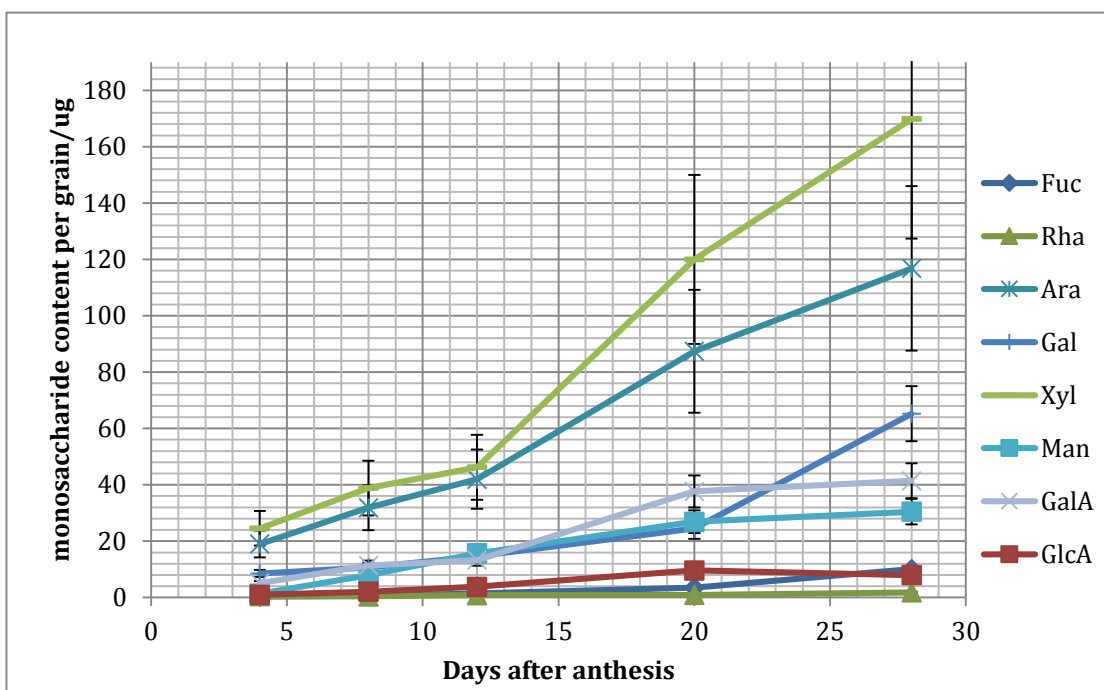


Figure 3.12. HPLC Monosaccharide content per grain in developing wheat grains. Average of 3 technical replicates based on an analysis of 100mg of milled starting material. Error bars denotes variance.

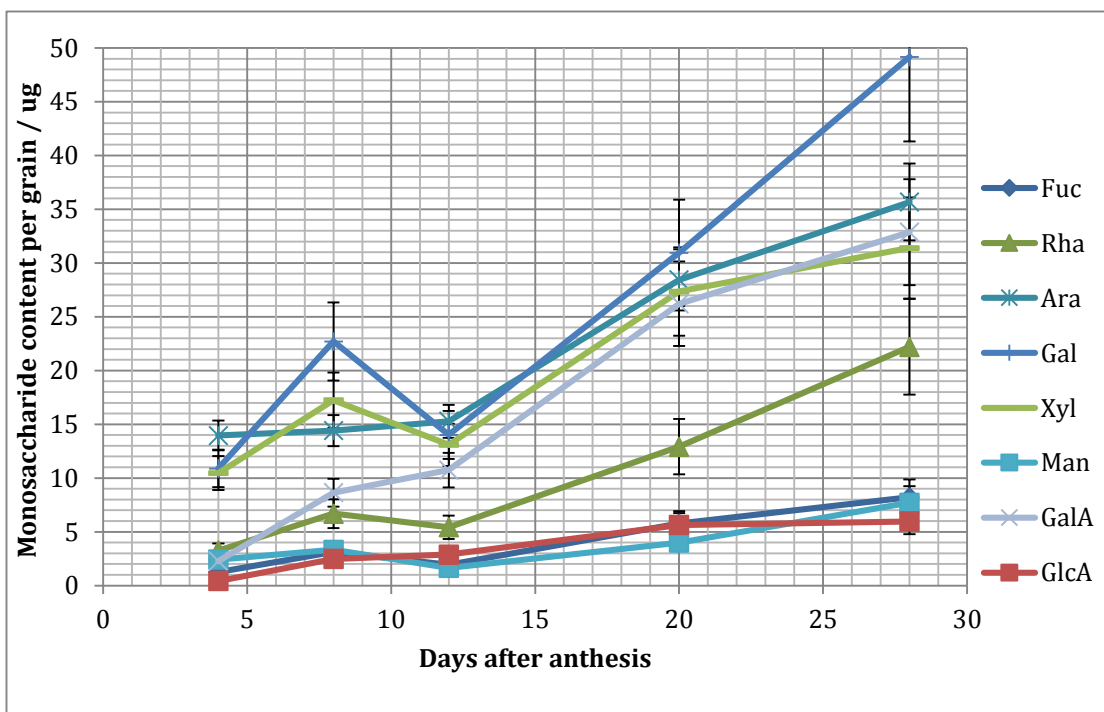


Figure 3.13. HPLC Monosaccharide content per grain in developing rice grains. Average of 3 technical replicates based on an analysis of 100mg of milled starting material. Error bars denotes variance.

3.2.4 Quantification of MLG content in developing wheat and rice grains with Megazyme MLG colorimetric assay kit.

3.2.4.1 Optimisation of the Megazyme MLG kit for detection in developing wheat and rice.

Analysis of mixed link β -glucan in cereal grains using conventional GC or HPLC monosaccharide analyses is theoretically possible but is practically challenging. The primary reason for this is the very high starch content of cereal grains, typically 70-80% w/w, compared to a total of 1-5% of cell wall monosaccharides. Any starch not removed by enzymatic or sequential solvent extraction methods can easily contaminate the total glucose content present in the cell wall. Other contamination can arise from glucose-based cell wall components such as cellulose, xyloglucan and callose or oligosaccharides such as stachyose or raffinose, and other simple sugars such as sucrose, which are not completely removed prior to analysis. Resistant starch is often undigested by α -amylases and pullanases, and can give significant glucose peaks in these chromatographic analyses. The glucose peak will also contain contributions from other glucosic polysaccharides. Typically a colorimetric technique is employed to avoid these problems, by digesting the MLG using lichenase, solubilizing the short glucose oligosaccharides from the cell wall, which can then be easily separated from the rest of the sample and converted to glucose with β -glucosidase. Colorimetric analysis of the glucose in solution is then used to quantify the MLG content. Wheat and rice starchy endosperms are reported to have similar levels of MLG at ~20% and 23% of cell wall respectively, but no data on how this polymer is accumulated throughout development was available.

Initial trials with the method provided by Megazyme International with their kit (Chapter 2.5.3.1), showed that the method was not sufficiently sensitive to allow accurate quantification of the much smaller amounts of MLG in wheat and rice compared to oat or barley grain cell walls, which the test was designed for. The protocol was tested with the dilution step reduced by 10 fold, and using white endosperm flour from wheat and rice as a test material. This allowed detection of MLG in both wheat and rice white flours (~0.2% of starting material) while still accurately detecting the much higher concentrations of barley and oat flours (containing 4.1% and 6% MLG respectively) with an accuracy of $\pm 0.1\%$ (Chapter 2.5.3.2).

Table 3.4. Detection of D-glucose (25-100 µg per cuvette) with Megazyme MLG kit for production of D-glucose standard calibration curve.

Sample	Abs @ 510nm	Glucose content/ µg
25 µg	0.259	26.98
25 µg	0.247	25.73
25 µg	0.264	27.50
50 µg	0.490	51.04
50 µg	0.443	46.15
50 µg	0.474	49.38
75 µg	0.743	77.40
75 µg	0.721	75.10
75 µg	0.751	78.23
100 µg	0.933	97.19
100 µg	0.951	99.06
100 µg	0.956	99.58
Barley std	0.334	34.79

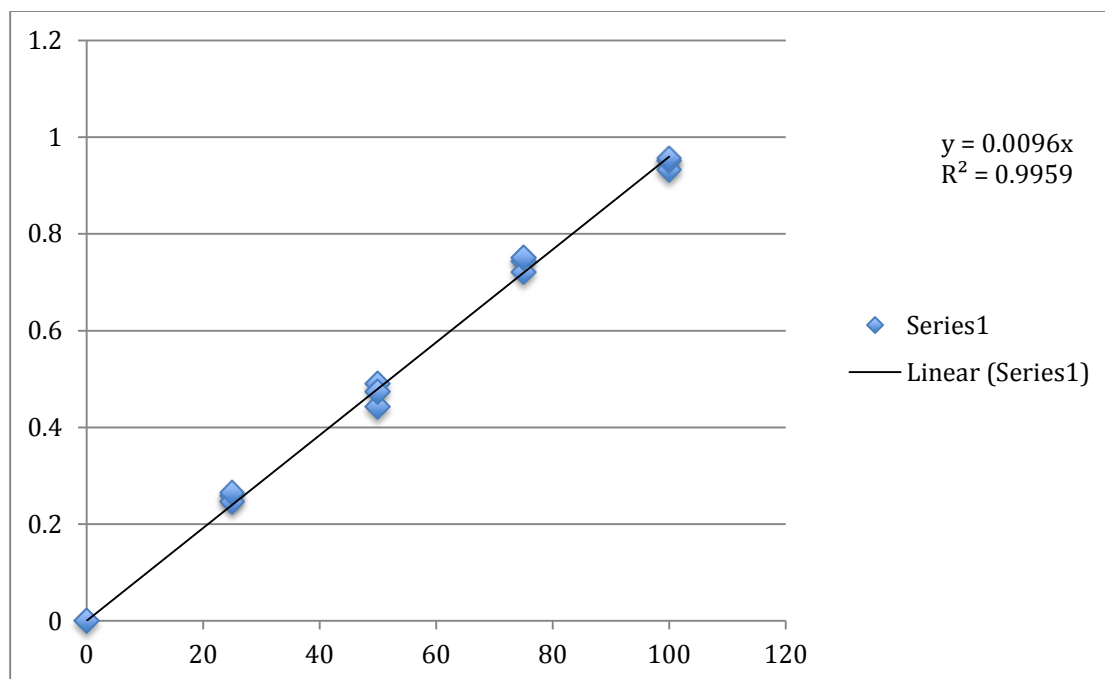


Figure 3.14. D-glucose absorbance response curve at 510 nm with GOPOD reagent.

3.2.4.2 Determination of MLG content of developing wheat and rice grain with optimised Megazyme procedure

MLG content expressed as mg/g of flour in developing wheat and rice grains decreases from the earliest stages of development at 4 DAA, when the grain is almost entirely composed of maternal tissue, to 28 DAA, when the maternal tissue is a minor component of the grain (Fig 3.15). However, when the MLG content values are converted to a per grain basis, the dynamics of MLG can be better ascertained. Wheat grains demonstrate an increase in MLG content from 4 DAA to 28 DAA, with the most pronounced increase being early in development (4-12 DAA) before tailing off towards maturity (Table 3.5, Fig 3.16). There is a ~3 fold increase from 4-28 DAA in $\mu\text{g} / \text{grain}$ of MLG content but the grain enlarges by about 10x (w/w), hence the observed reduction in mg/g of flour can be attributed to dilution of the MLG content by increases in other flour components. Rice conversely does not show a large change in MLG content per grain throughout the grain development period analysed (Fig. 3.16). This conflicts with the immunocytochemical analysis, which clearly shows a dramatic increase in the labelling intensity of MLG in the rice endosperm with development. Degradation of MLG in outer layers may occur at about the same rate as deposition of MLG in the endosperm, effectively masking the deposition of MLG when analysing wholegrain rice rather than specific tissue types.

Table 3.5. MLG content in developing wholegrain wheat and rice as detected with the megazyme MLG assay.

Sample	Days after anthesis	Average MLG content per gram of flour (mg)	Standard deviation (mg)	Average MLG content per grain (μg)	Standard deviation (μg)
Wheat					
	4	23.94	0.74	95.75	2.97
	8	21.26	0.66	170.07	5.27
	12	16.67	0.52	200.05	6.20
	20	9.08	0.28	254.20	7.88
	28	4.99	0.15	179.70	5.57
White flour					
	-	1.04	0.07	-	-
Rice					
	4	18.10	0.56	37.13	1.15
	8	5.94	0.18	42.09	1.30
	12	3.54	0.11	35.31	1.09
	20	1.85	0.06	36.16	1.12
	28	2.03	0.06	41.96	1.30
White flour					
	-	0.91	0.03	-	-

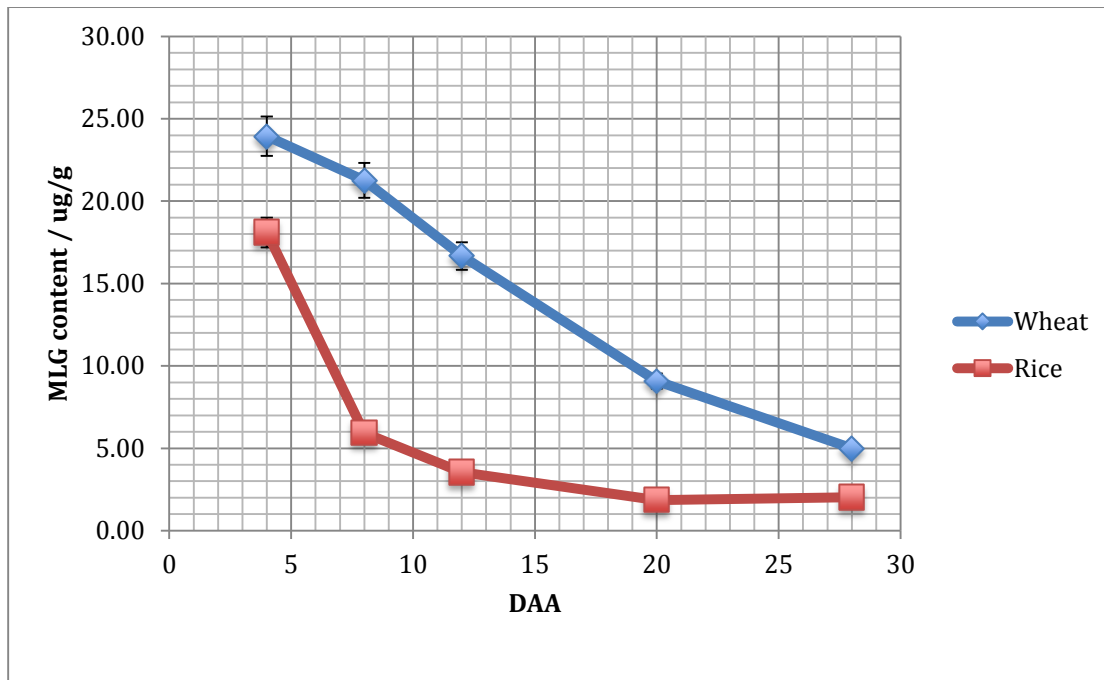


Figure 3.15. Average MLG content per gram of milled wholegrain tissue throughout development in wheat and rice, as detected colorimetrically by the Megazyme MLG assay kit. Each data point is the average of 3 technical replicates using separate tissue samples. Error bars denote 1 standard deviation.

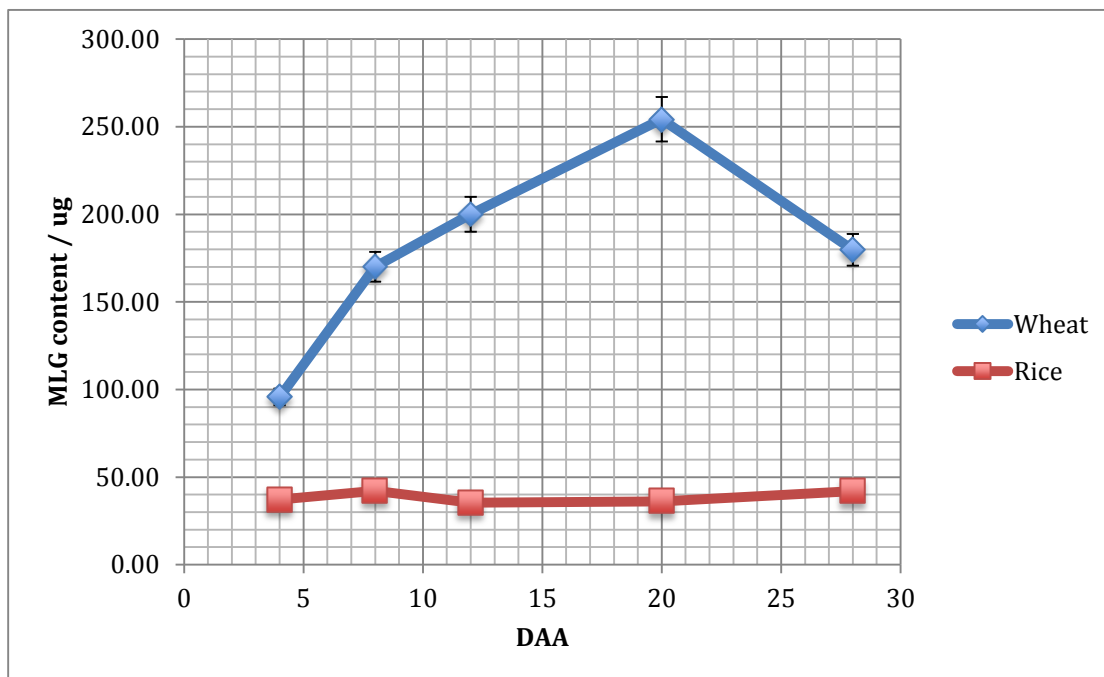


Figure 3.16. Average MLG content per wheat or rice wholegrain throughout development, as detected colorimetrically by the megazyme MLG assay kit.

Each data point is the average of 3 technical replicates using separate tissue samples. Error bars denote the variance of the data.

3.2.5 Colorimetric quantification of cellulose with anthrone reagent.

Cellulose has previously been reported to be a significant proportion of rice endosperm cell walls at around 23% (Shibuya et al. 1985) whereas wheat and other cereal crops are reported to be relatively low in cellulose (2-4% in wheat (Andersson et al. 2013)) in their endosperm cell walls. These figures are for mature grain samples, and no data have been published on the cellulose contents of developing cereal grains. To this end an experiment was carried out to quantify the cellulose content of developing grains using anthrone reagent. Anthrone reagent has been previously used for cellulose quantification due to its well-defined colour change in the presence of monosaccharides, although the colour change varies with the precise monosaccharide. This was used to construct a colorimetric assay modified from the method of Updegraff (1969), where cellulose was isolated from a plant material by an AIR prep followed by a acetic acid:nitric acid digestion to solubilize the other non-starch polysaccharides. The cellulose is then converted to glucose with concentrated sulphuric acid prior to colorimetric detection with the anthrone reagent. As anthrone reagent can be used to colorimetrically detect many monosaccharides, it is worth noting that the isolation method of the cellulose derived glucose is crucial to the specificity of the analysis.

Table 3.6. Average d-glucose content colorimetrically detected with anthrone reagent in concentrated sulphuric acid, of samples of known d-glucose concentration to produce a calibration or response curve for the subsequent analysis of cellulose content.

Average glucose content / nMol	Abs @ 620nm	±
50	0.15	
100	0.245	
150	0.333	
200	0.479	
300	0.685	
400	0.84	

Table 3.7. Colorimetric quantification of cellulose derived d-glucose of whole grain wheat and rice using anthrone reagent in a dilute sulphuric acid solution. Average results based on 3 technical repeats.

Sample	Abs @ 620nm	Glucose content in cuvette / nMol	Glucose content per gram of flour / mg	Glucose content per grain / μg
Wheat 8	0.889	422.37	3.80	30.41
Wheat 12	1.071	508.82	4.58	54.95
Wheat 20	0.689	328.12	2.95	91.03
Wheat 28	0.764	364.00	3.28	118.04
White flour	0.087	19.14	0.17	-
Rice 8	0.367	174.46	1.57	11.15
Rice 12	0.372	177.06	1.59	15.92
Rice 20	0.309	147.42	1.33	25.88
Rice 28	0.244	116.48	1.05	21.72
White flour	0.705	286.90	1.29	-

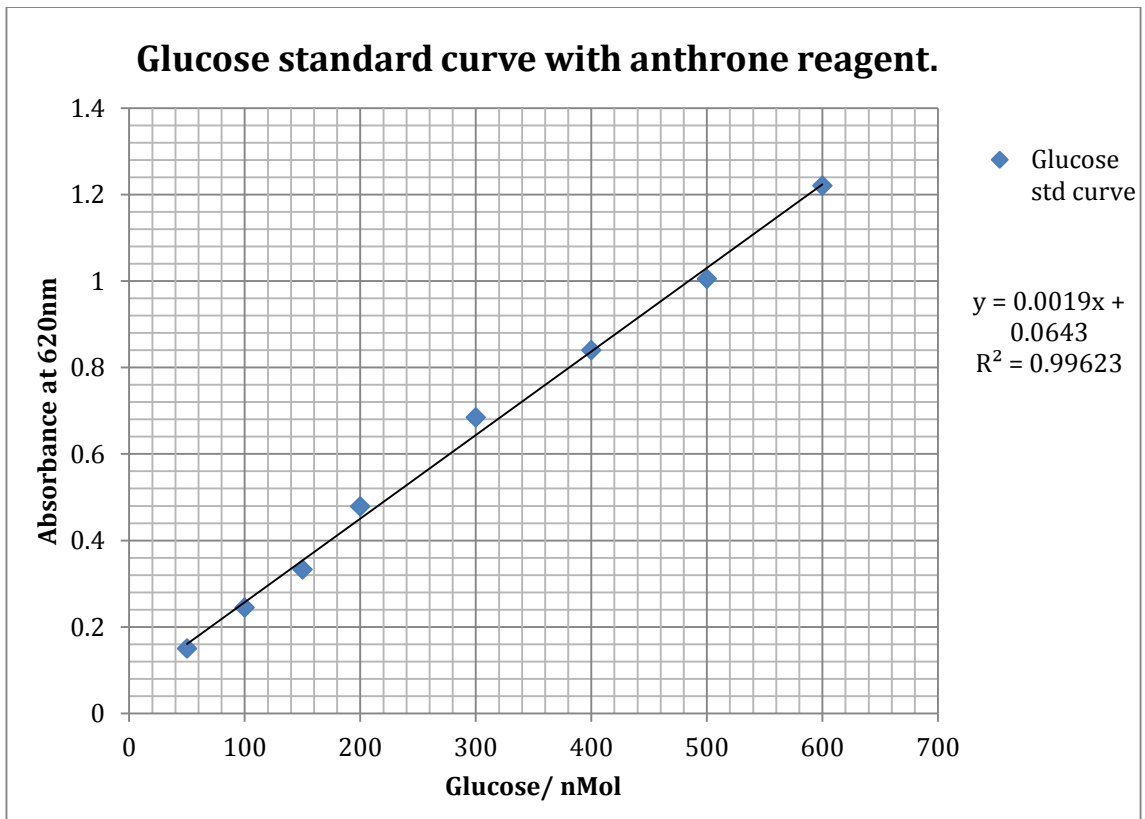


Figure 3.17. d-Glucose standard response curve with anthrone reagent, showing the working concentration of anthrone to be between 100 and 600nMol of d-glucose, based on an average of 3 technical repeats.

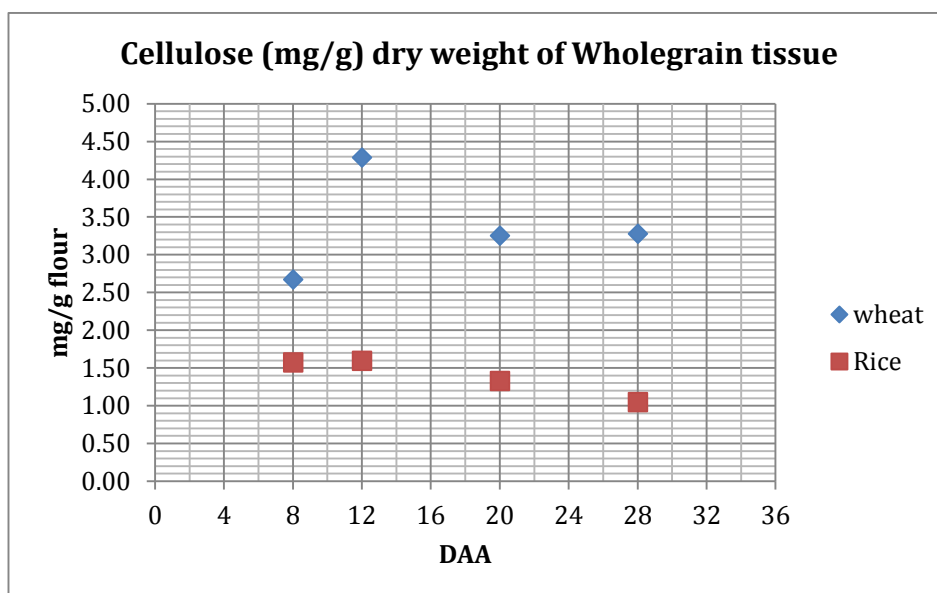


Figure 3.18. Average cellulose content per gram of milled wholegrain tissue in wheat and rice throughout development (based on triplicate technical repeats). Colorimetrically assayed using anthrone reagent.

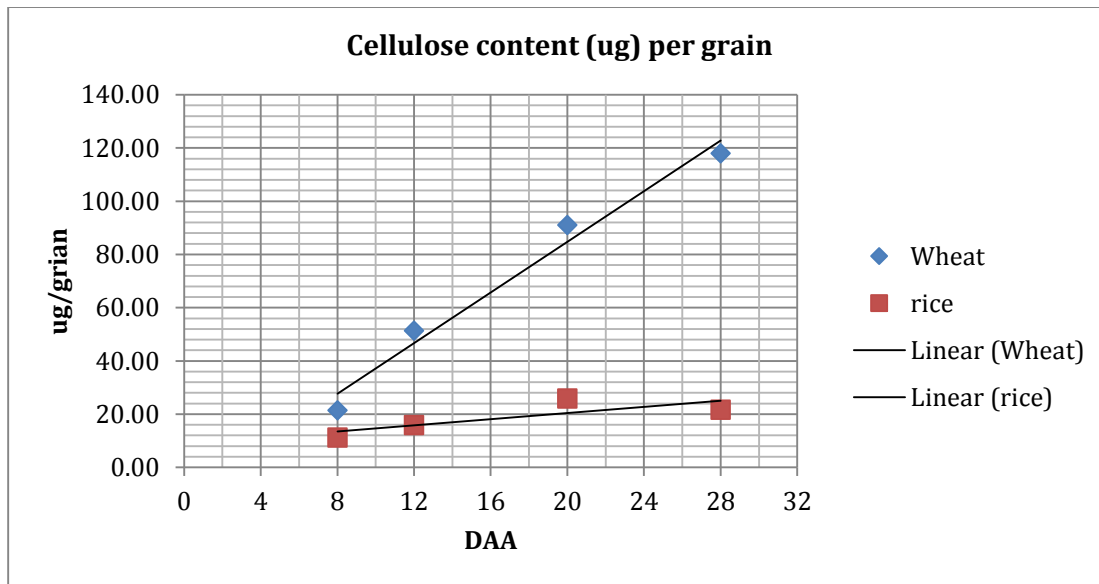


Figure 3.19. Average cellulose content per wheat and rice whole grains throughout development (based on triplicate technical repeats), colorimetrically assayed using anthrone reagent.

The colorimetric assay shows that the cellulose contents of both wheat and rice grains increase throughout grain development, however, the increase is much more pronounced in wheat. Both species have similar cellulose content at the earliest developmental stage analysed (8 DAA) of 21.37 and 11.15 μg of cellulose per grain for wheat and rice, respectively, which represents around 7% of the cell wall in both species. However by maturity the difference between the two species is very pronounced with rice reaching 26.61 μg and wheat almost 5 times higher at 118.04 μg per grain (Fig. 3.19). Cellulose content was also determined in white flour from mature grains of each species, showing that about a third of the cellulose content was derived from the starchy endosperm of wheat, and the remaining two thirds from the aleurone or maternal tissues removed by the pearling process. On the contrary, in rice a higher concentration of cellulose was determined in white flour than in whole grain, suggesting that the endosperm is more highly enriched in cellulose than the maternal tissues (Fig. 3.18). In wheat grains at 28 DAA, a cellulose content of 118.04 μg represents approximately 13% of the total cell wall which is significantly higher than previous reports of 2-4% (Andersson et al. 2013). The reported value of 2-4% was for wheat starchy endosperm cells: wholegrain samples contain significant amounts of maternal and embryonic tissues and would be expected to be more cellulose-rich than starchy endosperm tissue which may account for the 13% cellulose content detected in this assay, however the wheat

white flour sample did correlate to this previous report with a figure of 3.25% cellulose. The cellulose content determined by these analyses in white rice flour (20.0%) is comparable to the 23% cellulose reported for the starchy endosperm by Shibuya et al. (1985). The maternal and embryonic tissues in the whole grain sample would be expected to be rich in cellulose, thus the 7.25% cellulose content in 28 DAA wholegrain rice as determined in this experiment is unexpected. It may be the case that these differences may also be accounted for by differences in cultivar and growth conditions as (Lai et al. 2007) demonstrated that many other monosaccharides showed high variation among rice cultivars.

3.2.6 Klason-lignin content in developing wheat and rice grains.

Lignin is a significant component of vegetative plant tissue and in particular of vascular bundles. However, no lignin has been reported in the endosperm walls of wheat, and there are conflicting reports about the lignification of rice endosperm cell walls. Klason lignin was therefore determined in 100 mg of wholegrain flour at 4 developmental stages, and 1 gram of mature endosperm flour from both species. Klason lignin analysis is based on digesting all other cell wall components with 12M H₂SO₄, and measuring the remaining lignin. This is a widely used method to detect and quantify lignin, however some lignin is known to be acid-soluble and may be lost in this analyses.

3.2.6.1 Klason-Lignin content increases steadily throughout the development of both wheat and rice, but rises at a greater rate in wheat than in rice.

In both wheat and rice white flour no Klason lignin was detected, even when using 10 times as much starting material as with the wholegrain flours, this suggests that there is either very little or no lignin present in the endosperm of either species at maturity. Previous reports of lignin in rice endosperm may be a result of greater sensitivity, through the use of larger quantities of sample material. However in wholegrain flour of both species Klason lignin was detected and a linear increase was seen as development progressed (Fig. 3.20). Maternal tissues or aleurone cells may therefore be progressively lignified as the grain matures, it may be that the aleurone or embryo cells are the source of this lignification rather than the maternal tissues that have degraded into a crushed layer, as it seems unlikely that lignification would continue to increase after the maternal layers have undergone

PCD. Although there are no specific reports of lignin being present in the aleurone layer, as previous analyses combine maternal and aleuronic tissues together.

Table 3.8. Lignin content of milled wholegrain wheat and rice tissue throughout development, and in milled mature polished grains (white endosperm enriched flour) using Klason-lignin analysis.

<i>Sample</i>	<i>Starting material /mg</i>	<i>Lignin content / mg</i>	<i>Lignin content per grain / μg</i>
Wheat 8 DAA	100	20.5	164.0
Wheat 12 DAA	100	20.0	240.0
Wheat 20 DAA	100	20.3	568.4
Wheat 28 DAA	100	20.6	741.6
Wheat White flour	1000	0	0
Rice 8 DAA	100	6.7	47.5
Rice 12 DAA	100	6.9	68.9
Rice 20 DAA	100	8.6	167.7
Rice 28 DAA	100	12.0	248.6
Rice White Flour	1000	0	0

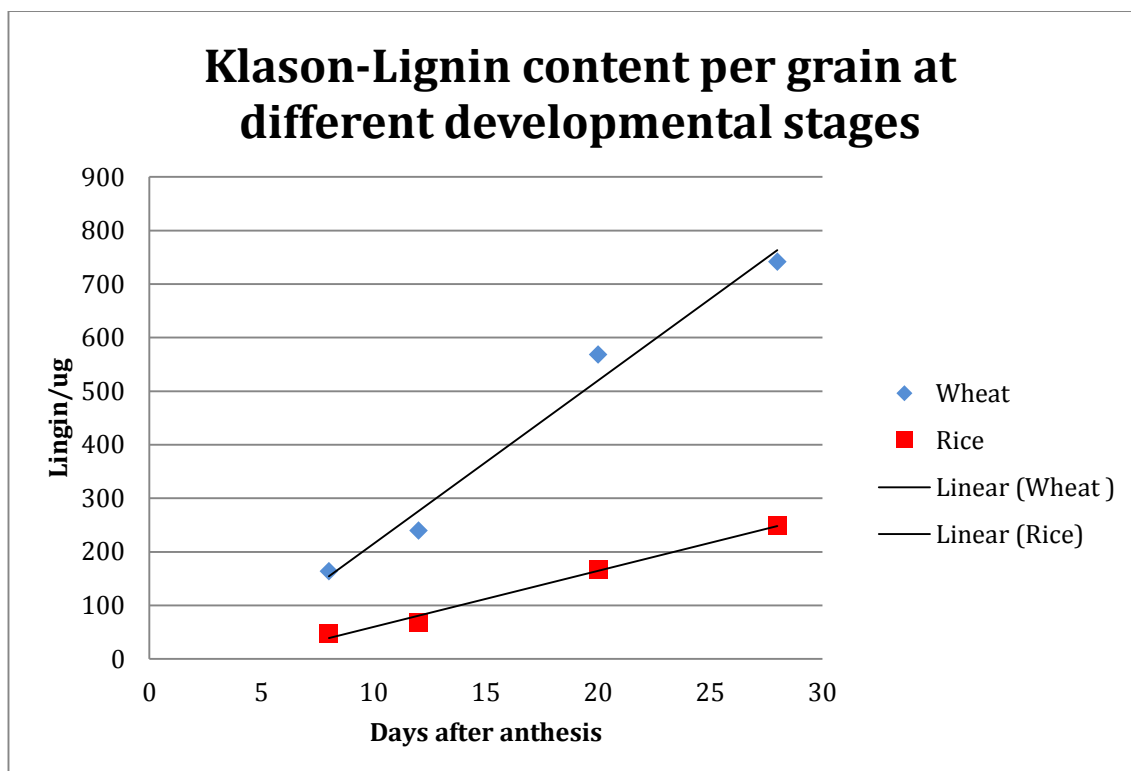


Figure 3.20. Klason-Lignin content per whole grain in wheat and rice throughout development. Results based on 1 technical repeat due to insufficient material.

3.2.7 Total cell wall composition quantification in developing wheat and rice grains.

The experiments detailed in this chapter have provided detailed insight into the dynamics of wheat and rice grain cell wall polysaccharides throughout development. However these analyses take each cell wall component in isolation and do not provide the full picture about cell wall deposition in wheat and rice grains at each developmental stage. By combining the data from the cellulose and MLG assays with the HPLC data, it is possible to calculate the relative percentage contribution of each monosaccharide and polysaccharide throughout the 5 developmental stages allowing direct comparison of the dynamics of cellulose, MLG and other cell wall components. The analysis of cellulose content at 4 DAA would have provided additional valuable information about the composition of the newly cellularised grains of both wheat and rice, but unfortunately insufficient plant material was available for this analysis.

Table 3.9. Table of cell wall composition (μg / grain) in developing wheat and rice grain, combining HPLC monosaccharide data, MLG and cellulose data.

Monosaccharide content per grain (μg)																					
Sample	DAA	Fuc	Rha	Ara	Gal	Xyl	Man	GalA	GlcA	Cellulose	MLG										
Rice	4.0	1.3	0.0	3.3	0.3	14.0	0.5	10.9	0.0	10.5	1.1	2.4	0.2	2.3	0.3	0.4	0.1	-	37.1	1.2	
	8.0	3.1	0.1	6.7	0.2	14.4	0.0	22.7	0.3	17.2	1.6	3.3	0.0	8.6	1.3	2.5	0.4	11.2	1.7	42.1	1.3
	12.0	2.0	0.1	5.4	0.4	15.3	1.3	14.0	1.0	13.1	2.0	1.7	0.2	10.7	1.6	2.9	0.4	15.9	2.4	34.9	1.1
	20.0	5.8	0.4	12.9	1.4	28.4	1.0	31.0	3.1	27.3	1.3	4.0	0.3	26.2	3.9	5.6	0.8	25.9	3.9	35.3	1.1
28.0	8.2	1.4	22.2	2.6	35.7	1.8	49.2	6.0	31.4	0.6	7.7	1.0	32.9	4.9	6.0	0.9	21.7	3.3	42.0	1.3	
Wheat	4.0	0.3	0.0	0.5	0.0	19.0	4.8	8.5	1.4	24.6	7.5	1.4	0.2	5.1	0.8	1.0	0.1	-	95.8	3.0	
	8.0	0.5	0.1	0.4	0.1	31.8	7.3	10.6	1.6	38.8	9.1	8.0	1.0	11.4	1.7	2.1	0.3	21.4	3.2	170.1	5.3
	12.0	1.4	0.2	0.8	0.1	42.0	8.4	14.6	2.3	46.2	11.9	15.7	2.9	13.3	2.0	3.8	0.6	51.4	7.7	200.1	6.2
	20.0	3.5	0.2	0.9	0.1	87.4	8.4	24.5	2.0	119.9	21.0	26.9	1.4	37.7	5.6	9.6	1.4	91.0	13.7	254.2	7.9
28.0	10.0	0.2	1.8	0.1	116.8	11.5	65.2	25.1	169.8	36.1	30.5	0.3	41.4	6.2	8.0	1.2	118.0	17.7	179.7	5.6	

3.2.7.1 Examining the contribution of each cell wall component as a percentage reveals that MLG is the major component of grain cell walls from 4-20 DAA in both species.

In both wheat and rice grains, MLG is the largest single cell wall component in early development representing 55% and 44% in wheat and rice respectively at 4 DAA, and remains the largest single cell wall component until 20 DAA when arabinoxylan becomes the most prevalent polysaccharide in both species. MLG content declines steadily during development to represent only 20% and 14% in 28 DAA wheat and rice, respectively (Table 3.10). In wheat, this decline is despite a 3-fold increase in total MLG content in the developing grain from 4-28 DAA and demonstrates the large-scale deposition of all other polysaccharides occurring within the developing wheat grain. In rice, MLG content fluctuates slightly throughout development but stays close to the initial content: 38 µg per grain at 4 DAA and 41.5 µg per grain at 28 DAA. Thus the decline in the cell wall percentage is entirely due to dilution by the increasing content of other polysaccharides. AX content increases in both species throughout development, but the percentage of the cell wall it represents does not differ greatly in either species with fluctuations from, from 26% at 4 DAA to 32% at 28 DAA, compared to rice, from 29% at 4 DAA to 24% at 28 DAA. Pectin, as represented by the total of fucose, rhamnose and galacturonic acid, changes dramatically in rice increasing from 7.95% at 4 DAA to almost a quarter of the cell wall at 28 DAA (21.1%) (Fig. 3.21). In wheat the change is less dramatic, but a significant pectin level is detected, with 6.3% of the cell wall consisting of pectin at cellularisation and 12.9% at maturity (Fig 3.22). Galactose, which would normally be discussed either in terms of RG-I side chains or as part of the AG peptide, represents a significant proportion of the mature cell wall in both species, at 7.2% in wheat and 16.4% in rice. The contribution of galactose in wheat and rice appears higher than expected, especially in 28 DAA rice grain. I suggest that as the galactan side chains on RG-I appear to co-localise with expanding and dividing cells in immunohistochemical experiments on developing rice grains (Fig. 5.10 g,i,k) that the RG-I in the rice embryo may be heavily substituted with galactan side-chains, to the extent that the overall grain cell wall composition is skewed by this. It is unlikely that a significant proportion of this figure is the result of AG peptides, as comparatively little arabinose was detected to make up for the presence of AX and AGP. Cellulose accounted for a similar proportion of the mature grain cell wall at 12.9% in wheat and 7.3% in rice. The period from 8 -12 DAA showed a noticeable increase in the cellulose content of the cell wall, from 7.9% to 12.1% in rice and 6.4% to 11.3% in

wheat, despite it being a period of relatively little cell wall deposition. In mature endosperms, the cellulose content was 7.3 % of the rice endosperm, whereas a larger value of 12.9% cellulose was detected in wheat. Both figures differ with the previously published reports (Mares and Stone 1973a; Bacic and Stone 1981; Shibuya et al. 1985), but the values reported for the white flour samples which should represent mainly mature endosperm tissue correlate closely to the figures previously published for wheat and rice endosperms (Shibuya et al. 1985; Andersson et al. 2013).

Table 3.10. Table of cell wall composition by percentage in developing wheat and rice grain, combining HPLC monosaccharide data, MLG and cellulose data.

		Average Percentage of cell wall / %										
Sample	DAA	Fuc	Rha	Ara	Gal	Xyl	Man	GalA	GlcA	Cellulose	MLG	
Rice	4.00	1.47	3.81	16.38	12.77	12.27	2.85	2.66	0.49		43.55	
	8.00	2.20	4.71	10.16	16.01	12.15	2.34	6.09	1.75	7.86	29.67	
	12.00	1.49	4.14	11.65	10.68	9.98	1.26	8.19	2.20	12.14	26.63	
	20.00	2.49	5.58	12.27	13.36	11.80	1.73	11.31	2.43	11.17	15.24	
	28.00	2.74	7.41	11.91	16.42	10.48	2.57	10.97	1.99	7.25	14.01	
White												
flour		3.99	7.49	9.88	17.18	8.80	2.72	13.66	2.15	14.11	20.02	
Wheat	4.00	0.18	0.30	10.97	4.93	14.18	0.80	2.96	0.57		55.30	
	8.00	0.15	0.13	9.39	3.13	11.45	2.35	3.35	0.61	6.30	50.13	
	12.00	0.31	0.18	9.27	3.23	10.20	3.47	2.93	0.84	11.35	44.13	
	20.00	0.45	0.12	11.39	3.19	15.64	3.51	4.91	1.25	11.87	33.15	
	28.00	1.10	0.20	12.80	7.15	18.61	3.34	4.54	0.87	12.94	19.69	
White												
flour		0.32	0.00	19.08	2.68	35.34	1.46	6.95	1.34	18.32	14.51	

Table 3.11. Summary table of percentage composition of developing wheat and rice grains, showing the relative contribution of the major polysaccharides.

		Hemicellulose				
		Total Hemicellulose	MLG	AX	Pectin	Cellulose
Rice	4	75.54	43.55	29.14	7.95	
	8	56.07	29.67	24.06	13.00	7.86
	12	51.70	26.63	23.82	13.81	12.14
	20	43.47	15.24	26.50	19.38	11.17
	28	40.96	14.01	24.38	21.13	7.25
	White flour	37.66	14.11	20.83	25.14	20.02
Wheat	4	81.83	55.30	25.72	3.44	
	8	73.93	50.13	21.45	3.63	6.30
	12	67.90	44.13	20.30	3.43	11.35
	20	64.94	33.15	28.29	5.48	11.87
	28	55.32	19.69	32.29	5.84	12.94
	White flour	85.49	20.73	63.11	8.23	3.25

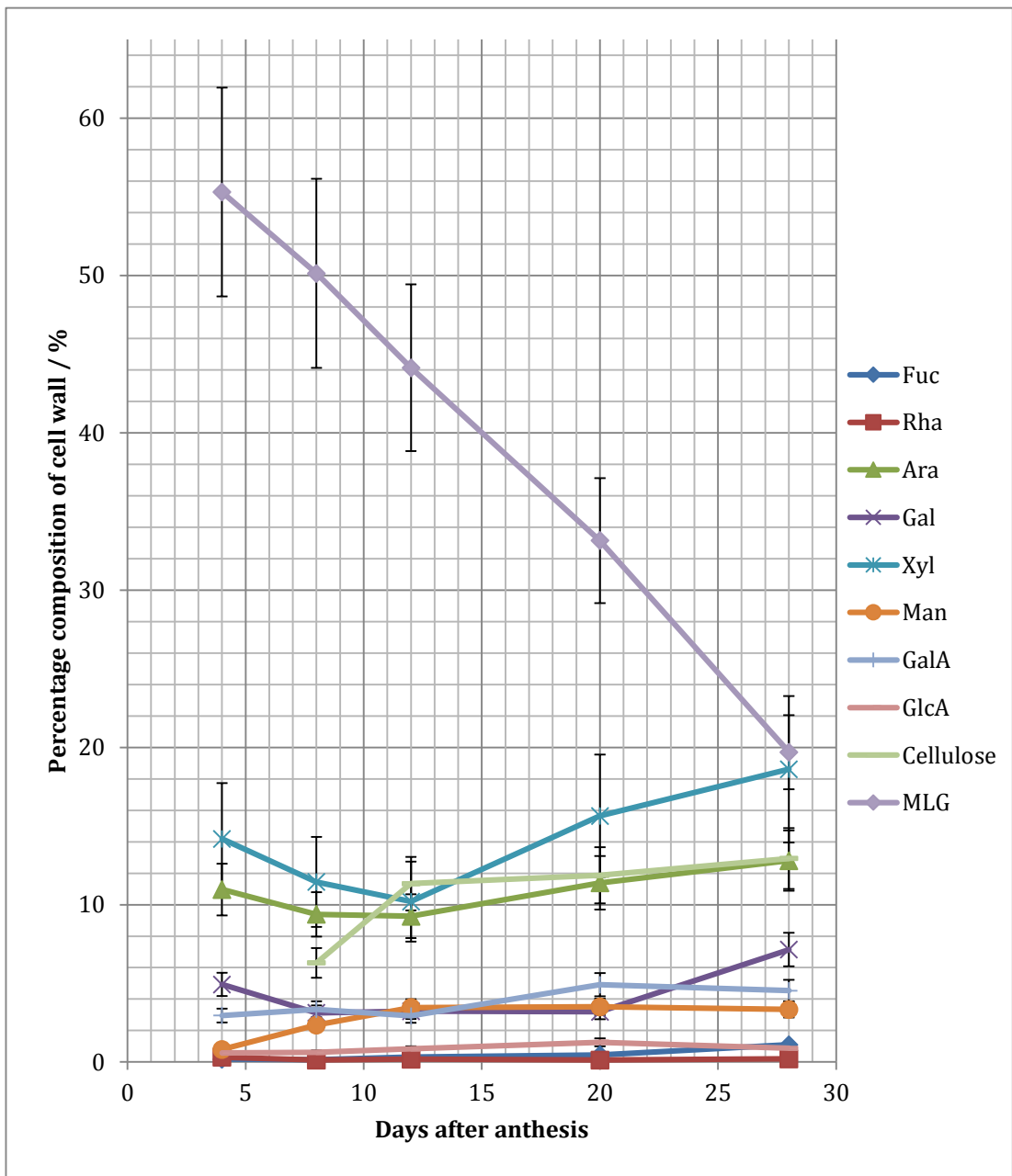


Figure 3.21. Combined cell wall composition of developing wheat grains, showing data from HPLC monosaccharide analysis, MLG and cellulose assays. Error bars denote 1 standard deviation.

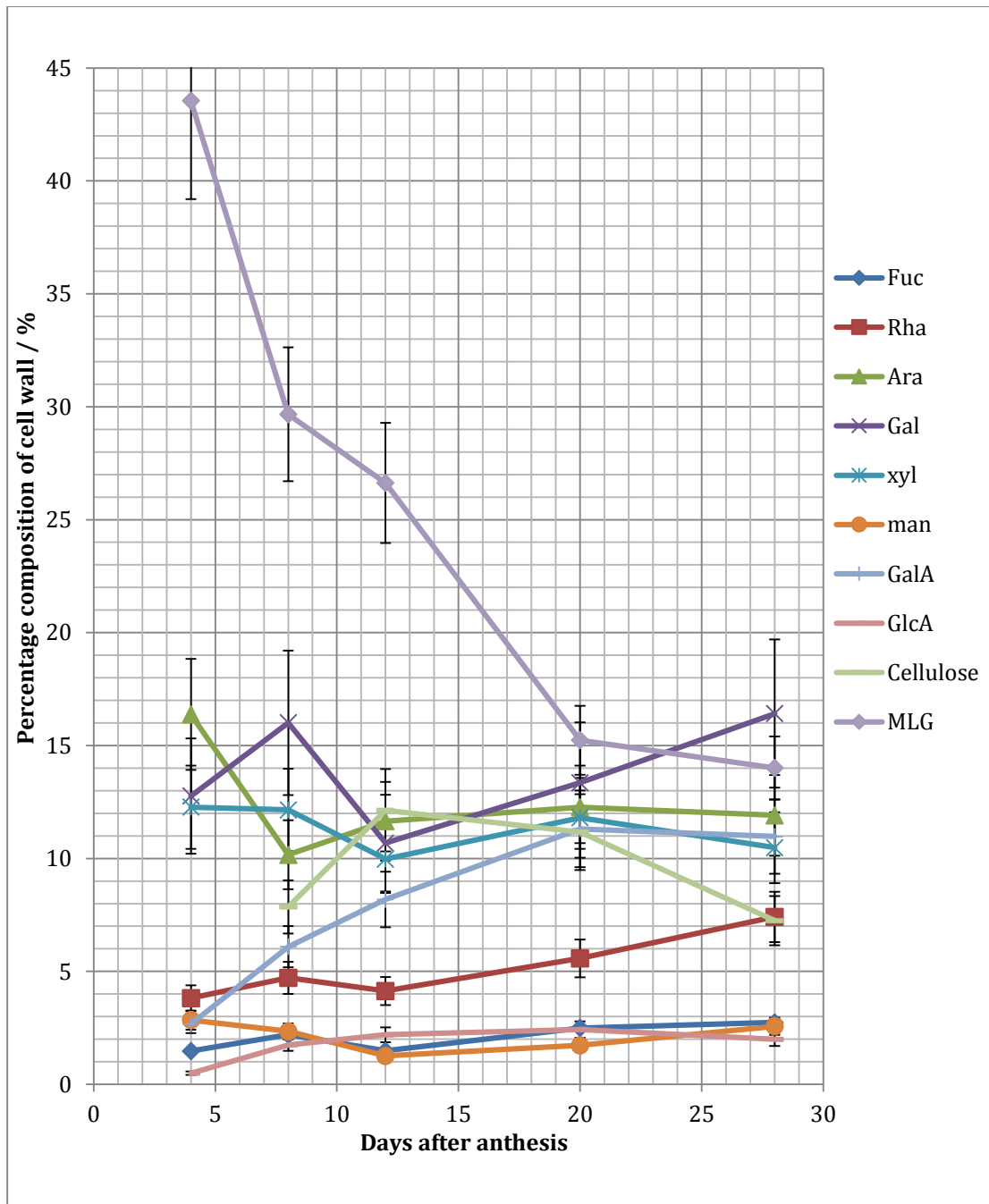


Figure 3.22. Combined cell wall composition of developing rice grains, showing data from HPLC monosaccharide analysis, MLG and cellulose assays. Error bars denote 1 standard deviation.

3.3 Discussion

Wheat wholegrain at 28 DAA is rich in MLG and AX with low contents of cellulose and pectin, whereas rice contains a more even distribution of these four major polysaccharides.

Physiologically mature (28 DAA) wheat wholegrain samples contain about 32% AX and 20% MLG with 13% cellulose and 6% pectin, 7% galactose and 3% mannose, whereas rice contains 24% AX, 14% MLG, 21 % pectin, 7% cellulose and 16% galactose. Wheat is enriched in arabinoxylan and MLG compared to rice, which contains higher percentages of pectin and galactose. This agrees well with previously reported endosperm cell wall analyses of rice (Shibuya et al. 1985; Lai et al. 2007) but few complete wholegrain analyses have been reported for wheat or rice, to provide direct comparisons. The white flour samples provide a more appropriate comparison, to these reports, and with only small discrepancies occurring between the published monosaccharide data and the data presented here (table 3.11). For example, wheat starchy endosperm cell walls are reported to contain 60-70% AX and 15-20% MLG, matching closely to the figures of 63% AX and 21% MLG. The high cellulose content reported for the whole grain wheat analyses may be expected as maternal and embryonic tissues are likely to have higher cellulose contents than endospermatic tissue. Conversely this appears not to be the case in wholegrain rice where the cellulose content is much lower than that of the endospermatic tissue. High galactose is present in both species relative to the galacturonic acid content, which may be indicative of contamination of the extracted cell wall material with AGP and galactose-containing water soluble oligosaccharides such as raffinose or stachyose.

3.3.1 Cell wall deposition in wheat and rice grains follows a consistent pattern between the five developmental stages examined.

Four clear phases of cell wall deposition were observed in developing grains of both wheat and rice, with each species transitions from one phase to the next at the same developmental stage. This suggests a correlation between the pattern of grain development in both species and the deposition of cell wall material. This pattern can be described as two phases with high rates of cell wall polysaccharide deposition (between 100%-500% increase in four days) generally followed by a reduced rate of deposition, with some monosaccharides showing a small overall

decrease in content per grain ($< \pm 40\%$) as summarised in Tables 3.14 and 3.15. This pattern of deposition does not agree with the patterns of grain weight increase (Fig. 3.1) or of starch and protein accumulation, all of which show a single phase of deposition followed by a decrease in rate, which produces a plateau at about 20-24 DAA. However these four phases of cell wall deposition do match the transitions between the five main stages of grain development. The first phase of cell wall deposition from 4-8 DAA shows the highest rate of cell wall deposition of all monosaccharides and coincides with the greatest change in endosperm size, with this phase reported as a period of expansion and cell division. Rapid cell expansion and cell division require significant production and deposition of cell wall material in order to facilitate these changes. MLG exhibits a small increase in content per grain in both species, but the significant deposition of all other polysaccharides at this time point results in an overall reduction in the percentage content of MLG in their cell walls. The second period from 8-12 DAA is the transition from rapid expansion and cell division to cell differentiation, with little cell division being reported and micrographs of grain structure showing only a small increase in cell size. These decreases in cell expansion and the rate of cell division generate less demand for cell wall deposition and this is reflected in the slower rates of deposition of most monosaccharides during this phase. From 12-20 DAA the grains of both species are depositing significant amounts of storage proteins and starch, and the grain expand to their maximal size at 20 DAA. This increase in grain size is due to both cell division and cell expansion and this, in addition to cell wall thickening of the aleurone cells, may require the significant increase in cell wall content seen from 12-20 DAA. The final phase from 20-28 DAA is a period of maturation and preparation for desiccation and exhibits a small reduction in overall grain size. This is mainly attributed to the decrease in grain moisture content between 20-28 DAA in wheat and it is likely a similar desiccation occurs in rice grains. The combination of reduced grain size and reduced rate of endosperm cell division in this period may cause the reduction in the cell wall deposition rate observed from 20-28 DAA in both species. Significantly, the pattern of cell wall deposition of two of the polymers does not follow this four phase pattern; MLG and cellulose both follow a simple pattern with a single deposition rate from 4 DAA to 20 DAA before a plateauing of the deposition rate. This may be explained by two scenarios. One possibility is that the deposition of these two polymers is differentially regulated from that of the other major polysaccharides. Alternatively, it

is possible that the explanation lays in the composition of the maternal tissue, which provides a high contribution to the overall cell wall composition in earlier stages of grain development and is probably rich in MLG and cellulose. Thus changes in the amount of maternal cell wall content may obscure the four phase pattern seen in other monosaccharides by rapid changes in the MLG content of the maternal tissue, as the maternal tissues degrades and are lost between 8-20 DAA. This effect may be less evident for other monosaccharides due to their lower proportions in the maternal tissues.

Table 3.12. Summary of wheat cell wall component content changes per grain during the 4 major grain phases.

Developmental Phase	Decrease in content	Large decrease in content >30%	Increase in content	Large increase in content >40%
Phase 1 (4 – 8 DAA)	Rha		Gal	All other cell wall components (58-474%)
Phase 2 (8 – 12 DAA)			Ara, Xyl, GalA, Gal, MLG	Fucose, Rha, Man, GlcA, Cellulose
Phase 3 (12 – 20 DAA)			MLG, Rha	All other cell wall components (67-184%)
Phase 4 (20 – 28 DAA)	GlcA	MLG	Ara, Man, GalA, Cellulose	Fucose, Rha, Gal, Xylose

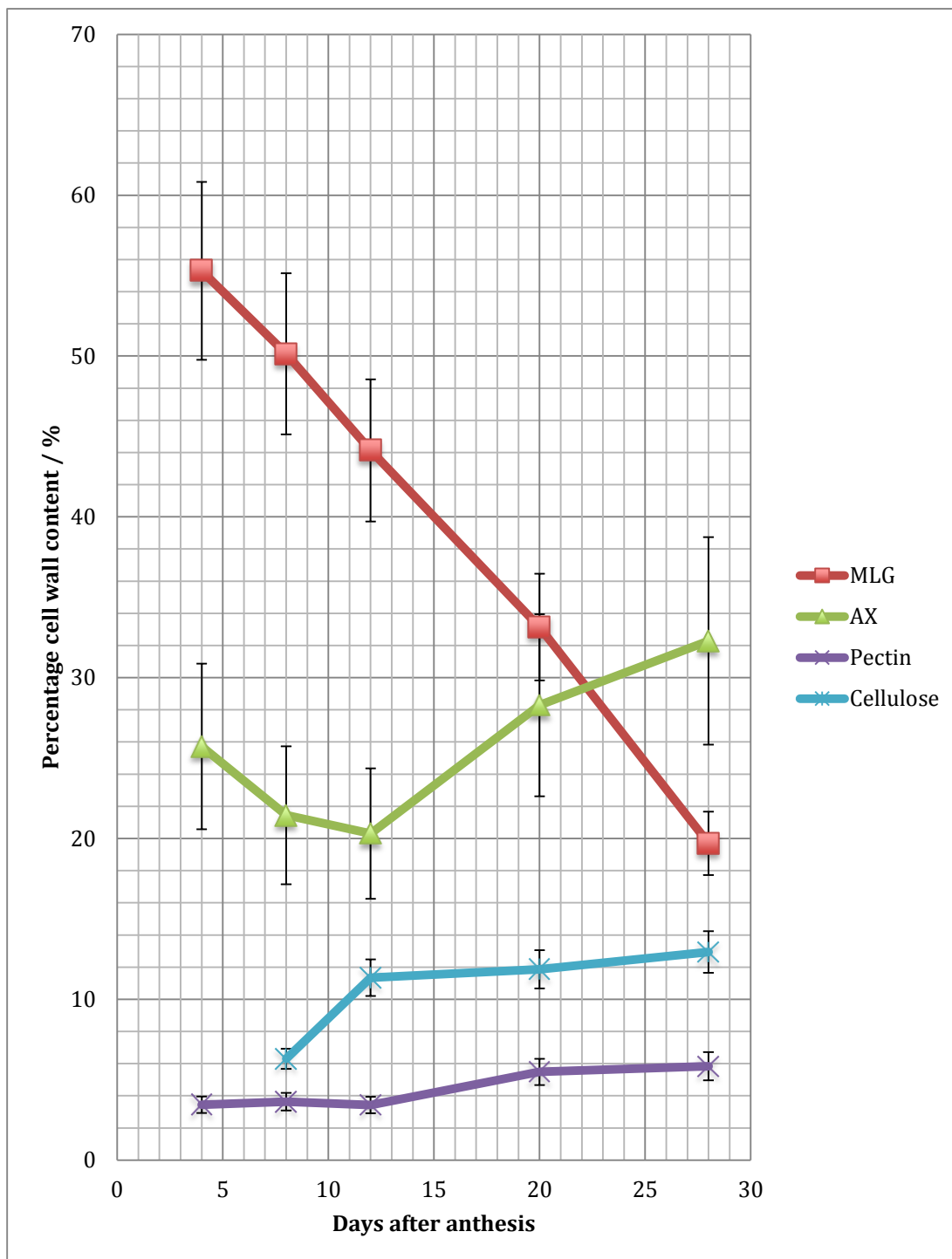


Figure 3.23. Summary of the developmental changes in percentage composition of wholegrain wheat cell walls in the major 4 polysaccharides. Error bars denote 1 standard deviation.

Table 3.13. Summary of rice cell wall component content changes per grain during the 4 major grain phases.

Developmental Phase	Decrease in content	Large decrease >30%	Increase in content	Large increase >40%
Phase 1 (4 – 8 DAA)			Ara, Man, MLG	All other cell wall components (~65-490%)
Phase 2 (8 – 12 DAA)	Rha, MLG, Gal, Xyl	Fuc, Man	Ara, GalA, GlcA	
Phase 3 (12 – 20 DAA)			MLG	All other cell wall components (~63-195%)
Phase 4 (20 – 28 DAA)	Cellulose		Ara, Xyl, GalA, GlcA, MLG	Fuc, Rha, Gal, Man

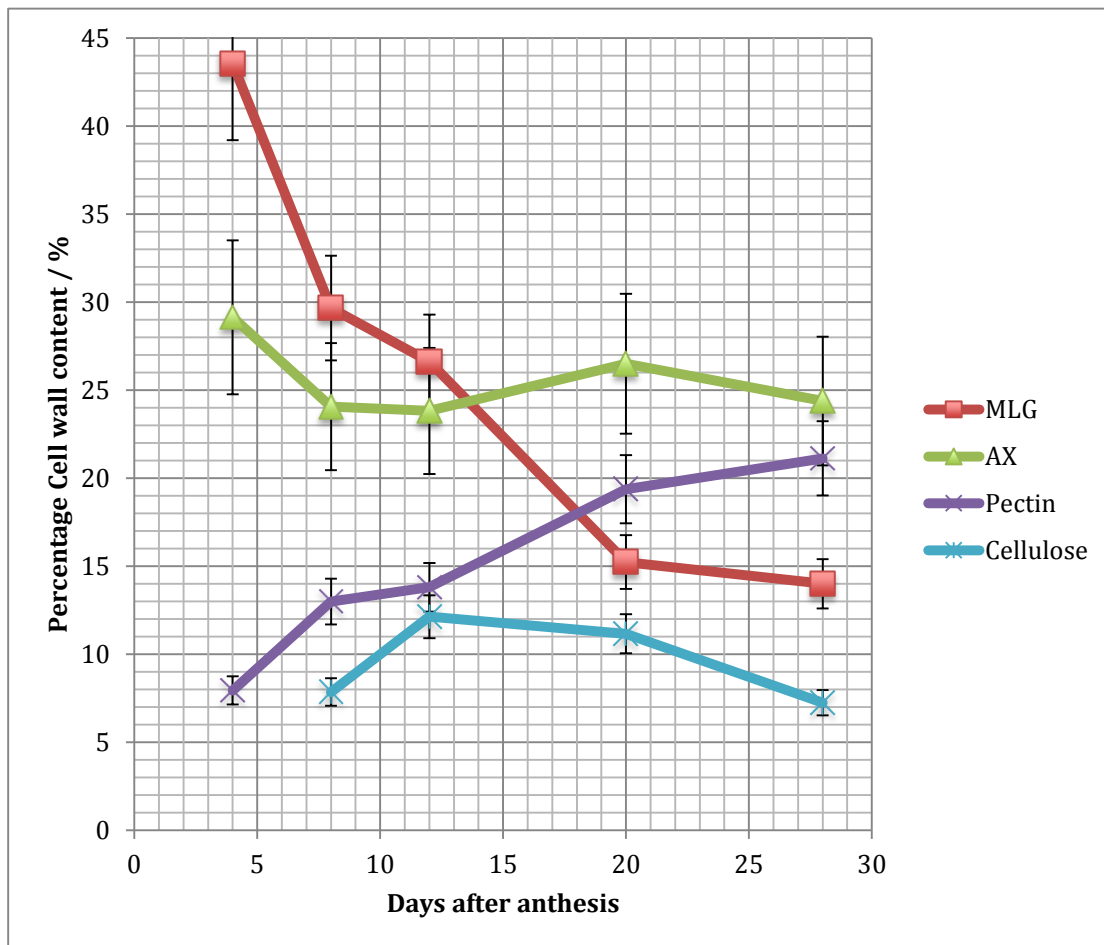


Figure 3.24. Summary of the developmental changes in percentage composition of wholegrain rice cell walls in the major 4 polysaccharides.

3.3.2 The percentage content of MLG and AX changes significantly in both species throughout development

MLG is a major polysaccharide in the early stages of grain development in wheat (55.3%) and rice grain (43.6%), but its percentage contribution declines steadily until maturity in wheat (19.7%) and 28 DAA in rice (14.0%). In the context of the other monosaccharides determined this is the largest single change in polysaccharide contribution during development in both species. This reduction in the percentage contribution is not a reduction in total MLG, which increases slowly throughout development (Fig. 3.9), but to the high rate of deposition of other monosaccharides during the course of grain development, which eclipses the small changes in total MLG content. Despite these changes MLG remains the second most abundant

polysaccharide, with only AX presenting a higher total content in both species. AX content increases between 4 DAA and 28 DAA in wheat with an increase from 25.7% to 33.3% in wholegrain samples, as shown by the total of arabinose and xylose. In rice a small decrease is detected, from 29.1% to 24.4% at 28 DAA. A smaller change in AX content is observed in rice grains where MLG and AX accounts for only 41.0% of the total cell wall compared to 55.3% in wheat.

3.3.3 Pectin content increases during grain development, increasing almost two-fold during the period from 4-28 DAA in wheat and three-fold in rice.

Pectin percentage content is ~4 times higher in rice than wheat grains at 28 DAA. Rice also contains higher levels of pectic monosaccharides (21.1%) at 28 DAA compared to wheat (5.8%), and similar levels of cellulose (7.3% rice, 12.9% wheat). This higher percentage of pectin in rice is a characteristic difference between the two species. Pectin content early in grain development (4 DAA) is similar in the two species with 7.9% in rice and 3.4% in wheat, indicating that the 4 DAA grain, which comprises mainly maternal tissue, is quite similar in composition between the two species. This demonstrates that subsequent changes in wholegrain cell wall content are a result of the increasing proportions of endosperm and embryonic tissues and of the concomitant degradation of the cell walls in the maternal tissues.

Most of the pectin content is accounted for by homogalacturonan as shown by the amount of galacturonic acid in the HPLC monosaccharide analyses. This accounts for 77% of 28 DAA wheat pectin (GalA+Rha+Fuc) and 55% of rice pectin not including RG-I sidechains. In wheat this value is very close to the figure of 80% reported by Mohnen (2008) for the relative contribution of HG in the pectic supramolecule, however in rice a larger difference is seen, which may be due to larger than expected fucose and rhamnose contents. RG-I side chains are impossible to assign accurately using monosaccharide analysis alone, as arabinose can contribute to RG-I, AGPs and AX structure, and galactose can contribute to both AGP and RG-I and several oligosaccharides. The galactose content of rice grains was determined as up to 16.4% of the total cell wall composition at 28 DAA, which is much higher than expected based on previous reports by (Shibuya et al. 1985) suggesting that the embryo contains the highest proportion of galactose at 7.8%. The conflicting values from the HPLC analysis require validation. In wheat grain the galactose content was also relatively high at about 7.2% of the total cell wall content, which is similar to the galacturonic acid value, and did not vary greatly

during development. Substantial proportions of AGP, up to 0.4% of dry weight, have been reported for wheat endosperm, which may have affected the analyses. Contamination from raffinose, which is a trisaccharide composed of galactose, fructose and glucose, would also contribute to higher than expected proportions of galactose in monosaccharide analyses. (MacArthur and D'Appolonia 1979; Henry 1985; Black et al. 1999; Shanmugavelan et al. 2013). Raffinose contamination may occur through co-precipitation with monosaccharides in the Englyst extraction protocol, as the raffinose is likely to be hydrolysed to the constituent monosaccharides along with the cell wall polysaccharides.

3.3.4 Cellulose content increases throughout development and appears to be a major component of rice endosperm tissue.

Total cellulose content increases in both species from 8-28 DAA, but no change is seen from 8 DAA to 28 DAA in the percentage contribution of the cellulose to the rice cell wall matrix compared with a large increase in wheat (6.3% to 12.9%). Cellulose is reported to be a minor component of wheat endosperm tissue at a 2-4% so the continued increase in cellulose content throughout grain development is unexpected. By comparing the white flour and wholegrain tissue analyses, it appears likely that either the aleurone layer and embryonic tissues accumulate significant amounts of cellulose, although (Antoine et al. 2003) report only 1.1-1.5% cellulose in the aleurone layer but up to 23.8% in the pericarp tissues. Both Shibuya et al. (1985) and Lai et al. (2007) have reported cellulose to be a significant component of rice endosperm tissue, which differs from reports for other cereal grains, where the levels are low (Knudsen 1997; Guillon et al. 2011). Whilst these reports have used different cultivars in their analyses, there are significant similarities in percentage compositions between the analyses. The high content of cellulose determined for rice white flour indicate that the rice endosperm is significantly enriched with cellulose and agrees with the value of 23% reported by Shibuya et al. (1985) for rice endosperm. Conversely the analyses of cellulose content in developing wholegrain are about half that reported by Shibuya et al. (1985) at only 7.3% at 28 DAA. Because the analyses of Shibuya et al. (1985) were on harvest mature grain tissues (~45-50 DAA) rather than physiologically mature grain tissue (28 DAA) it is possible that the cellulose content continues to increase during the period from 28-50 DAA. It is also possible that the cultivar and growth

conditions used here resulted in grain with significantly lower cellulose content than those analysed by (Shibuya et al. 1985).

3.3.5 The Klason lignin method appears unreliable with the small quantities of grain tissue available for analysis.

The Klason lignin assay is widely used for lignin quantification in plant tissues, however it does present some limitations. It does not provide a measure of all the lignin present in a given sample, as acid soluble lignin polysaccharides are lost during the harsh acid treatments, and additionally some cellular components that are not degraded by the acid may contribute to inflate the lignin value. The Klason lignin method in Chapter 2.5.4 was followed as it had been used successfully to analyse a few Arabidopsis seeds, rather than the larger scale methods typically employed which require large quantities (10 g or more) of starting material. However it is probable that the difficulty in measuring the small amounts of lignin collected (10 mg or less, balance accuracy ± 0.1 mg) and small fluctuations in the weight of the filter papers due to moisture content or other contaminants may have given artificially high results, despite efforts to minimise these problems. Considerably more lignin was detected than any other cell wall components at all time points in both species, for example in 28 DAA wheat 741 μg of lignin was detected compared to 333 μg of xylose+mannose per grain. In addition, insufficient material was available for technical replicates. It was therefore decided to exclude the lignin values from the analyses of the total cell wall composition in both species.

3.3.6 Deposition of protein and starch granules occur up to 4 days earlier in rice than in wheat grains. Whilst endosperm cell wall morphology is more uniform between the two species.

Both storage protein and starch deposition was seen to occur earlier in developing rice grains than in wheat, with starch granules appearing widespread in the central region at 4 DAA in rice, shortly after cellularisation with comparable levels of starch accumulation not appearing till 8 DAA in wheat grains. Protein bodies also accumulated much earlier in rice grains (about 6 DAA) compared to wheat (at 10 DAA) as detected by light microscopy. The onset of deposition of storage components in rice begins at an earlier developmental stage despite the overall developmental stages of wheat and rice proceeding at a similar rates after anthesis.

This indicates that the regulation of protein and starch deposition is likely to be controlled in a different way in the two species. The earlier development of starch granules in the central region of rice endosperm may be a consequence of the more ordered pattern of programmed cell death in rice grains, with the central region exhibiting PCD by 12 DAA which subsequently extends towards the aleurone cells. It is therefore likely that the cells of the central endosperm are older than those of the outer regions. This may also explain the apparent scarcity of protein deposition in the central region of the rice endosperm, as at 8 DAA the central cells may be preparing for the beginning of PCD. Differences in the rate of cell wall maturation were observed in the cell wall thickenings of the aleurone cells, which appeared slightly earlier in rice grains at 12 DAA compared to ~14 DAA in wheat, but no other visual differences were seen in the development of endosperm cell walls with Calcofluor White. The maternal parenchyma cells did show different behaviour during grain development in the two cereals, with these cells persisting much longer in wheat, at least until 20 DAA, with some cell layers often being seen at 28 DAA. Conversely, in rice, the maternal parenchyma cells were completely crushed by 12 DAA, with only traces of the compressed cell walls remaining. In both species the loss of the maternal pericarp is thought to be due to internal pressure created by the expanding grain crushing the outer layers against the glumes or palea and lemma (modified leaf structures which contain the developing grains and form the husk when desiccated) and have been proposed as key limitations in the maximal dimensions of the developing grain.

3.4 Conclusion

Grain development follows 4 key stages, which have previously been described in detail, and these appear to be synchronous in wheat and rice. Four distinct phases of cell wall deposition can be tracked between the 5 developmental stages examined with all non-glucosic polysaccharides displaying the same 4 phases of deposition. These phases are largely consistent between both species and presumably reflect the changing biological process occurring in the grain. However, small differences in the rates of deposition of individual monosaccharides were observed between species.

The percentage of MLG decreased during the development of both wheat and rice grains, while AX content increased. Pectic monosaccharides showed the single

largest increase of any cell wall components in the developing rice grain, from 7.9% to 21.1%, but little change was observed in wheat.

Wheat cell walls at 28 DAA are dominated by the presence of MLG and AX which together account for 55.3% of the total cell wall material, whereas rice grains at the same developmental stage have about equal proportions of AX, pectic polysaccharides at 24.4% and 21.1% each, with slightly less MLG at 14.0%, with cellulose and polysaccharides making up the remaining ~25% in both species.

CHAPTER 4: IMMUNOHISTOCHEMICAL ANALYSES OF WHEAT AND RICE

4.1 Introduction to antibodies and methodology

Plant cell wall architecture is highly complex while the structure of the cell wall matrix remains elusive in both primary and secondary cell wall systems. The cell walls of cereal endosperms appear to lack any secondary cell wall features and thus present an opportunity to study primary cell wall structure in isolation. Whilst relative proportions of cell wall polysaccharides can be routinely ascertained by use of chemical analyses, the spatial distribution of cell wall polysaccharides require the use of different methods. Few methods are available for the detection and analyses of the linkages between polysaccharides *in muro*, with immunofluorescence microscopy being the most used of these techniques; however this still requires the production of monoclonal or polyclonal antibodies to particular cell wall polysaccharides and their specific structural epitopes. Production of monoclonal antibodies (mAbs) can be an arduous and time consuming procedure, requiring the isolation and purification of a sample of the polysaccharide of interest, followed by the immunisation of an animal host (typically rats, mice or rabbits) with the purified sample often conjugated to bovine serum albumin, and subsequently the B cells of the host are extracted from the spleen and added to a culture of myeloma cells in order to produce hybridomas. Hybridomas are fusions of the B cells and the myeloma cells, in practice this can be facilitated in several ways including the use of polyethylene glycol or electroporation. Once the hybridomas have been isolated they are individually cultured before being characterised on western blot gels and probed with a sample of the initial sample to identify which lines are producing antibodies, which bind to the sample of interest. Additional characterisation of these monoclonal antibodies can be carried out with ELISA assays to quantify the binding affinity of the antibodies to the target molecule. However monoclonal antibodies have been shown to be very useful (Willats et al. 2001b; Guillon et al. 2004; Wilson et al. 2006; Verhertbruggen et al. 2009; Hervé et al. 2009; Chateigner-Boutin et al. 2014) in examining the structure of cell walls *in muro* without the potential for the truncations and alterations to polysaccharide structure that may occur as a

consequence of typical extraction procedures. A wide range of cell wall monoclonal antibodies are available at present, which can detect epitopes of almost all cell wall polysaccharides, and are often able to provide greater detail about the precise structure of a polysaccharide at that precise *in muro* location. For example, the methyl esterification state of HG can be examined by immunofluorescence microscopy using LM19 + LM20, which display specificities for low and highly methyl esterified HG epitopes respectively (Verhertbruggen et al. 2009). Unmasking of cell wall polysaccharides through the use of specific cell wall degrading enzymes is a very useful tool to provide further details about the spatial proximity of different cell wall polysaccharides *in muro*. If degradation of a specific polysaccharide, either partially or completely, results in a stronger signal from antibodies recognising a different polysaccharide, this represents a clue that the two polysaccharides exist within the same section of wall and may be in spatial proximity to one another. Degradation of one or more polysaccharide may allow the relatively large antibodies sufficient space to access epitopes on the other polysaccharide more readily.

It has previously been shown that plant cell walls are dynamic and adaptable structures able to change their architecture to respond to both biological signals and mechanical and osmotic stress (Wakabayashi et al. 1997; Verhertbruggen et al. 2013). In particular it has already been shown that in the early developing endosperms of both wheat and barley grains that a pre-set order of callose, arabinoxylan and mixed linkage β -glucan deposition takes place (Wilson et al. 2006; Pellny et al. 2012).

In the course of the current project we have examined the spatial and temporal distribution of cell wall polysaccharides in the developing grains of wheat and rice using a combination of monoclonal antibodies and unmasking by a lichenase and xylanase double digestion in order to compare and contrast the cell wall architectures within of these two poaecea, which have significantly different cell wall compositions at maturity.

As discussed above, gradients in the amounts of some cell wall polysaccharides across the wheat endosperm have been identified, but little is known about the factors controlling these gradients or their biological roles, and not all cell wall matrix polysaccharides have been studied in depth. It is possible that these gradients are related to cell age and lineage, since the sub-aleurone layer is thought to derive from periclinal cell divisions of aleurone cells, occurring later into grain development

than the divisions of central endosperm cells that give rise to the central starchy endosperm (Olsen et al. 1998; Olsen 2001). Although the initial formation of cell walls in the developing rice endosperm is well described and the polysaccharide composition of the mature grain has been reported, the sequence of deposition of individual wall polysaccharides has not been reported. Wheat and rice grain present important anatomical differences, first of all, the presence of a crease in wheat accommodating the vascular bundle and acting as the sole point of entry of assimilates in the endosperm. In rice, on the contrary, nutrients are unloaded from the phloem in the nucellar epidermis, and can move circumferentially to then enter the endosperm at different points via the aleurone cells. Cell wall composition and deposition dynamics in the two species may therefore reflect this difference in their grain physiology. The composition of the major polysaccharides in rice grain cell walls in particular is a matter of some debate in the literature (Mod et al. 1978; Shibuya et al. 1985; Lai et al. 2007) with significantly different compositions being proposed. The aim of the present study was therefore to conduct a comparative analysis to determine the temporal patterns of polymer deposition in cell walls of developing rice grain, focusing on the wholegrain, and to compare these with the pattern in wheat, which has been more thoroughly described.

Table 4.1. Cell wall directed monoclonal antibodies used in this study.

Antibody	Antigen	Reference
Arabinoxylans		
INRA-AX1	arabinoxylan	(Guillon et al. 2004)
LM28	glucuronoxylan	in preparation
Phenolic components		
LM12	feruloylated polysaccharides	(Pedersen et al. 2012)
INRA-COU1	coumaric acid	(Tranquet et al. 2009)
Mixed Linkage β Glucan		

MLG	mixed linkage β glucan	(Meikle et al. 1994)
Minor non-cellulosic polysaccharides		
Callose	1-3 β -glucan	(Meikle et al. 1991)
LM21	heteromannan	(Marcus et al. 2010)
LM25	xyloglucan	(Pedersen et al. 2012)
Pectic Homogalacturonan		
LM19	un-esterified homogalacturonan	(Verhertbruggen et al. 2009)
JIM7	partially methyl- esterified pectic HG	(Clausen et al. 2003)
LM20	methyl-esterified pectic HG	(Verhertbruggen et al. 2009)
Pectic Rhamnogalacturon an-I		
INRA-RU1	rhamnogalacturon an backbone	(Ralet et al. 2010)
LM5	(1-4)- β -D-galactan	(Jones et al. 1997)
LM6	(1-5)- α -L-arabinan	(Willats et al. 1998)

4.2 Results

Cell wall composition and distribution of polysaccharides within different tissues throughout grain development is a largely underexplored area, particularly in rice. Several studies exist in wheat documenting either particular phases of grain development or focus on particular polysaccharides but a complete examination of all the major polysaccharides throughout grain development was absent in both wheat and rice.

The precise spatial and temporal localisation of cell wall polysaccharides was probed with an array of cell wall polysaccharide specific monoclonal antibodies (table 5.1), in both wheat and rice grains. Grain tissue was carefully harvested and examined with immunofluorescence microscopy at 5 developmental time points to represent the 5 major phases of grain development; cellularisation (4 DAA), expansion (8 DAA), differentiation (12 DAA), storage component deposition (20 DAA), and maturation (28DAA). Calcofluor White 2mr was applied as a counter stain to all antibody labelled sections, this labels all β -glycan linkages in plant cell walls to produce fluorescence under UV excitation. β -glycans exist in many cell wall polysaccharides in plant cell walls including cellulose, callose, Mixed-link β glucan and xyloglucan, this provides a clear structural overview of all the cell walls in grain, allowing specific cells and cell types to be distinguished and to see how the grain proportions change throughout development.

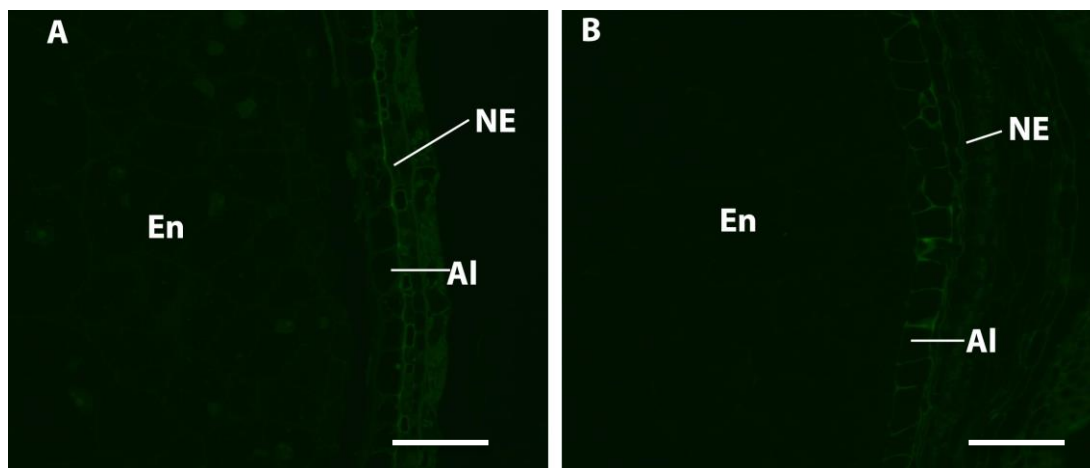


Figure 4.1. Autofluorescence control images of 12 DAA rice (A) and 12 DAA wheat (B) under 568nm Ar-Kr laser illumination. AI = aleurone, NE = nucellar epidermis, En = starchy endosperm. Bars = 100 μ m

4.2.1 Dynamics of non-cellulosic/non-pectic cell wall matrix glycans

4.2.1.1 Arabinoxylan (AX as detected with INRA-AX1 increases in labelling strength as development progresses in both wheat and rice in all tissues and wheat endosperm cell walls lacks the LM28 glucuronoxylan epitope that is widespread in rice endosperm cell walls

A combination of INRA-AX1 and LM28 monoclonal antibodies were used to detect different AX epitopes, LM28 for glucuronosylated xylans and INRA-AX1 for arabinosylated xylo-oligosaccharides (Guillon et al. 2004). The spatial patterns of AX epitope detection in developing wheat grain have been studied extensively (Guillon et al. 2004; McCartney et al. 2005; Philippe et al. 2006b; Robert et al. 2011; Dornez et al. 2011; Pellny et al. 2012). However AX distribution in developing rice grains has never been investigated with antibodies. In grains of wheat cv. Cadenza the INRA-AX1 epitope was detected in the cell walls of the nucellar epidermis and nucellar projection closest to the endosperm tissue at 8 DAA, while the modified aleurone cells in the crease region labelled strongly at 12 DAA, with weaker labelling extending radially across the endosperm towards the outer layer of cells, which are differentiated from the aleurone (Fig. 4.2 d). The strength of labelling increased towards maturity (28 DAA), when all of the endosperm cells were clearly labelled (Fig. 4.2 g). By contrast, in rice, labelling with INRA-AX1 was observed in all the starchy endosperm cells from as early as 6 DAA and increased in intensity throughout grain development. The aleurone cells displayed particularly strong labelling from 16 DAA, after they had visually differentiated with pronounced cell wall thickenings (Fig. 4.3 e). The presence of glucuronosylated xylan polysaccharides in developing wheat and rice grains was also examined using a recently isolated mAb, LM28 (Cornuault et al. 2015), which binds to a glucuronosyl-containing epitope widely present in heteroxylans, which was used for immunolocalisation of glucuronoxylan. However it should be noted that LM28 may recognise xylans that are both arabinosylated and glucuronosylated.

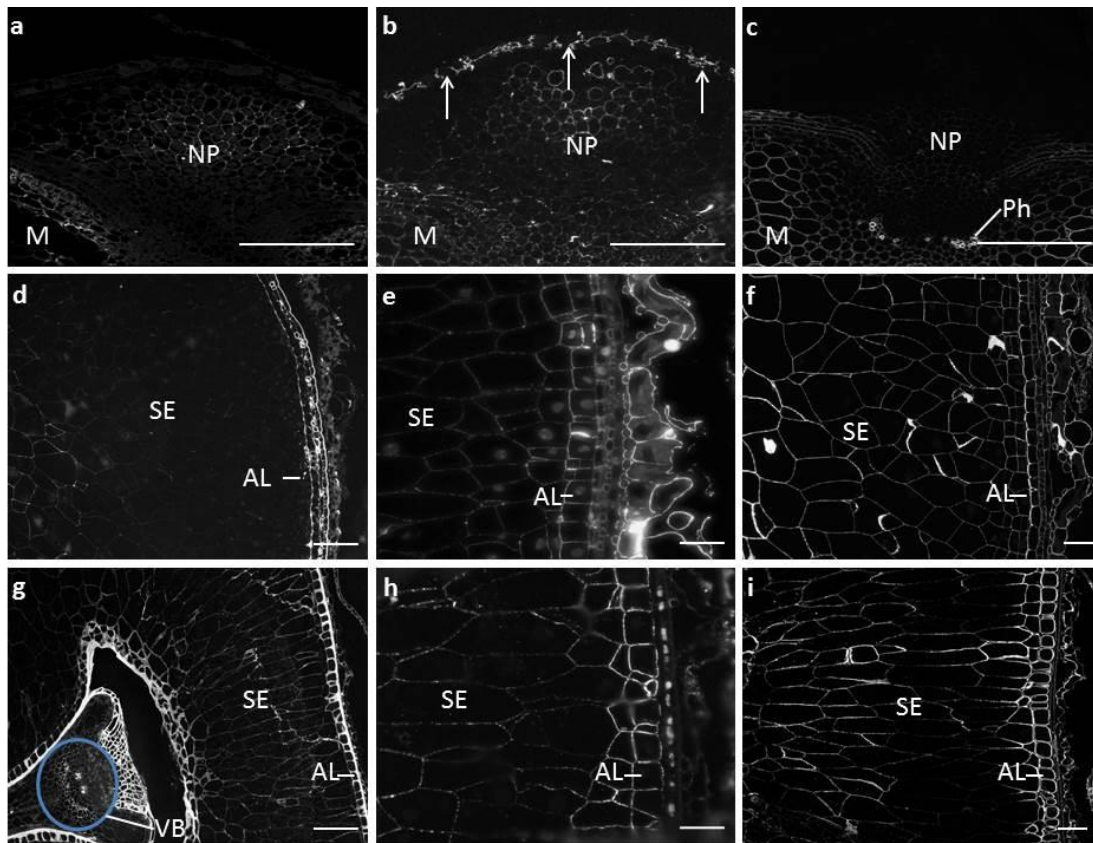


Figure 4.2. Indirect immunofluorescence detection of AX, callose and MLG in medial transverse sections of a wheat grain at 4 (a-c), 12 (d-f), and 28 DAA (g-i). Immunofluorescence detection of INRA-AX1 (a, d, g) and anti-callose (b, e, h) and anti-MLG (c, f, i). Al = aleurone, M = maternal pericarp, NP = nucellar projection, SE = starchy endosperm, VB = vascular bundle. Arrowheads indicate labelling of anticlinal cell wall extensions. Bars = 100 μ m, except D, G = 200 μ m

displayed clear labelling with the GUX mAb (Fig. 4.4 a, c) demonstrating a clear demarcation between the cell wall composition of the vegetative tissue of the maternal plant and that of the seed. From 20 DAA onwards the epitope was also abundant in the residual cell walls of the nucellar epidermis proximal to the aleurone tissues, but remained notably absent from the aleurone or endosperm tissues. Conversely, in rice grains, the GUX epitope was widespread throughout all tissue types examined from the earliest stage examined (shortly after the completion of cellularisation at 4 DAA) until the latest stage (28 DAA) (Fig. 4.4 b, d). The labelling of the endosperm by LM28 at 4 DAA was uniform and included all endosperm cell walls (Fig.4.4 b), however by 8 DAA has already become less distinct and uneven. By 28 DAA strong labelling by LM28 was detected only in aleurone and outer starchy endosperm cells whilst cells in the central region of starchy endosperm showed little or no labelling (fig. 4.4 d). The aleurone cells could be differentiated from the endosperm cells from 8 DAA with the presence of strong detection of the GUX epitope, which persisted until maturity.

4.2.1.2 Callose persists beyond cellularisation in the developing endosperm of both wheat and rice.

Callose (1,3- β -glucan) was detected in the extending anticlinal cell walls of both rice (Fig. 4.3 b) and wheat (Fig. 4.2 b) at cellularisation, and continued to be observed throughout the endosperm at all time points. Stronger labelling of the putative aleurone and sub-aleurone cells was also observed, compared with weaker punctate labelling of the central starchy endosperm cell walls (Fig. 4.3 d, f and 4.2 e, h). These results corroborate the data shown in several other studies (Morrison and Obrien 1976; Fineran et al. 1982; Stone and Clarke 1992; Brown et al. 1997; Li et al. 2003), although the study of Pellny et al (2012) no callose was detected in the starchy endosperm after 8 DAA.

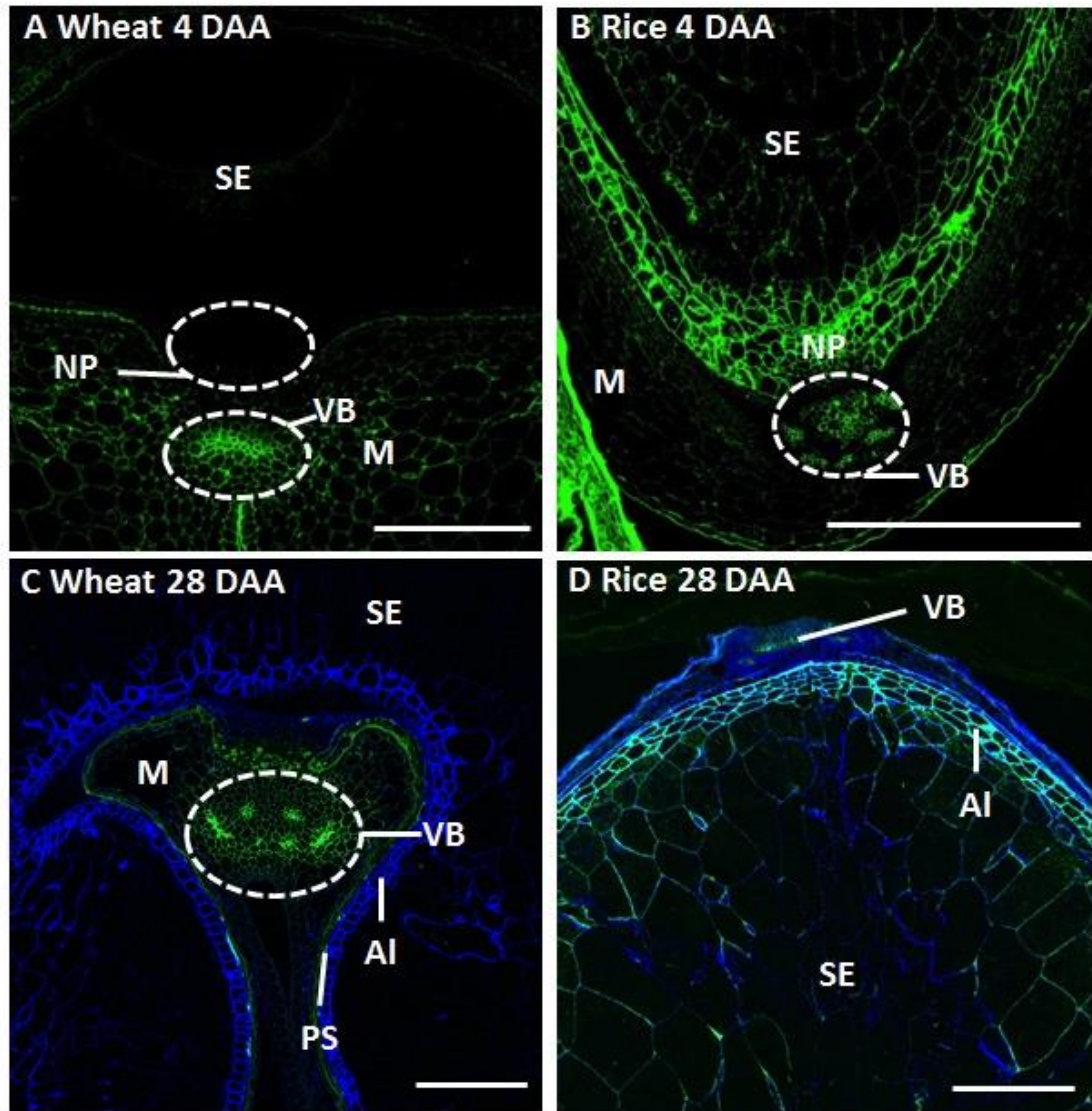


Figure 4.4. Indirect immunofluorescence detection of glucuronoxylan (GUX, LM28) in medial transverse sections of wheat (A, C) and rice (B, D) grains at 4 DAA (A, B) and 28 DAA (C, D). M = maternal pericarp, NP = nucellar projection, Al = aleurone, PS = pigment strand, SE = starchy endosperm, VB = vascular bundle, H = husk. Bar = 200 μ m

4.2.1.3 Mixed-linkage glucan is absent from the early endosperm cell walls of both wheat and rice prior to the detection of AX in both species. MLG is absent from the aleurone and nucellar epidermis of rice until 20 DAA, conversely in wheat these cells always display the strongest labelling for MLG.

During cellularisation, MLG was only detected in the maternal tissues of both species, primarily in the phloem vessels, nucellar epidermis and integuments. However, by 8 DAA the MLG antibody labelled the endosperm tissues of both species, and this labelling pattern remained throughout development (data not shown). Significantly, clear differences between the two species were observed at 12 DAA (Fig. 4.5). In wheat, the nucellar epidermis and aleurone cell walls are clearly labelled but in the labelling of cells immediately below the sub-aleurone layer (which are thought to be derived from recent divisions of aleurone cells and hence retain aleurone characteristics) was weaker than the central starchy endosperm cells (Fig. 4.5 a, c). This pattern is consistent with the previous study of (Philippe et al. 2006c).

By contrast, in rice, the vascular bundle, nucellar epidermis and aleurone cell walls were not labelled by the antibody, while labelling of sub-aleurone and starchy endosperm cells walls appears even and lack the polarisation exhibited in wheat (Fig. 4.5 b, d). By 20 DAA (data not shown) the aleurone cell walls of both species were prominently labelled and remained so throughout development suggesting significant remodelling, perhaps in response to the developing phases of grain development.

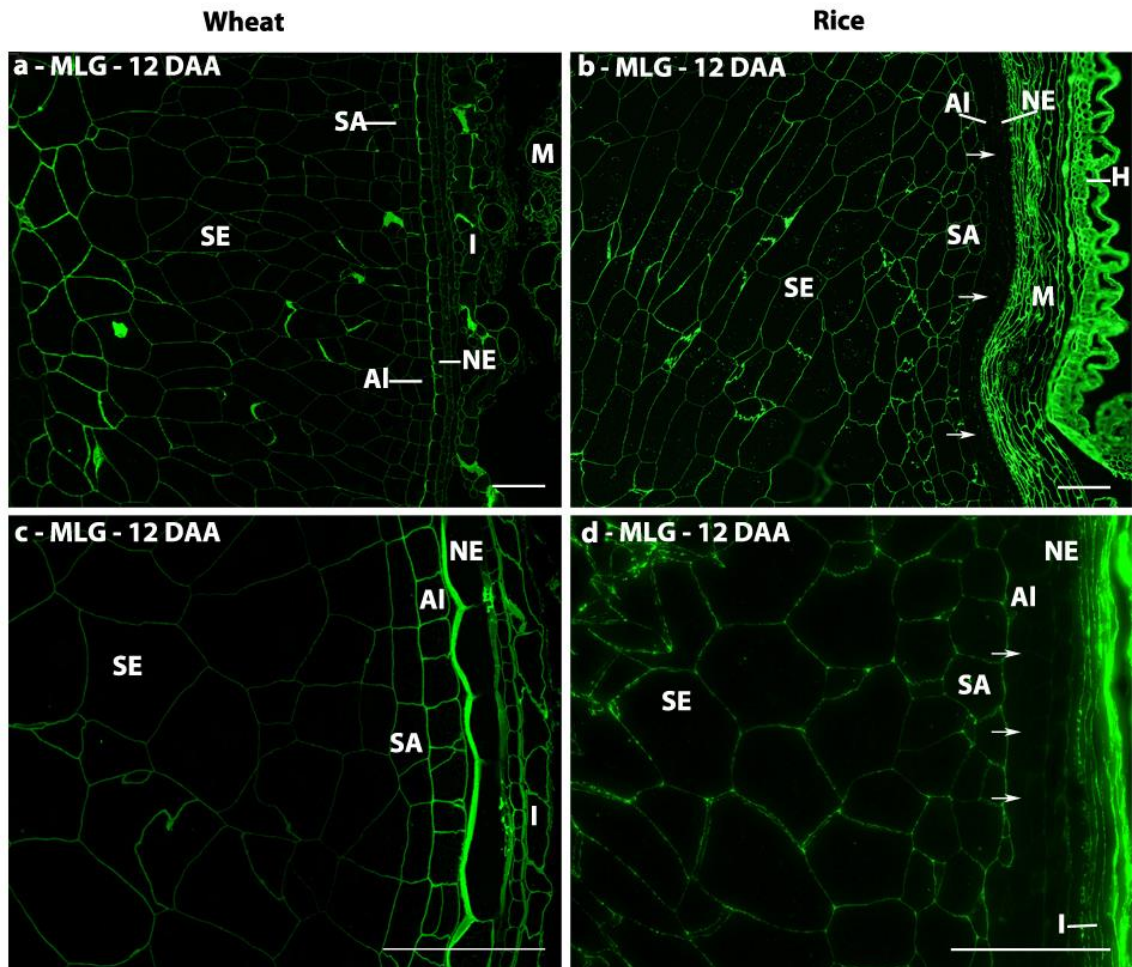


Figure 4.5. Indirect immunofluorescence detection of MLG in medial transverse sections of wheat (a, c) and rice (b, d) grains at 12 DAA. Arrowheads indicate absence of fluorescence labelling in the aleurone and nucellar epidermis. M = maternal pericarp, NP = nucellar projection, NE = nucellar epidermis, SA = sub-aleurone, AI = aleurone, I = Integuments, SE = starchy endosperm, VB = vascular bundle, H = husk. Bar = 100 μ m

4.2.1.4 Xyloglucan is detected in the anticlinal cell wall extensions of wheat and rice during cellularisation, and persists in the early endosperm cell walls, but can only be detected in the aleurone cells of rice at maturity.

The presence of xyloglucan in wheat cell walls has not been shown by biochemical analyses, however the study of Pellny et al. (2012) demonstrated the presence using the LM15 mAb (Pellny et al. 2012). Examination of wheat cell walls with the more recently generated LM25 xyloglucan antibody confirmed the presence of

xyloglucan in developing grains with abundant labelling of the walls undergoing cellularisation in the syncytial endosperm of both species, particularly those of the anticlinal cell wall extensions (Fig. 4.6 a, b). By 12 DAA no xyloglucan epitope was detectable in wheat (Fig. 4.6 c-f). However, in rice the cell wall of the aleurone cells retained significant labelling until 28 DAA (Fig. 4.6 f) but in wheat no LM25 epitope was detected in the aleurone cells at any stage (Fig. 4.6 e).

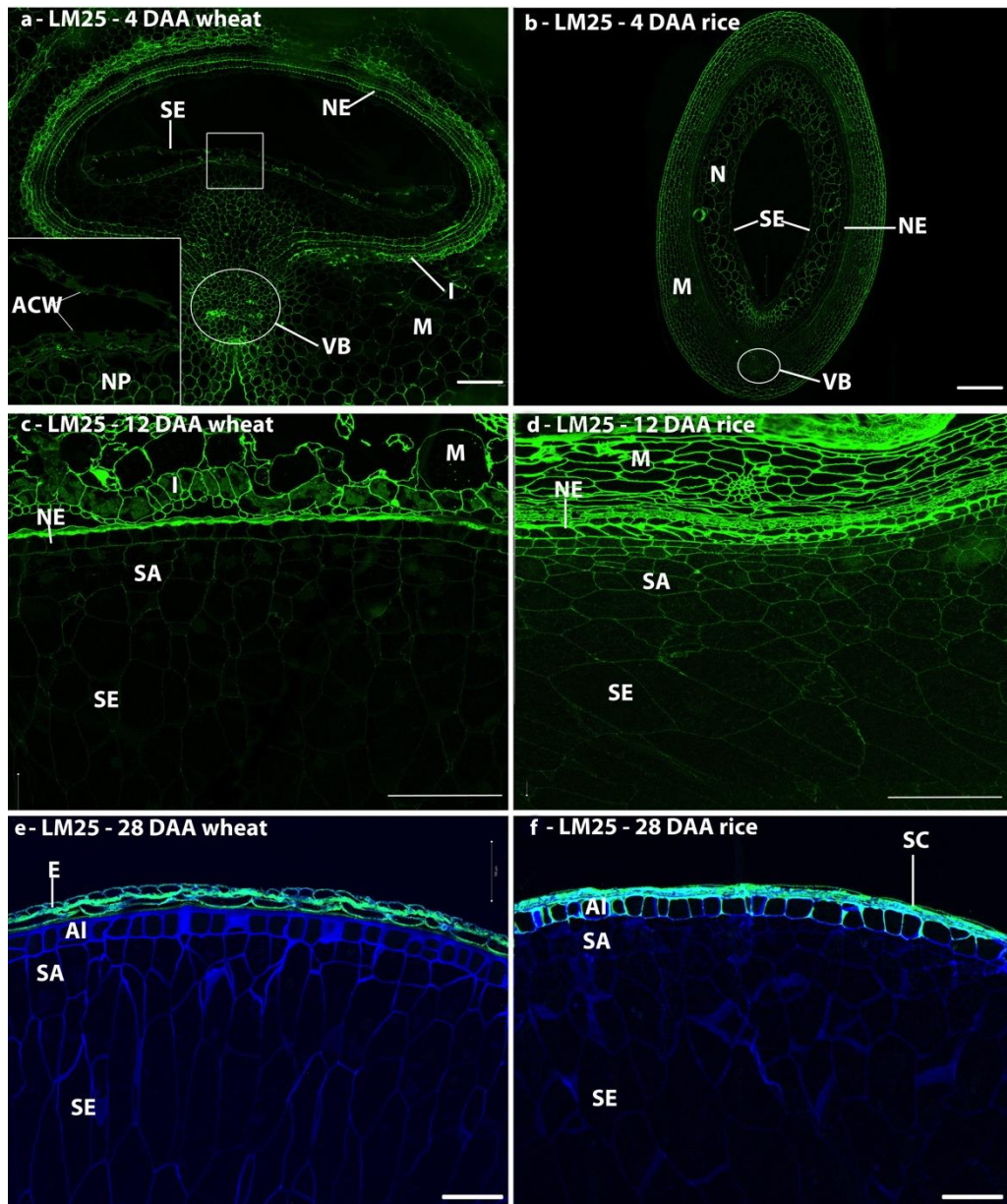


Figure 4.6. Indirect immunofluorescence detection of xyloglucan in medial transverse sections of wheat (a, c, e) and rice (b, d, f) grains at 4 (a, b), 12 (c, d), and 28 days after anthesis (e, f). Inset in micrograph a is a 4x enlargement of the boxed region, showing immunofluorescence labelling of the anticlinal cell walls. M = maternal pericarp, N = nucellus, NP = nucellar projection, NE =

nucellar epidermis, SA = sub-aleurone, AI = aleurone, I = integuments, SE = starchy endosperm, VB = vascular bundle, ACW = anticlinal cell wall.

Bar = 100 μm

4.2.1.5 Glucomannan is detected strongly in the endosperm cell walls of wheat, but cannot be detected at any developmental stage in rice endosperm.

Biochemical analyses have identified the presence of glucomannan in starchy endosperm and aleurone cell walls of wheat (Mares and Stone 1973b; Bacic and Stone 1981) and recent analyses with the LM21 heteromannan antibody detected heteromannan epitopes throughout development (Pellny et al. 2012). The immunolabelling data presented here corroborates the study of Pellny et al. (2012), with LM21 showing strong but uneven labelling of starchy endosperm and sub-aleurone cell walls (Fig. 4.7 a, c). In wheat grain from 12 DAA onwards (Fig. 4.7 c) the LM21 labelling was reduced in the aleurone cells with no signal detected at maturity. By contrast, no detection of the LM21 epitope in endosperm cell walls of rice was observed at any developmental stage, although it was observed in the outer maternal tissues (Fig. 4.7 b, d). This agrees with available cell wall composition data for rice endosperm, which rarely records mannans as present (Shibuya et al. 1985; Shibuya 1989). However, some reports particularly the study of (Lai et al 2004) mannans are recorded in small quantities in specific cultivars.

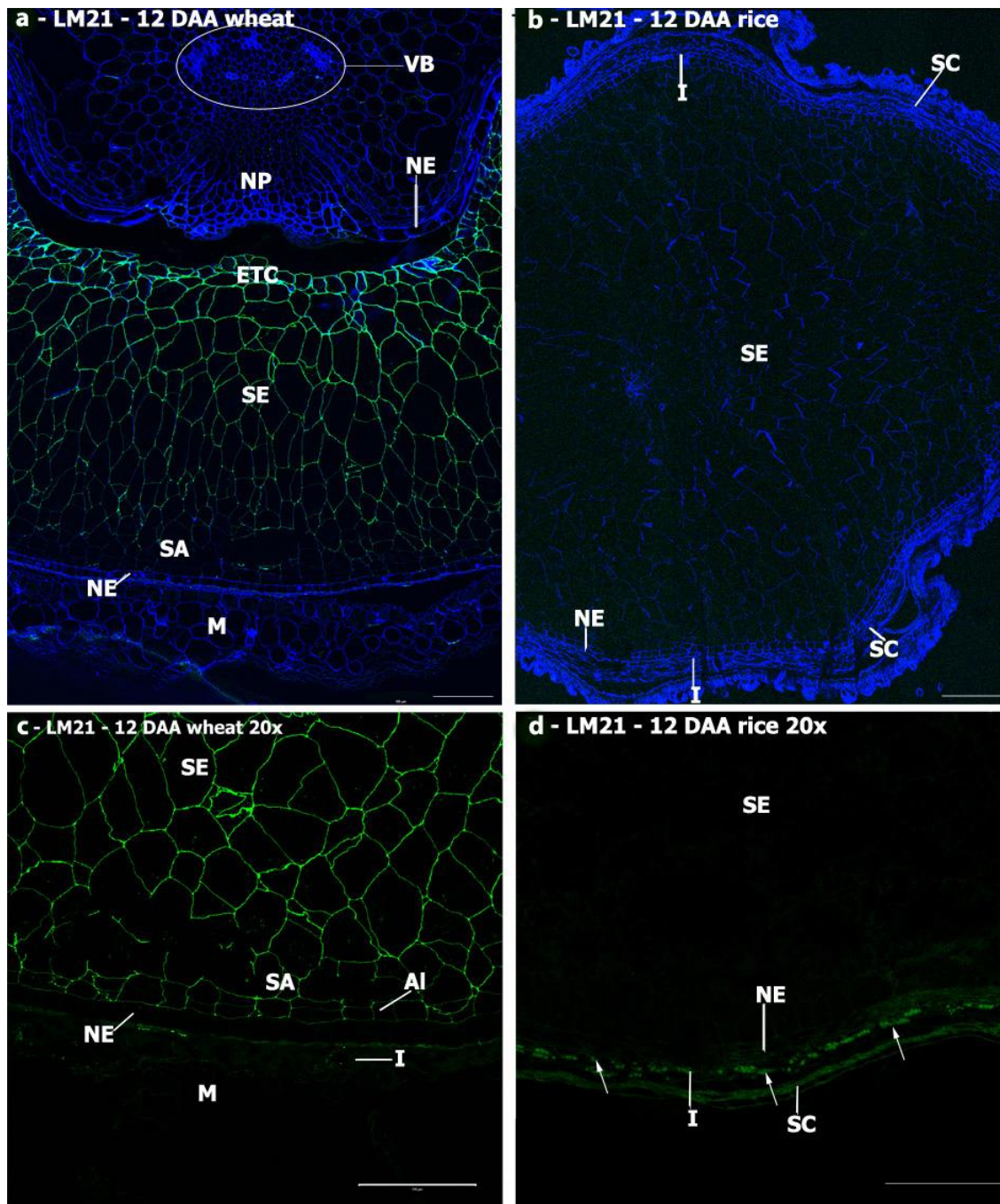


Figure 4.7. Indirect immunofluorescence detection of heteromannan in medial transverse sections of wheat (a, c) and rice (b, d) grains at 12 DAA.

Micrographs c and d are 4x enlargements of the outer endosperm regions of micrographs a and b to show that the heteromannan signal is present throughout the endosperm and sub aleurone tissues in wheat, but remains absent in rice. M = maternal pericarp, N = nucellus, NP = nucellar projection, NE = nucellar epidermis, SA = sub-aleurone, Al = aleurone, I= integuments, SE = starchy endosperm, VB = vascular bundle, ETC = endosperm transfer cells, SC = seed coat. Bar = 100 μ m

4.2.1.6 Dynamics of pectic polysaccharides

4.2.1.6.1 The presence of glycan domains of pectic supramolecules was studied using sets of antibody probes specific for HG and RG-I polysaccharides. Homogalacturonan methylation state appears to be cultivar dependant in wheat endosperm tissues, whereas LM19 was the major epitope detected in rice endosperm.

Monosaccharide analyses of wheat grain have not previously reported any pectin content. However, the recent study of Chateigner-Boutin et al. 2014 reported significant presence of HG and RG-I in the later stages of wheat grain development, and also demonstrated that the labelling could be made even stronger by the use of lichenase and xylanase to remove both AX and MLG. Using the JIM7 antibody, which recognised a methyl-esterified HG epitope, labelling signal could be clearly identified in the maternal tissues of wheat (Fig. 4.8). The crease region, in particular, was labelled throughout development, with no labelling of the endosperm tissues seen at any stage examined. The patterns of localisation of the LM19 epitope (specific for un-esterified HG) differed from those observed with JIM7. Specifically, the LM19 epitope was restricted to the cells of the nucellar projection, and displayed a gradient of labelling that was strongest in the cells closest to the endosperm cavity in the early stages of development (4-12 DAA) of wheat (Fig. 4.8 b). However these cells are degraded as development progresses and their collapsed walls label weakly after 12 DAA. This may be indicative of partially degraded cell walls (Fig. 4.8 d). The nucellar epidermis of wheat labelled strongly with LM19 at 12 DAA, and labelling persisted until 28 DAA (Fig. 4.8 d). By contrast, broader patterns of labelling with JIM7 and LM19, including the cell walls of the endosperm, aleurone cells as well as all maternal tissues (Fig. 4.8 f, h), were observed in rice. The LM19 epitope was the major epitope detected in the starchy endosperm of rice grain, indicating the presence of an unesterified form of HG.

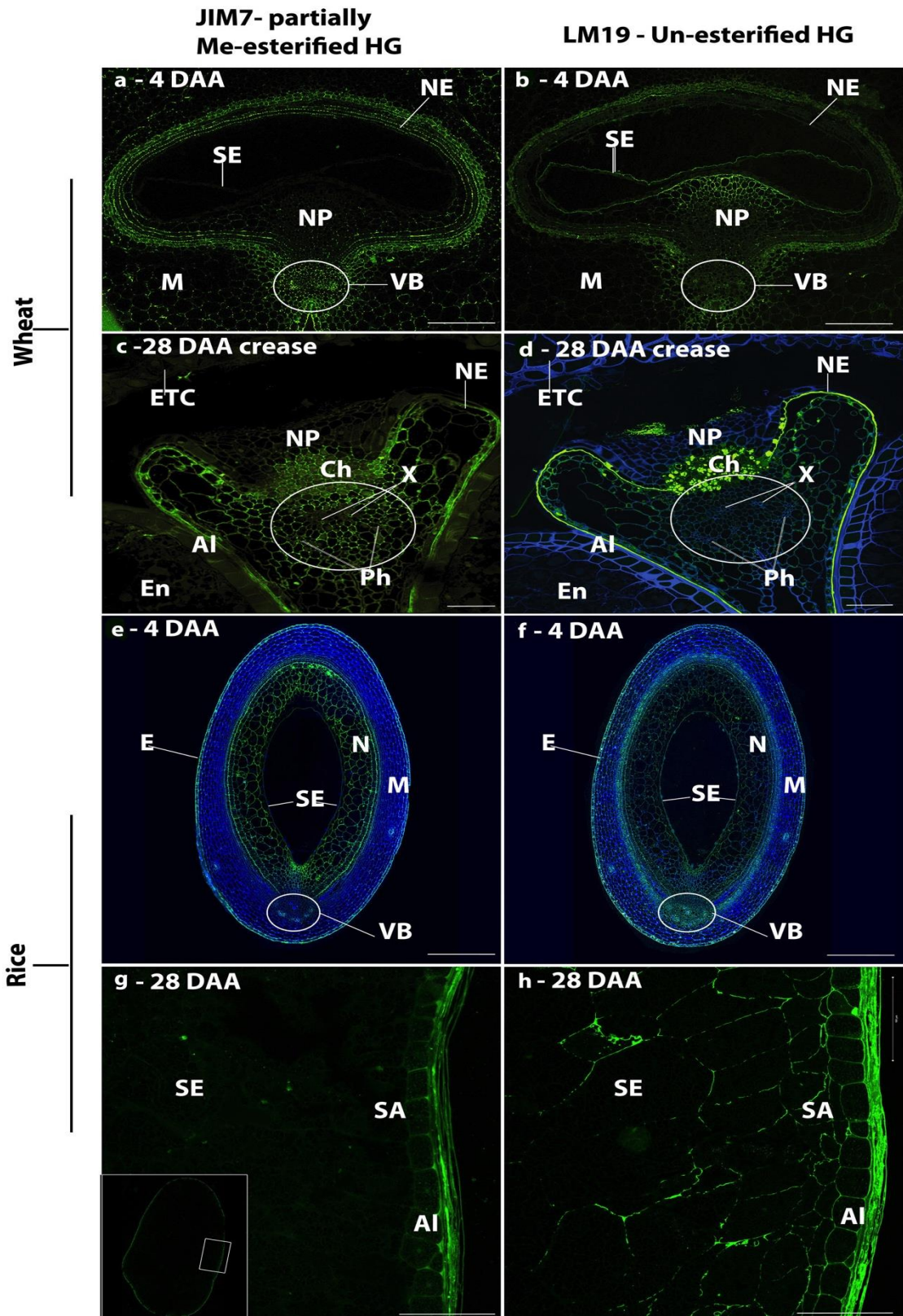


Fig 4.8. Indirect immunofluorescence detection of pectic HG in medial transverse sections of wheat (a-d) and rice (e-h) grains at 4 (a, b, e, f) and 28 DAA (c, d, g, h) using JIM7 and LM19 monoclonal antibodies. Inset in micrograph g is a lower magnification image with the boxed region indicating

the region imaged for micrographs g and h. M = maternal pericarp, N = nucellus, NP = nucellar projection, Ph = phloem, X = xylem, NE = nucellar epidermis, SA = sub-aleurone, Al = aleurone, I = integuments, SE = starchy endosperm, VB = vascular bundle, E = epidermis, Ch = chalazal region, ETC = endosperm transfer cells. Bar = 100 μ m

4.2.1.6.2 Rhamnogalacturonan-I backbone epitope detection is earlier in the endosperm of rice at (12 DAA) than in wheat (20 DAA).

The presence of RG-I was determined using the INRA-RU1 antibody specific for the RG-I backbone. In wheat, the cell wall of the starchy endosperm displayed weak labelling from 20 DAA with INRA-RU1, increasing in intensity by 28 DAA, but this labelling did not extend to the cells of the sub-aleurone and aleurone. A similar pattern was observed in rice at 12 DAA, but by 28 DAA the labelling was extended to include the cells of the aleurone and sub-aleurone (Fig. 4.9 b, d). Maternal tissues of both species exhibited stronger labelling by INRA- RU1 at all time-points, especially the cell walls of the vascular regions. This is consistent with the reported presence of significant proportions of pectic polysaccharides in these tissues (Shibuya et al. 1985; Hay and Spanswick 2006). In the maternal pericarp of wheat the RU1 epitope was localised at the triangular cell wall junction zones prior to 12 DAA, but at later stages these cells have been crushed during grain expansion and cannot be distinguished clearly. In rice, however, the INRA-RU1 epitope was more widely distributed throughout the walls of all pericarp cells and had no apparent specificity for cell wall junctions.

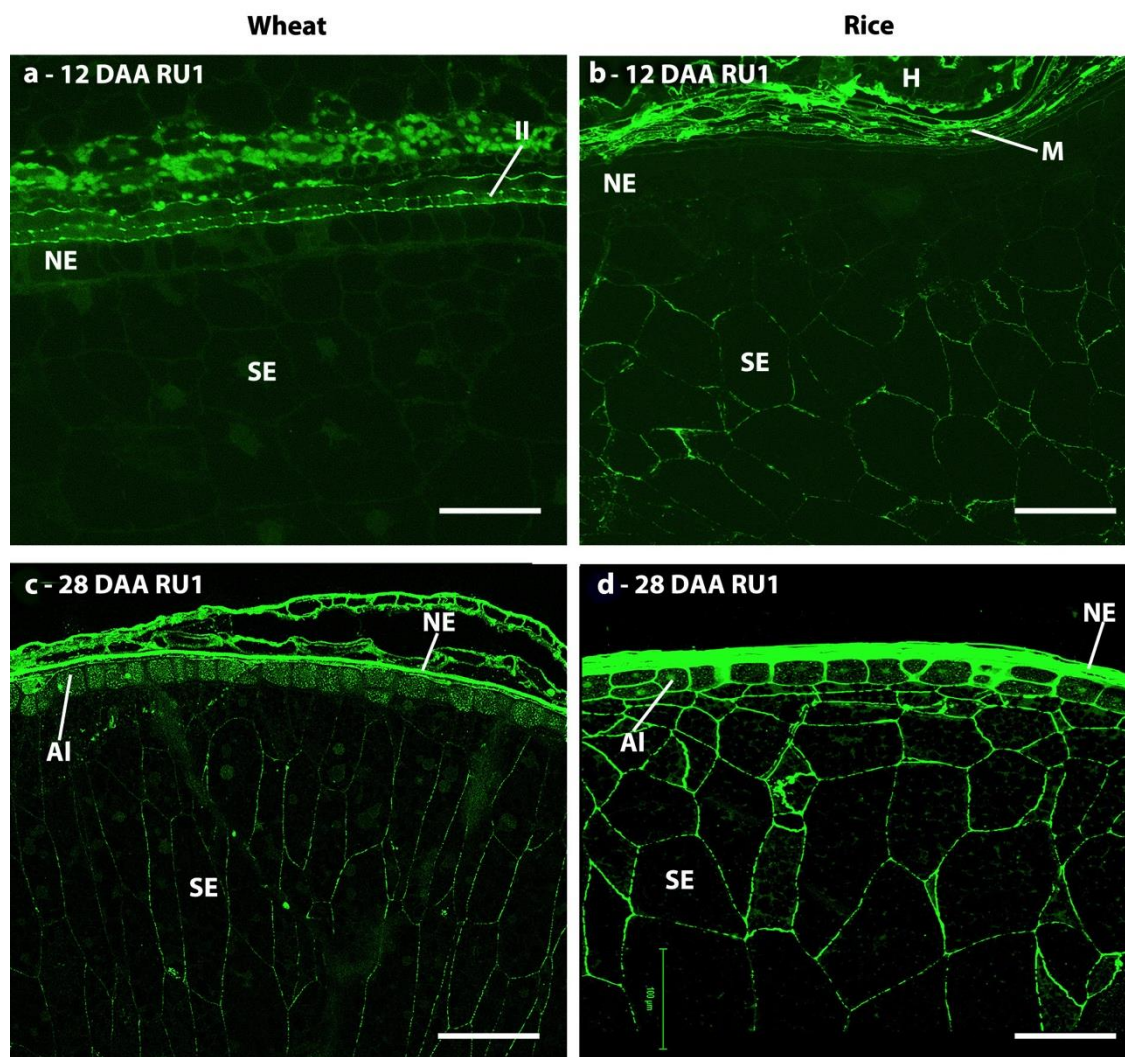


Figure 4.9. Indirect immunofluorescence detection of RG-I backbone in medial transverse sections of wheat (a, c) and rice (b, d) grains at 12 (a, b) and 28 days after anthesis (c, d). M = maternal pericarp, NE = nucellar epidermis, SA = sub-aleurone, AI = aleurone, I = integuments, SE = starchy endosperm, II = inner integuments, H = husk. Bar = 100 μ m

4.2.1.6.3 Galactan (LM5) and arabinan (LM6) RG-I Side chains can be detected earlier in development than RG-I back bone epitopes in both wheat and rice endosperm

Rhamnogalacturonan side chains were detected with two antibodies, LM5 for 1,4-galactan and LM6 for 1,5-arabinan. The only evidence for the presence of RG-I in wheat endosperm at early developmental stages is the weak and transient binding of LM6 from 8 DAA to 12 DAA (Fig. 4.10 d). However, labelling was absent by 28

DAA (Fig. 4.10 f). Conversely rice, shows ubiquitous labelling of arabinan in the starchy endosperm at all stages after cellularisation has been completed by LM6.

The LM5 and LM6 epitopes were weakly detected in the maternal tissues at all developmental stages in both species with the LM5 epitope being consistently more abundant in the inner pericarp tissues than in the outer pericarp tissues (Fig. 4.9 a). In wheat endosperm cells, the LM5 galactan epitope was not detected at any stage, whilst it was detected in the cellularising endosperm of rice, with every endosperm cell being labelled at 4 DAA (Fig. 4.10 g). Subsequently, the LM5 epitope became increasingly restricted to the outer layers of the endosperm, with only the aleurone and sub-aleurone being labelled by 12 DAA (Fig. 4.10 i) and only the aleurone cells at 28 DAA (Fig. 4.10 k). The LM6 arabinan epitope differed in its pattern of distribution in comparison to the LM5 epitope in rice, showing little or no labelling at 4 DAA (Fig. 4.10 h) then slowly increasing in distribution throughout development with weak detection in all endosperm cells by 8 DAA, all starchy endosperm and sub-aleurone cells being labelled at 28 DAA. The inner faces of the aleurone cell walls proximal to the cell membrane were most strongly labelled at 28 DAA (Fig. 4.10 l). It was also frequently observed that the LM6 epitope appeared to be surrounding circular intracellular structures, which did not appear to be protein bodies or nuclei.

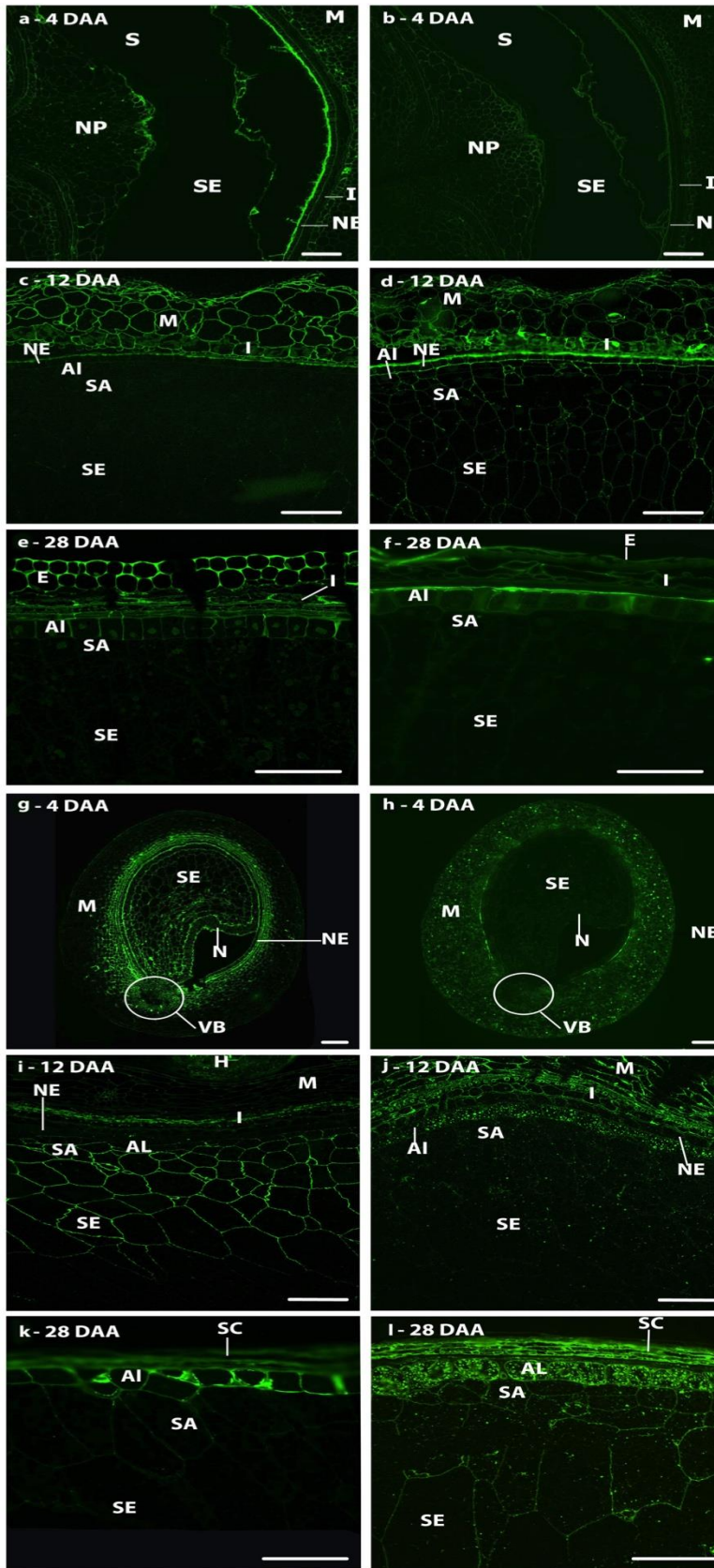


Figure 4.10. Indirect immunofluorescence detection of pectic arabinan and galactan as in medial transverse sections of wheat (A-F) and rice (G-L) grains

at 4 (A, B, G, H), 12 (C, D, I, J) and 28 days after anthesis (E, F, K, L), using LM5 (A, C, E, G, I, K) and LM6 (B, D, F, H, J, L) monoclonal antibodies. M = maternal pericarp, NE = nucellar epidermis, SA = sub-aleurone, AI = aleurone, I = integuments, SE = starchy endosperm, S = syncytium, I = integuments, SC = seed coat, H = husk, VB = vascular bundle, N = nucellus, NP = nucellar projection, E= epidermis. Bar = 100 μ m

4.2.1.7 Developmental dynamics of Phenolic polysaccharides.

4.2.1.7.1 Ferulic acid epitopes more prevalent in the endosperm cells proximal to the crease cavity in wheat grains after 20 DAA, in rice ferulic acid labelling was evenly distributed throughout the endosperm.

In rice, the LM12 epitope was found to be evenly distributed through out all the cells of the endosperm and maternal tissue by 12 DAA, with nucellar epidermis, phloem and the putative cells of the aleurone layer, displaying stronger labelling (Fig. 4.11 f). This distribution pattern did not change throughout grain development although the strength of the labelling in the endosperm cells increased towards 28 DAA (Fig. 4.11 g, h). In wheat, LM12 labelled the cells of the starchy endosperm only weakly from 20 DAA with those closer to the crease showing more pronounced labelling than in the outer regions (Fig. 4.11 c). The endosperm transfer cell region, nucellar projection, nucellar epidermis vascular bundle and epidermal tissue all showed strong and even labelling from 8 DAA and this persisted throughout development (Fig 4.11 b).

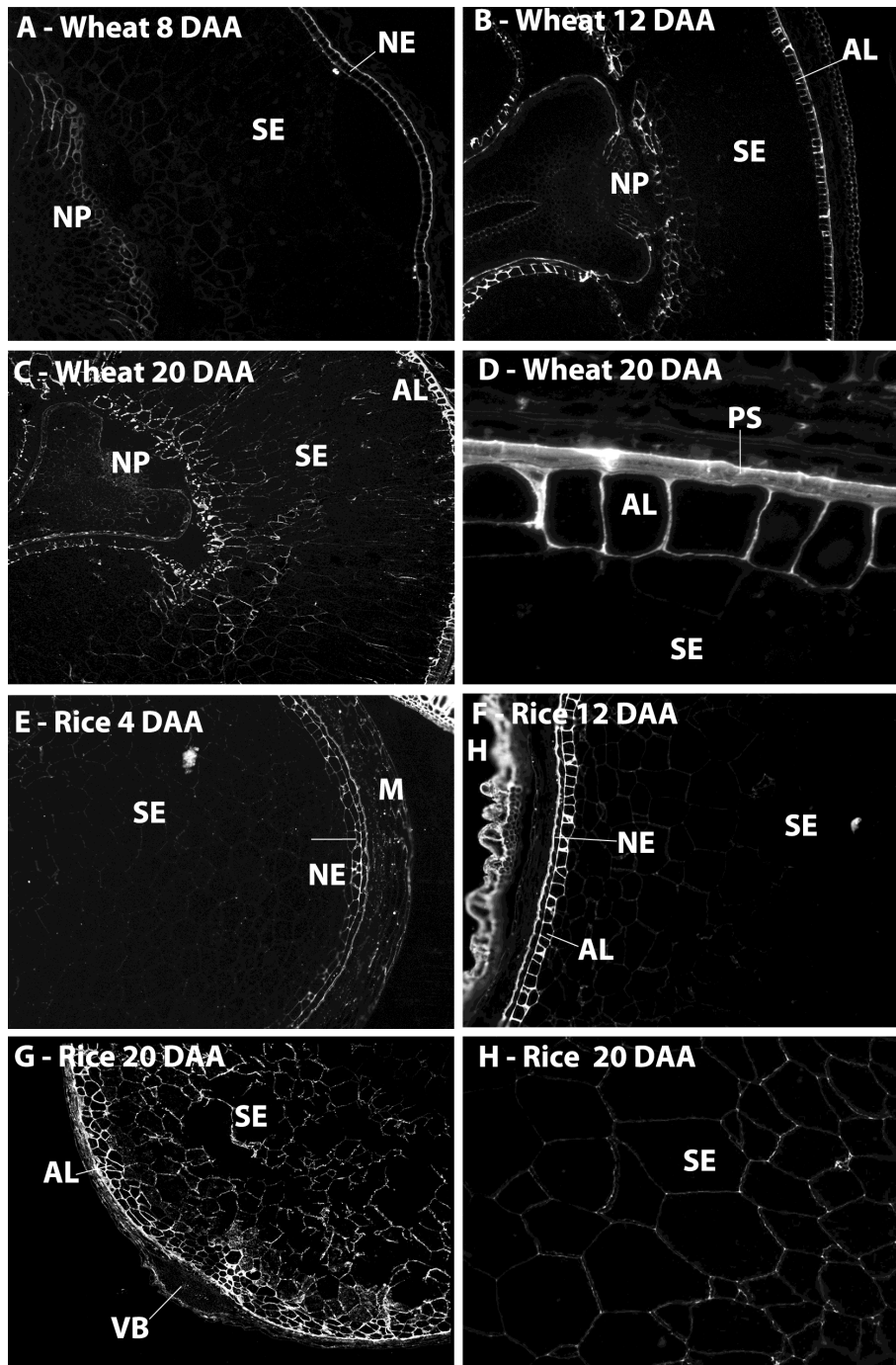


Fig 4.11. Indirect immunofluorescence detection of feruloylated polysaccharides in medial transverse sections of wheat (A-D) and rice (E-H) grains at 4 (E), 8 (A), 12 (B, F) and 20 DAA (C, D, G, H) using LM12 monoclonal antibody. Micrograph D and H are higher magnifications of C and G. M = maternal pericarp, NP = nucellar projection, NE = nucellar epidermis, SA = sub-aleurone, Al = aleurone, SE = starchy endosperm, VB = vascular bundle, PS = pigment strand. Bar = 100 µm

4.2.1.7.2 *p*-Coumaric acid is found in both the aleurone and endosperm cells at maturity in rice, but is detected only in the aleurone cells of wheat grains

In wheat, the INRA-COU1 *p*-coumaric acid epitope was initially localised only in the maternal tissues, which were labelled strongly, but at 12 DAA when the cells of the aleurone layer also became labelled (Fig. 4.12 a, b). This labelling did not initially extend to the aleurone cells proximal to the crease region (Fig. 4.12 a, b arrowheads), but the INRA-COU1 epitope was detected in these cells by 28 DAA (Fig 4.12 c). The distribution of *p*-coumaric acid in the aleurone cells at 28 DAA was restricted to a discrete layer within the wall rather than extending throughout the entire width of the wall as did the AX and MLG labelling. In rice, the INRA-COU1 showed a different pattern of localisation, compared to wheat, first appearing in the aleurone cells and endosperm transfer cells closest to the nucellar projection and vascular bundle at 12 DAA (Fig. 4.12 f) and then extending through the aleurone cells, showing uniform labelling throughout all aleurone cells by 28 DAA (Fig. 4.12 g, h).

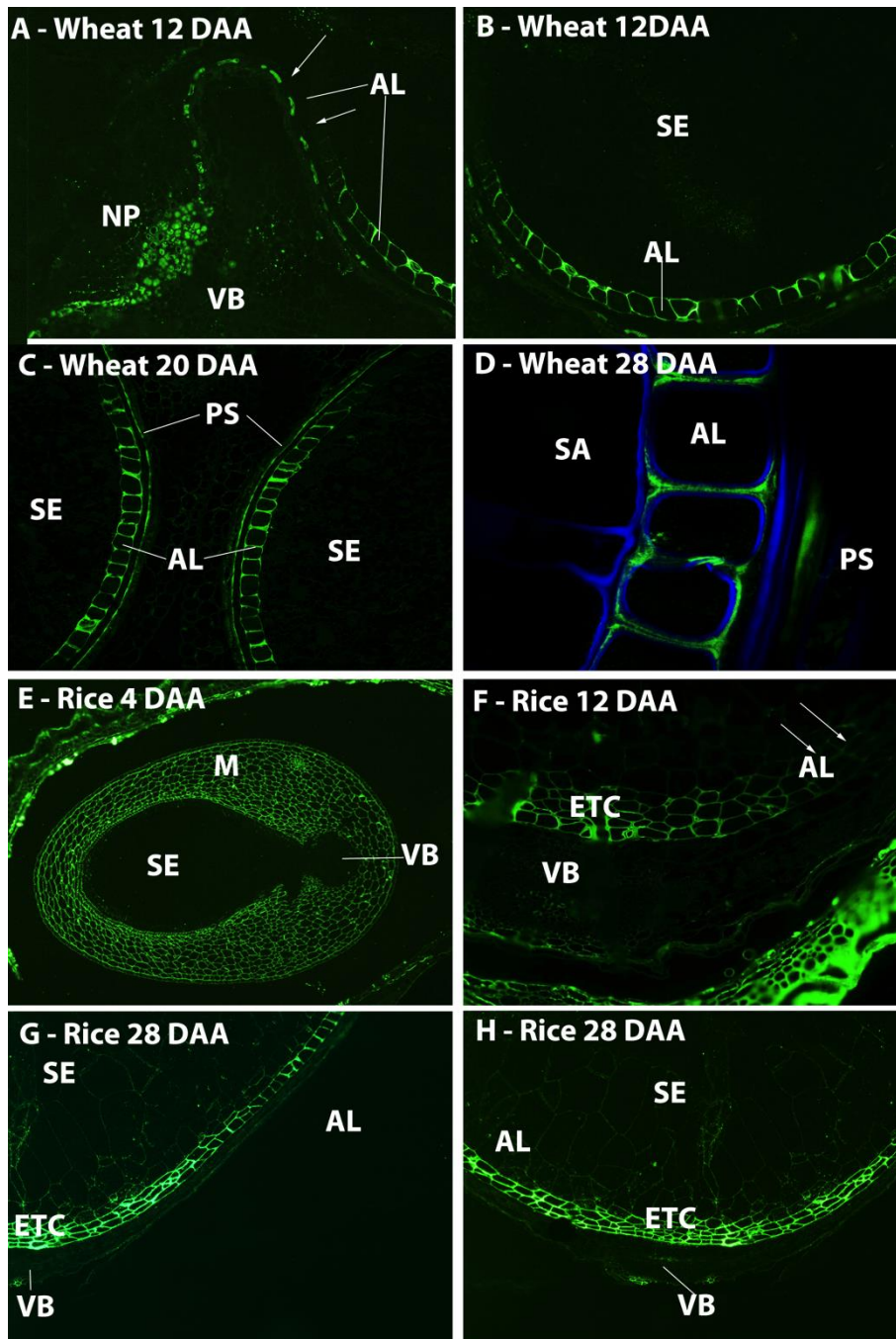


Fig 4.12. Indirect immunofluorescence detection of coumaric acid in medial transverse sections of wheat (A-D) and rice (E-H) grains at 4 (E), 12 (A, B, F), 20 (C) and 28 DAA (D, G, H) using INRA-COU1 monoclonal antibody. Arrowheads indicate aleurone cells unlabelled by INRA-COU1. M = maternal pericarp, NP = nucellar projection, NE = nucellar epidermis, SA = sub-aleurone, AL = aleurone, SE = starchy endosperm, VB = vascular bundle, PS = pigment strand, ETC = endosperm transfer cells. Bar = 100 µm

4.2.2 Unmasking of cell wall polysaccharides

Monoclonal antibodies are relatively large structures and antibodies raised to cell wall epitopes may in some cases be unable to bind to an epitope they recognise *in situ* due to the large quantities of other polysaccharides present, which may either prevent access directly through steric interference, or through decreasing the probability of the antibody making contact with the epitope. In these cases the use of enzymes to remove specific cell wall polysaccharides prior to immunolabelling can therefore provide additional information about the localisation of epitopes within plant cell walls (Marcus et al. 2010; Chateigner-Boutin et al. 2014) by revealing additional locations of certain epitopes or by causing their loss of an epitope from certain regions, thus providing insight into the possible proximity of the different cell wall polysaccharides *in muro*.

4.2.2.1 Unmasking of pectic epitopes with a lichenase xylanase (LX) dual enzymatic treatment.

An experiment was carried out to examine the epitope masking of pectic cell wall polysaccharides in wheat and rice. Previous work by Chateigner-Boutin et al. (2014), in which wheat grain homogalacturonan structure was probed using LM19, JIM7 and LM20 antibodies, specific for differing degrees of HG methyl esterification, demonstrated epitope masking of all pectic epitopes in the developing wheat grain. However, in most cases a combination of lichenase and xylanase (GH11) treatments was required to reveal the epitopes, suggesting that in wheat endosperm pectin is a minor component tightly associated with the other major polysaccharides, since almost all of the cell wall needs to be removed in order for the pectin specific monoclonal antibodies to access their epitopes. Lichenase is an enzyme that degrades mixed link β -glucan, through the hydrolysis of (1-4)- β -D-glucosidic linkages adjacent to (1-3)- β -D-glucosidic linkages. As part of this PhD work, lichenase xylanase (LX) double digest was conducted on sections prepared from cv. Cadenza wheat grains rather than the cv. Recital used by Chateigner-Boutin et al. (2014). While labelling of wheat endosperm cell walls with LM19 and JIM7 was observed at 20 DAA, after LX treatment, none was observed for LM20 (Fig. 4.13 e, f). This contrasts with what was observed by Chateigner-Boutin et al. (2014) in cv. Recital where LM20 was the major epitope recognised in wheat endosperm at a similar developmental time point. Labelling with LM20 in cv. Cadenza was restricted to the pigment strand in the maternal tissues at this stage. The LM19 epitope was concentrated in the endosperm transfer cells and the endosperm cells proximal to

the crease cavity, with weaker labelling being seen throughout the endosperm (Fig. 4.13 d). The JIM7 epitope labelled all endosperm cell walls, with weaker labelling proximally to the crease cavity.

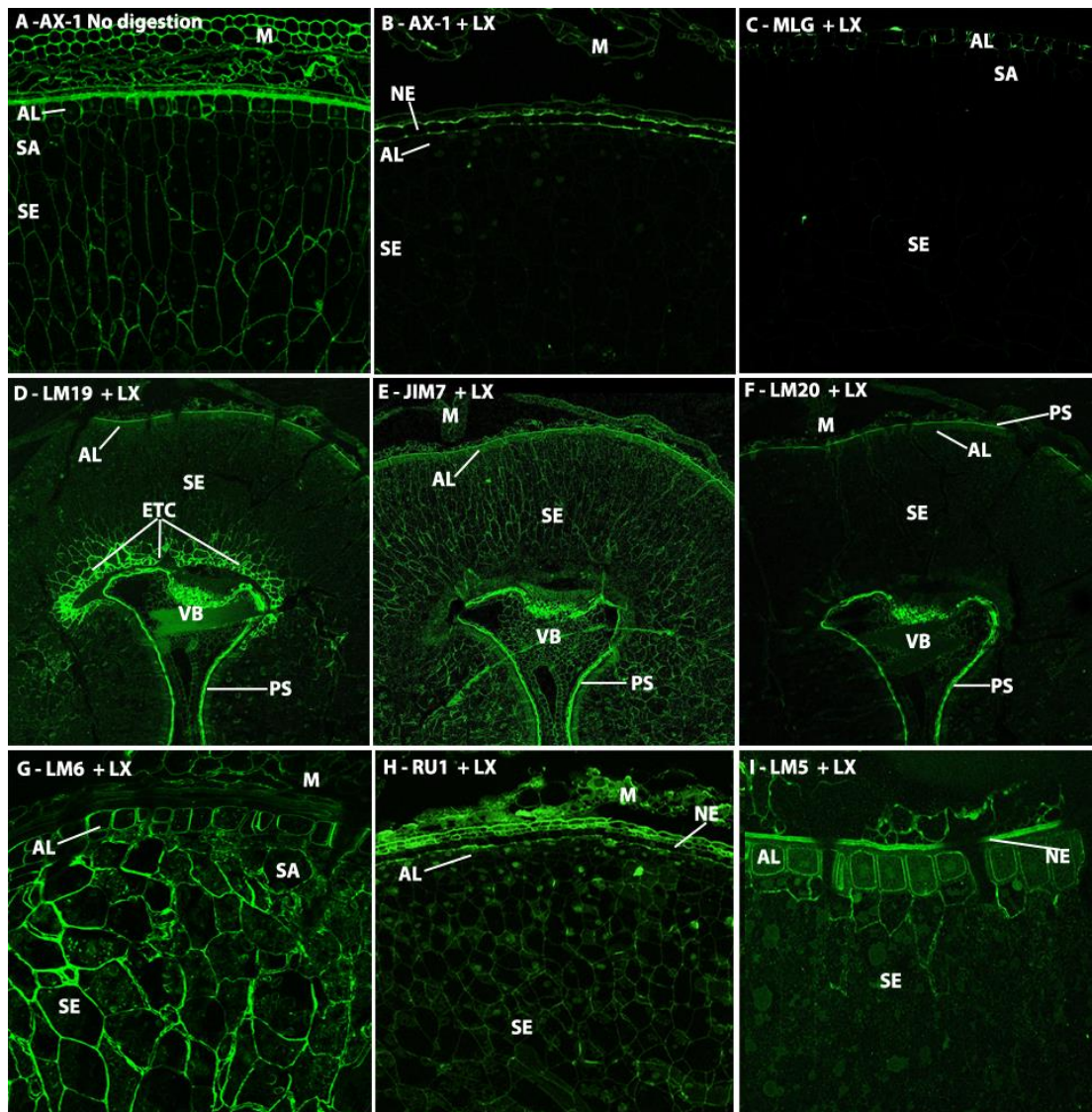


Figure 4.13. Indirect immunofluorescence detection of pectic epitopes in medial transverse sections of wheat grains at 20 DAA partially digested by lichenase and xylanase (LX) labelled with INRA-AX1 (A, B), Anti-MLG (C), LM19 (D), JIM7 (E), LM20 (F), LM6 (G), INRA-RU1 (H), LM5 (I) monoclonal antibodies. M = maternal pericarp, NP = nucellar projection, NE = nucellar epidermis, SA = sub-aleurone, Al = aleurone, SE = starchy endosperm, VB = vascular bundle, ETC = endosperm transfer cells, PS = pigment strand. Bar = 100 μ m

RG-I masking in cv. Cadenza was also examined using a LX digest, using INRA-RU1, LM5 and LM6 to detect the presence of revealed RG-I. Labelling patterns with all three antibodies were consistent with those reported by Chateigner-Boutin et al. (2014), with labelling by RU1 reported from as early as 12 DAA and was stronger in fluorescent intensity than prior to LX digestion (Fig. 4.12 g). LM6 epitopes were revealed to be more widely distributed amongst the starchy endosperm from 8 DAA (Fig. 4.12 h). While LM5 was only weakly revealed by enzymatic unmasking of the pigment strand, aleurone and some sub-aleurone cells (Fig. 4.12 i).

A comparative study of the enzymatic unmasking of rice pectic polysaccharide epitopes with a LX double digestion was also undertaken to see if similar changes in labelling patterns and chronology could be detected. Prior to LX digestion, only low methyl-esterified HG epitopes were labelled by LM19 in rice endosperm cell walls. While LM20 and JIM7 epitopes were both revealed by LX digestion to be evenly distributed throughout all starchy endosperm cells from 20 DAA (Fig 4.14 d, g). LM19 labelling was strengthened by LX unmasking but no change to its distribution pattern was observed. RG-I epitopes were not observed any earlier or across different tissues, but the labelling for RU1 and LM6 had a brighter fluorescence intensity and displayed less fluorescence noise after LX unmasking. LM5 labelling also showed no change in distribution pattern (Fig. 4.14 j), confirming the progressive restriction of the LM5 epitope to the outer endosperm and sub aleurone cells seen prior to unmasking (Fig 4.10 g, i, k) and thus proving it is not an artefact of epitope masking.

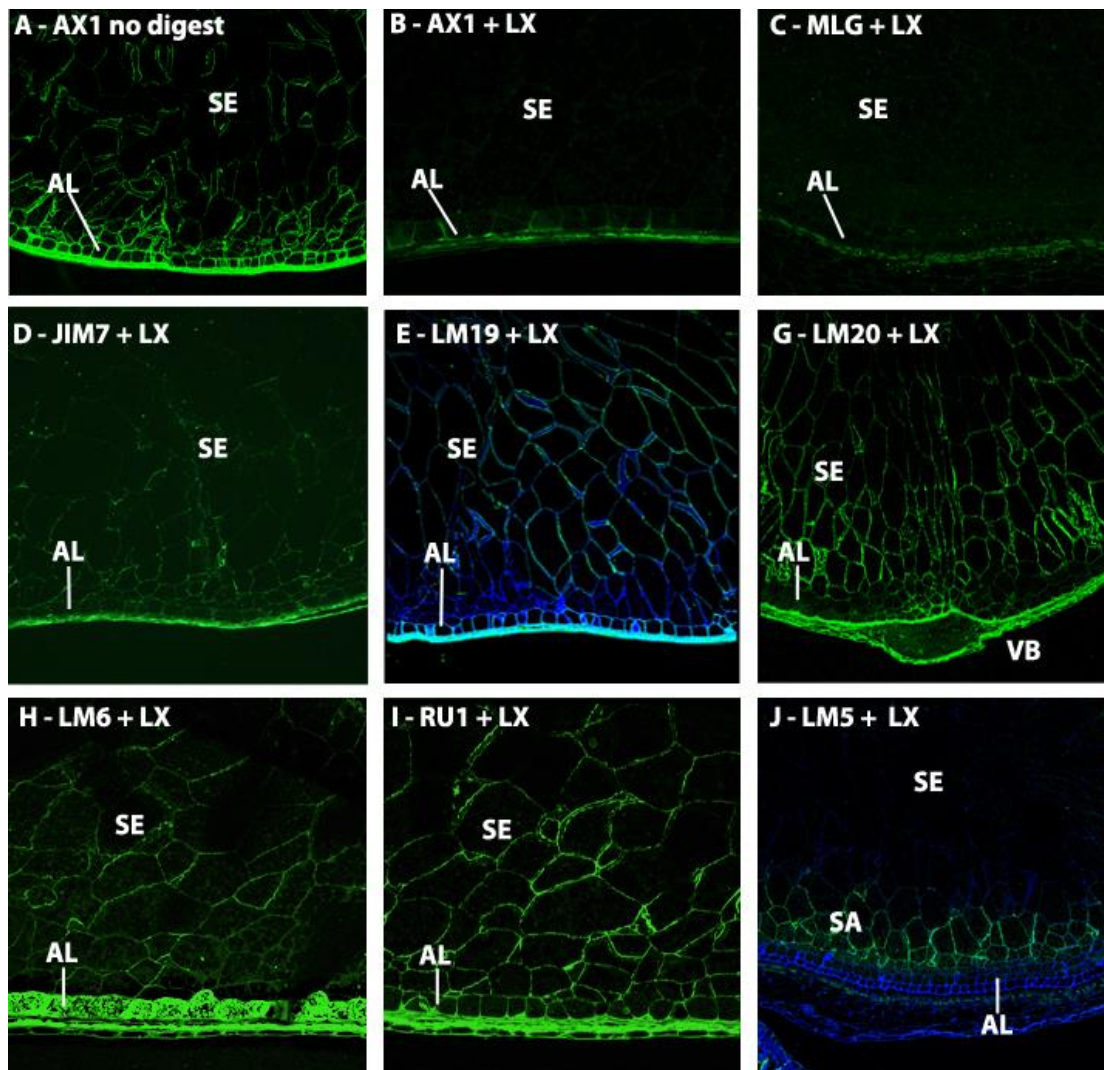


Figure 4.14. Indirect immunofluorescence detection of pectic epitopes in medial transverse sections of rice grains at 20 DAA partially digested by Lichenase and Xylanase (LX) labelled with INRA-AX1(A, B), Anti-MLG (C), JIM7 (D), LM19 (E), LM20 (F), LM6 (G), INRA-RU1 (H), LM5 (I) monoclonal antibodies. M = maternal pericarp, NP = nucellar projection, NE = nucellar epidermis, SA = sub-aleurone, Al = aleurone, SE = starchy endosperm, VB = vascular bundle, PS = pigment strand. Bar = 100 μ m

4.3 Discussion

4.3.1 Callose, arabinoxylan and Mixed link glucan exhibit a conserved order of deposition within the cellularising endosperm of wheat rice and barley.

Callose has long been reported to be one of the primary elements of cell plate formation during cellularisation in many species, including wheat and rice (Morrison and O'Brien 1976; Brown et al. 1997). Traditionally it has been reported to be transient, most likely being remodelled or remobilised after the end of cellularisation. This study confirms that the callose epitope can be detected in the extending anticlinal cell wall outgrowths and cell plates in wheat and rice, which occur during the syncytial stage of cellularisation, but also that detection remains possible until around 12 DAA. Specifically, in 12 DAA wheat, the periclinal cell walls of the aleurone cells and sub-aleurone cells were observed to have increased labelling intensity in comparison to the anticlinal walls implicating callose as a significant polysaccharide in the cell division and re-differentiation of the aleurone cells into sub-aleurone cells, which occurs up to at least 15 DAA (Evers 1970; Cochrane and Duffus 1981).

The endosperm cell walls of wheat and rice grain have been shown to be primarily hemicellulosic in nature, containing mainly AX and MLG, and to contain low to moderate levels of cellulose. Whilst wheat and rice have significant differences in the proportions of individual hemicelluloses, their spatial locations and kinetics of deposition are largely similar. Additionally, if reports of early cell wall deposition in wheat and barley (Wilson et al. 2006; Pellny et al. 2012) are considered, it appears that all three species follow the same sequence of deposition of callose, AX and MLG in the cellularising endosperm, suggesting that the factors regulating this early cell wall deposition in these grasses may be derived from a common ancestor. Hemicelluloses are likely to play a significant role in the mechanical structure of grain cell walls given that the deposition of these polysaccharides is conserved in homologous tissues.

Hemicelluloses have been proposed to be capable of crosslinking cellulose microfibrils to generate the basic load-bearing structure of the cell wall matrix (Scheller and Ulvskov 2010). However, the number of hemicelluloses, the variety of individual structures, and the dynamic modifications that they can undergo, are

indicative of a range of specific roles in cell wall matrices during cell wall formation and development.

Endosperm cell walls perform several distinct roles during grain development. In the early stages of grain development (4-12 DAA) they must be synthesised rapidly to allow grain expansion. Hydration level must also be regulated; allowing cell-to-cell exchange of soluble assimilates. Furthermore, their mechanical properties must match the changing biological conditions within the grain, by displaying sufficient flexibility and strength to accommodate grain expansion and subsequent desiccation. Finally, it has been postulated that cell walls may play a role in seed dormancy and germination, by acting both as a regulator of grain hydration and possibly as a secondary store of readily accessible carbohydrate for the germinating seedling. (Finch-Savage and Leubner-Metzger 2006).

By replacing most of the rigid and indigestible cellulose microfibrils with simpler hemicellulosic polysaccharides, the cell walls of cereals may be able to respond more rapidly and efficiently to the changes occurring within the developing grain.

AX deposition in the endosperm cell walls of rice follows the well characterised deposition pattern in wheat (Philippe et al 2006b) with the first evidence of its deposition coinciding with the cessation of the most rapid phase of grain expansion: as observed by labelling with the LM11 antibody at about 12 DAA in wheat (Gao et al. 1992; Shewry et al. 2012) and 8 DAA in rice (Hoshikawa 1973). However, previous studies of developing barley grain have shown that pre-treatment of sections with α -arabinofuranosidase to cleave arabinan side chains from the xylan backbone permits detection by LM11 from as early as 5 DAA (end of cellularisation) suggesting that a heavily substituted form of AX is initially deposited which cannot be recognised by this antibody without specific pretreatment (Wilson et al. 2006; Wilson et al. 2012). This would also be supported by reports of a steady decrease in AX substitution level in the course of wheat grain development (Toole et al. 2009). Rice endosperm appears to show a similar early deposition of AX that is detectable only after the use of arabinofuranosidase. In rice the AX also contains glucuronosyl substitutions as the LM28 epitope is detected at 4 DAA, significantly earlier than the INRA-AX1 epitope that is less sensitive for heavily substituted AX. Glucuronosyl substitutions of AX have been reported to be present in the pericarp and seed coat tissues of wheat (Fincher and Stone 2004). This study has demonstrated that the LM28 GUX epitope is only present in the maternal tissues of the wheat grain throughout development. This contrasts with rice, where the LM28 epitope was detected in both maternal and endosperm tissues at all stages of development,

although the precise pattern and intensity of labelling differed depending upon the developmental stage; suggesting a clear difference between the structure of AX in wheat and rice endosperm. Strong labelling by the LM12 and LM28 antibodies allows discrimination of the rice aleurone cells from the other endosperm cells from 8 DAA, significantly earlier than with other cell wall antibodies or microscopy stains. This suggests that accumulation of glucuronosyl and ferulic substitutions are some of the earliest detectable changes in the differentiation of rice aleurone cells. Little to no AX can be detected in these cells at 8 DAA with INRA AX-1, suggesting that glucuronosyl substitutions may interfere with AX detection with INRA AX-1 or that the AX is very heavily substituted. MLG is also deposited by 6 DAA in both wheat and rice with similar proportions being present at maturity in both species (~23 and 25% respectively). Whilst barley displays a much larger proportion of MLG at ~70-80%, deposition of this polysaccharide is also reported to occur slightly later than AX which is also reported in wheat (Wilson et al. 2006) and rice ((Palmer et al. 2015). The aleurone and nucellar epidermis showed a clear difference in MLG detection between wheat and rice, with MLG being undetectable during early development in rice (up to 20 DAA), although by 28 DAA the MLG epitope was strongly detected in the aleurone cells. Wheat behaves comparably with barley (Wilson et al. 2006; Wilson et al. 2012), with these tissues exhibiting clear labelling at all stages from 8 DAA. These differences in MLG detection may reflect the different assimilate transport pathway in rice where assimilate exchange from the vascular bundle to the endosperm cells is partially a circumferential process through the nucellar projection and aleurone (Oparka and Gates 1981a, b). By contrast, in wheat and barley all assimilates flow from the vascular bundle through the nucellar projection to diffuse into the endosperm. An important role of MLG in cell expansion of maize coleoptiles (Carpita 1984; Carpita et al. 2001) and root cells (Kozlova et al. 2012) has also been reported, perhaps indicating some grain expansion may be occurring in these cellular locations.

4.3.2 Xyloglucan is detected in the anticlinal cell walls of cellularising endosperm in wheat and rice.

In addition to callose, xyloglucan was present in the cell wall ingrowths in the syncytium, with the LM25 xyloglucan epitope being detected readily in both wheat and barley. Whilst Pellny et al. (2012) reported the presence of transcripts for xyloglucan synthase and immunodetection of xyloglucan in the developing

endosperm, xyloglucan has not been reported as a component of mature wheat endosperm. The transient detection of xyloglucan in cellularising endosperm is consistent with that reported in barley (Wilson et al. 2012) suggesting that there may be a conserved mechanism among grasses for the transition from a syncytial state to the cellularised endosperm. Although, no LM25 epitope was detected in the cellularising endosperm of rice, but since no other xyloglucan antibodies were used, the apparent absence may be due to a different xyloglucan structure being present. It is possible that xyloglucan may regulate the deposition of callose, in a similar way to how it regulates the deposition of cellulose fibrils (Zhou et al. 2007).

Glucomannan is a well-established component of wheat endosperm cell walls (Mares and Stone 1973b; Pellny et al. 2012) and its presence represents a distinctive difference with rice endosperm where glucomannan has not been observed by biochemical analysis or immunodetection, but for which mannose has been reported by monosaccharide analysis (Lai et al. 2007). The basis for these differences in cell wall polysaccharide composition between the two species will become clearer with increased understanding of the specific functions and properties of the matrix polymers.

4.3.3 Pectic polysaccharide structure during grain development

The pectic set of polysaccharides are a diverse and complex set of polymers containing domains of HG and RG-I and RG-II (Caffall and Mohnen 2009; Burton et al. 2010a), and are hypothesised to require around 50 unique glycosyl transferases to facilitate their construction, with *Arabidopsis thaliana* containing significant redundancy with almost 300 pectic glycosyl transferases in its genome. In comparison, the hemicelluloses appear simple and readily understood.

The presence of pectic polysaccharides in the cell walls of the rice was predicted by previous monosaccharide analyses, however the abundance and distribution is unique within the endosperm of the common cereal species, with all other species examined showing barely detectable levels of pectin (<2%) whilst rice endosperm walls are reported to contain 25% pectin. Unexpectedly, given the large proportion of pectin within the cell wall, no HG was detected in rice endosperm prior to 28 DAA, and then the only low esterified HG LM19 epitope. Maternal tissue at all stages displayed a combination of both the LM19 and JIM7 epitopes, which represent

partially methyl esterified HG. The JIM7 epitope was more evident in the epidermis, nucellar epidermis and vessels of the phloem and xylem, whereas the LM19 epitope was more widely distributed although the tissue of the vascular bundle region was more heavily labelled than surrounding tissues. In the context of HG biosynthesis, these are significant observations as HG is reported to be synthesised in a methyl-esterified form and then subjected to enzymatic de-esterification *in muro* (Atmodjo et al. 2013). A recent study (Chateigner-Boutin et al. 2014) reported that the enzymatic removal of MLG and AX allowed the detection of the highly methyl esterified HG epitope LM20 in wheat endosperm cell walls, confirming the presence of pectic HG, as previously suggested by the expression of GAUT genes transcripts in wheat endosperm; GAUT genes encode enzymes synthesising the HG backbone (Pellny et al. 2012).

4.3.4 LX unmasking of pectic polysaccharides during grain development.

Unmasking using lichenase and xylanase treatments in tandem following the method described by Chateigner-Boutin et al (2014) showed that homogalacturonan epitopes in both wheat and rice are masked by the presence of both arabinoxylan and MLG, with minimal unmasking being seen when either xylanase or lichenase are used as isolated treatments. Wheat to show cultivar specific methylation of the HG present, with LM20 being the major epitope detected in cv.Recital and a mixture of JIM7 and LM19 being seen in the endosperm cell walls of cv.Cadenza at similar developmental stages. Differences in AX substitution level have also been reported across a range of wheat cultivars in the Healthgrain diversity screen by (Toole et al. 2011), similar differences were observed with HG esterification levels. In rice, the only HG epitope detected prior to unmasking was the LM19 low methyl esterified epitope, but after unmasking both JIM7 and LM20 moderate and highly methyl esterified HG epitopes were widespread in almost all rice grain tissues, notably throughout the endosperm cells. This suggests that a wide range of methyl esterification states is present in the rice endosperm cell walls, and that the more highly methyl esterified regions of HG may be more tightly associated with AX or MLG.

The RG-I domains of pectic polysaccharides are highly heterogeneous, differing in the length of backbone chains, and the presence of numerous arabinan or galactan side chains of varying length and degree of branching. Surprisingly, epitopes directed towards the side chains of RG-I (LM5 - galactan and LM6 - arabinan) were

detected prior to any detection of the RG-I backbone epitope during grain development of both species. LM5 has not been shown to cross react with any other cell wall polysaccharide, but LM6 is known to cross react with AGP in some circumstances, so detection of LM6 at these stages may occur due to AGP, although LM5 galactan is indicative of RG-1 presence at these stages. Detection of the backbone itself in the earliest stages of development has remained elusive, perhaps because of masking by another cell wall polymer; alternatively structurally distinct side chains linked to an acidic backbone may be present, or perhaps INRA-RU1 is unable to bind to the RG-I back bone if heavily substituted. Unfortunately no competitive inhibition ELISA information was published on heavily substituted RG-I due to the difficulties in synthesising such complex molecules. Enzymatic deconstruction by Chateigner-Boutin et al. (2014) detected RG-I using the INRA-RU1 antibody from 11 DAA in wheat, suggesting that at least a partial masking may occur. Both scenarios point to dynamic remodelling of RG-I polymers during grain development and reinforce current views of the role of RG-I in the generation and modulation of cell wall mechanical properties (Caffall and Mohnen 2009). In cv. Cadenza RU1 epitopes were detected from 12 DAA with unmasking, and was seen to label more strongly than prior to unmasking at all subsequent developmental stages in the endosperm cell walls.

The LM5 galactan epitope was detected only in rice endosperm, from cellularisation, and was observed to become progressively more restricted to the two or three outermost cell layers of starchy endosperm cells, and aleurone and sub-aleurone as development progresses. The cells labelled by LM5 are most likely to be exhibiting the highest rates of cell expansion, supporting a role for galactan side chains in cell elongation, which has previously been reported in the Arabidopsis root (McCartney et al. 2003). No changes were seen in the distribution of LM5 labelling after LX unmasking, suggesting that the no masking of pectic galactan occurred in the inner endosperm cell walls. By contrast, the LM6 linear arabinan epitope was widely detected in the starchy endosperm of both species, albeit only up to 8 DAA in wheat, again coinciding with a phase of rapid cell expansion. Detection with LM6 persisted throughout development in rice. The arabinan side chain of pectin has been implicated in drought resistance in resurrection plants (Moore et al. 2008a) via regulation of the hydration state and water retention capacity of cell walls. A similar role may occur in the expanding endosperms of wheat and rice, regulating wall flexibility to allow for cellular expansion and tolerance of desiccation. Additionally, the LM6 epitope was detected at the inner face of the cell wall/ internal cell

organelles (Fig 5.10 I) after 20 DAA; here the epitope may represent linear arabinan chains in arabinogalactan-proteins (AGPs) (Lee et al. 2005) rather than RG-I.

4.3.5 Conclusion

The high level of sensitivity provided by mAbs allows the determination of the developmental dynamics of minor cell wall components, which are likely to provide important modifications to the structures and properties of cell walls. The near synchronous deposition of AX, MLG and callose in analogous cellular locations in wheat and rice implicates a role for these polymers in specific developmental stages, namely cellularisation for callose, and cell differentiation for AX and MLG. Xyloglucan can also now be included as a cell wall component at cellularisation. In comparative terms, glucomannan is a distinctive feature of wheat endosperm cell walls whilst pectic galactan and glucuronosylated arabinoxylan appear distinctive of rice endosperm cell walls. Pectic polysaccharides, notably RG-I, may play important roles in maintaining cell wall integrity during the rapid cell expansion in the grain after the termination of cellularisation.

CHAPTER 5: ARABINO GALACTAN PROTEINS: A CELL WALL COMPONENT?

5.1 Introduction

Arabinogalactan-proteins are a large family of highly glycosylated hydroxyproline-rich glycoproteins expressed throughout the plant kingdom and have been found in leaves, stems, roots, floral parts and seeds (Fincher and Stone 1974; Fincher et al. 1983; Nothnagel 1997). Arabinogalactans proteins have been attributed a wide range of functions, from developmental regulation, cell adhesion, and wound healing, to salt and drought tolerance (Showalter 2001; Van Hengel et al. 2002; Brownlee 2002; Johnson et al. 2003; Mashiguchi et al. 2004; Lamport et al. 2006; Ellis et al. 2010).

They were originally isolated from the aqueous growth medium of *Anogeissus leiocarpus* cell culture and characterized as arabinogalactan polysaccharides (Aspinall and Carlyle 1969; Aspinall et al. 1969; Aspinall and McNab 1969). Subsequently it has been shown that they contain a protein core that is heavily glycosylated (typically 90-95% of the total structure) on numerous hydroxyproline residues (Fincher et al. 1983). Classical arabinogalactan proteins are very large molecules (up to 120 kD) containing a protein core, which can range from 87-739 amino acids in length (Zhao et al. 2002; Showalter et al. 2010). This protein core is rich in hydroxyproline, alanine and serine and is generally deficient in tyrosine, phenylalanine, tryptophan and cysteine. The hydroxyproline residues are typically decorated with arabinogalactan (AG) modules which are currently thought to be composed of a β -(1-3)-linked galactopyranosyl backbone chains which in turn have (1-6)-linked galactopyranosyl side chains which can display a large range of length. Both the side chains and backbone can be decorated with single arabinofuranosyl substitutions at the O-3 position and the side chains can in turn be decorated with single arabinopyranosyl residues at the O-3 position (fig. 6.1). AG modules typically contain somewhere in the region of 100-120 sugar residues. And often represent 80-90% of the molecular weight of classical arabinogalactan proteins. In classical wheat arabinogalactan proteins the AG structure is reported to differ from the generic structure, as the β -1-6 galactan side chains may be additionally decorated

by arabinopyranosyl residues on the arabinofuranosyl residues substitutions present. These side chains also appear to contain glucuronic acid residues at the non-reducing termini (figure 6.1, (Tryfona et al. 2010))

In contrast to the relatively large protein cores of classical arabinogalactan proteins, arabinogalactan peptides (AGPs) contain a small relatively homologous peptide core of 15-25 amino acids in length. In cereals a 15 amino acid core containing 3 hydroxyproline residues is conserved (Wilkinson et al. 2013). These hydroxyproline residues are the sites for O-glycosylation with AG modules. The 15 amino acid peptide core is identical to the N-terminal pro peptide sequence of the grain softness protein GSP-1, and thus is thought to be a processing product of GSP-1. The relationship between these AGPs and GSP was demonstrated by Van den Bulck et al. (2005) Both AG proteins and AGPs are proteolysis resistant, which is thought to result from the substantial carbohydrate network that surrounds the protein or peptide core.

The biological roles and locations of GSP and wheat AGPs remain unknown, although they are often assumed to be present in the cell wall due to the large highly branched coat of arabinogalactan structures. GSP has been proposed to affect grain hardness phenotype in wheat grains, but this has not been proved.

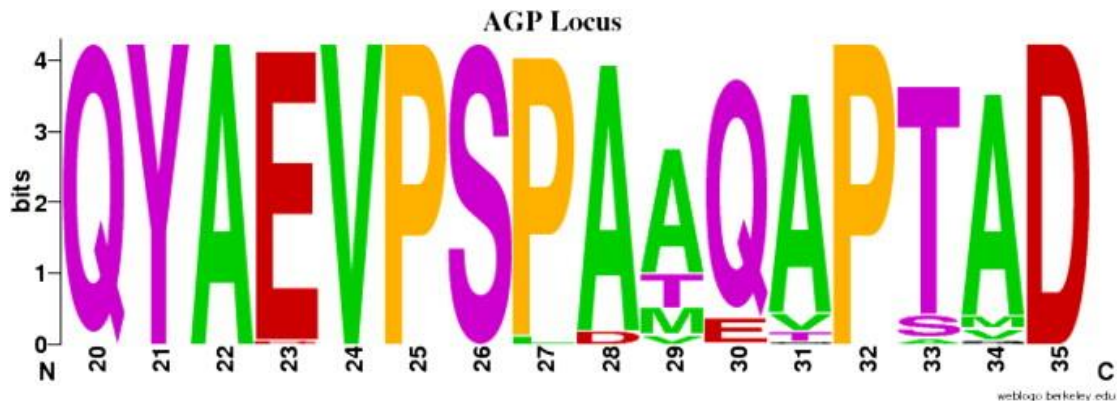


Fig 5.2. Consensus sequence of wheat arabinogalactan peptide across different wheat cultivars, as displayed with the Berkley logo software. Modified from Wilkinson et al. (2013).

Both AG proteins and AGPs can be isolated by the use of β -glucosyl Yariv reagent (1,3,5-tris(4- β -D-glucopyranosyloxyphenylazo)-2,4,6-trihydroxybenzene). This has been shown to be effective at precipitating the AG Proteins from a solution, however, the precise mechanism behind this remains unknown, (Yariv et al. 1962; Kitazawa et al. 2013) and some recently discovered AG peptide complexes, such as APAP-1 (Tan et al. 2013) cannot be isolated by this method.

5.2 Results

The cellular location of wheat AGPs has long been discussed in the literature, often in the context of them being cell wall proteins. However, no evidence has ever been provided for this. Exploiting wheat GSP RNAi lines produced by Dr Mark Wilkinson at Rothamsted Research and the two recently developed wheat AG peptide specific monoclonal antibodies (LM30 and 2H5/E4) (Wilkinson et al, in preparation), immunofluorescence analyses were conducted to determine the location of GSP/AGP in the developing wheat endosperm. The AGP antibodies were monoclonal antibodies raised specifically to AG peptide from wheat cv. Cadenza, which was extracted by Dr Alison Lovegrove (Rothamsted Research) using the method of Loosveld et al. (1997). These antibodies were pre-screened by direct ELISA and subsequently by western immunoblots against wheat flour preparations

to select those with the highest binding affinities to the water extracted wheat flour AGP (Wilkinson et al, in preparation). Wheat caryopses were collected from both null and RNAi transgenic lines at 8, 12 and 15 DAA, and were fixed and embedded prior to sectioning and labelling with the monoclonal antibodies. Comparison of the null and transgenic RNAi lines, which achieved a ~50% knockdown of GSP-1 when expressed under the control of the endosperm-specific high-molecular-weight glutenin-subunit (HMW-GS) promoter, should provide valuable insight into the dynamics as well as the localisation of the AG peptide within developing wheat grains. Previous immunofluorescence studies have been conducted using existing AG protein mAbs (LM2, MAC207, JIM13 and JIM16) in carrot root tip and arabidopsis pollen tube cells which produced both intracellular and membrane labelling patterns but provided no evidence for AG proteins as a cell wall matrix component. The binding pattern of these existing AG protein mAbs were compared with the newly produced wheat specific LM30 and 2H5/E4 antibodies to determine the specificity of antibody binding. It was decided to compare the antibodies directed to classical AG proteins as they are more likely to recognise the carbohydrate AG modules which make up more than 90% of the total, rather than the inaccessible protein or peptide cores.

5.2.1 Production of mAbs to water extractable wheat AGPs.

A range of monoclonal antibodies were produced by Susan Marcus at the University of Leeds, using wheat cadenza AGP isolated by Alison Lovegrove in Rothamsted Research using the method of Loosveld et al. (1997). Two monoclonal antibodies, LM30 and 2H5/E4 were selected based on having the strongest binding to wheat AG peptide in ELISA analysis (data not shown). Further analysis with western blot analysis to compare binding of LM30 and LM2 to wheat AGP demonstrated a similar binding pattern with a weaker band seen at around 48 kD in both mAb binding patterns, however upon the addition of arabinofuranosidase a clear difference in the binding sensitivity between the antibodies was seen, with little or no effect on binding of LM2, whereas LM30 binding was almost completely abolished (fig 5.3 A). This suggests that LM30 likely binds to an arabinose chains of the AG structure. The sensitivity of LM30 binding was further analysed with ELISA, which showed that treatment with arabinofuranosidase (Megazyme, E-AFASE) removes almost all binding at a concentration of 0.4 µg/ml while a family 51 (GH51) arabinofuranosidase also reduced, LM30 binding to AGP but requires nearly 20 µg/ml to reach a similar reduction (Figure 5.3 B). Almost no binding was observed to other commercially available AG protein preparations including larch

arabinogalactan, acacia gum Arabic and sugar beet arabinan, indicating that the epitope recognise on wheat AGP does not exist in these other arabinogalactan or linear arabinan fractions (Figure 5.3 B). All LM30 characterisation was carried out by Sue Marcus at the University of Leeds.

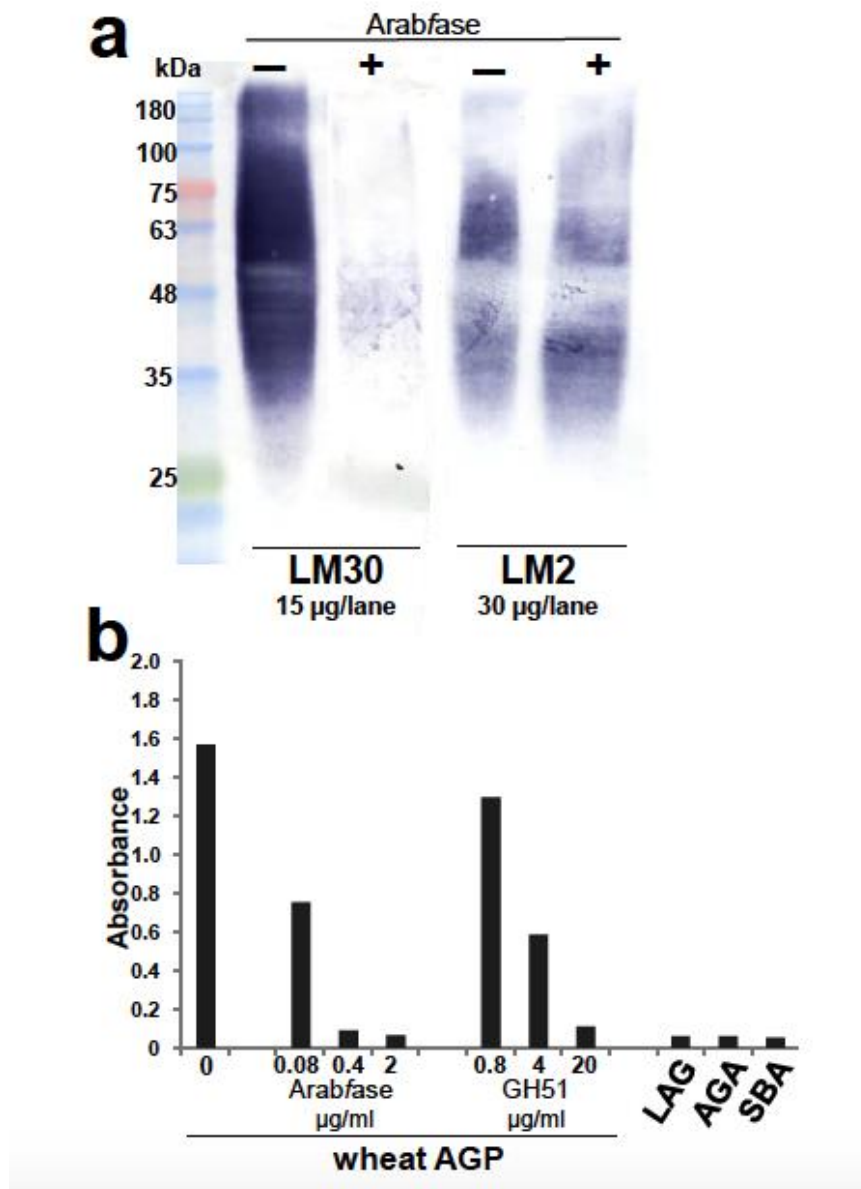


Fig 5.3. Analysis of LM30 binding to wheat grain AGP. **A.** Western blot of LM30 binding to wheat grain AGP (loaded on to SDS-PAGE gel at 15 µg/lane) and sensitivity to an arabinofuranosidase (Arabfase) used at 10 µg/ml prior to loading. For comparison the LM2 AG protein antibody binds weakly to the wheat grain AGP (loaded on to SDS-PAGE gel at 30 µg/lane) and binding was unaffected by Arabfase. Ladder shows molecular weight markers in kDa. **B.** ELISA of LM30 binding to wheat grain AGP at 10 µg/ml and sensitivity to Megazyme arabinofuranosidase (Arabfase) and a family 51

arabinofuranosidase (GH51) used at indicated concentrations in microtitre plate wells prior to probing with LM30. LM30 binding was removed by arabinofuranosidase action on wheat-AGP. LM30 showed no binding to larch arabinogalactan (LAG), Acacia sp. gum Arabic (AGA) or sugar beet arabinan (SBA) all coated on to microtitre plate wells 50 µg/ml). Standard deviation of absorbance <0.01 units in all cases. Kindly conducted and supplied by Sue Marcus.

5.2.2 Immunolabeling of paraformaldehyde fixed sections.

Two mAb lines were selected based on reactions with an aqueous extract of wheat cv. Cadenza flour using ELISA and immunoblotting data from Sue Marcus. The two antibodies were given the designations LM30 and 2H5/E4, based on the strength of their reactivity against a simple aqueous extract of wheat cv. Cadenza flour. Thin sections of resin-embedded 8 and 12 DAA wheat grains fixed using a paraformaldehyde:glutaraldehyde solution were probed with mAbs LM30 and 2H5/E4 in order to locate the AGPs. Both antibodies gave consistent labelling, with the epitopes being widely distributed in both maternal and starchy endosperm tissues (Fig 5.4). The nuclei showed the strongest labelling, however punctate labelling was also observed throughout the outer regions of endosperm cells and sometimes surrounding small intracellular objects, which appear to starch granules due to the characteristic refractive properties when visualised under brightfield microscopy. (Fig 5.4 b, d-f). The 8 DAA sections were labelled in the outer regions of the cells, and the starch granules in the maternal tissue were clearly labelled (Fig 5.4 b, d). By 12 DAA, the intensity of the labelling was reduced in the maternal tissues and fewer starch granules were apparent, however these starch granules are known to be digested to provide additional assimilates for the developing endosperm (Fig 5.4 e, f). However, no protein bodies, Golgi bodies or vacuoles were labelled at either time point with either antibody.

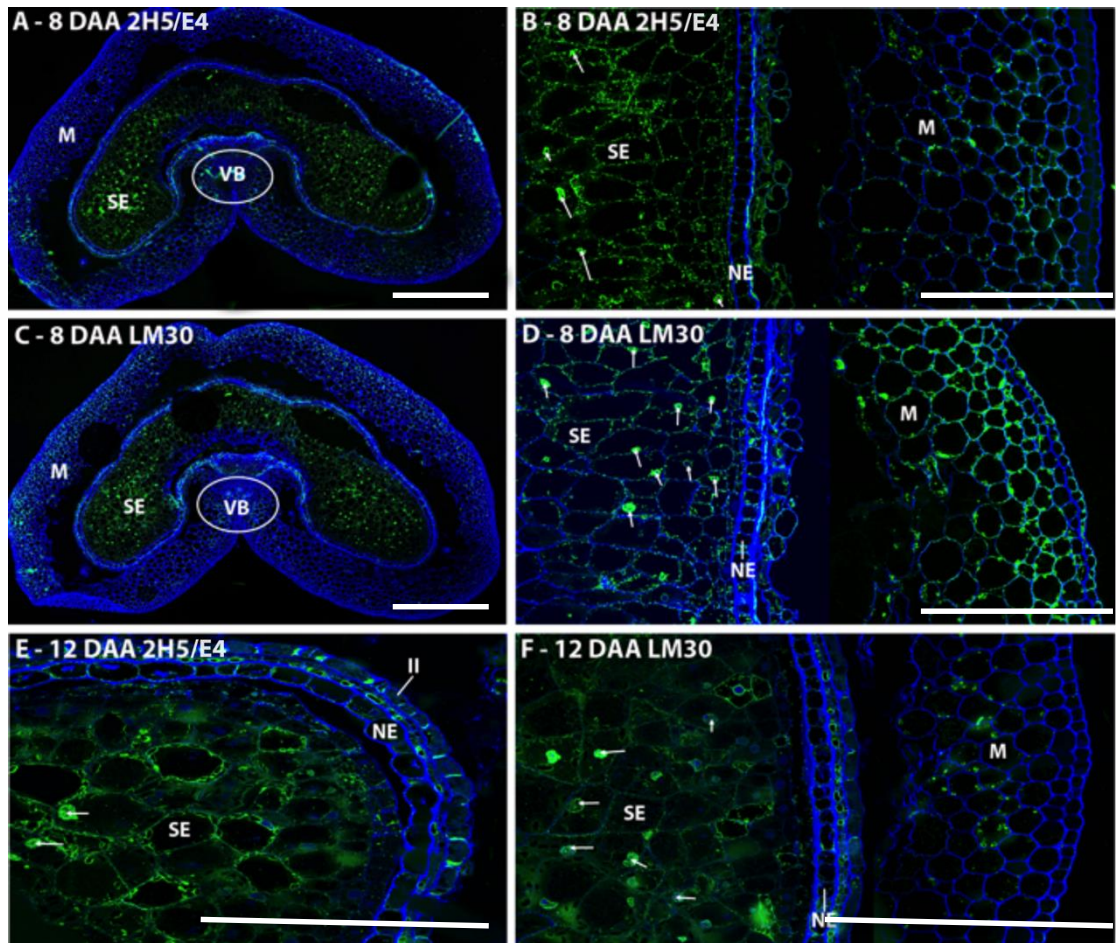


Figure 5.4. Immunofluorescence labelling of AGPs with LM30 (C, D, F) and 2H5/E4 (A, B, E) on paraformaldehyde fixed 1 μm thick medial transverse wheat grain sections at 8 DAA (A-D) and 12 DAA (E, F). Antibody labelling (green) showing the widespread distribution of epitope throughout the endosperm and maternal tissues, counterstained with calcofluor white to indicate cell walls (blue) where no colocalisation was detected. Arrowheads indicate nuclei labelling, SE = starchy endosperm, M = maternal pericarp, NE = nucellar epidermis, II = inner integument, VB = vascular bundle. Bars 250 μm (A, C), 100 μm (B, D-F).

5.2.3 Comparison of different monoclonal antibody lines from the initial immunisation protocol.

A selection of both available AG protein antibodies and other mAbs produced by the initial immunisation with wheat AGPs were used to probe the null segregant wheat grain sections fixed by HPF. HPF fixation was trialled as an alternative to paraformaldehyde fixation due to the unexpected antibody labelling seen in the paraformaldehyde fixed wheat sections. Further four antibodies from the initial AGP

immunisation procedure (4H8, 5C9, 7F3, 8E11) and four commercially available antibodies (JIM13, JIM16, LM2, MAC207) were also tested. The antibodies 4H8, 5C9, 7F3 and 8E11 gave very similar patterns of localisation to that of the 2H5/E4 and LM30 antibodies, however with significantly lower fluorescence intensities and were therefore imaged using slightly longer exposures (1000 ms) rather than the one used with 2H5/E4 and LM30 (500 ms). Subtle changes to the localisation pattern were also noted between the 6 wheat AGPs antibodies, with 7F3 and 8E11 showing the lowest levels of labelling of the aleurone cells (Fig 5.7 C, D), and 8E11 not labelling the integuments (Fig 5.7 D), unlike the other wheat AGPs antibodies. The characteristic labelling of the cell membrane was observed with all 6 wheat AGP antibodies (Fig 5.6, Fig 6.7 A-D). In contrast, when using JIM13 and MAC207 antibodies no labelling of endosperm or aleurone cells was observed (Fig 5.7 E, F). Labelling was restricted to the maternal tissues with the strongest labelling detected in the cross-cells and integuments. However, the internal surface of aleurone cell wall and the maternal cells were labelled with LM2 (Fig 5.7 H). Differences in the labelling of epidermal cells were detected between LM2, JIM13 and MAC207; LM2 and MAC207 labelled the cell membrane, whereas JIM13 labelled the outer surface of the epidermal cell walls. JIM16 exhibited a labelling pattern that partially mimicked that of the wheat AGP antibodies (Fig 5.7 G), with a clear labelling of the cell membrane area of most endosperm cells and the aleurone cells, but the labelling was very weak (requiring exposures of ~2000 ms to produce an appropriate micrograph), and did not include the intracellular labelling visualised by 2H5/E4 and LM30.

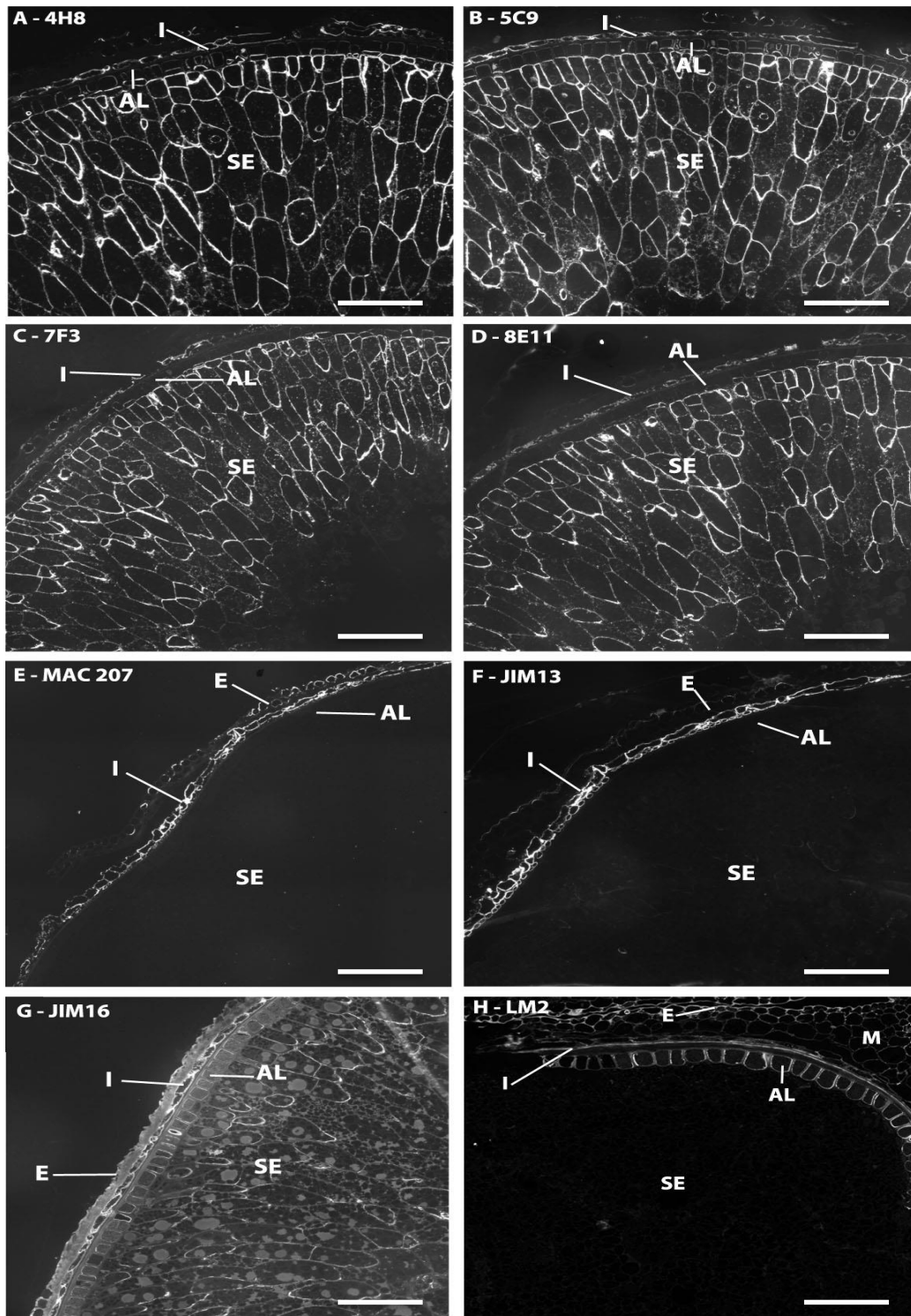


Figure 5.5. Immunofluorescence labelling of AGPs with 4H8 (A), 5C9 (B), 7F3 (C), 8E11 (D), MAC207 (E), JIM13 (F), JIM16 (G) and LM2 (H) on high pressure frozen 1 μ m thick medial transverse null segregant wheat grain sections at 15 DAA (A-H). Micrograph G exposed for 2000 ms compared with 1000 ms in all other micrographs to demonstrate no weak intracellular labelling is detected. SE = starchy endosperm, ETC = endosperm transfer cells, Al = aleurone, I = integuments, E = epidermis. Bars 250 μ m (A-H) .

5.2.4 Immunolabelling of *gsp-1* RNAi Lines

Monoclonal antibodies LM30 and 2H5/E4 were used to probe high pressure frozen (HPF) sections of RNAi seeds and their null segregants at 15 DAA. Paraformaldehyde fixation gave a very broad labelling pattern, and the labelling of nuclei and starch granules was unexpected, although GSP-1 has been reported to be associated with the surface of starch granules. Whilst the N-terminal 15 amino acids of GSP-1 is homologous to the amino acid sequence in wheat AG peptides, no other link between the two molecules has yet to be identified, although it is postulated that the AG peptide sequence is cleaved from the full length GSP-1 sequence. High pressure freezing (HPF) has been reported to give superior fixation of labile cellular component in comparison to standard paraformaldehyde fixation in plant tissues (Kiss et al. 1990; Studer et al. 1992; Galway et al. 1993; Kaneko and Walther 1995). The immunofluorescence experiment was therefore repeated on HPF fixed sections to confirm the binding pattern. Labelling of null segregants with both antibodies in the HPF sections was virtually indistinguishable, and showing the epitopes to be located at the cell membrane of all cell types, however significant labelling was also detected intracellularly in the starchy endosperm cells (Fig 6.5). This intracellular labelling appears to be partially surrounding protein bodies and starch granules, and is more prominent towards the cell extremities, indicating that it is probably cytoplasmic labelling (Fig 6.5 E, G, H). However, unlike the paraformaldehyde-fixed sections no labelling was seen in the nuclei of any cell, and no co-localization could be detected when the sections were treated with propidium iodide (Fig 6.5 B, D) (a histochemical counterstain that labels double stranded DNA) (Jones and Kniss 1987).

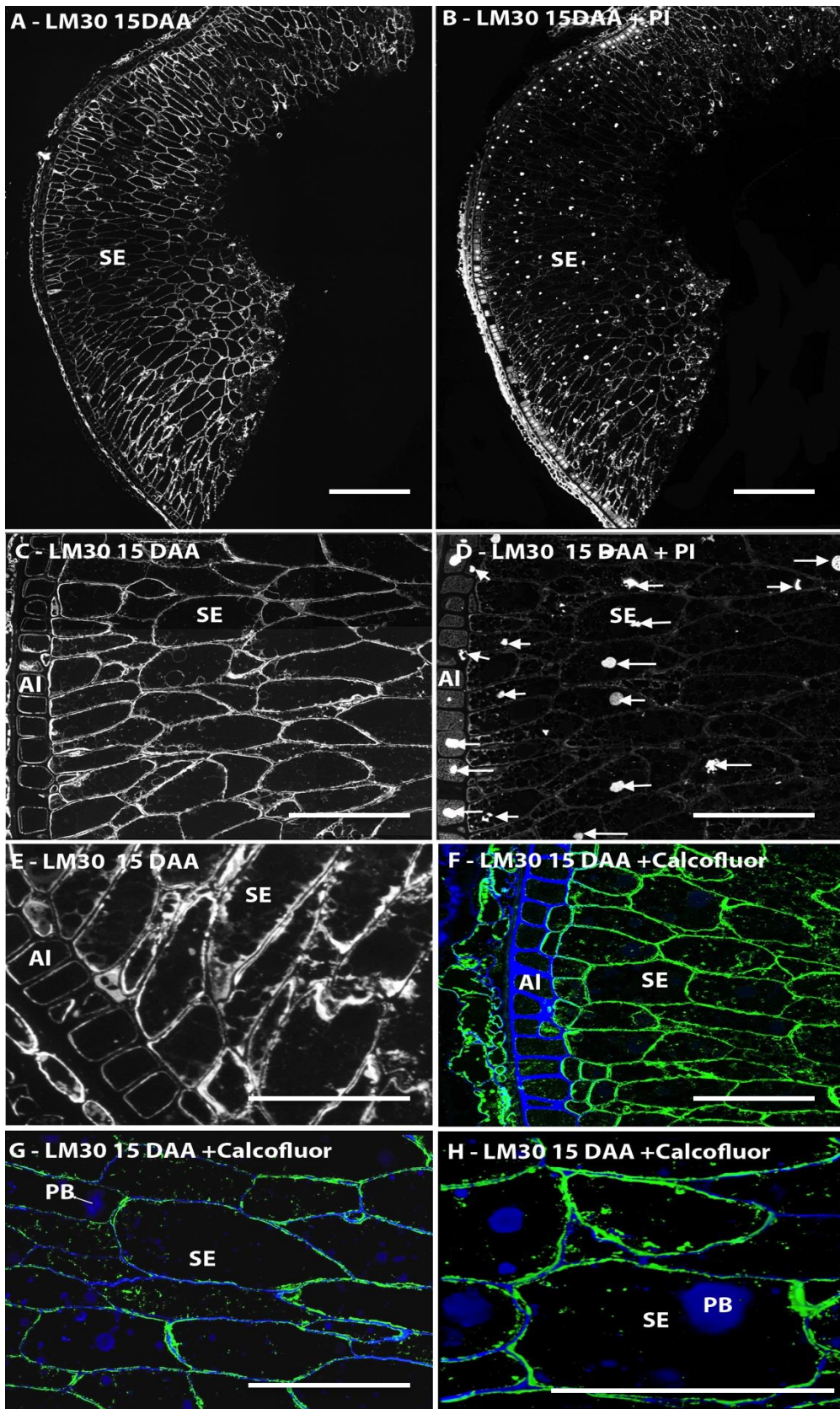


Figure 5.6. Immunofluorescence labelling of AGPs with LM30 (A-H) on high pressure frozen 1 µm thick medial transverse wheat grain sections null segregants at 15 DAA (A-H). Micrograph D counterstained with propidium

iodide, Arrowheads indicate nuclei labelling with propidium iodide.

Micrographs F-H counterstained with calcofluor 2mr (blue) to demonstrate no co-localization of the AGP epitope and the cell wall. SE = starchy endosperm, M = maternal pericarp, II = inner integument. Bars 250 μm (A, B), 100 μm (C-H).

5.2.5 Immunolabelling of HPF fixed *gsp-1* RNAi lines reveals labelling is restricted to the cell membrane.

RNAi lines were kindly supplied by Mark Wilkinson. Caryopses were collected at 15 DAA and fixed by high pressure freezing and sectioned by Paola Tosi. The HPF RNAi sections showed the same labelling at the cell membranes as the null segregants, however, the labelling appeared weaker and was not always continuous around each cell (Fig 6.6). Conversely, no cytoplasmic labelling could be detected with either LM30 or 2H5/E4 labelling in the RNAi sections, even with much longer exposure settings (1500 ms compared to 500 ms, Fig 6.6 D), suggesting that the ~50% reduction in AGPs reported by HNMR in the RNAi lines (data not shown) may represent removal of the cytosolic AGPs component.

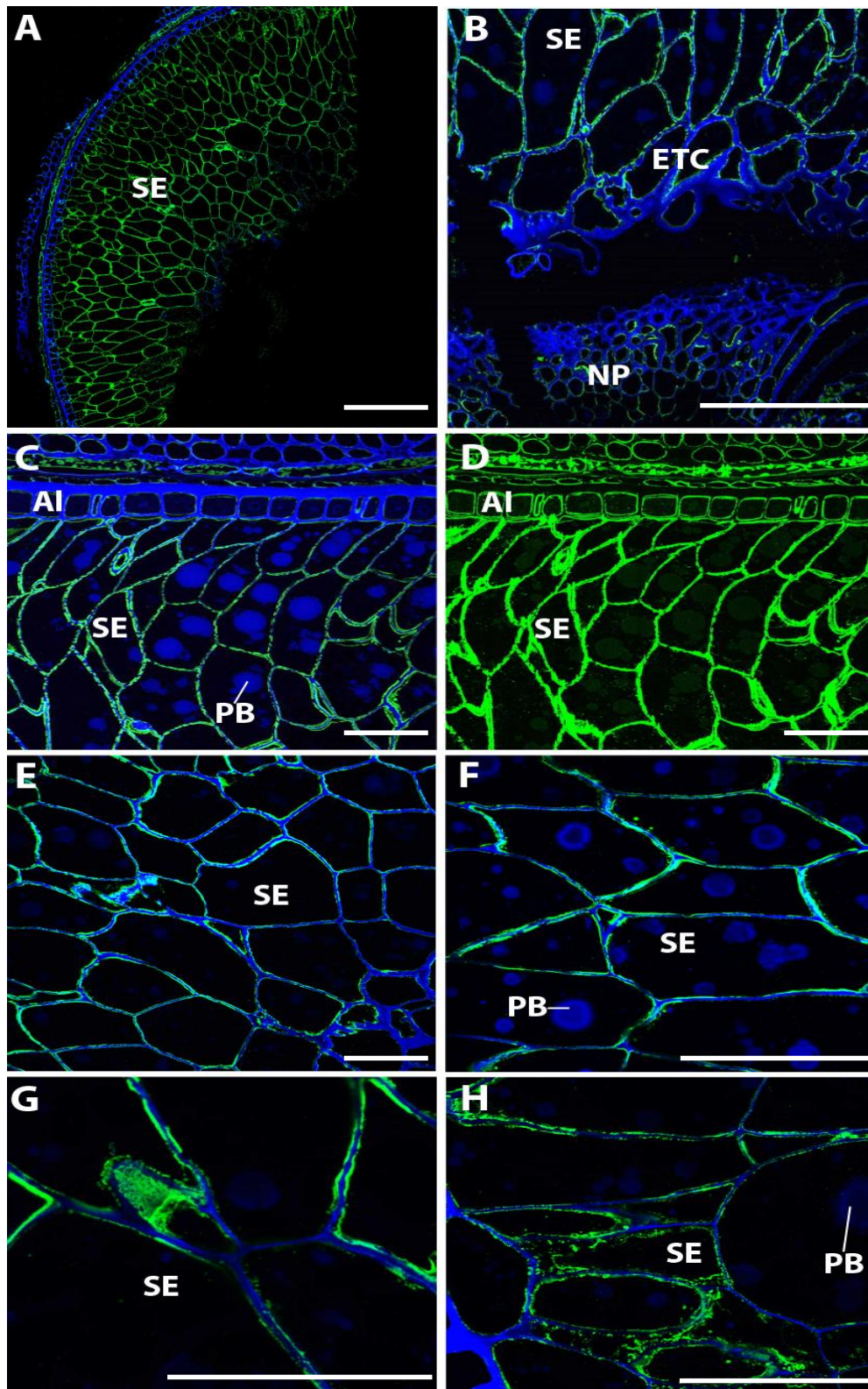


Figure 5.7. Immunofluorescence labelling of AGPs with LM30 (A-H) on high pressure frozen 1 µm thick medial transverse RNAi *gsp-1* wheat grain sections at 15 DAA (A-H). Micrograph D exposed for 1500 ms compared with 500 ms in all other micrographs to demonstrate no weak intracellular labelling is detected. Micrographs F-H counterstained with Calcofluor 2mr (blue) to

demonstrate no co-localization of the AGP epitope (green) and the cell wall. SE = starchy endosperm, ETC = endosperm transfer cells, AI = aleurone, NP = nucellar projection, PB = protein body. Bars 250 μ m (A), 100 μ m (B-H) .

5.3 Discussion

AG peptides have long been considered to be constituent elements of plant cell surfaces and particularly as elements of the cell wall matrix, due largely to their characteristic molecular structure, with large levels of O-glycosylation of the central peptide chain. However, immunolabelling work carried out as part of this thesis on wheat grain sections prepared by HPF and using monoclonal antibodies raised specifically to wheat flour AGP demonstrates that, at least in wheat, this is not the case: the AG peptide is not associated with cell walls. The AGPs was widely distributed throughout all endosperm cells in developing wheat grains, with two particular locations being evident. Firstly at the cell membrane/ cell wall face, with no co-localisation being observed with the cell wall structure, visualised using a β -glycan stain (Calcofluor White 2mr), and secondly a strong intracellular location, which appears to be cytoplasmic. The cytoplasmic localisation appears to be sensitive to the RNAi knockdown of the *gsp-1* gene in wheat grains, with no labelling at this location being visualised in the RNAi sections. It is unclear at present how or why AGPs are localised to the membrane, as there are no known GPI anchors, unlike in several wheat and rice arabinogalactan proteins, and no known functions for it have been postulated for this location. GPI anchors are common cell membrane attachment domains in membrane bound proteins, and have commonly been reported in classical AG proteins, It is also possible that these AGP molecules are associated with other membrane bound proteins. The resistance of the labelling to RNAi knockdown may be in part due to the promoter selected for RNAi line, an HMW-GS promoter that is known to be expressed from about 8-12 DAA and has is expressed more strongly in the central regions of the endosperm. It is possible that synthesis of the AGPs may begin prior to the activation of the RNAi transcript, with the labelling in cell membrane representing AGPs in its final location while further AGP expression is reduced by the RNAi transcript. AGPs are known to undergo post-translational glycosylation in the Golgi apparatus, and the glycan is likely to be further modified in the vacuole. It remains possible that some of the small punctate labelling visualised in the intracellular labelling may represent very small vacuoles, which have been reported to be numerous in developing wheat endosperm cells.

Unlike the full length GSP (which may also be affected by the RNAi transcript) there is no evidence from binding patterns to support AGPs affecting grain hardness through interaction with starch granules in the starchy endosperm. However the labelling of maternal pericarp starch granules was observed in the 8 and 12 DAA paraformaldehyde fixed sections and requires repeating in HPF fixed sections to identify if this also an artefact of the fixation protocol. Given the significant amount of AGPs present in mature wheat grains 0.4 mg/g (which is similar to wheat soluble AX content) it is probable that it plays a significant role. Reports that arabinan and galactan chains regulate flexibility and hydration state in the pectic structures of resurrection plants (Moore et al. 2008a; Moore et al. 2013), suggest that the broad network of arabinan side chains extending from the AGPs may be able to act similarly, with the whole molecule acting as an osmoregulator molecule modulating grain desiccation and dormancy prior to grain germination. However, AGPs could also act as a part of a calcium signalling cascade at the cell membrane as proposed by Lamport et al. (2014) for classical AG proteins, or simply as a form of storage carbohydrate that is easily digestible during germination.

CHAPTER 6: DISCUSSION

This project has determined the morphological and compositional changes in the developing cell walls of wheat and rice grains, showing that mAbs directed to cell wall epitopes can provide detailed spatial and temporal information about the location and modification of the major components. Monoclonal antibodies allow for relatively high resolution and highly specific detection of epitopes within a sample material and can detect the presence or absence of an epitope. The wide array of available monoclonal antibodies provides tools to detect almost the whole range of cell wall polysaccharides, which allows for very sensitive analysis of cell wall dynamics and the assessment of the structural heterogeneity within a single cell wall. Grain development in both species follows 4 phases, and the changing biological processes at these different phases require changes to the overall composition of the cell walls, both in terms of monosaccharide content and in terms of specific structures as detected by mAbs. The combination of chemical and immunochemical studies of the cell walls in two different grain species across development shows that the major components of endosperm cell walls are deposited in the same order and that this agrees with previous reports of developing barley grains. However, it also provides novel details about the microstructure of the cell walls, and through the use of enzymatic unmasking, novel insights into the structure and distribution of pectin within both grains. AX and MLG are major components of grain cell walls in both species and appear to be deposited and regulated in a similar manner, with pectin and cellulose making up significant proportions of the rest of the cell wall. However the starchy endosperm cells of both species appear to contain polysaccharides, which are not present in the other species, wheat endosperm is rich in a mannan epitope whilst glucuronoxylan and pectic galactan are widely detected in rice endosperms.

Gradients of composition in cereal grains are widely reported in wheat, with AX substitution level, and protein distribution being clear examples. The work presented here shows that gradients in composition also occur in some cell wall components, (Toole et al. 2009; Toole et al. 2010), and that the deposition of protein bodies appears to be spatially regulated with more protein deposition occurring in the outer regions of the endosperm and sub-aleurone cells in wheat grains. AGPs have long

been considered to be cell wall components of cereal grains, however, the generation and use of mAbs to wheat AGPs has led to the conclusion that AGPs are likely to be found in the cytoplasm or in the membrane/cell wall face in wheat.

Whilst current reports show a synchronous pattern of grain development in both wheat and rice after cellularisation, the use of histochemical stains labelling proteins and starch shows that the accumulation of these storage components is not synchronous between the two species. Previous studies have examined developing grain of the two species in isolation; direct comparisons between equivalent developmental stages have not previously been available. Using CBB to stain protein deposits, it is clear that both species accumulate protein bodies in a manner comparable to that previously reported. Wheat protein bodies cannot be detected with light microscopy prior to 8 DAA whilst in rice, numerous protein bodies are detected at 6 DAA, showing an earlier initiation of protein deposition in rice compared to wheat, however, by 12-14 DAA comparable numbers of protein bodies are seen in both species and this persists until maturity. A clear gradient in protein deposition can be seen from the earliest stages of protein deposition, with the outer regions of the endosperm and putative sub aleurone cells showing the greatest concentration of protein while the inner endosperm regions accumulate comparably little protein. This pattern is maintained in both species throughout development, but the transition from high to low protein content is more pronounced in rice grains where a sharp decline in protein content is seen after only a few endosperm cell layers as reported by Ohdaira et al. (2011). Conversely starch content is higher in the central region of the endosperm and lower in the sub aleurone cells, with rice producing dense starch deposits in the central regions from 6 DAA, whereas relatively sparse starch deposits are detected in wheat until after 12 DAA. These differences show that whilst the same patterns of storage product localisation are occurring in both species there is asynchrony in the relationship of deposition to the developmental phase of the grain between the two species.

Determination of the monosaccharide composition of the cell walls of developing wheat and rice grains at 5 key stages, showed clear transitions in all non-glucosic polysaccharides between each developmental stage producing 4 phases of cell wall deposition within both wheat and rice grains, which occurred synchronously between both species. The 4 phases can be described as a two phases of high rates of cell wall deposition (phases 1 and 3; at least doubling the monosaccharide content, which coincide with known phases of rapid cell division or grain expansion

in both species) interspersed by periods of more moderate cell wall deposition (phases 2 and 4; up to 50% increases in monosaccharide contents but small declines in some monosaccharides, which coincide with periods of very little grain expansion or cell division and re-differentiation). During phases 2 and 4, greater variation occurs between monosaccharides with some components showing moderate rates of accumulation (as summarised in Tables 3.14 and 3.15). These differences are probably due to modulation of cell wall properties to adapt to the changing biological requirements within the grain, for example continued deposition of rhamnose and fucose and galactose in phase 4 are likely to reflect increased pectin content and in particular pectic RG, which has been implicated in generating cell wall plasticity and modulating cell wall hydration state (Moore et al. 2008a; Moore et al. 2013). The changes in phases phase 2 and 4 may give interesting insights into the *in muro* characteristics of cell wall polysaccharides, which still remain relatively obscure. However, the preparation and analysis of tissue-specific monosaccharide preparations rather than the wholegrain analyses presented here may give significantly different results due to the ratios of tissues differing markedly between developmental stages. However, at 28 DAA most of cell wall monosaccharides will be derived from endosperm tissue.

Prior to phase 1, cellularisation in cereal endosperms generates the first round of endosperm cells. Xyloglucan has previously been reported as a key polysaccharide in the cell wall extension during cellularisation in barley by detection with monoclonal antibodies and also in angiosperm cell plates (Rodkiewicz 1970; Wilson et al. 2012). LM25 binding was seen in both wheat and rice anticlinal cell wall extensions, confirming the presence of xyloglucan in the formation of the first cell walls during cellularisation. It is likely that cellulose or callose are also deposited in conjunction with the xyloglucan, although no callose was detected prior to the completion of cellularisation in wheat or barley (Wilson et al. 2012; Pellny et al. 2012). Xyloglucan was only detected transiently at the earliest stages of grain development in both wheat and rice grains, with detection disappearing by 8 DAA. This transient detection may reflect its function in accelerating cell wall deposition and expansion through the cellulose network during the earliest stages of grain development as reported in *A. thaliana* stems (Kaida et al. 2010).

The temporal pattern of cell wall deposition within both wheat and rice continued to align with that previously reported in barley (Wilson et al. 2012) with all three species showing xyloglucan and callose as the first polysaccharides detected during

cellularisation followed by arabinoxylan epitopes shortly after the completion of cellularisation and subsequently MLG is first detected between the completion of cellularisation and 2 days afterwards (4-6 DAA in wheat and rice grains). This conserved sequence of cell wall polysaccharide deposition despite the vastly different final cell wall compositions suggests that a conserved sequence exists between these 3 species and that it may extend to all cereal grains. If this is the case then it is highly likely that it is a process inherited from a mutual ancestor.

Both cellulose and MLG displayed significantly different patterns of deposition to the four-phase pattern described above. MLG concentration decreased dramatically throughout development in both species. This indicates that the maternal tissues surrounding the grain are likely to be highly enriched with MLG and that the decline in content can at least in part be attributed to the loss and degradation of these tissues during development. Moreover, the rapid expansion of grain weight and relatively small increase in cell wall content generates a significant dilution affecting the concentration of MLG detected in these samples. However, MLG content per grain increases steadily from 4-20 DAA in wheat showing that MLG deposition is still a significant part of endosperm development. Rice grains appear to exhibit very little change in total grain MLG throughout development which, taken with the increasingly strong labelling of MLG epitopes in the immunofluorescence experiments, suggests that the MLG deposition may occur at a similar rate to the loss of MLG from maternal tissues. MLG content in wholegrain wheat or rice caryopses has not been analysed during grain development before, so no comparison can be made to help explain this pattern.

Cellulose also lacks the four-phase deposition pattern with the content of cellulose per grain increasing in a relatively linear fashion from 8-28 DAA in both species, however this occurred at a much faster rate in wheat than in rice. As both of these MLG and cellulose are likely to be very significant components of vegetative cereal tissue, their deposition pattern may be heavily affected by the concomitant loss of large amounts of maternal tissue and the growth of the embryonic axis (which is likely to have a vegetative tissue type of cell wall composition based on reports of rice (Shibuya et al. 1985)).

The cell wall composition of the mature whole wheat and rice grains differ significantly, with wheat composed of around 75% AX and MLG (50 and 25%

respectively) and smaller components of cellulose (12%) and pectin (6%). Rice is also mainly composed of AX and MLG ~50%, but also contains large proportions of cellulose (23%) and pectin (~25%). It appears that wheat grains have a similar cell wall composition as rice grains, based both on the monosaccharide analyses and on the identical deposition patterns of AX, MLG, callose and xyloglucan detected through immunofluorescence studies (Chapter 5) in early cellularisation. The main differences in the cell walls of the two species appear to be a greater accumulation of AX in wheat grains with an increase from 32 to 52% (from 4-28 DAA) combined with lower levels of pectin and cellulose, whereas rice AX content increased from 18-24% during the same period. These final cell wall compositions agree well with previously reported values for wheat and rice endosperm cell wall composition. However, no direct comparisons are available for whole grain analyses and greater differences were observed between the two data sets. This is due to the higher proportions of maternal and embryonic tissues in whole grain analyses, which are likely to contain higher MLG, cellulose and pectin levels than endosperm tissues (Shibuya et al. 1985; Antoine et al. 2003; Parker et al. 2005).

Rice exhibits GUX epitopes widely throughout both maternal and endospermatic tissues at all stages of development after cellularisation, and detection of this epitope is consistently stronger and earlier than with xylan or arabinoxylan antibodies. GUX epitopes were not detected in wheat endospermatic tissues at any stage, but were widely detected in maternal tissues at all stages. This clear separation in the structure of a major cell wall polymer within the grains of both species shows pronounced differences of comparable cell walls within both species. Glucuronic acid monosaccharides were detected in both species, at all time points, however due to the wholegrain makeup of the samples analysed it was not possible to separate the endospermatic and maternal tissues, whereas by utilising LM28 mAb it was possible to discriminate the two tissues and detect the presence of glucuronoxylan epitopes in wheat maternal tissues only. It may be possible that the much higher percentage composition of AX in wheat allows for greater strengthening of the cell wall through more ferulic dimerization compared to the GUX type of AX seen in rice grains, where structural rigidity may be generated by the significantly larger content of cellulose microfibrils present.

Pectin has only recently been identified as a component of wheat endosperm cell walls through immunohistochemical studies utilising unmasking techniques. Through the use of monosaccharide analysis, wheat grain pectin can be quantified

to 5-6% and this percentage composition remains relatively unchanged in the wheat grain throughout development, suggesting that this level may be required to correctly form the middle lamellae between cell walls and to maintain cell to cell adhesion. Rice has long been reported to have significantly higher pectin contents, with previous reports of between 15 and 25 % of the endosperm cell wall (Shibuya et al. 1985; Lai et al. 2007). In the earliest stages of grain development about 6% pectin is also determined, when mostly maternal tissues are present, but as endosperm development progresses this figure rises steadily to a peak of 23% at maturity, indicating that rice endosperm is highly enriched in pectin compared to wheat cell walls. The presence of pectin in both species is an important discovery, as pectin has yet to be reported in the endosperms of other cereal species, the focus of previous research being dominated by AX and MLG. The detection of pectin in other cereal species endosperms would strengthen the hypothesis that a small proportion of pectin is essential for correct assembly and function of the endosperm cell wall.

Pectin was widely detected with mAbs in wheat and rice grains in all tissue types, however detection was only found in the later stages of grain development, prior to enzymatic unmasking of grain sections. This correlates with the study of Chateigner-Boutin et al. (2014), which showed enhanced detection of RG-I and HG epitopes in wheat grains with a lichenase-xylanase double digestion of the cell wall. The methylesterification state of pectic homogalacturonan in cereal endosperms appears to be consistently regulated across the grain, although differing methylesterification states were detected between Cv. Recital (Chateigner-Boutin et al. 2014) and Cv. Cadenza. The necessity to remove around 80-90% of the endosperm cell wall in order to visualise pectin at early stages of grain development, suggests that either very little pectin is present in wheat endosperm cell walls or that it is very closely spatially associated with other major cell wall polysaccharides rendering it inaccessible to relatively large mAb molecules.

Significantly the RG-I of wheat grains appeared to lack galactan side chains (as detected by LM5) at any stage of development. Pectic galactan is detected clearly in developing rice endosperm, which diminishes in a sequential pattern from the central region first before extending to the outer regions by maturity. This pattern was not modified by the use of enzymatic unmasking and appears to correlate with the maturation and PCD of endosperm cells within the rice grain, implicating a role in cell expansion or regulation of cell wall plasticity.

The use of mAbs and enzymatic unmasking has revealed complex and dynamic processes of cell wall deposition within both wheat and rice grains, with significant similarities between the two species seen at key developmental stages despite very different cell wall compositions. Dynamics within each major polysaccharide can be seen with significant changes in the fine structure as indicated by epitope detection patterns.

The location and function of AGP has long been hypothesised since its first discovery in wheat by Fincher and Stone (1974). Many studies have implicated it as a cell wall protein, likely embedded in the cell wall matrix with an unknown function (Fincher et al. 1983; Showalter 2001; Lamport et al. 2006; Ellis et al. 2010). Through the generation of specific monoclonal antibodies to wheat flour AGP extract it can be concluded that in wheat grains, AGPs are unlikely to be a cell wall component. However the partial cytosolic and cell membrane localisation pattern detected using LM30 and 2H5/E4 does continue to raise questions about the significance of AGP within cereal endosperms where in wheat it accounts for as much as 0.4% of the dry weight of mature grains (Loosveld et al. 1997). Several hypotheses have been raised in the past about the function of AGPs, with molecular roles as varied as cell wall proteins, to signalling molecules and storage media being presented. No known membrane bound anchor exists within wheat AGPs therefore interaction with the membrane is likely to be through a different method, perhaps via a protein-protein interaction. The AG modules attached to the peptide core confer water-solubility to AGP and thus their cytosolic type localisation is logical. It may be the case that the AGP directed mAbs are specific for an epitope in the AG coat of the module due to the loss of binding after α -arabinofuranosidase treatment. Whilst a high degree of specificity has been seen during the characterisation of these mAbs it may be the case that the epitope is present on other proteins in wheat, which may contain membrane anchors, and this would explain the loss of the cytosolic type labelling in the RNAi knockdown lines and minimal effect on the plasma membrane type labelling. Another potential explanation for the sole loss of cytosolic labelling in RNAi lines may be that the HMW-GS promoter used for the RNAi transcript only begins transcription around 7-8 DAA, therefore the cytosolic location maybe a temporary transport or modification location, prior to association with the plasma membrane, and some AGP may be produced prior to the activation of the RNAi transcript. The membrane bound localisation may also represent another membrane bound protein exhibiting the epitope recognised by LM30.

Immunofluorescence labelling with both LM30 and 2H5/E4 demonstrated that significant changes in the localisation pattern existed dependant upon the fixation method. The chemical fixation showed widespread distribution of the epitope in including surrounding starch granules and heavily labelling cell nuclei. This contrasts strongly with the membrane bound and cytosolic labelling seen in the HPF sections. It is likely that as chemical fixation is not instantaneous and does not preserve labile molecules as well as HPF that the changes in localisation patterns are due to imperfect preservation.

Whilst the structure of AG modules has been studied for some time a definitive structure has yet to be identified (Tryfona et al. 2010). Using pre-existing AG protein mAbs several differing types of labelling patterns were seen within serial wheat grain sections, suggesting that different epitopes are being recognised between the different antibodies, and that depending upon the cell type these may be differentially regulated. For instance some of these antibodies were restricted to labelling maternal tissues with others restricted to endospermatic tissues, suggesting that classical AG proteins can be structurally different, with these differences probably occurring in the AG coat structure. The spatial regulation of AG proteins, which may contain different structural characteristics is a novel discovery and may indicate that they have slightly different roles within the grain.

The role of AGPs and AG proteins still remains unknown, however the clarification of the wheat AGPs being localised to the cytoplasm and plasma membrane in developing wheat grains, may correlate with some of the previously proposed roles, such as signalling molecules, or as osmoregulators, however the plasma membrane localisation requires further investigation through the use of Immunogold transmission electron microscopy. Whilst Peter Shewry believes that some of the punctate cytoplasmic labelling may represent deposition many tiny vacuoles (which have previously been reported at this stage of grain development), as it has previously been suggested that some modification may occur in vacuoles. The large quantities produced within the developing wheat grain may also imply a storage product role, as the arabinan and galactan would be a readily transportable, digestible sugar source for the germinating embryo.

6.1 Conclusions

In conclusion, both wheat and rice grains present complex and dynamic processes of cell wall deposition, as revealed by our studies based on immunohistochemistry

with monoclonal antibodies raised against polysaccharide-specific epitopes and enzymatic unmasking. The mature grain of these two cereals present very different cell wall compositions, significant similarities between the two species could be observed in the pattern of deposition of their cell wall polysaccharides, which occurs according to a 4-phase pattern coinciding with the changing developmental and biological demands within the grain. In particular a sequential pattern of polysaccharide deposition during cellularisation, previously reported in barley. By using newly developed mAbs against wheat AGP we were also able to establish that AGPs are not part of the cell wall matrix, as previously proposed; however additional analysis is required to conclude whether AGPs are cytosolic or plasma membrane bound.

CHAPTER 7: BIBLIOGRAPHY

- Ahn J-W, Verma R, Kim M, Lee J-Y, Kim Y-K, Bang J-W, Reiter W-D, Pai H-S (2006) Depletion of UDP-D-apiose/UDP-D-xylose synthases results in rhamnogalacturonan-II deficiency, cell wall thickening, and cell death in higher plants. *J Biol Chem* 281 (19):13708-13716
- Akita K, Ishimizu T, Tsukamoto T, Ando T, Hase S (2002) Successive glycosyltransfer activity and enzymatic characterization of pectic polygalacturonate 4- α -galacturonosyltransferase solubilized from pollen tubes of *Petunia axillaris* using pyridylaminated oligogalacturonates as substrates. *Plant Physiol* 130 (1):374-379
- Albersheim P, Darvill A, Roberts K, Sederoff R, Staehelin A (2010) *Plant cell walls*. Garland Science,
- Alejandro S, Lee Y, Tohge T, Sudre D, Osorio S, Park J, Bovet L, Lee Y, Geldner N, Fernie AR (2012) AtABCG29 is a monolignol transporter involved in lignin biosynthesis. *Curr Biol* 22 (13):1207-1212
- Anders N, Wilkinson MD, Lovegrove A, Freeman J, Tryfona T, Pellny TK, Weimar T, Mortimer JC, Stott K, Baker JM (2012) Glycosyl transferases in family 61 mediate arabinofuranosyl transfer onto xylan in grasses. *PNAS* 109 (3):989-993
- Anderson CT, Carroll A, Akhmetova L, Somerville C (2010) Real-time imaging of cellulose reorientation during cell wall expansion in *Arabidopsis* roots. *Plant Physiol* 152 (2):787-796
- Anderson JW, Baird P, Davis RH, Ferreri S, Knudtson M, Koraym A, Waters V, Williams CL (2009) Health benefits of dietary fiber. *Nutr Rev* 67 (4):188-205
- Anderson OD, Greene FC, Yip RE, Halford NG, Shewry PR, Malpica-Romero JM (1989) Nucleotide sequences of the two high-molecular-weight glutenin genes from the D-genome of a hexaploid bread wheat, *Triticum aestivum* L. cv Cheyenne. *Nucleic Acids Res* 17 (1):461-462
- Andersson AA, Andersson R, Piironen V, Lampi A-M, Nyström L, Boros D, Fraš A, Gebruers K, Courtin CM, Delcour JA (2013) Contents of dietary fibre components and their relation to associated bioactive components in whole grain wheat samples from the HEALTHGRAIN diversity screen. *Food Chem* 136 (3):1243-1248
- Antoine C, Peyron S, Mabilille F, Lapierre C, Bouchet B, Abecassis J, Rouau X (2003) Individual contribution of grain outer layers and their cell wall structure to the mechanical properties of wheat bran. *J Agr Food Chem* 51 (7):2026-2033

- Asaoka M, Okuno K, Fuwa H (1985a) Effect of environmental temperature at the milky stage on amylose content and fine structure of amylopectin of waxy and nonwaxy endosperm starches of rice (*Oryza sativa* L.). *Agri Biol Chem* 49 (2):373-379
- Asaoka M, Okuno K, Sugimoto Y, Fuwa H (1985b) Developmental changes in the structure of endosperm starch of rice (*Oryza sativa* L.). *Agri Biol Chem* 49 (7):1973-1978
- Aspinall G, Carlyle J (1969) *Anogeissus leiocarpus* gum. Part IV. Exterior chains of leiocarpan A. *J Chem Soc* (5):851-856
- Aspinall G, Carlyle J, McNab J, Rudowski A (1969) *Anogeissus leiocarpus* gum. Part II. Fractionation of the gum and partial hydrolysis of leiocarpan A. *J Chem Soc* (5):840-845
- Aspinall G, McNab J (1969) *Anogeissus leiocarpus* gum. Part III. Interior chains of leiocarpan A. *J Chem Soc* (5):845-851
- Atmodjo MA, Hao ZY, Mohnen D (2013) Evolving views of pectin biosynthesis. *Annu Rev Plant Biol* 64:747-+. doi:DOI 10.1146/annurev-arplant-042811-105534
- Bacic A, Stone B (1980) A (1-3)-linked and (1-4)-linked β -D-glucan in the endosperm cell-walls of wheat. *Carbohyd Res* 82 (2):372-377
- Bacic A, Stone B (1981) Chemistry and organization of aleurone cell wall components from wheat and barley. *Funct Plant Biology* 8 (5):475-495
- Barron C, Parker ML, Mills ENC, Rouau X, Wilson RH (2005) FTIR imaging of wheat endosperm cell walls in situ reveals compositional and architectural heterogeneity related to grain hardness. *Planta* 220 (5):667-677
- Barron C, Robert P, Guillon F, Saulnier L, Rouau X (2006) Structural heterogeneity of wheat arabinoxylans revealed by Raman spectroscopy. *Carbohyd Res* 341 (9):1186-1191
- Barron C, Rouau X (2008) FTIR and Raman signatures of wheat grain peripheral tissues. *Cereal Chem* 85 (5):619-625
- Bartels D, Altosaar I, Harberd NP, Barker RF, Thompson RD (1986) Molecular analysis of γ -gliadin gene families at the complex Gli-1 locus of bread wheat (*T. aestivum* L.). *Theor Appl Genet* 72 (6):845-853. doi:10.1007/BF00266556
- Baskin TI (2001) On the alignment of cellulose microfibrils by cortical microtubules: a review and a model. *Protoplasma* 215 (1-4):150-171
- Bates B, Lennox A, Swan G (2011) National Diet and Nutrition Survey (NDNS). Headline results from years 1 and 2 (combined) of the rolling programme (2008/2009 – 2009/10). London: The stationery Office
- Bechtel D, Juliano B (1980) Formation of protein bodies in the starchy endosperm of rice (*Oryza sativa* L.): a re-investigation. *Ann Bot -London* 45 (5):503-509
- Becraft PW, Asuncion-Crabb Y (2000) Positional cues specify and maintain aleurone cell fate in maize endosperm development. *Development* 127 (18):4039-4048

- Becraft PW, Yi GB (2011) Regulation of aleurone development in cereal grains. *J Exp Bot* 62 (5):1669-1675
- Beňová-Kákošová A, Dignonnet C, Goubet F, Ranocha P, Jauneau A, Pesquet E, Barbier O, Zhang Z, Capek P, Dupree P (2006) Galactoglucomannans increase cell population density and alter the protoxylem/metaxylem tracheary element ratio in xylogenic cultures of *Zinnia*. *Plant Physiol* 142 (2):696-709
- Berthet S, Demont-Caulet N, Pollet B, Bidzinski P, Cézard L, Le Bris P, Borrega N, Hervé J, Blondet E, Balzergue S (2011) Disruption of LACCASE4 and 17 results in tissue-specific alterations to lignification of *Arabidopsis thaliana* stems. *Plant Cell* 23 (3):1124-1137
- Bertoft E (1986) Hydrolysis of amylopectin by the α -amylase of *B. subtilis*. *Carbohydr Res* 149 (2):379-387
- Bewley JD, Black M (1994) Seed development and maturation. In: *Seeds*. Springer, pp 35-115
- Bingham SA, Williams DRR, Cummings JH (1985) Dietary fiber consumption in Britain - new estimates and their relation to large bowel-cancer mortality. *Brit J Cancer* 52 (3):399-402
- Bjorck I, Ostman E, Kristensen M, Anson NM, Price RK, Haenen GRMM, Havenaar R, Knudsen KEB, Frid A, Mykkanen H, Welch RW, Riccardi G (2012) Cereal grains for nutrition and health benefits: Overview of results from *in vitro*, animal and human studies in the HEALTHGRAIN project. *Trends Food Sci Tech* 25 (2):87-100
- Black M, Corbineau F, Gee H, Côme D (1999) Water content, raffinose, and dehydrins in the induction of desiccation tolerance in immature wheat embryos. *Plant Physiol* 120 (2):463-472
- Boerjan W, Ralph J, Baucher M (2003) Lignin biosynthesis. *Annu Rev Plant Biol* 54 (1):519-546
- Böhm N, Kulicke W-M (1999) Rheological studies of barley (1-3),(1-4)- β -glucan in concentrated solution: mechanistic and kinetic investigation of the gel formation. *Carbohydr Res* 315 (3):302-311
- Bouton S, Leboeuf E, Mouille G, Leydecker M-T, Talbotec J, Granier F, Lahaye M, Höfte H, Truong H-N (2002) QUASIMODO1 encodes a putative membrane-bound glycosyltransferase required for normal pectin synthesis and cell adhesion in *Arabidopsis*. *Plant Cell* 14 (10):2577-2590
- Briarty L, Hughes C, Evers A (1979) The developing endosperm of wheat—a stereological analysis. *Ann Bot -London* 44 (6):641-658
- Bringmann M, Li E, Sampathkumar A, Kocabek T, Hauser M-T, Persson S (2012) POM-POM2/cellulose synthase interacting1 is essential for the functional association of cellulose synthase and microtubules in *Arabidopsis*. *Plant Cell* 24 (1):163-177

- Bromley JR, Busse- Wicher M, Tryfona T, Mortimer JC, Zhang Z, Brown DM, Dupree P (2013) GUX1 and GUX2 glucuronyltransferases decorate distinct domains of glucuronoxylan with different substitution patterns. *Plant J* 74 (3):423-434
- Brown DM, Goubet F, Wong VW, Goodacre R, Stephens E, Dupree P, Turner SR (2007) Comparison of five xylan synthesis mutants reveals new insight into the mechanisms of xylan synthesis. *Plant J* 52 (6):1154-1168
- Brown DM, Zhang Z, Stephens E, Dupree P, Turner SR (2009) Characterization of IRX10 and IRX10- like reveals an essential role in glucuronoxylan biosynthesis in Arabidopsis. *Plant J* 57 (4):732-746
- Brown RC, Lemmon BE, Olsen OA (1994) Endosperm development in barley: microtubule involvement in the morphogenetic pathway. *Plant Cell* 6 (9):1241-1252
- Brown RC, Lemmon BE, Olsen OA (1996a) Polarization in early differentiation of cereal grain endosperm. *Mol Biol Cell* 7:1759-1759
- Brown RC, Lemmon BE, Stone BA, Olsen OA (1997) Cell wall (1-3)- and (1-3),(1-4)- β -glucans during early grain development in rice (*Oryza sativa L*). *Planta* 202 (4):414-426
- Brown RM, Saxena IM, Kudlicka K (1996b) Cellulose biosynthesis in higher plants. *Trends Plant Sci* 1 (5):149-156
- Brownlee C (2002) Role of the extracellular matrix in cell–cell signalling: paracrine paradigms. *Curr Opin Plant Biol* 5 (5):396-401
- Brummell DA (2006) Cell wall disassembly in ripening fruit. *Funct Plant Biol* 33 (2):103-119
- Buckeridge MS, Rayon C, Urbanowicz B, Tiné MAS, Carpita NC (2004) Mixed linkage (1-3),(1-4)- β -D-glucans of grasses. *Cereal Chem* 81 (1):115-127
- Buckeridge MS, Vergara CE, Carpita NC (1999) The mechanism of synthesis of a mixed-linkage (1-3),(1-4) β -D-glucan in maize. Evidence for multiple sites of glucosyl transfer in the synthase complex. *Plant Physiol* 120 (4):1105-1116
- Buckeridge MS, Vergara CE, Carpita NC (2001) Insight into multi-site mechanisms of glycosyl transfer in (1-4)- β -D-glycans provided by the cereal mixed-linkage (1-3),(1-4) β -D-glucan synthase. *Phytochemistry* 57 (7):1045-1053
- Buffetto F, Ropartz D, Zhang X, Gilbert H, Guillon F, Ralet M-C (2014) Recovery and fine structure variability of RG-II sub-domains in wine (*Vitis vinifera Cv. Merlot*). *Ann Bot -London*:mcb097
- Bunzel M, Ralph J, Funk C, Steinhart H (2003) Isolation and identification of a ferulic acid dehydrotrimer from saponified maize bran insoluble fiber. *Eur Food Res Technol* 217 (2):128-133
- Bunzel M, Ralph J, Marita JM, Hatfield RD, Steinhart H (2001) Diferulates as structural components in soluble and insoluble cereal dietary fibre. *J Sci Food Agri* 81 (7):653-660

- Burton RA, Fincher GB (2009) (1-3),(1-4)- β -d-glucans in cell walls of the Poaceae, lower plants, and fungi: a tale of two linkages. *Mol Plant* 2 (5):873-882
- Burton RA, Fincher GB (2012) Current challenges in cell wall biology in the cereals and grasses. *Frontier Plant Sci* 3
- Burton RA, Gidley MJ, Fincher GB (2010a) Heterogeneity in the chemistry, structure and function of plant cell walls. *Nat Chem Biol* 6 (10):724-732. doi:Doi 10.1038/Nchembio.439
- Burton RA, Gidley MJ, Fincher GB (2010b) Heterogeneity in the chemistry, structure and function of plant cell walls. *Nat Chem Biol* 6 (10):724-732
- Busse-Wicher M, Gomes TC, Tryfona T, Nikolovski N, Stott K, Grantham NJ, Bolam DN, Skaf MS, Dupree P (2014) The pattern of xylan acetylation suggests xylan may interact with cellulose microfibrils as a twofold helical screw in the secondary plant cell wall of *Arabidopsis thaliana*. *Plant J* 79 (3):492-506
- Buttriss J (2009) Fibre and health. *Agro Food Ind Hi Tec* 20 (3):4-8
- Cade JE, Burley VJ, Greenwood DC (2007) Dietary fibre and risk of breast cancer in the UK women's cohort study. *Int J Epidemiol* 36 (2):431-438
- Caffall KH, Mohnen D (2009) The structure, function, and biosynthesis of plant cell wall pectic polysaccharides. *Carbohydr Res* 344 (14):1879-1900
- Cagam Cagampang GB, Cruz LJ, Espiritu SG, Santiago RG, Juliano BO, Upton EM, Hester EE, Meredith O, Wren J, Yoshino D (1966) Studies on the extraction and composition of rice proteins. *Cereal Chem* 43 (2):145-155
- Cardoso SM, Ferreira JA, Mafra I, Silva AM, Coimbra MA (2007) Structural ripening-related changes of the arabinan-rich pectic polysaccharides from olive pulp cell walls. *J Agr Food Chem* 55 (17):7124-7130
- Carpita NC (1984) Cell-wall development in maize coleoptiles. *Plant Physiol* 76 (1):205-212
- Carpita NC, Defernez M, Findlay K, Wells B, Shoue DA, Catchpole G, Wilson RH, McCann MC (2001) Cell wall architecture of the elongating maize coleoptile. *Plant Physiol* 127 (2):551-565
- Carpita NC, Gibeaut DM (1993) Structural models of primary cell walls in flowering plants: consistency of molecular structure with the physical properties of the walls during growth. *Plant J* 3 (1):1-30
- Carvajal-Millan E, Landillon V, Morel M-H, Rouau X, Doublier J-L, Micard V (2005) Arabinoxylan gels: Impact of the feruloylation degree on their structure and properties. *Biomacromolecules* 6 (1):309-317
- Chateigner-Boutin AL, Bouchet B, Alvarado C, Bakan B, Guillon F (2014) The wheat grain contains pectic domains exhibiting specific spatial and development-associated distribution. *Plos One* 9 (2)
- Chen F, Tobimatsu Y, Havkin-Frenkel D, Dixon RA, Ralph J (2012a) A polymer of caffeyl alcohol in plant seeds. *PNAS* 109 (5):1772-1777

- Chen F, Tobimatsu Y, Jackson L, Nakashima J, Ralph J, Dixon RA (2013) Novel seed coat lignins in the *Cactaceae*: structure, distribution and implications for the evolution of lignin diversity. *Plant J* 73 (2):201-211
- Chen X, Vega-Sánchez ME, Verhertbruggen Y, Chiniquy D, Canlas PE, Fagerström A, Prak L, Christensen U, Oikawa A, Chern M (2012b) Inactivation of OsIRX10 leads to decreased xylan content in rice culm cell walls and improved biomass saccharification. *Mol Plant* 6:570-573
- Chiotelli E, Le Meste M (2002) Effect of small and large wheat starch granules on thermomechanical behavior of starch. *Cereal Chem* 79 (2):286-293
- Cochrane M, Duffus C (1981) Endosperm cell number in barley. *Nature* 289:399-401
- Cornuault V, Buffetto F, Rydahl MG, Marcus SE, Torode TA, Xue J, Crépeau M-J, Faria-Blanc N, Willats WG, Dupree P (2015) Monoclonal antibodies indicate low-abundance links between heteroxylan and other glycans of plant cell walls. *Planta*:1-14
- Cui W, Wood P, Blackwell B, Nikiforuk J (2000) Physicochemical properties and structural characterization by two-dimensional NMR spectroscopy of wheat β -D-glucan—comparison with other cereal β -D-glucans. *Carbohydr Polym* 41 (3):249-258
- D'Ovidio R, Mattei B, Roberti S, Bellincampi D (2004) Polygalacturonases, polygalacturonase-inhibiting proteins and pectic oligomers in plant–pathogen interactions. *BBA - Proteins Proteom* 1696 (2):237-244
- Dahl R, Staehelin LA (1989) High-pressure freezing for the preservation of biological structure: Theory and practice. *J Electron Microscop Tech* 13 (3):165-174
- Dale EM, Housley TL (1986) Sucrose synthase activity in developing wheat endosperms differing in maximum weight. *Plant Physiol* 82 (1):7-10
- Darlington H, Tecsi L, Harris N, Griggs D, Cantrell I, Shewry P (2000) Starch granule associated proteins in barley and wheat. *J Cereal Sci* 32 (1):21-29
- Darvill AG, Albersheim P, McNeil M, Lau JM, York WS, Stevenson TT, Thomas J, Doares S, Gollin DJ, Chelf P (1985) Structure and function of plant cell wall polysaccharides. *J Cell Sci* 1985 (Supplement 2):203-217
- Davin LB, Wang H-B, Crowell AL, Bedgar DL, Martin DM, Sarkanen S, Lewis NG (1997) Stereoselective bimolecular phenoxy radical coupling by an auxiliary (dirigent) protein without an active center. *Science* 275 (5298):362-367
- DeMason DA, Sexton R, Gorman M, Reid J (1985) Structure and biochemistry of endosperm breakdown in date palm (*Phoenix dactylifera* L.) seeds. *Protoplasma* 126 (3):159-167
- Dhugga KS, Barreiro R, Whitten B, Stecca K, Hazebroek J, Randhawa GS, Dolan M, Kinney AJ, Tomes D, Nichols S (2004) Guar seed β -mannan synthase is a member of the cellulose synthase super gene family. *Science* 303 (5656):363-366

- Diet A, Link B, Seifert GJ, Schellenberg B, Wagner U, Pauly M, Reiter W-D, Ringli C (2006) The Arabidopsis root hair cell wall formation mutant *lrx1* is suppressed by mutations in the RHM1 gene encoding a UDP-L-rhamnose synthase. *Plant Cell* 18 (7):1630-1641
- Doblin MS, Pettolino FA, Wilson SM, Campbell R, Burton RA, Fincher GB, Newbigin E, Bacic A (2009) A barley cellulose synthase-like CSLH gene mediates (1-3),(1-4)- β -D-glucan synthesis in transgenic Arabidopsis. *PNAS* 106 (14):5996-6001
- Donaldson LA (2001) Lignification and lignin topochemistry—an ultrastructural view. *Phytochemistry* 57 (6):859-873
- Dornez E, Cuyvers S, Holopainen U, Nordlund E, Poutanen K, Delcour JA, Courtin CM (2011) Inactive fluorescently labeled xylanase as a novel probe for microscopic analysis of arabinoxylan containing cereal cell walls. *J Agr Food Chem* 59 (12):6369-6375
- Dupont FM, Altenbach SB (2003) Molecular and biochemical impacts of environmental factors on wheat grain development and protein synthesis. *J Cereal Sci* 38 (2):133-146
- Ebringerová A, Hromádková Z, Heinze T (2005) Hemicellulose. In: *Polysaccharides i*. Springer, pp 1-67
- Edashige Y, Ishii T (1998) Rhamnogalacturonan II from cell walls of *Cryptomeria japonica*. *Phytochemistry* 49 (3):681-690
- Edwards ME, Dickson CA, Chengappa S, Sidebottom C, Gidley MJ, Reid J (1999) Molecular characterisation of a membrane-bound galactosyltransferase of plant cell wall matrix polysaccharide biosynthesis. *Plant J* 19 (6):691-697
- Egelund J, Damager I, Faber K, Olsen C-E, Ulvskov P, Petersen BL (2008) Functional characterisation of a putative rhamnogalacturonan II specific xylosyltransferase. *FEBS letters* 582 (21):3217-3222
- Egelund J, Petersen BL, Motawia MS, Damager I, Faik A, Olsen CE, Ishii T, Clausen H, Ulvskov P, Geshi N (2006) *Arabidopsis thaliana* RGXT1 and RGXT2 encode Golgi-localized (1, 3)- α -D-xylosyltransferases involved in the synthesis of pectic rhamnogalacturonan-II. *Plant Cell* 18 (10):2593-2607
- Ellis M, Egelund J, Schultz CJ, Bacic A (2010) Arabinogalactan-proteins: key regulators at the cell surface? *Plant Physiol* 153 (2):403-419
- Englyst HN, Quigley ME, Hudson G, Cummings J (1992) Determination of dietary fibre as non-starch polysaccharides by gas-liquid chromatography. *Analyst* 117 (11):1707-1714
- Englyst HN, Quigley ME, Hudson GJ (1994) Determination of dietary fibre as non-starch polysaccharides with gas-liquid chromatographic, high-performance liquid chromatographic or spectrophotometric measurement of constituent sugars. *Analyst* 119 (7):1497-1509

- Eshtiaghi M, Stute R, Knorr D (1994) High-Pressure and Freezing Pretreatment Effects on Drying, Rehydration, Texture and Color of Green Beans, Carrots and Potatoes. *J Food Sci* 59 (6):1168-1170
- Evers AD (1970) Development of endosperm of wheat. *Ann Bot -London* 34 (136):547-&
- Fannon JE, Hauber RJ, BeMiller JN (1992) Surface pores of starch granules. *Cereal Chem* 69 (3):284-288
- Fenwick K, Apperley D, Cosgrove D, Jarvis M (1999) Polymer mobility in cell walls of cucumber hypocotyls. *Phytochemistry* 51 (1):17-22
- Fernandes AN, Thomas LH, Altaner CM, Callow P, Forsyth VT, Apperley DC, Kennedy CJ, Jarvis MC (2011) Nanostructure of cellulose microfibrils in spruce wood. *PNAS* 108 (47):1195-1203
- Finch-Savage WE, Leubner-Metzger G (2006) Seed dormancy and the control of germination. *New Phytologist* 171 (3):501-523
- Fincher G, Stone B (1974) A water-soluble arabinogalactan-peptide from wheat endosperm. *Aust J Biol Sci* 27 (2):117-132
- Fincher G, Stone B (2004) Chemistry of non-starch polysaccharides.
- Fincher GB, Burton RA (2014) Evolution and Development of Cell Walls in Cereal Grains. *Frontiers in Plant Science* 5. doi:10.3389/fpls.2014.00456
- Fincher GB, Stone BA, Clarke AE (1983) Arabinogalactan-proteins: structure, biosynthesis, and function. *Annu Rev Plant Physiol* 34 (1):47-70
- Fineran BA, Wild DJC, Ingerfeld M (1982) Initial wall formation in the endosperm of wheat, *Triticum aestivum* - a re-evaluation. *Can J Bot* 60 (9):1776-1795
- French D (1984) Organization of starch granules. *Starch: Chemistry and technology* 2:183-247
- Funk C, Ralph J, Steinhart H, Bunzel M (2005) Isolation and structural characterisation of 8-O-4/8-O-4-and 8-8/8-O-4-coupled dehydrotriferulic acids from maize bran. *Phytochemistry* 66 (3):363-371
- Furukawa S, Mizuma T, Kiyokawa Y, Masumura T, Tanaka K, Wakai Y (2003) Distribution of storage proteins in low-glutelin rice seed determined using a fluorescent antibody. *J Biosci Bioeng* 96 (5):467-473
- Gallant DJ, Bouchet B, Baldwin PM (1997) Microscopy of starch: evidence of a new level of granule organization. *Carbohydr Polym* 32 (3):177-191
- Galway M, Rennie P, Fowke L (1993) Ultrastructure of the endocytotic pathway in glutaraldehyde-fixed and high-pressure frozen/freeze-substituted protoplasts of white spruce (*Picea glauca*). *J Cell Sci* 106 (3):847-858
- Gao XP, Francis D, Ormrod JC, Bennett MD (1992) Changes in cell number and cell-division activity during endosperm development in allohexaploid wheat, *Triticum aestivum* L. *J Exp Bot* 43 (257):1603-1609

- Gemen R, de Vries JF, Slavin JL (2011) Relationship between molecular structure of cereal dietary fiber and health effects: focus on glucose/insulin response and gut health. *Nutr Rev* 69 (1):22-33
- Gillmor CS, Poindexter P, Lorieau J, Palcic MM, Somerville C (2002) α -Glucosidase I is required for cellulose biosynthesis and morphogenesis in Arabidopsis. *J Cell Biol* 156 (6):1003-1013
- Goubet F, Barton CJ, Mortimer JC, Yu X, Zhang Z, Miles GP, Richens J, Liepman AH, Seffen K, Dupree P (2009) Cell wall glucomannan in Arabidopsis is synthesised by CSLA glycosyltransferases, and influences the progression of embryogenesis. *Plant J* 60 (3):527-538
- Goubet F, Mohnen D (1999) Subcellular localization and topology of homogalacturonan methyltransferase in suspension-cultured *Nicotiana tabacum* cells. *Planta* 209 (1):112-117
- Gross KC, Sams CE (1984) Changes in cell wall neutral sugar composition during fruit ripening: a species survey. *Phytochemistry* 23 (11):2457-2461
- Guillon F, Bouchet B, Jamme F, Robert P, Quemener B, Barron C, Larre C, Dumas P, Saulnier L (2011) *Brachypodium distachyon* grain: characterization of endosperm cell walls. *J Exp Bot* 62 (3):1001-1015
- Guillon F, Tranquet O, Quillien L, Utile JP, Ortiz JJO, Saulnier L (2004) Generation of polyclonal and monoclonal antibodies against arabinoxylans and their use for immunocytochemical location of arabinoxylans in cell walls of endosperm of wheat. *J Cereal Sci* 40 (2):167-182. doi:DOI 10.1016/j.jcs.2004.06.004
- Gupta RB, Batey IL, Macritchie F (1992) Relationships between protein-composition and functional-properties of wheat flours. *Cereal Chem* 69 (2):125-131
- Ha M-A, Viëtor RJ, Jardine GD, Apperley DC, Jarvis MC (2005) Conformation and mobility of the arabinan and galactan side-chains of pectin. *Phytochemistry* 66 (15):1817-1824
- Ha MA, Apperley DC, Evans BW, Huxham IM, Jardine WG, Viëtor RJ, Reis D, Vian B, Jarvis MC (1998) Fine structure in cellulose microfibrils: NMR evidence from onion and quince. *Plant J* 16 (2):183-190
- Hao Z, Mohnen D (2014) A review of xylan and lignin biosynthesis: foundation for studying Arabidopsis irregular xylem mutants with pleiotropic phenotypes. *Crit Rev Biochem Mol* 49 (3):212-241
- Harholt J, Jensen JK, Sørensen SO, Orfila C, Pauly M, Scheller HV (2006) ARABINAN DEFICIENT 1 is a putative arabinosyltransferase involved in biosynthesis of pectic arabinan in Arabidopsis. *Plant Physiol* 140 (1):49-58
- Harholt J, Suttangkakul A, Scheller HV (2010) Biosynthesis of pectin. *Plant Physiol* 153 (2):384-395
- Harris D, Bulone V, Ding S-Y, DeBolt S (2010) Tools for cellulose analysis in plant cell walls. *Plant Physiol* 153 (2):420-426

- Harris N, Juliano B (1977) Ultrastructure of endosperm protein bodies in developing rice grains differing in protein content. *Ann Bot -London* 41 (1):1-5
- Hay JO, Spanswick RM (2006) Mechanical and enzymatic separation of ripening rice (*Oryza sativa* L.) caryopsis tissues. *Seed Sci Res* 16 (3):223-227
- Hayashi T, Marsden MP, Delmer DP (1987) Pea xyloglucan and cellulose VI. Xyloglucan-cellulose interactions *in vitro* and *in vivo*. *Plant Physiol* 83 (2):384-389
- Hazen SP, Scott-Craig JS, Walton JD (2002) Cellulose synthase-like genes of rice. *Plant Physiol* 128 (2):336-340
- Henry RJ (1985) A comparison of the non-starch carbohydrates in cereal grains. *J Sci Food Agri* 36 (12):1243-1253
- Hervé C, Rogowski A, Gilbert HJ, Paul Knox J (2009) Enzymatic treatments reveal differential capacities for xylan recognition and degradation in primary and secondary plant cell walls. *Plant J* 58 (3):413-422
- Hesselman K, Elwinger K, Nilsson M, Thomke S (1981) The effect of β -glucanase supplementation, stage of ripeness, and storage treatment of barley in diets fed to broiler-chickens. *Poultry Sci* 60 (12):2664-2671
- Hizukuri S (1986) Polymodal distribution of the chain lengths of amylopectins, and its significance. *Carbohyd Res* 147 (2):342-347
- Hoshikawa K (1973) Morphogenesis of Endosperm Tissue in Rice. *JARQ - JPN Agri Res Q* 7 (3):153-159
- Hsia C, Anderson O (2001) Isolation and characterization of wheat ω -gliadin genes. *Theor Appl Genet* 103 (1):37-44
- Huber KC, BeMiller JN (1997) Visualization of channels and cavities of corn and sorghum starch granules. *Cereal Chem* 74 (5):537-541
- Iiyama K, Lam TB-T, Stone BA (1994) Covalent cross-links in the cell wall. *Plant Physiol* 104 (2):315
- Immerzeel P, Eppink MM, De Vries SC, Schols HA, Voragen AG (2006) Carrot arabinogalactan proteins are interlinked with pectins. *Physiol Plantarum* 128 (1):18-28
- Ishii T (1997a) O-acetylated oligosaccharides from pectins of potato tuber cell walls. *Plant Physiol* 113 (4):1265-1272
- Ishii T (1997b) Structure and functions of feruloylated polysaccharides. *Plant Sci* 127 (2):111-127
- Ishii T, Ichita J, Matsue H, Ono H, Maeda I (2002) Fluorescent labeling of pectic oligosaccharides with 2-aminobenzamide and enzyme assay for pectin. *Carbohyd Res* 337 (11):1023-1032
- Ishii T, Matsunaga T, Pellerin P, O'Neill MA, Darvill A, Albersheim P (1999) The plant cell wall polysaccharide rhamnogalacturonan II self-assembles into a covalently cross-linked dimer. *J Biol Chem* 274 (19):13098-13104

- Ishimaru T, Matsuda T, Ohsugi R, Yamagishi T (2003) Morphological development of rice caryopses located at the different positions in a panicle from early to middle stage of grain filling. *Funct Plant Biol* 30 (11):1139-1149
- Jeffries TW (1994) Biodegradation of lignin and hemicelluloses. In: *Biochemistry of microbial degradation*. Springer, pp 233-277
- Jenner C, Ugalde T, Aspinall D (1991) The physiology of starch and protein deposition in the endosperm of wheat. *Funct Plant Biol* 18 (3):211-226
- Jing Y-p, Liu D-t, Li D-l, Li X-g, Zeng X, Gu Y-j, Wang Z (2013) Development of starch endosperm cells and amyloplasts in wheat. *J Triticeae Crops* 4:34-41
- Johnson KL, Jones BJ, Bacic A, Schultz CJ (2003) The fasciclin-like arabinogalactan proteins of Arabidopsis. A multigene family of putative cell adhesion molecules. *Plant Physiol* 133 (4):1911-1925
- Jones KH, Kniss DA (1987) Propidium iodide as a nuclear counterstain for immunofluorescence studies on cells in culture. *J Histochem Cytochem* 35 (1):123-125
- Jones L, Milne JL, Ashford D, McCann MC, McQueen-Mason SJ (2005) A conserved functional role of pectic polymers in stomatal guard cells from a range of plant species. *Planta* 221 (2):255-264
- Jones L, Milne JL, Ashford D, McQueen-Mason SJ (2003) Cell wall arabinan is essential for guard cell function. *PNAS* 100 (20):11783-11788
- Jones L, Seymour GB, Knox JP (1997) Localization of pectic galactan in tomato cell walls using a monoclonal antibody specific to (1-4)- β -D-galactan. *Plant Physiol* 113 (4):1405-1412
- Juliano BO (1985a) Cooperative tests on cooking properties of milled rice. *Cereal Food World* 30 (9):651-656
- Juliano BO (1985b) *Rice: chemistry and technology*. American Association of Cereal Chemists, St Paul, MN,
- Kaida R, Sugawara S, Negoro K, Maki H, Hayashi T, Kaneko TS (2010) Acceleration of cell growth by xyloglucan oligosaccharides in suspension-cultured tobacco cells. *Mol Plant* 3 (3):549-554
- Kainuma K, Preiss J (1988) Structure and chemistry of the starch granule. *Carbohydrates* 14:141-180
- Kaneda M, Rensing KH, Wong JC, Banno B, Mansfield SD, Samuels AL (2008) Tracking monolignols during wood development in lodgepole pine. *Plant Physiol* 147 (4):1750-1760
- Kaneko Y, Walther P (1995) Comparison of ultrastructure of germinating pea leaves prepared by high-pressure freezing–freeze substitution and conventional chemical fixation. *J Electron Microsc* 44 (2):104-109
- Kawagoe Y, Suzuki K, Tasaki M, Yasuda H, Akagi K, Katoh E, Nishizawa NK, Ogawa M, Takaiwa F (2005) The critical role of disulfide bond formation in protein sorting in the endosperm of rice. *Plant Cell* 17 (4):1141-1153

- Kerstens S, Verbelen JP (2002) Cellulose orientation in the outer epidermal wall of angiosperm roots: implications for biosystematics. *Ann Bot -London* 90 (5):669-676
- Kiemle SN, Zhang X, Esker AR, Toriz G, Gatenholm P, Cosgrove DJ (2014) Role of (1-3),(1-4)- β -glucan in cell walls: interaction with cellulose. *Biomacromolecules* 15 (5):1727-1736
- Kim H-S, Huber KC (2008) Channels within soft wheat starch A-and B-type granules. *J Cereal Sci* 48 (1):159-172
- Kim WT, Li XX, Okita TW (1993) Expression of storage protein multigene families in developing rice endosperm. *Plant Cell Physiol* 34 (4):595-603
- Kiss J, Giddings Jr TH, Staehelin L, Sack F (1990) Comparison of the ultrastructure of conventionally fixed and high pressure frozen/freeze substituted root tips of *Nicotiana* and *Arabidopsis*. *Protoplasma* 157:64-74
- Kitazawa K, Tryfona T, Yoshimi Y, Hayashi Y, Kawauchi S, Antonov L, Tanaka H, Takahashi T, Kaneko S, Dupree P (2013) β -Galactosyl yariv reagent binds to the β -(1-3)-galactan of arabinogalactan proteins. *Plant Physiol* 161 (3):1117-1126
- Knox JP, Linstead PJ, King J, Cooper C, Roberts K (1990) Pectin esterification is spatially regulated both within cell-walls and between developing-tissues of root apices. *Planta* 181 (4):512-521
- Knudsen KEB (1997) Carbohydrate and lignin contents of plant materials used in animal feeding. *Anim Feed Sci Tech* 67 (4):319-338
- Ko Y-T, Dong Y-L, Hsieh Y-F, Kuo J-C (2009) Morphology, associated protein analysis, and identification of 58-kDa starch synthase in mungbean (*Vigna radiata* L. cv. KPS1) starch granule preparations. *J Agr Food Chem* 57 (10):4426-4432
- Kobayashi H, Ikeda TM, Nagata K (2013) Spatial and temporal progress of programmed cell death in the developing starchy endosperm of rice. *Planta* 237 (5):1393-1400
- Kobayashi M, Matoh T, Azuma J (1996) Two chains of rhamnogalacturonan II are cross-linked by borate-diol ester bonds in higher plant cell walls. *Plant Physiol* 110 (3):1017-1020
- Kozlova L, Snegireva A, Gorshkova T (2012) Distribution and structure of mixed linkage glucan at different stages of elongation of maize root cells. *Rus J Plant Physiol* 59 (3):339-347
- Kurek I, Kawagoe Y, Jacob-Wilk D, Doblin M, Delmer D (2002) Dimerization of cotton fiber cellulose synthase catalytic subunits occurs via oxidation of the zinc-binding domains. *PNAS* 99 (17):11109-11114
- Lai VM, Lu S, He WH, Chen HH (2007) Non-starch polysaccharide compositions of rice grains with respect to rice variety and degree of milling. *Food Chem* 101 (3):1205-1210

- Lampert DT, Kieliszewski MJ, Showalter AM (2006) Salt stress upregulates periplasmic arabinogalactan proteins: using salt stress to analyse AGP function. *New Phytol* 169 (3):479-492
- Lampert DT, Varnai P, Seal CE (2014) Back to the future with the AGP–Ca²⁺ flux capacitor. *Ann Bot -London* 114 (6):1069-1085
- Lau JM, McNeil M, Darvill AG, Albersheim P (1987) Treatment of rhamnogalacturonan I with lithium in ethylenediamine. *Carbohydr Res* 168 (2):245-274
- Lazaridou A, Biliaderis C (2007) Molecular aspects of cereal β -glucan functionality: Physical properties, technological applications and physiological effects. *J Cereal Sci* 46 (2):101-118
- Lazaridou A, Biliaderis C, Micha-Screttas M, Steele BR (2004) A comparative study on structure–function relations of mixed-linkage (1-3),(1-4) linear β -d-glucans. *Food Hydrocolloid* 18 (5):837-855
- Leclere L, Van Cutsem P, Michiels C (2013) Anti-cancer activities of pH-or heat-modified pectin. *Frontier Pharmacology* 4:128
- Ledbetter M, Porter K (1963) A "microtubule" in plant cell fine structure. *J Cell Biology* 19 (1):239-250
- Lee C, Zhong R, Ye Z-H (2012) Arabidopsis family GT43 members are xylan xylosyltransferases required for the elongation of the xylan backbone. *Plant Cell Physiol* 53 (1):135-143
- Lee KJD, Sakata Y, Mau SL, Pettolino F, Bacic A, Quatrano RS, Knight CD, Knox JP (2005) Arabinogalactan proteins are required for apical cell extension in the moss *Physcomitrella patens*. *Plant Cell* 17 (11):3051-3065. doi:DOI 10.1105/tpc.105.034413
- Lewis NG, Yamamoto E (1990) Lignin: occurrence, biogenesis and biodegradation. *Annu Rev Plant Biol* 41 (1):455-496
- Li J, Burton RA, Harvey AJ, Hrmova M, Wardak AZ, Stone BA, Fincher GB (2003) Biochemical evidence linking a putative callose synthase gene with (1-3)- β -D-glucan biosynthesis in barley. *Plant Mol Biol* 53 (1):213-225
- Liepman AH, Nairn CJ, Willats WG, Sørensen I, Roberts AW, Keegstra K (2007) Functional genomic analysis supports conservation of function among cellulose synthase-like a gene family members and suggests diverse roles of mannans in plants. *Plant Physiol* 143 (4):1881-1893
- Liepman AH, Wilkerson CG, Keegstra K (2005) Expression of cellulose synthase-like (Csl) genes in insect cells reveals that CslA family members encode mannan synthases. *PNAS* 102 (6):2221-2226
- Lin T-Y, Elbein AD, Su J-C (1966) Substrate specificity in pectin synthesis. *Biochem Biophys Res Comms* 22 (6):650-657
- Liu XL, Liu L, Niu QK, Xia C, Yang KZ, Li R, Chen LQ, Zhang XQ, Zhou Y, Ye D (2011) MALE GAMETOPHYTE DEFECTIVE 4 encodes a rhamnogalacturonan II

- xylosyltransferase and is important for growth of pollen tubes and roots in Arabidopsis. *Plant J* 65 (4):647-660
- Lonsdale JE, McDonald KL, Jones RL (1999) High pressure freezing and freeze substitution reveal new aspects of fine structure and maintain protein antigenicity in barley aleurone cells. *Plant J* 17 (2):221-229
- Loosveld A-MA, Grobet PJ, Delcour JA (1997) Contents and structural features of water-extractable arabinogalactan in wheat flour fractions. *J Agr Food Chem* 45 (6):1998-2002
- Lovegrove A, Wilkinson MD, Freeman J, Pellny TK, Tosi P, Saulnier L, Shewry PR, Mitchell RA (2013) RNA interference suppression of genes in glycosyl transferase families 43 and 47 in wheat starchy endosperm causes large decreases in arabinoxylan content. *Plant Physiol* 163 (1):95-107
- MacArthur L, D'Appolonia B (1979) Comparison of oat and wheat carbohydrates. I. Sugars. *Cereal Chem* 56 (5):455-457
- Macquet A, Ralet M-C, Loudet O, Kronenberger J, Mouille G, Marion-Poll A, North HM (2007) A naturally occurring mutation in an Arabidopsis accession affects a β -D-galactosidase that increases the hydrophilic potential of rhamnogalacturonan I in seed mucilage. *Plant Cell* 19 (12):3990-4006
- Marcus SE, Blake AW, Benians TA, Lee KJ, Poyser C, Donaldson L, Leroux O, Rogowski A, Petersen HL, Boraston A (2010) Restricted access of proteins to mannan polysaccharides in intact plant cell walls. *Plant J* 64 (2):191-203
- Mares D, Stone B (1973a) Studies on wheat endosperm II. Properties of the wall components and studies on their organization in the wall. *Aust J Biol Sci* 26 (4):813-830
- Mares DJ, Norstog K, Stone BA (1975) Early stages in development of wheat endosperm .1. Change from free nuclear to cellular endosperm. *Aust J Bot* 23 (2):311-326
- Mares DJ, Stone BA (1973b) Studies on wheat endosperm .1. chemical composition and ultrastructure of cell-walls. *Aust J Biol Sci* 26 (4):793-812
- Mashiguchi K, Yamaguchi I, Suzuki Y (2004) Isolation and identification of glycosylphosphatidylinositol-anchored arabinogalactan proteins and novel β -glucosyl Yariv-reactive proteins from seeds of rice (*Oryza sativa*). *Plant Cell Physiol* 45 (12):1817-1829
- McCartney L, Knox JP (2002) Regulation of pectic polysaccharide domains in relation to cell development and cell properties in the pea testa. *J Exp Bot* 53 (369):707-713
- McCartney L, Marcus SE, Knox JP (2005) Monoclonal antibodies to plant cell wall xylans and arabinoxylans. *J Histochem Cytochem* 53 (4):543-546
- McCartney L, Ormerod AP, Gidley MJ, Knox JP (2000) Temporal and spatial regulation of pectic (1-4)- β -D-galactan in cell walls of developing pea cotyledons: implications for mechanical properties. *Plant J* 22 (2):105-113

- McCartney L, Steele-King CG, Jordan E, Knox JP (2003) Cell wall pectic (1-4)- β -D-galactan marks the acceleration of cell elongation in the Arabidopsis seedling root meristem. *Plant J* 33 (3):447-454
- McDonald K (1999) High-pressure freezing for preservation of high resolution fine structure and antigenicity for immunolabeling. In: *Electron microscopy methods and protocols*. Springer, pp 77-97
- McNeil M, Darvill AG, Albersheim P (1980) Structure of plant cell walls. Rhamnogalacturonan I, a structurally complex pectic polysaccharide in the walls of suspension-cultured sycamore cells. *Plant Physiol* 66 (6):1128-1134
- Meikle PJ, Bonig I, Hoogenraad NJ, Clarke AE, Stone BA (1991) The location of (1-3)- β -glucans in the walls of pollen tubes of *Nicotiana-alata* using a (1-3)- β -glucan-specific monoclonal antibody. *Planta* 185 (1):1-8
- Meikle PJ, Hoogenraad NJ, Bonig I, Clarke AE, Stone BA (1994) A (1-3),(1-4)- β -glucan-specific monoclonal antibody and its use in the quantitation and immunocytochemical location of (1-3),(1-4)- β -glucans. *Plant J* 5 (1):1-9
- Melton LD, McNeil M, Darvill AG, Albersheim P, Dell A (1986) Structural characterization of oligosaccharides isolated from the pectic polysaccharide rhamnogalacturonan II. *Carbohyd Res* 146 (2):279-305
- Meredith P (1981) Large and small starch granules in wheat—are they really different? *Starch* 33 (2):40-44
- Miao Y-C, Liu C-J (2010) ATP-binding cassette-like transporters are involved in the transport of lignin precursors across plasma and vacuolar membranes. *PNAS* 107 (52):22728-22733
- Mills ENC, Parker ML, Wellner N, Toole G, Feeney K, Shewry PR (2005) Chemical imaging: the distribution of ions and molecules in developing and mature wheat grain. *J Cereal Sci* 41 (2):193-201
- Mitsuda H, Yasumoto K, Murakami K, Kusano T, Kishida H (1967) Studies on the proteinaceous subcellular particles in rice endosperm: Electron-microscopy and isolation. *Agri Biol Chem* 31 (3):293-300
- Mod RR, Conkerton EJ, Ory RL, Normand FL (1978) Hemicellulose composition of dietary fiber of milled rice and rice bran. *J Agr Food Chem* 26 (5):1031-1035
- Mohnen D (2008) Pectin structure and biosynthesis. *Curr Opin Plant Biol* 11 (3):266-277
- Molina-Hidalgo FJ, Franco AR, Villatoro C, Medina-Puche L, Mercado JA, Hidalgo MA, Monfort A, Caballero JL, Muñoz-Blanco J, Blanco-Portales R (2013) The strawberry (*Fragaria x ananassa*) fruit-specific rhamnogalacturonate lyase 1 (FaRGLyase1) gene encodes an enzyme involved in the degradation of cell-wall middle lamellae. *J Exp Bot* 64 (6):1471-1483
- Moore JP, Farrant JM, Driouich A (2008a) A role for pectin-associated arabinans in maintaining the flexibility of the plant cell wall during water deficit stress. *Plant signaling & behavior* 3 (2):102-104

- Moore JP, Nguema-Ona EE, Vicré-Gibouin M, Sørensen I, Willats WG, Driouich A, Farrant JM (2013) Arabinose-rich polymers as an evolutionary strategy to plasticize resurrection plant cell walls against desiccation. *Planta* 237 (3):739-754
- Moore JP, Vicré-Gibouin M, Farrant JM, Driouich A (2008b) Adaptations of higher plant cell walls to water loss: drought vs desiccation. *Physiol Plantarum* 134 (2):237-245
- Moreira L (2008) An overview of mannan structure and mannan-degrading enzyme systems. *Appl Microbiol Biotech* 79 (2):165-178
- Morgan JL, Strumillo J, Zimmer J (2013) Crystallographic snapshot of cellulose synthesis and membrane translocation. *Nature* 493 (7431):181-186
- Morrison IN, O'Brien TP (1976) Cytokinesis in Developing Wheat-Grain - Division with and without a Phragmoplast. *Planta* 130 (1):57-67
- Mortimer JC, Miles GP, Brown DM, Zhang Z, Segura MP, Weimar T, Yu X, Seffen KA, Stephens E, Turner SR (2010) Absence of branches from xylan in *Arabidopsis gux* mutants reveals potential for simplification of lignocellulosic biomass. *PNAS* 107 (40):17409-17414
- Mouille G, Ralet MC, Cavelier C, Eland C, Effroy D, Hématy K, McCartney L, Truong HN, Gaudon V, Thibault JF (2007) Homogalacturonan synthesis in *Arabidopsis thaliana* requires a Golgi-localized protein with a putative methyltransferase domain. *Plant J* 50 (4):605-614
- Mujer CV, Ramirez DA, Mendoza EMT (1984) α -d-galactosidase deficiency in coconut endosperm: its possible pleiotropic effects in makapuno. *Phytochemistry* 23 (4):893-894
- Muller S, Vensel WH, Kasarda DD, Kohler P, Wieser H (1998) Disulphide bonds of adjacent cysteine residues in low molecular weight subunits of wheat glutenin. *J Cereal Sci* 27 (2):109-116
- Myers AM, Morell MK, James MG, Ball SG (2000) Recent progress toward understanding biosynthesis of the amylopectin crystal. *Plant Physiol* 122 (4):989-998
- Nakamura A, Furuta H, Maeda H, NAGAMATSU Y, Yoshimoto A (2001) Analysis of structural components and molecular construction of soybean soluble polysaccharides by stepwise enzymatic degradation. *Biosci Biotech Bioch* 65 (10):2249-2258
- Nakamura Y, Umemoto T, Takahata Y, Komae K, Amano E, Satoh H (1996) Changes in structure of starch and enzyme activities affected by sugary mutations in developing rice endosperm. Possible role of starch debranching enzyme (R-enzyme) in amylopectin biosynthesis. *Physiol Plantarum* 97 (3):491-498
- Nakamura Y, Yuki K, Park S-Y, Ohya T (1989) Carbohydrate metabolism in the developing endosperm of rice grains. *Plant Cell Physiol* 30 (6):833-839

- Newman RH, Hill SJ, Harris PJ (2013) Wide-angle x-ray scattering and solid-state nuclear magnetic resonance data combined to test models for cellulose microfibrils in mung bean cell walls. *Plant Physiol* 163 (4):1558-1567
- Ng JK, Schröder R, Brummell DA, Sutherland PW, Hallett IC, Smith BG, Melton LD, Johnston JW (2015) Lower cell wall pectin solubilisation and galactose loss during early fruit development in apple (*Malus x domestica*) cultivar 'Scifresh' are associated with slower softening rate. *J Plant Physiol* 176:129-137
- Noguchi K, Yasumori M, Imai T, Naito S, Matsunaga T, Oda H, Hayashi H, Chino M, Fujiwara T (1997) bor1-1, an *Arabidopsis thaliana* mutant that requires a high level of boron. *Plant Physiol* 115 (3):901-906
- Nothnagel EA (1997) Proteoglycans and related components in plant cells. *Int Rev Cytol* 174:195-291
- Nyman ME, Bjorck IM (1989) *In vivo* effects of phytic acid and polyphenols on the bioavailability of polysaccharides and other nutrients. *J Food Sci* 54 (5):1332-1335
- O'Neill MA, Eberhard S, Albersheim P, Darvill AG (2001) Requirement of borate cross-linking of cell wall rhamnogalacturonan II for *Arabidopsis* growth. *Science* 294 (5543):846-849
- O'Neill MA, Ishii T, Albersheim P, Darvill AG (2004) Rhamnogalacturonan II: structure and function of a borate cross-linked cell wall pectic polysaccharide. *Annu Rev Plant Biol* 55:109-139
- O'Neill MA, Warrenfeltz D, Kates K, Pellerin P, Doco T, Darvill AG, Albersheim P (1996) Rhamnogalacturonan-II, a pectic polysaccharide in the walls of growing plant cell, forms a dimer that is covalently cross-linked by a borate ester *in vitro* conditions for the formation and hydrolysis of the dimer. *J Biol Chem* 271 (37):22923-22930
- Obel N, Porchia A, Scheller H (2003) Intracellular feruloylation of arabinoxylan in wheat: evidence for feruloyl-glucose as precursor. *Planta* 216 (4):620-629
- Øbro J, Harholt J, Scheller HV, Orfila C (2004) Rhamnogalacturonan I in *Solanum tuberosum* tubers contains complex arabinogalactan structures. *Phytochemistry* 65 (10):1429-1438
- Ogawa M, Kay P, Wilson S, Swain SM (2009) ARABIDOPSIS DEHISCENCE ZONE POLYGALACTURONASE1 (ADPG1), ADPG2, and QUARTET2 are polygalacturonases required for cell separation during reproductive development in *Arabidopsis*. *Plant Cell* 21 (1):216-233
- Ogawa M, Kumamaru T, Satoh H, Iwata N, Omura T, Kasai Z, Tanaka K (1987) Purification of protein body-I of rice seed and its polypeptide composition. *Plant and Cell Physiology* 28 (8):1517-1527
- Ohdaira Y, Masumura T, Nakatsuka N, Shigemitsu T, Saito Y, Sasaki R (2011) Analysis of storage protein distribution in rice grain of seed-protein mutant cultivars by immunofluorescence microscopy. *Plant Prod Sci* 14 (3):219-228

- Oka T, Nemoto T, Jigami Y (2007) Functional analysis of *Arabidopsis thaliana* RHM2/MUM4, a multidomain protein involved in UDP-D-glucose to UDP-L-rhamnose conversion. *J Biol Chem* 282 (8):5389-5403
- Okita TW, Hwang YS, Hnilo J, Kim WT, Aryan AP, Larson R, Krishnan HB (1989) Structure and expression of the rice glutelin multigene family. *J Biol Chem* 264 (21):12573-12581
- Okita TW, Kim WT, Krishnan HB, Hnilo J, Hwang YS (1988) Immunological relationship and structure of wheat and rice seed proteins. *Abstr Pap Am Chem S* 195:106-111
- Olsen OA (2001) Endosperm development: Cellularization and cell fate specification. *Annu Rev Plant Phys* 52:233-267
- Olsen OA, Lemmon B, Brown R (1998) A model for aleurone development. *Trends Plant Sci* 3 (5):168-169
- Oosterveld A, Voragen AG, Schols HA (2002) Characterization of hop pectins shows the presence of an arabinogalactan-protein. *Carbohydr Poly* 49 (4):407-413
- Oparka K, Harris N (1982) Rice protein-body formation: all types are initiated by dilation of the endoplasmic reticulum. *Planta* 154 (2):184-188
- Oparka KJ, Gates P (1981a) Transport of assimilates in the developing caryopsis of rice (*Oryza-Sativa-l*) - the pathways of water and assimilated carbon. *Planta* 152 (5):388-396
- Oparka KJ, Gates P (1981b) Transport of assimilates in the developing caryopsis of rice (*Oryza-Sativa-L*) - Ultrastructure of the pericarp vascular bundle and its connections with the aleurone layer. *Planta* 151 (6):561-573
- Oparka KJ, Gates PJ (1982) Ultrastructure of the developing pigment strand of rice (*Oryza-Sativa-L*) in relation to its role in solute transport. *Protoplasma* 113 (1):33-43
- Orfila C, Sørensen SO, Harholt J, Geshi N, Crombie H, Truong H-N, Reid JG, Knox JP, Scheller HV (2005) QUASIMODO1 is expressed in vascular tissue of *Arabidopsis thaliana* inflorescence stems, and affects homogalacturonan and xylan biosynthesis. *Planta* 222 (4):613-622
- Palmer R, Cornuault V, Marcus SE, Knox JP, Shewry PR, Tosi P (2015) Comparative in situ analyses of cell wall matrix polysaccharide dynamics in developing rice and wheat grain. *Planta* 241 (3):669-685
- Palmiano EP, Almazan AM, Juliano BO (1968) Physicochemical properties of protein of developing and mature rice grain. *Cereal Chem* 45 (1):1-12
- Parker ML, Ng A, Waldron KW (2005) The phenolic acid and polysaccharide composition of cell walls of bran layers of mature wheat (*Triticum aestivum* L. cv. Avalon) grains. *J Sci Food Agri* 85 (15):2539-2547
- Pattathil S, Avci U, Baldwin D, Swennes AG, McGill JA, Popper Z, Bootten T, Albert A, Davis RH, Chennareddy C (2010) A comprehensive toolkit of plant cell wall glycan-directed monoclonal antibodies. *Plant physiology* 153 (2):514-525

- Peaucelle A, Braybrook S, Höfte H (2012) Cell wall mechanics and growth control in plants: the role of pectins revisited. *Front Plant Sci* 3
- Pedersen HL, Fangel JU, McCleary B, Ruzanski C, Rydahl MG, Ralet MC, Farkas V, von Schantz L, Marcus SE, Andersen MCF, Field R, Ohlin M, Knox JP, Clausen MH, Willats WGT (2012) Versatile High Resolution Oligosaccharide Microarrays for Plant Glycobiology and Cell Wall Research. *J Biol Chem* 287 (47)
- Pellny TK, Lovegrove A, Freeman J, Tosi P, Love CG, Knox JP, Shewry PR, Mitchell RAC (2012) Cell walls of developing wheat starchy endosperm: comparison of composition and RNA-Seq transcriptome. *Plant Physiol* 158 (2):612-627
- Peña MJ, Carpita NC (2004) Loss of highly branched arabinans and debranching of rhamnogalacturonan I accompany loss of firm texture and cell separation during prolonged storage of apple. *Plant Physiol* 135 (3):1305-1313
- Peña MJ, Zhong R, Zhou G-K, Richardson EA, O'Neill MA, Darvill AG, York WS, Ye Z-H (2007) Arabidopsis irregular xylem8 and irregular xylem9: implications for the complexity of glucuronoxylan biosynthesis. *Plant Cell* 19 (2):549-563
- Penfield S, Meissner RC, Shoue DA, Carpita NC, Bevan MW (2001) MYB61 is required for mucilage deposition and extrusion in the Arabidopsis seed coat. *Plant Cell* 13 (12):2777-2791
- Peng M, Gao M, Båga M, Hucl P, Chibbar RN (2000) Starch-branching enzymes preferentially associated with A-type starch granules in wheat endosperm. *Plant Physiol* 124 (1):265-272
- Pérez S, Rodriguez-Carvajal M, Doco T (2003) A complex plant cell wall polysaccharide: rhamnogalacturonan II. A structure in quest of a function. *Biochimie* 85 (1):109-121
- Philippe S, Barron C, Robert P, Devaux MF, Saulnier L, Guillon F (2006a) Characterization using Raman microspectroscopy of arabinoxylans in the walls of different cell types during the development of wheat endosperm. *J Agr Food Chem* 54 (14):5113-5119
- Philippe S, Robert P, Barron C, Saulnier L, Guillon F (2006b) Deposition of cell wall polysaccharides in wheat endosperm during grain development: Fourier transform-infrared microspectroscopy study. *J Agr Food Chem* 54 (6):2303-2308
- Philippe S, Saulnier L, Guillon F (2006c) Arabinoxylan and (1-3),(1-4)- β -glucan deposition in cell walls during wheat endosperm development. *Planta* 224 (2):449-461
- Philippe S, Tranquet O, Utile JP, Saulnier L, Guillon F (2007) Investigation of ferulate deposition in endosperm cell walls of mature and developing wheat grains by using a polyclonal antibody. *Planta* 225 (5):1287-1299
- Piber M, Koehler P (2005) Identification of dehydro-ferulic acid-tyrosine in rye and wheat: evidence for a covalent cross-link between arabinoxylans and proteins. *J Agr Food Chem* 53 (13):5276-5284

- Piot O, Autran JC, Manfait M (2001) Investigation by confocal Raman microspectroscopy of the molecular factors responsible for grain cohesion in the *Triticum aestivum* bread wheat. Role of the cell walls in the starchy endosperm. *J Cereal Sci* 34 (2):191-205
- Radford J, Vesik M, Overall R (1998) Callose deposition at plasmodesmata. *Protoplasma* 201 (1-2):30-37
- Ralet MC, Tranquet O, Poulain D, Moise A, Guillon F (2010) Monoclonal antibodies to rhamnogalacturonan I backbone. *Planta* 231 (6):1373-1383
- Ralph J, Quideau S, Grabber JH, Hatfield RD (1994) Identification and synthesis of new ferulic acid dehydrodimers present in grass cell walls. *J Chem Soc* (23):3485-3498
- Redgwell RJ, Fischer M, Kendal E, MacRae EA (1997) Galactose loss and fruit ripening: high-molecular-weight arabinogalactans in the pectic polysaccharides of fruit cell walls. *Planta* 203 (2):174-181
- Reid JG (1997) Carbohydrate metabolism: structural carbohydrates. *Plant Biochem*:205-236
- Reiter WD, Chapple C, Somerville CR (1997) Mutants of *Arabidopsis thaliana* with altered cell wall polysaccharide composition. *Plant J* 12 (2):335-345
- Renard CM, Jarvis MC (1999) A cross-polarization, magic-angle-spinning, ¹³C-nuclear-magnetic-resonance study of polysaccharides in sugar beet cell walls. *Plant Physiol* 119 (4):1315-1322
- Richmond TA, Somerville CR (2000) The cellulose synthase superfamily. *Plant Physiol* 124 (2):495-498
- Ridley BL, O'Neill MA, Mohnen D (2001) Pectins: structure, biosynthesis, and oligogalacturonide-related signaling. *Phytochemistry* 57 (6):929-967
- Robert P, Jamme F, Barron C, Bouchet B, Saulnier L, Dumas P, Guillon F (2011) Change in wall composition of transfer and aleurone cells during wheat grain development. *Planta* 233 (2):393-406
- Robert P, Marquis M, Barron C, Guillon F, Saulnier L (2005) FT-IR investigation of cell wall polysaccharides from cereal grains. Arabinoxylan infrared assignment. *J Agr Food Chem* 53 (18):7014-7018
- Robin J (1974) Lint-nerized starches. Gel filtration and enzymatic studies of insoluble residues from prolonged acid treatment of potato starch. *Cereal Chem* 51:389-406
- Rodkiewicz B (1970) Callose in cell walls during megasporogenesis in angiosperms. *Planta* 93 (1):39-47
- Roland J, Vian B, Reis D (1975) Observations with cytochemistry and ultracryotomy on the fine structure of the expanding walls in actively elongating plant cells. *J Cell Sci* 19 (2):239-259

- Rouau X, Cheynier V, Surget A, Gloux D, Barron C, Meudec E, Louis-Montero J, Criton M (2003) A dehydrotrimer of ferulic acid from maize bran. *Phytochemistry* 63 (8):899-903
- Roulin S, Buchala AJ, Fincher GB (2002) Induction of (1-3)(1-4)- β -d-glucan hydrolases in leaves of dark-incubated barley seedlings. *Planta* 215 (1):51-59
- Rubin R, Levanony H, Galili G (1992) Evidence for the presence of two different types of protein bodies in wheat endosperm. *Plant Physiol* 99 (2):718-724
- Sabelli PA, Larkins BA (2009) The development of endosperm in grasses. *Plant Physiol* 149 (1):14-26
- Samuels AL, Giddings TH, Staehelin LA (1995) Cytokinesis in tobacco by-2 and root-tip cells - a new model of cell plate formation in higher-plants. *J Cell Biol* 130 (6):1345-1357
- Savatin DV, Ferrari S, Sicilia F, De Lorenzo G (2011) Oligogalacturonide-auxin antagonism does not require posttranscriptional gene silencing or stabilization of auxin response repressors in Arabidopsis. *Plant Physiol* 157 (3):1163-1174
- Scheller HV, Doong RL, Ridley BL, Mohnen D (1999) Pectin biosynthesis: a solubilized α 1, 4-galacturonosyltransferase from tobacco catalyzes the transfer of galacturonic acid from UDP-galacturonic acid onto the non-reducing end of homogalacturonan. *Planta* 207 (4):512-517
- Scheller HV, Ulvskov P (2010) Hemicelluloses. *Plant Biol* 61 (1):263-289
- Scott Jr TA, Melvin EH (1953) Determination of dextran with anthrone. *Anal Chem* 25 (11):1656-1661
- Shanmugavelan P, Kim SY, Kim JB, Kim HW, Cho SM, Kim SN, Kim SY, Cho YS, Kim HR (2013) Evaluation of sugar content and composition in commonly consumed Korean vegetables, fruits, cereals, seed plants, and leaves by HPLC-ELSD. *Carbohydr Res* 380:112-117
- Shewry PR, Mitchell RAC, Tosi P, Wan YF, Underwood C, Lovegrove A, Freeman J, Toole GA, Mills ENC, Ward JL (2012) An integrated study of grain development of wheat (cv. Hereward). *J Cereal Sci* 56 (1):21-30
- Shewry PR, Sayanova O, Tatham AS, Tamas L, Turner M, Richard G, Hickman D, Fido R, Halford NG, Greenfield J, Grimwade B, Thomson N, Miles M, Freedman R, Napier J (1995) Structure, assembly and targeting of wheat storage proteins. *J Plant Physiol* 145 (5-6):620-625
- Shewry PR, Tatham AS, Halford NG (2001) Nutritional control of storage protein synthesis in developing grain of wheat and barley. *Plant Growth Regul* 34 (1):105-111
- Shewry PR, Underwood C, Wan YF, Lovegrove A, Bhandari D, Toole G, Mills ENC, Denyer K, Mitchell RAC (2009) Storage product synthesis and accumulation in developing grains of wheat. *J Cereal Sci* 50 (1):106-112

- Shibuya N (1989) Comparative-studies on the cell-wall polymers obtained from different parts of rice grains. *Acs Sym Ser* 399:333-344
- Shibuya N, Misaki A, Iwasaki T (1983) The structure of arabinoxylan and arabinoglucuronoxylan isolated from rice endosperm cell-wall. *Agri Biol Chem* 47 (10):2223-2230
- Shibuya N, Nakane R (1984) Pectic Polysaccharides of rice endosperm cell-walls. *Phytochemistry* 23 (7):1425-1429
- Shibuya N, Nakane R, Yasui A, Tanaka K, Iwasaki T (1985) Comparative studies on cell-wall preparations from rice bran, germ, and endosperm. *Cereal Chem* 62 (4):252-258
- Showalter A (2001) Arabinogalactan-proteins: structure, expression and function. *Cell Mol Life Sci* 58 (10):1399-1417
- Showalter AM, Keppler BD, Lichtenberg J, Gu D, Welch LR (2010) A bioinformatics approach to the identification, classification, and analysis of hydroxyproline-rich glycoproteins. *Plant Physiol* 153 (2):485-513
- Singh B, Jenner C (1982) Association between concentration of organic nutrients in the grain, endosperm cell number and grain dry weight within the ear of wheat. *Funct Plant Biol* 9 (1):83-95
- Skjøt M, Pauly M, Bush MS, Borkhardt B, McCann MC, Ulvskov P (2002) Direct interference with rhamnogalacturonan I biosynthesis in Golgi vesicles. *Plant Physiol* 129 (1):95-102
- Slabaugh E, Davis JK, Haigler CH, Yingling YG, Zimmer J (2014) Cellulose synthases: new insights from crystallography and modeling. *Trends Plant Sci* 19 (2):99-106
- Slavin J, Jacobs DR (2010) Dietary fiber: All fibers are not alike. *Nutr Health Ser*:13-24
- Somerville C (2006) Cellulose synthesis in higher plants. *Annu Rev Cell Dev Biol* 22:53-78
- Sørensen I, Pettolino FA, Wilson SM, Doblin MS, Johansen B, Bacic A, Willats WG (2008) Mixed-linkage (1-3),(1-4)- β -d-glucan is not unique to the Poales and is an abundant component of *Equisetum arvense* cell walls. *Plant J* 54 (3):510-521
- Sørensen SO, Pauly M, Bush M, Skjøt M, McCann MC, Borkhardt B, Ulvskov P (2000) Pectin engineering: modification of potato pectin by *in vivo* expression of an endo-(1-4)- β -D-galactanase. *PNAS* 97 (13):7639-7644
- Spyropoulos C, Reid J (1985) Regulation of α -galactosidase activity and the hydrolysis of galactomannan in the endosperm of the fenugreek (*Trigonella foenum-graecum* L.) seed. *Planta* 166 (2):271-275
- Staelin L, Giddings T, Levy S, Lynch M, Moore P, Swords K Organization of the secretory pathway of cell wall glycoproteins and complex polysaccharides in

- plant cells. In: Endocytosis, exocytosis and vesicle traffic in plants (Seminar Series 45), 1991. pp 183-198
- Staudte R, Woodward J, Fincher G, Stone B (1983) Water-soluble (1-3),(1-4)- β -D-glucans from barley (*Hordeum vulgare*) endosperm. III. Distribution of cellotriosyl and cellotetraosyl residues. *Carbohydr Polym* 3 (4):299-312
- Stevenson TT, Darvill AG, Albersheim P (1988) Structural features of the plant cell-wall polysaccharide rhamnogalacturonan-II. *Carbohydrate Res* 182 (2):207-226
- Stone BA, Clarke AE (1992) Chemistry and biology of (1-3)- β -Glucans. La Trobe University Press, Australia
- Studer D, Hennecke H, Müller M (1992) High-pressure freezing of soybean nodules leads to an improved preservation of ultrastructure. *Planta* 188 (2):155-163
- Tan K-S, Hoson T, Masuda Y, Kamisaka S (1992) Effect of ferulic and *p*-coumaric acids on *Oryza* coleoptile growth and the mechanical properties of cell walls. *J Plant Physiol* 140 (4):460-465
- Tan KS, Hoson T, Masuda Y, Kamisaka S (1991) Correlation between cell wall extensibility and the content of diferulic and ferulic acids in cell walls of *Oryza sativa* coleoptiles grown under water and in air. *Phys Planta* 83 (3):397-403
- Tan L, Eberhard S, Pattathil S, Warder C, Glushka J, Yuan C, Hao Z, Zhu X, Avci U, Miller JS (2013) An Arabidopsis cell wall proteoglycan consists of pectin and arabinoxylan covalently linked to an arabinogalactan protein. *Plant Cell* 25 (1):270-287
- Tanaka K, Sugimoto T, Ogawa M, Kasai Z (1980) Isolation and characterization of two types of protein bodies in the rice endosperm. *Agri Biol Chem* 44 (7):1633-1639
- Tashiro T, Wardlaw I (1990) The response to high temperature shock and humidity changes prior to and during the early stages of grain development in wheat. *Funct Plant Biol* 17 (5):551-561
- Tester RF, Karkalas J, Qi X (2004) Starch—composition, fine structure and architecture. *J Cereal Sci* 39 (2):151-165
- Tetlow IJ (2011) Starch biosynthesis in developing seeds. *Seed Sci Res* 21 (1):5-32
- Thomas JR, Darvill AG, Albersheim P (1989) Isolation and structural characterization of the pectic polysaccharide rhamnogalacturonan II from walls of suspension-cultured rice cells. *Carbohydr Res* 185 (2):261-277
- Thomas LH, Forsyth VT, Šturcová A, Kennedy CJ, May RP, Altaner CM, Apperley DC, Wess TJ, Jarvis MC (2013) Structure of cellulose microfibrils in primary cell walls from collenchyma. *Plant Physiol* 161 (1):465-476
- Threapleton DE, Greenwood DC, Evans CEL, Cleghorn CL, Nykjaer C, Woodhead C, Cade JE, Gale CP, Burley VJ (2013) Dietary fiber intake and risk of first stroke a systematic review and meta-analysis. *Stroke* 44 (5):1360-1368

- Tian F, Tao K, Xiao G, Cao S (1998) Determination of the soluble non-starch polysaccharides in rice and wheat bran by gas chromatography. *Se Pu* 16 (2):123-125
- Toole GA, Barron C, Le Gall G, Colquhoun IJ, Shewry PR, Mills ENC (2009) Remodelling of arabinoxylan in wheat (*Triticum aestivum*) endosperm cell walls during grain filling. *Planta* 229 (3):667-680
- Toole GA, Le Gall G, Colquhoun IJ, Johnson P, Bedo Z, Saulnier L, Shewry PR, Mills ENC (2011) Spectroscopic analysis of diversity of arabinoxylan structures in endosperm cell walls of wheat cultivars (*Triticum aestivum*) in the HEALTHGRAIN Diversity Collection. *J Agr Food Chem* 59 (13):7075-7082
- Toole GA, Le Gall G, Colquhoun IJ, Nemeth C, Saulnier L, Lovegrove A, Pellny T, Wilkinson MD, Freeman J, Mitchell RAC, Mills ENC, Shewry PR (2010) Temporal and spatial changes in cell wall composition in developing grains of wheat cv. Hereward. *Planta* 232 (3):677-689
- Toole GA, Wilson RH, Parker ML, Wellner NK, Wheeler TR, Shewry PR, Mills ENC (2007) The effect of environment on endosperm cell-wall development in *Triticum aestivum* during grain filling: an infrared spectroscopic imaging study. *Planta* 225 (6):1393-1403
- Tosh SM, Brummer Y, Wood PJ, Wang Q, Weisz J (2004) Evaluation of structure in the formation of gels by structurally diverse (1→3)(1→4)-β-D-glucans from four cereal and one lichen species. *Carbohydrate Polymers* 57 (3):249-259
- Tosi P, Gritsch CS, He JB, Shewry PR (2011) Distribution of gluten proteins in bread wheat (*Triticum aestivum*) grain. *Ann Bot -London* 108 (1):23-35
- Tosi P, Parker M, Gritsch CS, Carzaniga R, Martin B, Shewry PR (2009) Trafficking of storage proteins in developing grain of wheat. *J Exp Bot* 60 (3):979-991
- Tranquet O, Saulnier L, Utile J-P, Ralph J, Guillon F (2009) Monoclonal antibodies to *p*-coumarate. *Phytochem* 70 (11):1366-1373
- Tryfona T, Liang H-C, Kotake T, Kaneko S, Marsh J, Ichinose H, Lovegrove A, Tsumuraya Y, Shewry PR, Stephens E, Dupree P (2010) Carbohydrate structural analysis of wheat flour arabinogalactan protein. *Carbohydr Res* 345 (18):2648-2656
- Ugalde T, Jenner C (1990) Substrate gradients and regional patterns of dry matter deposition within developing wheat endosperm. II. Amino acids and protein. *Functional Plant Biology* 17 (4):395-406
- Updegraff DM (1969) Semimicro determination of cellulose in biological materials. *Analytical Biochemistry* 32 (3):420-424
- Urbanowicz BR, Rayon C, Carpita NC (2004) Topology of the maize mixed linkage (1-3),(1-4)-β-D-glucan synthase at the Golgi membrane. *Plant Physiol* 134 (2):758-768
- Van den Bulck K, Swennen K, Loosveldt AMA, Courtin CM, Brijs K, Proost P, Van Damme J, Van Campenhout S, Mort A, Delcour JA (2005) Isolation of cereal

arabinogalactan-peptides and structural comparison of their carbohydrate and peptide moieties. *J Cereal Sci* 41 (1):59-67

- Van Hengel AJ, Van Kammen A, De Vries SC (2002) A relationship between seed development, Arabinogalactan-proteins (AGPs) and the AGP mediated promotion of somatic embryogenesis. *Physiologia Plantarum* 114 (4):637-644
- Vanholme R, Morreel K, Ralph J, Boerjan W (2008) Lignin engineering. *Curr Opin Plant Biol* 11 (3):278-285
- Verhertbruggen Y, Marcus SE, Chen J, Knox JP (2013) Cell wall pectic arabinans influence the mechanical properties of *Arabidopsis thaliana* inflorescence stems and their response to mechanical stress. *Plant Cell Physiol* 54 (8):1278-1288
- Verhertbruggen Y, Marcus SE, Haeger A, Ordaz-Ortiz JJ, Knox JP (2009) An extended set of monoclonal antibodies to pectic homogalacturonan. *Carbohyd Res* 344 (14):1858-1862
- Verma DPS, Hong ZL (2001) Plant callose synthase complexes. *Plant Mol Biol* 47 (6):693-701
- Vignon M, Heux L, Malainine M-E, Mahrouz M (2004) Arabinan–cellulose composite in *Opuntia ficus-indica* prickly pear spines. *Carbohyd Res* 339 (1):123-131
- Vincken J-P, Schols HA, Oomen RJ, McCann MC, Ulvskov P, Voragen AG, Visser RG (2003) If homogalacturonan were a side chain of rhamnogalacturonan I. Implications for cell wall architecture. *Plant Physiol* 132 (4):1781-1789
- Vogel J (2008) Unique aspects of the grass cell wall. *Curr Opin Plant Biol* 11 (3):301-307
- Vogel K, Johnson V, Mattern P (1978) Protein and lysine contents of endosperm and bran of the parents and progenies of crosses of common wheat. *Crop Sci* 18 (5):751-754
- Voragen A, Pilnik W, Thibault J-F, Axelos M, Renard CM (1995) 10 Pectins. In: *Food polysaccharides and their applications*, pp 287-339
- Wakabayashi K, Hoson T, Kamisaka S (1997) Osmotic stress suppresses cell wall stiffening and the increase in cell wall-bound ferulic and diferulic acids in wheat coleoptiles. *Plant physiology* 113 (3):967-973
- Walbot V (1994) Overview of key steps in aleurone development. In: *The Maize Handbook*. Springer, pp 78-80
- Wang HL, Offler CE, Patrick JW (1994) Nucellar projection transfer cells in the developing wheat-grain. *Protoplasma* 182 (1-2):39-52
- Wang N, Fisher DB (1994) The use of fluorescent tracers to characterize the post-phloem transport pathway in maternal tissues of developing wheat grains. *Plant Physiol* 104 (1):17-27

- Wang T, Park YB, Daniel JC, Hong M (2015) Cellulose-Pectin Spatial Contacts Are Inherent to Never-Dried *Arabidopsis thaliana* Primary Cell Walls: Evidence from Solid-State NMR. *Plant physiology* 168 871-884
- Wilkinson MD, Castells-Brooke N, Shewry PR (2013) Diversity of sequences encoded by the Gsp-1 genes in wheat and other grass species. *J Cereal Sci* 57 (1):1-9
- Willats WG, McCartney L, Mackie W, Knox JP (2001a) Pectin: cell biology and prospects for functional analysis. In: *Plant Cell Walls*. Springer, pp 9-27
- Willats WG, Orfila C, Limberg G, Buchholt HC, van Alebeek G-JW, Voragen AG, Marcus SE, Christensen TM, Mikkelsen JD, Murray BS (2001b) Modulation of the degree and pattern of methyl-esterification of pectic homogalacturonan in plant cell walls. Implications for pectin methyl esterase action, matrix properties and cell adhesion. *J Biol Chem* 276 (22):19404-19413
- Willats WG, Steele-King CG, Marcus SE, Knox JP (1999) Side chains of pectic polysaccharides are regulated in relation to cell proliferation and cell differentiation. *Plant J* 20 (6):619-628
- Willats WGT, Marcus SE, Knox JP (1998) Generation of a monoclonal antibody specific to (1-5)- α -L-arabinan. *Carbohyd Res* 308 (1-2):149-152
- Wilson SM, Burton RA, Collins HM, Doblin MS, Pettolino FA, Shirley N, Fincher GB, Bacic A (2012) Pattern of deposition of cell wall polysaccharides and transcript abundance of related cell wall synthesis genes during differentiation in barley endosperm. *Plant physiology* 159 (2):655-670
- Wilson SM, Burton RA, Doblin MS, Stone BA, Newbigin EJ, Fincher GB, Bacic A (2006) Temporal and spatial appearance of wall polysaccharides during cellularization of barley (*Hordeum vulgare*) endosperm. *Planta* 224 (3):655-667
- Wolf S, Mouille G, Pelloux J (2009) Homogalacturonan methyl-esterification and plant development. *Mol Plant* 2 (5):851-860
- Woodward J, Fincher G, Stone B (1983a) Water-soluble (1-3),(1-4)- β -D-glucans from barley (*Hordeum vulgare*) endosperm. II. Fine structure. *Carbohyd Polym* 3 (3):207-225
- Woodward J, Phillips D, Fincher G (1983b) Water-soluble (1-3),(1-4)- β -D-glucans from barley (*Hordeum vulgare*) endosperm. I. Physicochemical properties. *Carbohyd Polym* 3 (2):143-156
- Woodward J, Phillips D, Fincher G (1988) Water-soluble (1-3)(1-4)- β -D-glucans from barley (*Hordeum vulgare*) endosperm. IV. Comparison of 40°C and 65°C soluble fractions. *Carbohyd Polym* 8 (2):85-97
- Wu AM, Rihouey C, Seveno M, Hörnblad E, Singh SK, Matsunaga T, Ishii T, Lerouge P, Marchant A (2009) The *Arabidopsis* IRX10 and IRX10-LIKE glycosyltransferases are critical for glucuronoxylan biosynthesis during secondary cell wall formation. *Plant J* 57 (4):718-731

- Xu J-H, Messing J (2008) Organization of the prolamin gene family provides insight into the evolution of the maize genome and gene duplications in grass species. *PNAS* 105 (38):14330-14335
- Xue X, Fry SC (2012) Evolution of mixed-linkage (1-3),(1-4)- β -D-glucan (MLG) and xyloglucan in *Equisetum* (horsetails) and other monilophytes. *Ann Bot - London* 109 (5):873-886
- Yamagata H, Sugimoto T, Tanaka K, Kasai Z (1982) Biosynthesis of storage proteins in developing rice seeds. *Plant physiology* 70 (4):1094-1100
- Yamagata H, Tanaka K (1986) The site of synthesis and accumulation of rice storage proteins. *Plant Cell Physiol* 27 (1):135-145
- Yang J, Zhang J, Huang Z, Wang Z, Zhu Q, Liu L (2002) Correlation of cytokinin levels in the endosperms and roots with cell number and cell division activity during endosperm development in rice. *Ann Bot -London* 90 (3):369-377
- Yapo BM (2011) Pectic substances: From simple pectic polysaccharides to complex pectins—A new hypothetical model. *Carbohydr Polym* 86 (2):373-385
- Yariv J, Rapport M, Graf L (1962) The interaction of glycosides and saccharides with antibody to the corresponding phenylazo glycosides. *Biochem J* 85 (2):383
- Yi G, Lauter AM, Scott MP, Becraft PW (2011) The thick aleurone1 mutant defines a negative regulation of maize aleurone cell fate that functions downstream of defective kernel1. *Plant Physiol* 156 (4):1826-1836
- Yin Y, Huang J, Xu Y (2009) The cellulose synthase superfamily in fully sequenced plants and algae. *BMC Plant Biol* 9 (1):99
- Yin Y-a, Qi J-c, Li W-h, Cao L-p, Wang Z-b (2012) Formation and developmental characteristics of A-and B-type starch granules in wheat endosperm. *J Integ Agr* 11 (1):73-81
- Young TE, Gallie DR (1999) Analysis of programmed cell death in wheat endosperm reveals differences in endosperm development between cereals. *Plant Mol Biol* 39 (5):915-926
- Zablackis E, Huang J, Muller B, Darvill AG, Albersheim P (1995) Characterization of the cell-wall polysaccharides of *Arabidopsis thaliana* leaves. *Plant Physiol* 107 (4):1129-1138
- Zee SY (1972a) Transfer cells and vascular tissue distribution in vegetative nodes of rice. *Aust J Bot* 20 (1):41-48
- Zee SY (1972b) Vascular tissue and transfer cell distribution in rice spikelet. *Aust J Biol Sci* 25 (2):411-414
- Zee SY, Obrian TP (1971) Vascular tissue of lodicules of wheat. *Aust J Biol Sci* 24 (4):805-809
- Zee SY, Obrian TP (1971a) Aleurone transfer cells and other structural features of spikelet of millet. *Aust J Biol Sci* 24 (2):391-396
- Zee SY, Obrian TP (1971b) Vascular transfer cells in wheat spikelet. *Aust J Biol Sci* 24 (1):35-50

- Zeeman SC, Tiessen A, Pilling E, Kato KL, Donald AM, Smith AM (2002) Starch synthesis in Arabidopsis. Granule synthesis, composition, and structure. *Plant Physiol* 129 (2):516-529
- Zhao ZD, Tan L, Showalter AM, Lamport DTA, Kieliszewski MJ (2002) Tomato LeAGP-1 arabinogalactan-protein purified from transgenic tobacco corroborates the Hyp contiguity hypothesis. *Plant J* 31 (4):431-444
- Zhou Q, Rutland MW, Teeri TT, Brumer H (2007) Xyloglucan in cellulose modification. *Cellulose* 14 (6):625-641
- Zykwinska A, Rondeau-Mouro C, Garnier C, Thibault J-F, Ralet M-C (2006) Alkaline extractability of pectic arabinan and galactan and their mobility in sugar beet and potato cell walls. *Carbohydr Polym* 65 (4):510-520
- Zykwinska AW, Ralet M-CJ, Garnier CD, Thibault J-FJ (2005) Evidence for *in vitro* binding of pectin side chains to cellulose. *Plant Physiol* 139 (1):397-407